Targeting NF-κB signaling in macrophages through drug repurposing

A thesis submitted for the degree of Doctor of Philosophy in Molecular Cell Biology in Health and Disease

University of Oxford

Trinity Term 2024



Annabell Roberti

Magdalen College

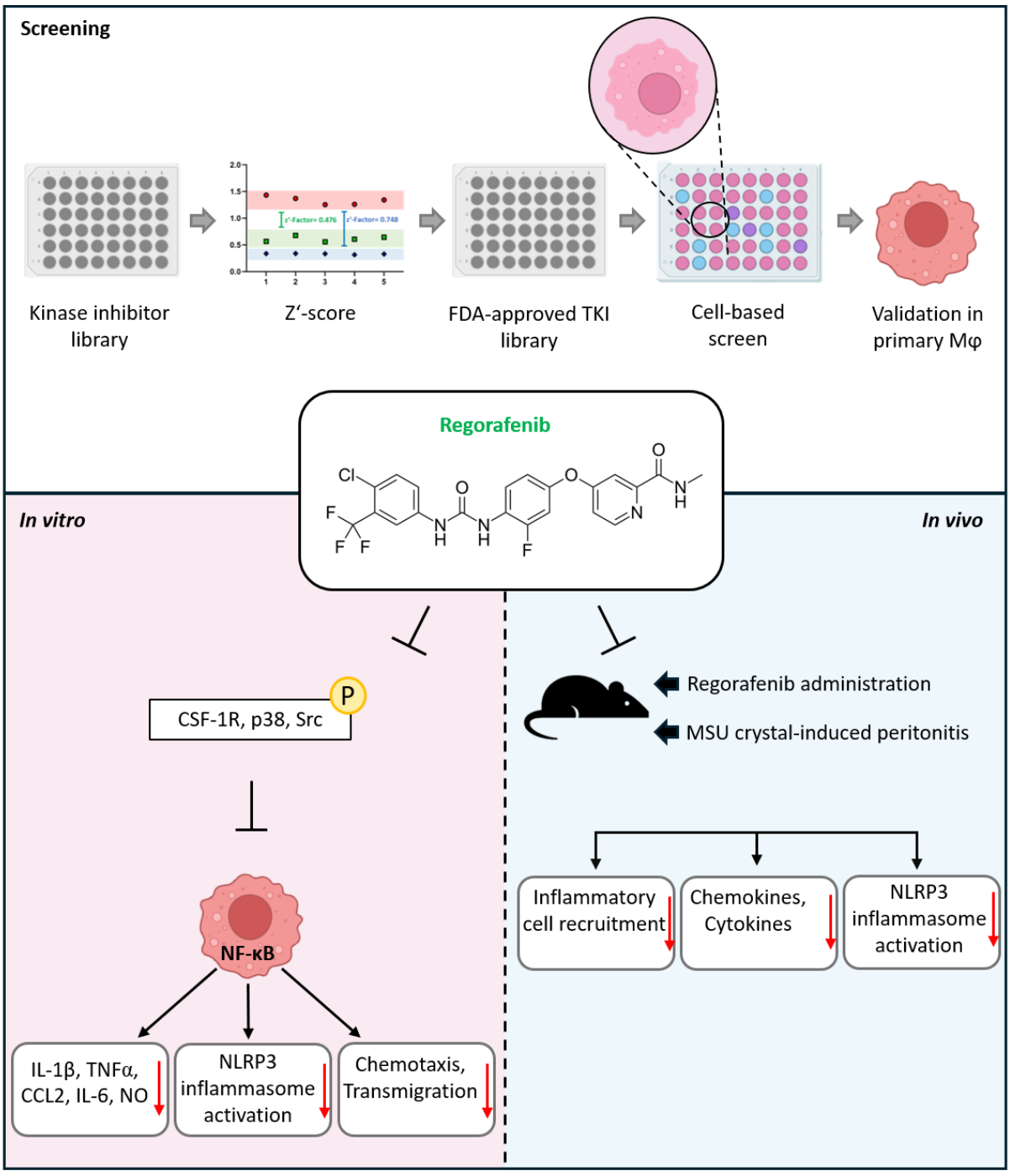
Sir William Dunn School of Pathology

Abstract

Inflammation driven by dysregulated NF-κB signaling is a defining feature of many human diseases. Significant side-effect profiles of current anti-inflammatory medicines create an unmet need for new anti-inflammatory drugs. Drug repurposing, the use of approved medicines for novel indications, is an attractive alternative to *de novo* drug development. Here, I aimed to identify FDA-approved medicines that inhibit NF-κB activation and reduce inflammation. Using NF-κB reporter cell lines, I identified regorafenib and sorafenib as NF-κB inhibitors in macrophages. Both drugs effectively reduced pro-inflammatory mediator production in primary murine and human macrophages and inhibited monosodium urate (MSU) crystal-induced NF-κB-mediated NLRP3 inflammasome priming in murine bone marrow-derived macrophages (BMDMs). In MSU crystal-induced peritonitis, a model of acute inflammation, prophylactic administration with regorafenib reduced peritoneal neutrophil influx and pro-inflammatory cytokine and chemokine production compared to vehicle at 4 h and inhibited neutrophil and monocyte recruitment at 16 h post-MSU crystal injection. Importantly, similar anti-inflammatory effects were observed after therapeutic intraperitoneal regorafenib administration. Mechanistically, regorafenib reduced inflammation *in vivo* by attenuating NF-κB-dependent NLRP3 inflammasome priming, reducing peritoneal IL-1β and ASC levels and suppressing pro-Caspase-1 production in peritoneal exudate cells. It further inhibited NF-κB-mediated MSU crystal-induced CCL2 chemokine production and retained monocytes in their splenic reservoir. In addition, regorafenib reduced circulating neutrophil numbers *in vivo* and inhibited transendothelial neutrophil migration *in vitro*.

The findings of this thesis demonstrate that a macrophage-based drug repurposing strategy can be employed to identify FDA-approved medicines with previously unreported NF-κB inhibitory and anti-inflammatory properties *in vitro* and *in vivo*.

Graphical Abstract



Acknowledgements

I would like to thank the following people, without whom I would not have been able to complete this thesis, and without whom I would not have made it through my DPhil.

First, I am deeply thankful to my supervisor Professor David Greaves, whose insight and knowledge into the project steered me through this research. Thank you for allowing me to work in your lab over the past four years and for your help in the PSB, even if it meant an early start to the day. My sincere thanks also go to Professor Asif Iqbal and his lab members Dr. Jenefa Begum and Areeba Fatima. Thank you for allowing me to work in Birmingham, for the warm welcome to the lab and your help with completing my experiments (sorry for all the extra work!).

I would like to express my appreciation to the Medical Research Council, Magdalen College and the Dunn School as they provided me with funding for my research and academic travels.

I am particularly grateful to the Dunn School staff, who supported me throughout my journey and helped me with guidance and training. Thank you, Lucinda Risius and Professor Anton van der Merwe, for always having an open ear. Thank you to the workshop team who helped us move labs twice (and even went through the rubble to rescue our western blot tank). To Bobby and Vasiliki- thank you for training and advising me on my flow cytometry experiments. Special thanks to Linda Randall and Nicky Hamp from the PSB for your help with documents, and hands on-help with my animal experiments. I am grateful for the chance to do my DPhil at such a welcoming and supportive department, which made working in Oxford such a fun, enriching and social experience, even through a global pandemic and the collapse of our lab ceiling.

Next, I would like to thank my DPhil viva examiners Professor Chris O'Callaghan and Professor Jean-Michel Sallenave for making the viva as enjoyable as possible. Thank you for your insights, advice and feedback.

I would also like to thank Professor Siamon Gordon. It was a privilege to work with you. Thank you for sharing your vast macrophage knowledge and historical insights with me and for mentoring me throughout my DPhil.

Thank you to Prof. Michael Ehrmann for giving me the opportunity to work in your lab for encouraging me to apply to Oxford. And thank you to Dr. Melisa Merdanovic for the supervision and training. I would not have gotten into this PhD programme otherwise.

To all past and present members of the Greaves lab- including honorary members: Agata, Laura, Vincent, Josh, Gareth, Conan, Ada, Lili and Isobel- thank you for creating such a friendly atmosphere both in and outside the lab. It has been great to work with you, share cake or wine and cheese, go to lab formals or punt around the River Cherwell.

Dr. Gareth Hartley, my time in Oxford would have been a lot less enjoyable without you. Thank you for being my emotional support, chauffeur and proofreader. Thank you for bearing with me during my ups and downs.

Finally, I would like to thank my family, especially my parents: Thank you for supporting me throughout my entire academic journey, being my support hotline, encouraging me after failed experiments and taking me on holiday to relax. I could not have done it without you.

Abbreviations

AGM	Aorta-gonad-mesonephros
AI	Artificial intelligence
AIM2	Absent in melanoma 2
ALR	AIM2-like receptors
ALT	Alanine aminotransferase
Arg-1	Arginase 1
AP-1	Activator protein 1
APC	Antigen-presenting cell
ASC	Apoptosis-associated speck-like protein containing a CARD
AST	Aspartate aminotransferase
ATP	Adenosine triphosphate
AUC	Area under curve
BMDM	Bone marrow-derived macrophage
BSA	Bovine serum albumin
BTK	Bruton's tyrosine kinase
CD	Cluster of differentiation
CI	Cell index
CLR	C-type lectin receptor
CO_2	Carbon dioxide
CREB	cAMP response element binding protein
CSF-1	Colony stimulating factor 1
CSF-1R	Colony stimulating factor 1 receptor
CV	Cardiovascular

DAMP	Damage-associated molecular pattern
DAPI	4′,6-diamidino-2-phenylindole
DC	Dendritic cell
DMARD	Disease-modifying antirheumatic drug
DMEM	Dulbecco’s modified eagle media
DMSO	Dimethyl sulfoxide
DNA	Deoxyribonucleic acid
ds	Double-stranded
EC	Endothelial cell
EDTA	Ethylenediaminetetraacetic acid
EGFR	Endothelial growth factor receptor
FACS	Fluorescence-activated cell sorting
FBS	Fetal bovine serum
FDA	Federal drug association
FLT3	Fms-related receptor tyrosine kinase 3
FLS	Fibroblast-like synoviocytes
FMO	Fluorescence minus one
FSC	Forward scatter
GC	Glucocorticoid
GI	Gastrointestinal
GMP	Granulocyte-macrophage progenitor
GPCR	G-protein coupled receptor
GR	Glucocorticoid receptor
h	Hour
HCC	Hepatocellular carcinoma
HDBEC	Human Dermal Blood Endothelial Cell
HEPES	4-(2-hydroxyethyl)-1-piperazineethanesulfonic acid
HKLM	Heat-killed Listeria monocytogenes

HSC	Haematopoietic stem cell
HUVECs	Human Umbilical Vein Endothelial Cells
IBD	Inflammatory bowel disease
IC	Immune complex
IFN	Interferon
IKK	Inhibitor of κB kinase
IL	Interleukin
IRF	Interferon-regulatory factor
ISG	Interferon stimulated gene
iNOS	Inducible nitric oxide synthase
i.p.	Intraperitoneal
IκB	Inhibitor of κB
JAK	Janus kinase
kDa	Kilodalton
LDH	Lactate dehydrogenase
LPS	Lipopolysaccharide
mAB	Monoclonal antibody
MDM	Monocyte-derived macrophage
MDSC	Myeloid-derived suppressor cell
MHC	Major histocompatibility complex
MPO	Myeloperoxidase
MS	Multiple sclerosis
MSU	Monosodium urate crystal
NF-κB	Nuclear factor kappa B
NK	Natural killer cell
NLR	NOD-like receptors
NLRP3	NLR family pyrin domain containing 3

NO	Nitric oxide
NOD	Nucleotide oligomerization domain
NSAID	Non-steroidal anti-inflammatory drug
OD	Optical Density
oxLDL	Oxidized low density lipoprotein
OXPHOS	Oxidative phosphorylation
P/S	Penicillin plus streptomycin
PAMP	Pathogen-associated molecular pattern
PBS	Phosphate-buffered saline
PCR	Polymerase chain reaction
PDGFR	Platelet-derived growth factor receptor
PECs	Peritoneal exudate cells
PFA	Paraformaldehyde
PMA	Phorbol 12-myristate 13-acetate
PMN	Polymorphonuclear neutrophil
Poly(I:C)	Polyinosinic:polycytidylic acid
PRR	Pattern recognition receptor
RA	Rheumatoid arthritis
RANTES	Regulated on activation, normal T cell expressed and secreted
RIG-I	Retinoic acid inducible gene I)
RLR	RIG-I-like receptor
RNA	Ribonucleic acid
ROS	Reactive oxygen species
ROCK	Rho-associated protein kinase
RPMI	Roswell Park Memorial Institute
RT	Room temperature
RT-PCR	Reverse transcription PCR
RTK	Receptor tyrosine kinase

SEAP	Secreted alkaline phosphatase
SFK	Src family kinase
SLE	Systemic lupus erythematosus
ss	Single stranded
SSC	Side scatter
STING	Stimulator of interferon genes
TBS	Tris-buffered saline
TGF-β	Transforming Growth Factor β
Th	T helper
TK	Tyrosine kinase
TKI	Tyrosine kinase inhibitor
TLR	Toll like receptor
TNFα	Tumor necrosis factor α
VEGFR	Vascular endothelial growth factor receptor
ZIP	Zymosan-induced peritonitis

Contents

Chapter 1: Introduction 1
1.1 Inflammation 1
1.1.1 Historical overview 1
1.1.2 Acute and chronic inflammation 2
1.2 The innate immune system 4
1.2.1 Neutrophils 4
1.2.2 Monocytes 6
1.2.2.1 Monocyte and neutrophil transendothelial migration in inflammation 7
1.2.2.2 Leukocyte chemotaxis 9
1.2.2.21 Neutrophil and monocyte chemotaxis 10
1.2.2.2.2 Macrophage chemotaxis 12
1.2.3 Eosinophils 13
1.2.4 Basophils and Mast cells 14
1.2.6 Dendritic cells 15
1.3. Macrophages 16
1.3.1 Embryonic and monocyte-derived macrophage populations 16
1.3.2 Macrophage phenotypes 18
1.3.3 Macrophage mediators of inflammation 21
1.3.3.1 Cytokines 21
1.3.3.2 Chemokines 22
1.3.3.3 Nitric Oxide 23
1.3.4 Macrophages in inflammatory pathologies 23
1.3.4.1 Macrophages in gout 24
1.3.4.2 Macrophages in Rheumatoid Arthritis 26
1.4 Inflammatory signaling pathways 28
1.4.1 Extracellular and intracellular pathogen recognition 28
1.4.2 TLR4 signaling 31
1.4.2 Inflammatory signaling pathways 33
1.4.2.1 NF-κB signaling 33
1.4.2.2 The NLRP3 inflammasome 35
1.5 Tyrosine kinase signaling in inflammation 37

1.5.1 VEGFR 38
1.5.2 PDGFR 39
1.5.3 CSF-1R 40
1.5.4 Src family kinases 41
1.5.5 BTK 43
1.6 Current anti-inflammatory medicines 44
1.6.1 NSAIDs 44
1.6.2 Glucocorticoids 45
1.6.3 DMARDs 47
1.6.5 Limitations of current anti-inflammatory medicines 48
1.7 Original hypothesis and experimental aims 50
Chapter 2: Materials and Methods 52
2.1 Reagents 52
2.2 Animal experiments 53
2.2.1 Animal husbandry 53
2.2.2 MSU crystal-induced peritonitis (prophylactic model) 53
2.2.3 MSU crystal-induced peritonitis (therapeutic model) 54
2.3 Cell culture 55
2.3.1 RAW-Blue macrophage reporter cells 55
2.3.2 THP1-Dual monocyte reporter cells 55
2.3.3 THP1-ASC-GFP monocyte reporter cells 55
2.3.4 Murine bone marrow-derived macrophages 56
2.3.5 Human monocytes and neutrophils 57
2.3.6 Primary human dermal blood endothelial cells 58
2.4 NF-κB-SEAP Reporter Assay 58
2.5 Cell viability assays 58
2.6 RT-qPCR 59
2.7 Cytokine quantification 59
2.8 Western Blotting 60
2.9 Flow cytometry 61
2.10 xCELLigence Chemotaxis assay 62
2.11 Static migration assay 63
2.12 Imagestream 64
2.13 Inflammasome activation and priming 65
2.14 Nitric oxide quantification 65
2.15 Cytospin and staining 65

2.16 Statistical analysis 65

Chapter 3: Screen of FDA-approved medicines in NF-κB reporter assay identifies drug repurposing candidates with anti-inflammatory properties 66

3.1 Introduction 66

3.1.1 Drug repurposing vs. *de novo* drug development 66

3.1.2 Experimental drug repurposing strategies 67

3.1.2.1 Target-based drug repurposing strategies 68

3.1.2.2 In vitro phenotypic drug repurposing strategies 69

3.1.2.3 In vivo phenotypic drug repurposing strategies 70

3.1.2.4 Organoid-based phenotypic drug repurposing strategies 71

3.1.3 Repurposing NF-κB inhibitors to treat inflammation 71

3.2 Rationale and experimental aims of the chapter 74

3.3 Results: 75

3.3.1 Screen of tyrosine kinase inhibitor library for NF-κB inhibition in RAW-Blue and THP1-Dual reporter cell lines 75

3.3.2 Screen of FDA-approved tyrosine kinase inhibitors for NF-κB inhibition in RAW-Blue and THP1-Dual reporter cell lines 83

3.3.3 Validation of the anti-inflammatory activity of repurposing candidates in primary murine macrophages 90

3.3.4 Anti-inflammatory activity of regorafenib and sorafenib on human MDMs 93

3.3.5 Effect of regorafenib and sorafenib on NF-κB signaling in macrophages 94

3.3.6 Effect of regorafenib and sorafenib on tyrosine kinase phosphorylation in macrophages 96

3.3.7 Effect of regorafenib on macrophage polarization 98

3.3.8 Effect of regorafenib and sorafenib on TLR4 surface expression 100

3.3.9 Effect of regorafenib and sorafenib on DAMP- and PAMP-induced inflammation in cell lines and primary macrophages 103

3.4 Discussion 106

3.4.1 Cell-based reporter screens for anti-NF-κB and anti-inflammatory activity 107

3.4.2 Identification of regorafenib and sorafenib as inhibitors of macrophage NF-κB 110

3.4.2.1 Novel anti-inflammatory effects of regorafenib and sorafenib in macrophage inflammation 112

3.4.2.2 Regorafenib affects primary murine macrophage polarization 114

3.4.3.3 Regorafenib and sorafenib inhibit NF-κB-driven macrophage inflammation in response to a wide variety of stimuli 115

3.4.3 Limitations of the studies reported in this chapter 117

3.4.4 Summary 117

Chapter 4: Regorafenib reduces acute inflammation in MSU crystal-induced peritonitis by inhibiting NF-κB-dependent NLRP3 inflammasome priming 119

4.1 Introduction 119
4.1.1 Mouse models of acute inflammation 119
4.1.1.1 Experimental endotoxemia 119
4.1.1.2 Subcutaneous air pouch models 119
4.1.1.3 Peritonitis models 120
4.1.1.3.1 MSU crystal-induced peritonitis 120
4.1.2 Repurposing tyrosine kinase inhibitors in acute inflammation 124
4.1.3 MSU crystal-induced peritonitis in drug repurposing studies 125
4.2 Original hypothesis and experimental aims of this chapter 126
4.3 Results 127
4.3.1 Effect of regorafenib and sorafenib on NLRP3 inflammasome activation in macrophages 127
4.3.2 Selection of an appropriate *in vivo* model of acute inflammation 132
4.3.3 Effect of prophylactic oral regorafenib and sorafenib administration on MSU crystal-induced peritonitis at 4 h 135
4.3.3.1 Effect on peritoneal cell recruitment 137
4.3.3.2 Effect on peritoneal cytokine and chemokine production 137
4.3.3.3 Effect on PEC cytokine gene expression 139
4.3.3.4 Effect on NLRP3 inflammasome markers in the peritoneum 140
4.3.4 Effect of prophylactic oral regorafenib administration on MSU crystal-induced peritonitis at 16 h 140
4.3.4.1 Effect on peritoneal cell recruitment 141
4.3.5 Effect of prophylactic and therapeutic oral regorafenib administration on MSU crystal-induced peritonitis at 16 h 142
4.3.5.1 Effect on peritoneal cell recruitment 142
4.3.5.2 Effect on peritoneal cytokine and chemokine production 143
4.3.5.3 Effect on NLRP3 inflammasome activation in PECs 143
4.3.6 Effect of prophylactic oral regorafenib administration on MSU crystal-induced peritonitis in female mice at 4 h 145
4.3.6.1 Effect on peritoneal cell recruitment 145
4.3.6.2 Effect on peritoneal cytokine and chemokine production 146
4.3.6.3 Effect on NLRP3 inflammasome activation in the peritoneum 146
4.3.7 Comparison of effects of regorafenib and NSAID indomethacin on MSU-crystal-induced peritonitis at 16 h 148
4.3.7.1 Effects on peritoneal cell recruitment 148
4.3.7.2 Effects on peritoneal cytokine and chemokine production 149
4.3.7.3 Effects on NF-κB and NLRP3 inflammasome activation in PECs 149
4.3.7.4 Toxicity of oral regorafenib and indomethacin administration 151

4.3.7.5 Gastrointestinal toxicity of indomethacin compared to regorafenib 152
4.3.8 Effect of therapeutic oral regorafenib administration on MSU crystal-induced peritonitis at 16 h 153
4.3.8.1 Effect of peritoneal cell recruitment 153
4.3.8.2 Effect on peritoneal cytokine and chemokine production 154
4.3.9 Effect of therapeutic intraperitoneal regorafenib administration on MSU crystal-induced peritonitis at 16 h 155
4.3.9.1 Effect on peritoneal cell recruitment 155
4.3.9.2 Effect on peritoneal cytokine and chemokine production 155
4.3.10 Identification of a non-inflammatory vehicle for intraperitoneal drug delivery 157
4.3.11 Effect of therapeutic intraperitoneal regorafenib administration on MSU crystal-induced peritonitis at 16 h (new vehicle) 159
4.3.11.1 Effect on peritoneal cell recruitment 159
4.3.11.2 Effect on peritoneal cytokine and chemokine production 160
4.4 Discussion 161
4.4.1 Regorafenib and sorafenib reduce inflammation in a mouse model of acute inflammation 161
4.4.2 *In vivo* mechanism of regorafenib in acute inflammation 162
4.4.4 Targeting NF-κB and the NLRP3 inflammasome in acute inflammation 163
4.4.5 TKIs - a new class of anti-inflammatory medicines? 165
4.4.6 Challenges of TKIs as therapeutics for inflammatory diseases 168
4.4.7 Limitations of the studies reported in this chapter 174
4.4.8 Summary 179
Chapter 5: Regorafenib modulates leukocyte mobilization, transendothelial migration and chemotaxis 180
5.1 Introduction 180
5.1.1 Assays to measure immune cell adhesion, transendothelial migration and chemotaxis 180
5.1.1.1 Chemotaxis assays 181
5.1.1.2 Adhesion and transmigration assays 186
5.1.2 Targeting leukocyte recruitment in inflammation 188
5.1.2.1 Targeting tyrosine kinases in leukocyte adhesion and chemotaxis 188
5.1.2.2 Targeting leukocyte chemokines in inflammation 191
5.1.3 The role of NF-κB in leukocyte adhesion, transendothelial migration and chemotaxis in inflammation 193
5.1.4 Drug repurposing to target leukocyte adhesion, transendothelial migration and chemotaxis 194
5.1.4.1 Targeting monocyte/neutrophil adhesion and transendothelial migration 194
5.1.4.2 Targeting monocyte/neutrophil chemotaxis 196

5.2 Original hypothesis and experimental aims of the chapter 198
5.3 Results 199
5.3.1 Effect of regorafenib and sorafenib on macrophage and monocyte chemotaxis . 199
5.3.1.1 C5a-elicited macrophage chemotaxis 200
5.3.3.2 CSF-1-elicited macrophage chemotaxis 201
5.3.3.3 CCL2-elicited monocyte chemotaxis 203
5.3.2 Effect of regorafenib on human primary neutrophil and monocyte endothelial cell adhesion 204
5.3.2.1 Effect on ECs during monocyte adhesion and migration 205
5.3.2.2 Effect on monocytes during EC adhesion and migration 207
5.3.2.3 Effect on ECs during neutrophil adhesion and migration 209
5.3.2.4 Effect on neutrophils during EC adhesion and migration 210
5.3.3 Effect of regorafenib on myeloid cell mobilization *in vivo* 212
5.4 Discussion 214
5.4.1 Targeting tyrosine kinases to modulate leukocyte adhesion, transendothelial migration and chemotaxis 215
5.4.2.2 Targeting tyrosine kinases to suppress leukocyte mobilization in acute inflammation 217
5.5 Limitations of this study 218
5.6 Summary 220
Chapter 6: Conclusions and future work 221
6.1 Summary and discussion of key findings 221
6.2 The future of TKIs regorafenib and sorafenib as therapeutics for inflammatory diseases 223
References 232
Appendices 281
Appendix 1. Publications 281
Appendix 2. IRF pathway activation assessment in THP1-Dual cells stimulated with Poly(I:C) and Poly(I:C)/LyoVec 281
Appendix 3. Project Contributions 282

List of Figures

Fig. 1. 1 Acute and chronic inflammatory responses 3
Fig. 1. 2 Transendothelial leukocyte migration 9
Fig. 1. 3 Chemokine signaling through GPCRs in leukocytes 11
Fig. 1. 4 The role of macrophages in joint homeostasis and gouty joint inflammation. 25
Fig. 1. 5 TLR signaling in inflammation 31
Fig. 1. 6 The canonical and non-canonical NF-κB signaling pathways 34
Fig. 1. 7 Overview of inflammasomes and their activators 35
Fig. 1. 8 Priming and activation of the NLRP3 inflammasome 37
Fig. 1. 9 Tyrosine kinase signaling in inflammation 39
Fig. 2. 1 Characterization of day 7 BMDMs by flow cytometry 57
Fig. 2. 2 Quantification of leukocyte adhesion, activation and migration in static migration assays 63
Fig. 3. 1: Drug repurposing approaches 67
Fig. 3. 2 Reproducible and reliable cell-based screen to identify compounds with unknown NF-κB inhibitory activity 75
Fig. 3. 3 Drug repurposing screen identifies kinase inhibitors with unknown NF-κB inhibitory activity 80
Fig. 3. 4 Tool compound screen in NF-κB reporter assay identifies potential drug repurposing targets 82
Fig. 3. 5 Screen of FDA-approved medicines in NF-κB reporter assay identifies drug repurposing candidates 88
Fig. 3. 6 Regorafenib and sorafenib reduce inflammatory gene expression in primary murine macrophages 91
Fig. 3. 7 Regorafenib and sorafenib reduce inflammatory mediator production in primary murine macrophages 92
Fig. 3. 8 Regorafenib and sorafenib reduce inflammation in human macrophages 93
Fig. 3. 9 Regorafenib and sorafenib reduce NF-κB signaling in macrophages 95
Fig. 3. 10 Regorafenib and sorafenib reduce pro-inflammatory signaling in macrophages 97
Fig. 3. 11 Regorafenib and sorafenib modulate macrophage polarization in vitro 99
Fig. 3. 12 Regorafenib and sorafenib do not affect TLR2/4 expression or TLR4 internalization in BMDMs 102
Fig. 3. 13 Regorafenib and sorafenib reduce macrophage inflammation in response to a wide variety of stimuli 104
Fig. 3. 14 NF-κB activation by TLR and TNF-R signaling pathways in innate immune cells 110
Fig. 3. 15 Chemical structures of sorafenib and regorafenib 115
Fig. 4. 1 Initiation of inflammation in MSU crystal-induced peritonitis 123
Fig. 4. 2 Regorafenib and sorafenib inhibit NF-κB-mediated NLRP3 inflammasome priming in macrophages 128
Fig. 4. 3 Regorafenib reduces NF-κB activation and ASC speck formation in macrophages 130
Fig. 4. 4 Regorafenib and sorafenib inhibit crystal-induced NLRP3 inflammasome activation in macrophages 131
Fig. 4. 5 Design of MSU crystal-induced peritonitis study 134
Fig. 4. 6 Intraperitoneal MSU crystal injection causes acute local inflammation 136
Fig. 4. 7 Prophylactic regorafenib or sorafenib administration reduces inflammation in MSU crystal-induced peritonitis at 4 h 138

Fig. 4. 8 Prophylactic regorafenib administration does not affect inflammation in MSU crystal-induced peritonitis at 16 h 141
Fig. 4. 9 Prophylactic and therapeutic regorafenib administration reduces inflammation in MSU crystal-induced peritonitis at 16 h 144
Fig. 4. 10 Prophylactic regorafenib treatment reduces inflammation in MSU crystal-induced peritonitis in female mice 147
Fig. 4. 11 Regorafenib and indomethacin both have anti-inflammatory effects in MSU crystal-induced peritonitis 150
Fig. 4. 12 Liver and gastrointestinal toxicity of regorafenib and indomethacin in MSU crystal-induced peritonitis 151
Fig. 4. 13 Therapeutic oral regorafenib administration has mild anti-inflammatory effects in MSU crystal-induced peritonitis 154
Fig. 4. 14 Therapeutic i.p. regorafenib administration has mild anti-inflammatory effects in MSU crystal-induced peritonitis 156
Fig. 4. 15 Vehicle optimization for i.p. regorafenib delivery 158
Fig. 4. 16 Therapeutic regorafenib administration reduces inflammation in MSU crystal-induced peritonitis (new vehicle) 160
Fig. 4. 17 Sorafenib in complex with its target p38α 171
Fig. 5. 1 Chemotaxis assays 1 182
Fig. 5. 2 Chemotaxis assays 2 185
Fig. 5. 3 Adhesion and transmigration assays 187
Fig. 5. 4 Tyrosine kinases in leukocyte extravasation and chemotaxis 189
Fig. 5. 5 TKI inhibition by regorafenib or sorafenib does not affect BMDM chemotaxis towards C5a 200
Fig. 5. 6 TKI inhibition by regorafenib or sorafenib reduces BMDM chemotaxis towards CSF-1 202
Fig. 5. 7 TKI inhibition by regorafenib reduces THP1-Dual monocyte chemotaxis towards CCL2 204
Fig. 5. 8 Regorafenib EC pre-treatment does not affect monocyte adhesion or transmigration 206
Fig. 5. 9 Regorafenib monocyte pre-treatment does not affect adhesion or endothelial transmigration. 208
Fig. 5. 10 Regorafenib EC pre-treatment reduces neutrophil transmigration 209
Fig. 5. 11 Regorafenib neutrophil pre-treatment reduces endothelial transmigration 211
Fig. 5. 12 Regorafenib retains monocytes in the spleen and reduces circulating neutrophil numbers 213
Fig. 5. 13 Tyrosine kinases in leukocyte extravasation and chemotaxis 216

List of Tables

Table 1. 1 M1 and M2 macrophage properties 20
Table 1. 2 Features and ligands of Toll-like receptors ..... **Error! Bookmark not defined.**
Table 1. 3 Adverse effects of current anti-inflammatory medicines **Error! Bookmark not defined.**
Table 2. 1 List of mouse primers ..... **Error! Bookmark not defined.**
Table 2. 2 List of primary antibodies used in this study ..... **Error! Bookmark not defined.**
Table 2. 3 List of fluorophores used in this study ..... **Error! Bookmark not defined.**
Table 3. 1 Comparison of time, success rate and cost of drug repurposing versus de novo drug development strategies ..... **Error! Bookmark not defined.**
Table 3. 2 Drug repurposing candidates for inflammatory diseases targeting NF-κB signaling. ..... **Error! Bookmark not defined.**
Table 3. 3 Compounds with anti-inflammatory activity identified with NF-κB reporter assay ..... **Error! Bookmark not defined.**
Table 3. 4 Drugs with anti-inflammatory effect identified with NF-κB reporter assay ..... **Error! Bookmark not defined.**
Table 3. 5: IC_{50} values of inhibition of NF-κB activity in Quanti-Blue assay in reporter cell lines ..... **Error! Bookmark not defined.**
Table 3. 6 IC_{50} values for inhibition of pro-inflammatory mediator production in BMDMs **Error! Bookmark not defined.**
Table 3.7 IC_{50} values of NF-κB inhibition in THP1-Dual monocytes stimulated with different PAMPs and DAMPs ..... **Error! Bookmark not defined.**
Table 3. 8 Target profiles of regorafenib and sorafenib ..... **Error! Bookmark not defined.**
Table 4. 1 Reference values for liver toxicity and cell death markers in the serum ..... **Error! Bookmark not defined.**
Table 4. 2 NLRP3 inflammasome inhibitors in clinical trials .... **Error! Bookmark not defined.**

Chapter 1: Introduction

1.1 Inflammation

1.1.1 Historical overview

Inflammation is defined as the immune response which protects the body from tissue injury or infection [1]. It is an essential process to ensure the survival of organisms as demonstrated by the presence of defense systems across species, ranging from bacteria, *Drosophila*, the Atlantic horseshoe crab and dinosaurs, with signs of inflammatory responses in their fossilized bones [1-4]. Inflammation has been described by many ancient cultures, including the Egyptians and the Greeks, who recognized inflammation as the first step of wound repair in response to tissue injury. Roman encyclopedist Aulus Cornelius Celsus was the first to describe redness, swelling, heat and pain as four of the main symptoms of inflammation. Around 150 years later, physician Galen of Pergamon added impaired function as a fifth symptom [5, 6]. In his 1893 lectures, Elie Metchnikoff described mononuclear leukocyte and neutrophil chemotaxis, macrophage amoeboid migration and their phagocytosis of foreign stimuli or organisms [7, 8]. He had first observed phagocyte recruitment to the site of tissue injury when he introduced a rose thorn into the tissue of starfish larvae [9].

Metchnikoff viewed inflammation in the context of harmony and disharmony: while physiological inflammation aims to establish harmony in organisms with inherent disharmony, pathological inflammation occurs in response to infection or tissue injury and involves phagocytes that try to re-establish harmony [10]. In 1929, Walter Cannon coined the term “homeostasis” (from Greek *homoios*= similar and *stasis*= standing still) to describe this phenomenon, emphasizing the dynamic properties of the term [11]. He wrote: “The coordinated physiological reactions which maintain most of the steady states in the body are so complex, and are so peculiar to the living organism, that it has been suggested (Cannon, 1926) that a specific designation for these states be employed – homeostasis” [11]. Homeostasis is therefore the ability of organisms to self-regulate their environment to maintain a steady state and prevent drastic disturbances, such as inflammation during cell stress, tissue

injury or infection [12, 13]. Therefore, an inflammatory response aims to eliminate irritants, initiate tissue repair and to re-establish tissue homeostasis.

1.1.2 Acute and chronic inflammation

Upon stimulation by tissue injury or pathogens, acute inflammation initiation is mediated by resident immune cells such as macrophages (Fig. 1.1A). This results in the production of pro-inflammatory mediators like cytokines and chemokines, which activate pro-inflammatory signaling pathways. As a consequence, the recruitment of granulocytes and mononuclear phagocytes from the blood is initiated [14]. Infiltrating leukocytes, including neutrophils, take up and eliminate pathogens and tissue debris [15]. Once the inflammatory stimulus is removed, the resolution phase of inflammation is initiated, which describes the period between peak inflammatory cell infiltration and the restoration of functional homeostasis [14, 16].

Inflammation resolution is an active process, during which pro-inflammatory signaling is dampened, the synthesis of pro-inflammatory mediators is halted and remaining mediators are actively catabolized to prevent further leukocyte recruitment [16-18]. Recruited leukocytes can re-enter circulation or exit through the lymphatic drainage system but the majority of PMNs undergo apoptosis and are cleared by macrophages, which mediate tissue repair [14, 16, 17].

In the final phase of post-resolution, damaged tissue is repaired and adapted homeostasis is established. The number of memory T and B cells increases and myeloid-derived suppressor cells (MDSCs), natural killer (NK) cells as well as monocyte-derived dendritic cells (DCs) can be detected [14, 19, 20]. Monocyte-derived macrophages can persist in the tissue and tissue-resident macrophages, which leave the inflamed tissue during the onset of inflammation (macrophage disappearance reaction), re-appear [14, 16, 21].

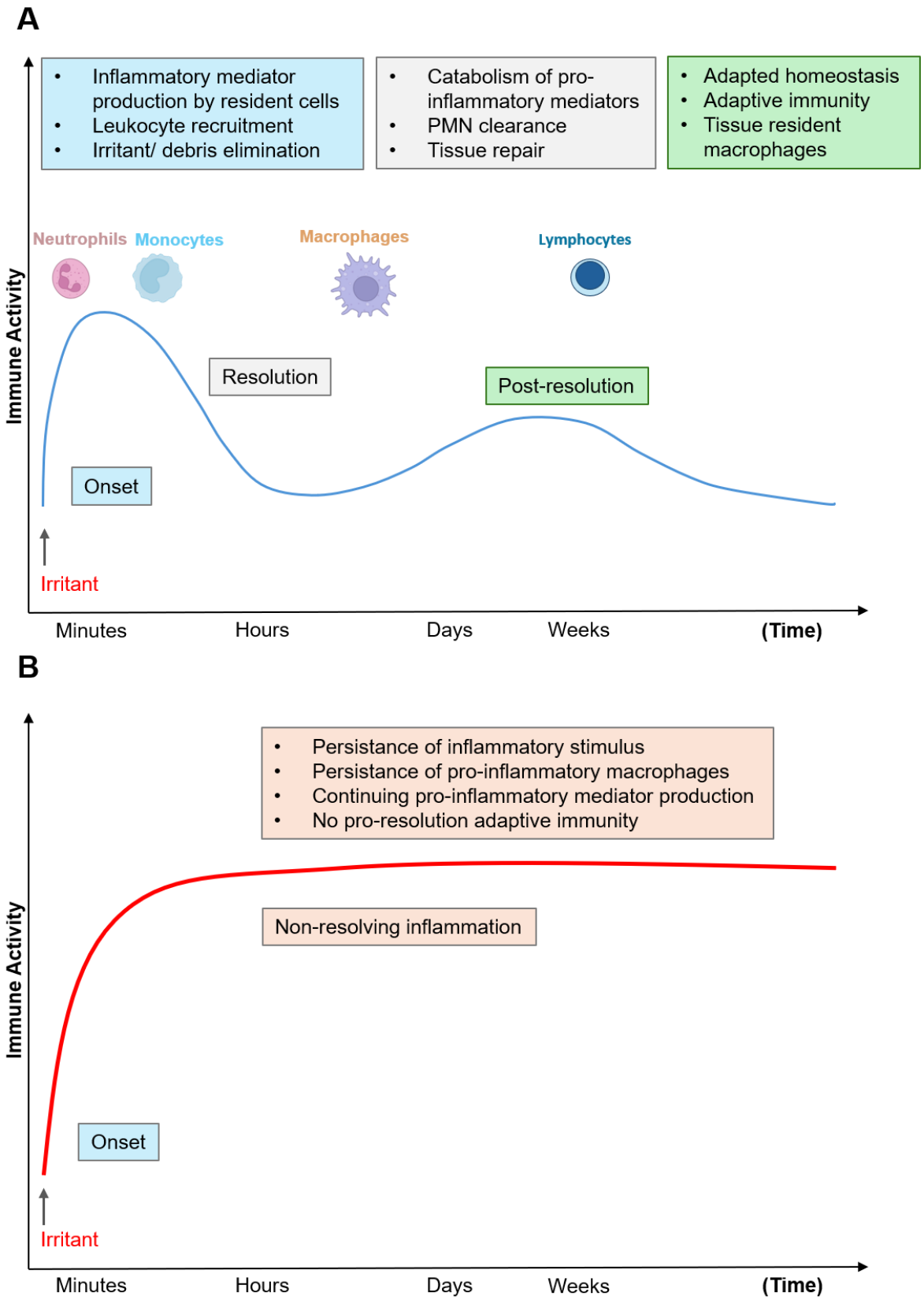


Fig. 1. 1 Acute and chronic inflammatory responses. Acute inflammation is initiated by an irritant, which is recognized by tissue resident cells. These cells mediate inflammation onset by producing pro-inflammatory mediators and recruit leukocytes to clear the inflammatory stimulus. Following the removal of the irritant, the active resolution phase is initiated, during which macrophages produce pro-resolution mediators and pro-inflammatory mediators are catabolized. PMNs undergo apoptosis or re-enter circulation and the tissue is repaired. During post-resolution, tissue resident macrophage repopulate the tissue and adapted homeostasis is established. Adapted from [14, 16].

When the magnitude or duration of inflammation is dysregulated or the inflammatory stimulus cannot be cleared, resolution is not initiated, resulting in pathological inflammation associated with chronic inflammatory diseases such as rheumatoid arthritis (RA) or systemic lupus erythematosus (SLE) [14, 16]. Here, macrophages continue to produce pro-inflammatory mediators, which recruit more leukocytes, thus exacerbating inflammation (Fig.1.1B). As a consequence, inflammation persists as tissue repair and homeostasis cannot be established and tissue damage occurs.

1.2 The innate immune system

The innate immune system constitutes the first line of defense which is encountered by pathogens. Innate immune cells recognize pathogen-associated molecular patterns (PAMPs), which are conserved components of pathogens, or endogenous damage-associated molecular patterns (DAMPs) through pattern recognition receptors (PRRs) [22]. Examples of PAMPs are lipopolysaccharides (LPS) of the bacterial cell wall or zymosan from yeast cell wall, while DAMPs include uric acid or extracellular ATP [23].

Innate immune cells express five types of PRRs based on their protein domain homology. They include Toll-like receptors (TLRs) and C-type lectin receptors (CLRs), which are bound to the cell surface or endolysosomal compartments, as well as cytosolic nucleotide oligomerization domain (NOD)-like receptors (NLRs), retinoic acid-inducible gene-I (RIG-I)-like receptors (RLRs) and absent in melanoma-2 (AIM2)-like receptors (ALRs) [24]. The receptors recognize their ligand through a ligand recognition domain and subsequently recruit adaptor molecules through their effector domain, initiating inflammatory downstream signaling pathways. This results in the production of pro-inflammatory cytokines, chemokines, adhesion molecules and growth factors and consequently leads to the activation and recruitment of additional immune cells [25].

1.2.1 Neutrophils

Neutrophils, which are also referred to as polymorphonuclear neutrophils (PMNs) due to the varying structure of their nucleus, are the first leukocytes that are recruited to sites of

inflammation [15]. They are continually produced in the bone marrow at a rate of approximately 10^{11} per day and are the most abundant white blood cells in the blood, making up 50 – 70% of circulating leukocytes in the human body [26]. In the bone marrow, granulocyte-macrophage progenitors (GMPs) differentiate into pre-neutrophils, which then form immature neutrophils and subsequently mature neutrophils. Both immature and mature neutrophils can enter blood circulation and tissues during inflammation, but only mature neutrophils are released from the bone marrow during steady-state conditions [27, 28]. As neutrophils mature in the bone marrow, they contain different types of granules. GMPs contain primary/azurophilic granules (markers: MPO, CD63), while pre-neutrophils also express secondary/specific granules (markers: lactoferrin, lipocalin 2, CD66b). Tertiary/gelatinase granules (markers: gelatinase B, CD11b) as well as secretory vesicles (markers: alkaline phosphatase, albumin, CD45, Mac-1/CD11b, CD13) can be found mostly in mature neutrophils in addition to primary and secondary granules [27-29]. Ficolin-1-rich granules, a fourth granule type, have also been reported [30]. In addition to these markers, neutrophil granules also include other contents, such as microbicidal proteins, proteases and adhesion molecules [29].

Neutrophils are retained in the bone marrow through CXCR4 and are released into the blood upon initiation of CXCR2 signaling. The release process can be further enhanced by G-CSF and other mobilization chemokines, such as CXCL1, which are produced during inflammation [28]. As neutrophils are rapidly recruited during the onset of inflammation, marginated reservoirs exist not only in the bone marrow but also in the lung, spleen and liver [31].

Upon inflammatory stimulation, an initial priming stimulus, such as pro-inflammatory cytokines like TNFα and IL-1β or contact with activated endothelial cells followed by a second stimulus, consisting of PAMPs and DAMPs, growth factors or chemokines, are required for neutrophil activation [15]. Such activating chemokines are CXCL8/IL-8 (CXCL1/KC in mice), CXCL2 and CXCL5 (LIX), which additionally induce endothelial adhesion and create a gradient, directing neutrophil chemotaxis [15, 32]. After adhesion and intra-vascular migration, neutrophils undergo transendothelial migration to reach the affected tissue [33]. Once activated,

neutrophils eliminate the inflammatory stimulus through phagocytosis, the release of cytotoxic granular contents, the production of reactive oxygen species (ROS) or by ejecting their DNA in the form of extracellular traps (NETs) [32]. They also secrete cytokines and chemokines to amplify the inflammatory response [26]. Once “pioneer” neutrophils have reached the site of inflammation for example, they produce swarm-initiating molecules including LTB4, IL-8 and CXCL2 to promote activation and recruitment of other neutrophils in a process called neutrophil swarming [34, 35].

To limit tissue damage, neutrophils have short life spans and have limited ability for protein synthesis after maturation. However, studies have shown that their life span can be extended through cytokines such as TNFα, IL-6 or IL-1β as well as through PAMPs like LPS [36-39].

After the removal of the inflammatory insult, neutrophils secrete monocyte chemoattractant CCL2. Additionally, they produce “find me” signals upon initiation of apoptosis to recruit monocytes to promote their phagocytosis and the clearance of cell debris [15]. Through reverse migration, neutrophils are also able to leave the site of inflammation and re-enter blood vessels [40]. While neutropenia is associated with impaired immune responses and increased risk of infection [41], neutrophilia is linked to chronic inflammatory conditions like obesity, rheumatic diseases or inflammatory bowel disease (IBD) [42].

1.2.2 Monocytes

Monocytes were named by Pappenheim in 1910 [43]. They originate from progenitors in the bone marrow and are recruited to the site of inflammation from reservoirs in the spleen, lungs or bone marrow [44]. In mice, circulating monocytes can be divided into two subsets: classical Ly6C^{hi} monocytes have high surface levels of CCR2 and this chemokine receptor mediates their rapid recruitment to sites of inflammation, where they can differentiate into inflammatory macrophages or dendritic cells [44, 45]. In addition, they were shown to give rise to intestinal macrophages [44]. Non-classical Ly6C^{lo} monocytes express low levels of CCR2 but high levels of CX_3CR1 [45]. They have a patrolling function in small blood vessels and upon recruitment to inflammatory sites, they may differentiate into pro-resolving macrophages and mediate

tissue repair [45, 46]. CCL2 production is initiated rapidly at sites of inflammation and is essential for Ly6C^{hi} monocyte recruitment from the bone marrow [47]. In humans, CD14^{+}/CD16^{-} monocytes are the equivalent to Ly6C^{hi} monocytes in mice, whereas human CD14^{lo}/CD16^{+} monocytes are analogous to non-classical murine Ly6C^{lo} monocytes [48]. Intermediate monocyte populations have also been identified and are characterized by Ly6C^{int} in mice or CD14^{+}/CD16^{+} in humans. They express CX_3CR1 levels comparable to those in non-classical monocytes but do not have a patrolling function and exhibit many features of classical monocytes, such as phagocytosis and ROS production [48, 49]. Classical monocytes represent the largest monocyte subset and account for 80-90% of all monocytes, while non-classical and intermediate monocytes make up 10-20% of monocytes in the human body [50].

1.2.2.1 Monocyte and neutrophil transendothelial migration in inflammation

The first description of leukocyte rolling and transmigration through the vessel wall during inflammation was provided by Wagner in 1839 and Dutrochet in 1824, respectively [5]. This was followed by Cohnheim's detailed reports on leukocyte adhesion and transmigration, highlighting the role of the inflamed endothelium in the process [6, 51].

Indeed, neutrophils and monocytes can be activated indirectly through contact with activated endothelial cells (ECs) in addition to direct exposure to inflammatory mediators. ECs become activated by inflammatory cytokines including TNFα, IL-6 or IL-1β, which are produced by tissue-resident macrophages upon recognition of an inflammatory stimulus (Fig. 1.2). Thus, ECs up-regulate the expression of adhesion molecules including selectins, which recognize glycoprotein ligands [52-54]. Reversible leukocyte capture is mediated by the binding of PSGL-1 and L-selectin on neutrophils or monocytes to P- and E-selectin on ECs [53]. Ly6C^{hi} monocytes have higher surface levels of PSGL-1 than Ly6C^{lo} populations, resulting in preferential recruitment of this population [55]. This induces the activation of integrins, which undergo conformational changes leading to increased affinity. In addition, captured leukocytes can induce the capture of other circulating leukocytes with surface L-selectin by interaction with PSGL-1 [56].

Binding of E-/P-selectins to their ligands on monocytes or neutrophils slows down their rolling movement and allows them to interact with chemokines presented by proteoglycans on ECs [57]. The chemokines are recognized by GPCRs on leukocytes and induce rapid inside-out signaling: integrins LFA-1 or Mac-1 on neutrophils or monocytes as well as VLA-4 on monocytes become activated and undergo conformational changes. In addition, outside-in signaling triggered by force acting on mechanosensory L-selectin leads to activation of LFA-1. Together, this results in further deceleration of captured leukocytes and eventually their arrest by firm interaction of ICAM-1 and VCAM-1 on ECs with leukocyte LFA-1, Mac-1 and VLA-4 [57, 58]. After adhesion, the force acting on LFA-1 induces signaling pathways resulting in increased intracellular calcium levels, triggering morphological changes and polarization of leukocytes [53]. Mediated by the interaction of Mac-1 and ICAM-1/2, they directionally migrate along the endothelium, following gradients of chemokines, adhesion receptors or EC stiffness [53, 57]. During this process, chemokine receptors and high-affinity integrins re-localize to the leading edge of the immune cell while low-affinity adhesion molecules are distributed on the trailing end to further polarize the cell [57].

Once leukocytes arrive at their preferred site for endothelial transmigration, they can leave the vasculature mostly by paracellular but also by transcellular migration [57, 58] (Fig. 1.2). Paracellular migration requires leukocytes to cross endothelial tight and adherens junctions. Tight junctions consist of occludins, claudins and junctional adhesion molecules A-C (JAM A-C). The latter bind to integrins LFA-1 and Mac-1 on the surface of monocytes. Vascular endothelial cadherin (VE-cadherin) on ECs mediates vascular permeability at adherens junctions but does not directly interact with monocytes, unlike endothelial adhesion molecules PECAM-1 and CD99. Leukocyte selectins and VCAM/ICAM trigger EC signaling resulting in increased intracellular calcium concentrations, causing the phosphorylation of VE-cadherin [57, 58].

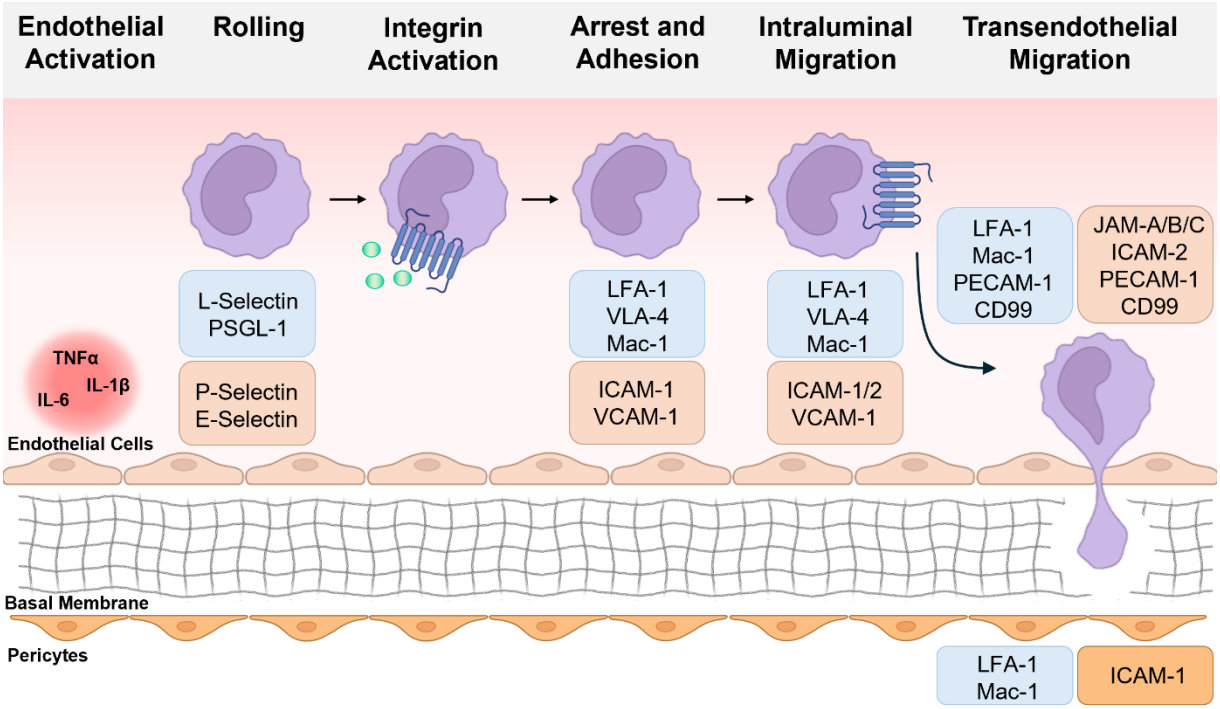


Fig. 1. 2 Transendothelial leukocyte migration. Inflammatory cytokine production by resident tissue macrophages activates endothelial cells, resulting in capture and rolling of leukocytes on the vascular endothelium. Chemokines and shear forces activate leukocyte integrins, triggering firm adhesion and directional intraluminal migration. At appropriate sites, leukocytes migrate through the endothelial cell layer, the basal membrane and through gaps between pericytes to reach the site of inflammation. Figure adapted from [59] and includes findings described in [53, 57-60]. Created with BioRender and PowerPoint.

In addition, the LFA-1 - ICAM-1 interaction induces Src and Pyk2 activation, which phosphorylate tyrosine residues on VE-cadherin. As a result, VE-cadherin dissociates and permits leukocyte transmigration through the junction [57, 58]. Interestingly, TNFα on endothelial cells was also shown to induce phosphorylation of cadherin [61]. Then, leukocytes cross the basal membrane at sites of low laminin or collagen IV density and migrate through the pericyte layer [58]. Pericytes express ICAM-1, which interacts with leukocyte LFA-1 and Mac-1, as well as chemokines and cytokines to support migration and modulate effector functions [52, 58, 60].

1.2.2.2 Leukocyte chemotaxis

First described by Leber in 1888, directed leukocyte migration following the gradient of a chemoattractant or chemorepellent is called chemotaxis and is an essential process in inflammation [62, 63]. The chemotactic process can be characterized based on the initiating signal: Haptotaxis describes directional migration towards surface-attached chemoattractants,

fugetaxis defines chemotaxis away from chemorepellents and necrotaxis is characterized by cell migration towards or away from factors released by apoptotic or necrotic cells [64]. In contrast, chemokinesis describes non-directional cell movement upon stimulation [65]. In order to undergo directional amoeboid migration, leukocytes polarize and form a leading edge with protruding pseudopodia to sense environmental signals, and a uropod, which contains large numbers of mitochondria and mediates cell adhesion [64].

1.2.2.21 Neutrophil and monocyte chemotaxis

Leukocytes recognize chemoattractants through surface G-protein coupled receptors (GPCRs). Chemoattractants can be divided into lipids (mostly arachidonic acid-derived eicosanoids like leukotriene B4 or PAF), chemokines (e.g. CXCL1/KC, CCL2/MCP-1, CXCL2/MIP-2, CXCL5/LIX), N-formylated peptides (e.g. bacterial fMPL) and complement anaphylotoxins like C5a [66, 67]. Binding of chemoattractants to the respective leukocyte GPCR initiates Gαi- or Gβγ signaling, resulting in cell polarization and chemotaxis (Fig. 1.3) [66, 68].

Upon sensing chemoattractant gradients through their GPCRs, neutrophils and monocytes polarize and initiate migration. Signaling pathways initiated by Gβγ have been well investigated and are thought to be the main mediators of chemotaxis [69]. The Gβγ heterodimer activates PI3Kγ, which generates PIP_3 and thus enables Gβγ to directly bind to and activate P-Rex1, Dock2 and PIXα/PAK1. P-Rex1, Dock2 and PIXα/PAK1 are guanine nucleotide exchange factors (GEFs) for Rac and Cdc42 and activate the small GTPases by stimulating GDP release and GTP binding [69-75]. Once activated, Rac and Cdc42 activate WASP and SCAR/WAVE, which mediate actin polymerization and thus pseudopodia formation on the leading edge, causing directional cell migration [76, 77]. To promote chemotaxis, a positive feedback loop has been described, which results in further PIP_3 generation at the leading edge upon PI3K and Rac-mediated F-actin polymerization [69, 78]. In addition, the Gβγ dimer activates PLCβ, which causes DAG and IP_3 production leading to an increase in intracellular calcium levels, which in turn activates PKC [73]. Together with PI3Kγ-activated Akt, PKC phosphorylates and

inactivates GSK3. Consequently, GSK3 can no longer phosphorylate and inhibit slingshot2 (SSH2), which dephosphorylates and activates cofilin, resulting in further F-actin formation in the leading edge [79].

Upon GTP binding, $G\alpha_{i2}$ subunits can bind to the complex consisting of ELMO1 and Dock180, which activate Rac by acting as GEFs [80]. $G\alpha_{i2}$-GTP can also induce Homer3 and mTORC2/PKC signaling pathways, resulting in F-actin polymerization and cell polarization [69, 81]. $G\alpha_{i2}$-GDP regulates the directionality of migration by binding to LGN/AGS3, which results in recruitment of the mlnsc/Par3/αPKC complex. This causes pseudopodia stabilization at the leading edge and directional migration [82]. In addition, $G\alpha_{12/13}$ can activate GEF115 and thus trigger RhoA/ROCK activation in the uropod of the cell, which causes myosin II assembly [83-85].

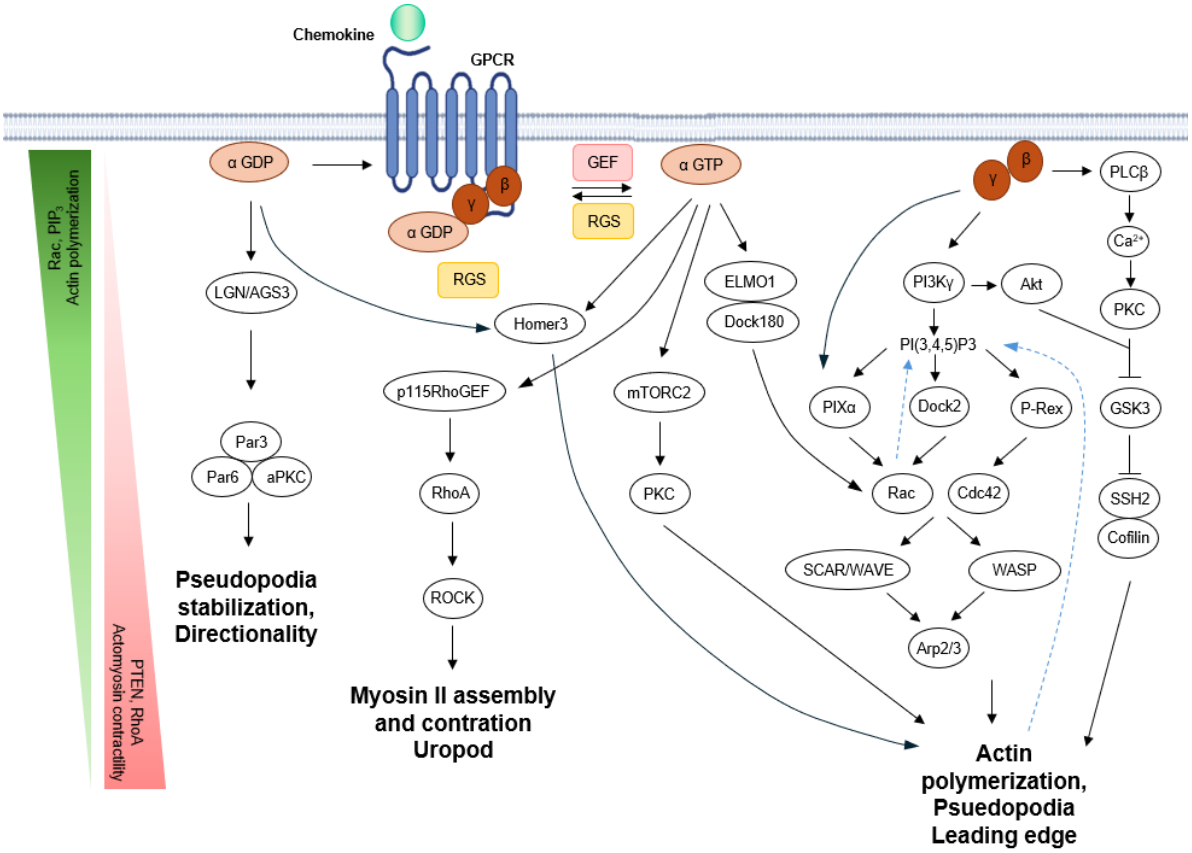


Fig. 1. 3 Chemokine signaling through GPCRs in leukocytes. Binding of chemokines to their respective chemokine receptor activates PLCβ signaling and PI3K-mediated PIP_3 production through Gβγ, resulting in the activation of Rac and Cdc42 through GEFs PIXα, P-Rex and Dock2. This causes actin polymerization at the leading edge through SCAR/WAVE- and WASP-mediated Arp2/3 activation. Positive feedback loops are indicated by blue arrows. $G\alpha_{i2}$-GTP initiates RhoA/ROCK activation at the uropod, resulting in actomyosin assembly and contractility. $G\alpha_{i2}$-GDP mediates contractility. Cell polarization and directional migration are regulated by gradients of PTEN and RhoA activation at the trailing end and PIP_3 production and Rac activation at the leading edge. Figure generated with PowerPoint and BioRender and adapted from [69, 86].

As described above, polarized PIP_3 production is essential for pseudopodia formation and directional cell migration [73, 87, 88]. The PIP_3 gradient required for chemotaxis may be modulated by PTEN, which can dephosphorylate PIP_3 and is localized in the uropod of the migrating cell [70, 89, 90]. PTEN localization depends on PIXα and RhoA/ROCK [70, 91]. In the trailing end of the cell, actin-myosin filaments contract upon RhoA/ROCK activation, causing tail-retraction, which pushes the migrating cell forward [86].

1.2.2.2.2 Macrophage chemotaxis

Unlike neutrophils and monocytes, which move through amoeboid migration, macrophages can use both amoeboid and mesenchymal motility depending on their environment [64, 92]. Mesenchymal migration is slower and the leading edge and the trailing end of the migrating cell are less defined, with lamellipodia extending from the cell. During mesenchymal migration, the cell strongly adheres to the surrounding tissue and remodels the surrounding extracellular matrix [93]. The expression of integrins, which mediate tight adhesion, differentially modulates the migratory behavior of distinct macrophage populations [92]. Both amoeboid and mesenchymal migration require the activation of Rac and Cdc42 through PI3K at the leading edge, resulting in the downstream activation of Scar/WAVE and WASP or Akt/PKC signaling and the initiation of actin polymerization, causing the formation of filopodia or lamellipodia. In mesenchymal migration, lamellipodia at the uropod activate PIP2, WASP, Scar and Arp2/3, which results in the branching of actin filaments. Adhesion complexes mediate firm attachment to the extracellular matrix [69, 94]. Firmins mDia1/2 are activated by Rho GTPases and generate firm adhesion points [64]. Adhesion is released through ROCK, calpain and calcineurin, which modulate Rac and myosin II activity at the rear of the cell [94].

Monocytes and macrophages can initiate chemotaxis in response to the activation of surface receptor tyrosine kinases, such as CSF-1R [95]. Upon CSF-1 binding, the RTK auto-phosphorylates and PI3K is activated [96], resulting in downstream activation of Cdc42 and Rac at the leading edge and Rho at the uropod, causing cell polarization and actin polymerization as well as adhesion/contractility required for macrophage chemotaxis [97, 98].

CSF-1 is known to be an important chemoattractant for macrophages and monocytes [99-102], which recruits them to sites of inflammation. In RA, synovial endothelial cells produce high amounts of CSF-1, which recruits monocytes and macrophages and promotes osteoclastogenesis. This can be inhibited by CSF-1 neutralizing antibodies [103].

1.2.3 Eosinophils

Eosinophils are named after the acidic dye eosin, which stains the basic granules in their cytoplasm a dark red color. They develop in the bone marrow and eosinophil differentiation is promoted by cytokines IL-3, IL-5 and GM-CSF. IL-5 induces eosinophil exit from the bone marrow into the bloodstream [104]. Eosinophils make up 2-5 % of leukocytes in the human blood, where they have a half-life of 8-18 h. Chemokines including CCL11 can induce their migration into tissues like the lamina propria of the gastrointestinal tract, where eosinophils survive for 2-5 days, but their life span can be enhanced to up to 14 days by cytokines such as IL-5 [104, 105]. The cytoplasmic granules of eosinophils are bound to the membrane and degranulation, whereby the granules fuse with the membrane to release their contents, is triggered by pathogen stimulation of surface IgA receptors. The granules contain leukotrienes, acid phosphatase, eosinophil peroxidase (EPO), eosinophil-derived neurotoxin (EDN), eosinophil cationic protein (ECP) and eosinophil major basic protein (MBP) [105, 106].

ECP and EDN have RNase activity and were shown to be involved in the anti-viral responses against viruses such as RSV or pneumonia virus in mice [104, 107, 108]. In addition, eosinophils are involved in the anti-fungal immune response [109]. Upon exposure to bacteria, eosinophils can release mitochondrial DNA together with ECP and MBP to eliminate the pathogens [106].

In addition, the cells release histaminase and aryl sulphatase to inactivate histamine and leukotrienes produced by mast cells to attenuate inflammatory responses and granulocyte infiltration [105, 110]. However, eosinophil degranulation is associated with asthma, as EPO and leukotrienes can cause tissue damage, increase vascular permeability and induce bronchoconstriction and mucus hypersecretion [110]. Further, MBP can cause bronchial

toxicity and airway hyperreactivity and further exacerbate inflammation by inducing basophil and mast cell degranulation [104].

1.2.4 Basophils and Mast cells

Basophils are the least abundant granulocytes in the blood and make up less than 0.2 % of leukocytes. They are derived from basophil-eosinophil progenitor cells in the bone marrow, from where they enter the blood and can remain in circulation for up to 2 weeks [27, 105]. Their name is derived from their staining properties, as sulfated proteoglycans (e.g. heparin) in their granules can be stained dark blue by basic dyes [111].

In contrast to basophils, mast cells do not circulate in the blood. They are derived from the bone marrow, which they exit in the form of progenitor cells. These progenitor cells quickly migrate from the blood into tissues, where they differentiate into mucosal mast cells (MMCs) or connective tissue mast cells (CTMCs). T cells are required to induce the proliferation of MMCs but not CTMCs [105, 112]. To effectively detect pathogens, mast cells are located near blood vessels, nerve endings, lymphatic vessels and other immune cells in the tissue [113].

Basophil and mast cell granules contain heparin, leukotrienes, histamine, serine proteinases, sulfated glucosaminoglycans, platelet-activating factor (PAF), eosinophil chemotactic factor of anaphylaxis (ECF-A) as well as neutrophil chemoattractants. Allergens result in the cross-linking of IgE molecules that are bound to surface FcεRI receptors on basophils to cause degranulation [105, 110]. In addition to allergens, stimuli like cold, trauma, cationic platelet-derived proteins, insect venom, PAMP-induced TLR activation, C5a-induced C5a-R activation, cytokines or lysosomal neutrophil granules can trigger basophil or mast cell degranulation [110, 113]. Granular contents such as histamine are required for an inflammatory host defense response against parasites but can also cause allergy symptoms [105]. Histamine binds to H_1 receptors on the vessel wall and enhances vascular permeability by causing EC contraction, gap formation and edema. In addition, activated basophils and mast cells were found to be a source of inflammatory mediators including TNFα, IFN-γ and GM-CSF [27, 110]. Thus, mast

cell and basophil degranulation is associated with pathologies including asthma or anaphylaxis [113, 114].

1.2.6 Dendritic cells

Dendritic cells (DCs) are professional antigen-presenting cells (APCs) and are thus important links between the innate and adaptive immune response. They are both key players in host defense from pathogens or DAMPs as well as inducers of immune tolerance [115]. Dendritic cells were first described by Steinman and Cohn in 1973 as a novel cell type named for their cellular morphology characterized by “processes of varying length” [116].

Steady-state DCs originate from a common DC precursor cell (CDP), which differentiates into two DC subsets: pre-classical DCs (pre-cDCs) and plasmacytoid DCs (pDCs). Pre-cDCs can give rise to cDC1 and cDC2 populations [117, 118]. Plasmacytoid DCs recognize viruses via TLR7/9 and STING and initiate the transcription and production of type I and III interferons and pro-inflammatory cytokines, such as TNFα or IL-6, via IRF3/7 or NF-κB, respectively [117, 119]. cDC1s present intracellular antigens via MHCI and induce $CD8^+$ T cell activation to promote Th1 and NK induction through IL-12. To detect PAMPs and DAMPs, they express TLR3/9/10 and produce type I and III interferons. cDC2s express TLR2/6/4/5/8, lectins, NOD-like receptors and RIG-I-like receptors and can consequently respond to a wide range of stimuli, such as LPS, fungi or poly(I:C). Human cDC2s produce pro-inflammatory cytokines IL-12, IL-1, IL-23, TNFα and IL-8 and activate $CD8^+$ T cells as well as $CD4^+$ Th1, Th2 and Th17 cells [117, 120].

Upon PAMP or DAMP recognition, DCs mature and migrate to draining lymph nodes where they present the antigen on surface MHC molecules to T cells, which can recognize specific antigens and co-stimulatory molecules. During maturation, DCs reorganize their cytoskeleton to become less adhesive and promote migration. In addition, they upregulate the expression of co-stimulatory molecules CD80 and CD86, MHC expression, chemokine receptor CCR7 expression and the secretion of pro-inflammatory cytokines, while their phagocytic capacity decreases [115]. CCR7 upregulation allows DCs to migrate to lymphoid organs which express

high levels of CCR7 ligands CCL19 and CCL21 [121]. In T cell zones of the lymph nodes, DCs present antigens to naive T cells. DCs process intracellular pathogens and present them on MHCI molecules to $CD8^+$ T cells, while extracellular pathogens or apoptotic/necrotic cells are endocytosed and antigens are presented on MHCII molecules to T helper cells [122]. Naïve $CD4^+$ T cells subsequently differentiate into Th1, Th2, Th17 or Treg cells depending on the cytokines produced by the DCs as well as their maturation state [115, 123].

If DCs encounter apoptotic or necrotic cells, they are taken up and these “tolerogenic DCs”, which are in the state of immaturity or intermediate maturity, present their antigens to T cells with fewer co-stimulatory molecules and MHC molecules. In addition, they increase the expression of inhibitory molecules and the production of anti-inflammatory cytokines to induce T cell apoptosis, anergy and the development of Treg cells [115, 124].

1.3. Macrophages

The critical role of macrophages (from Greek *macros phagein*= big eater) in host defense was first described by Elie Metchnikoff, the “father of innate immunity”, as he observed phagocyte recruitment in response to inflammation caused by foreign objects, dead cells or infection [9, 125, 126]. In his review “Das retikulo-endotheliale System” in 1924, Aschoff systematically characterized the reticuloendothelial system (RES) by summarizing previous findings and described the cells’ distribution across various tissues as well as their protective, storage and secretory functions. He considered the defining feature of cells of the RES to be “the intensity, the frequency of phagocytosis” based on vital staining [127]. As new findings emerged, van Furth, Cohn, Hirsch and others introduced the mononuclear phagocyte system (MPS) in the 1960s, which included macrophages, monocytes as well as their precursors in the bone marrow based on “similarities in the morphology, function, origin, and kinetics of the phagocytes” [128]. Of note, DCs were originally excluded but were later added after Steinman identified them as a novel cell type distinct from macrophages [116, 129, 130].

1.3.1 Embryonic and monocyte-derived macrophage populations

Aschoff wrote that "Metchnikoff [was] the first to – even though not explicitly- speak of one system of dispersed cells in the body" [127]. In local tissues, macrophages are key not only for host defense but also for development. They mediate tissue repair and carry out nurturing functions and thus are crucial to maintaining homeostasis [131, 132]. Based on Dobzhansky's statement on evolution [133], Gordon states that "nothing in macrophage biology makes sense except in the light of homeostasis" [134].

It was originally believed that tissue-resident macrophages, such as resident peritoneal macrophages, originate from circulating monocytes [135]. Later, the characterization of spleen macrophages revealed their "dual origin", indicating the presence of two distinct macrophage populations: monocyte-derived macrophages and self-renewing splenic macrophages [136]. More recently, Yona et *al*. and Hashimoto and colleagues demonstrated that resident tissue macrophages, such as alveolar, splenic and peritoneal macrophages as well as microglia and Kupffer cells originate from embryonic yolk sac-derived macrophages and fetal liver-derived macrophages, which can self-renew under physiological conditions so that they do not rely on monocytes to maintain the reservoir [21, 137]. Alternatively, they can proliferate during inflammation in the adult organism [138]. During inflammation, bone marrow-derived Ly6C^{hi} monocytes infiltrate affected tissues and differentiate into monocyte-derived macrophages, which can persist after inflammation resolution together with embryonic tissue-resident macrophages [14, 16, 21]. It is worth noting that most tissue-resident macrophages in the intestine as well as certain tissue macrophage populations in the skin, lung, heart and spleen are derived from monocytes [44, 139-142].

In the embryo, macrophages are generated even before haematopoietic stem cells (HSCs) [143]. There are three phases of haematopoiesis in the embryo: the first one occurs in blood clusters of the yolk sac (primitive haematopoiesis) and generates erythrocyte, megakaryocyte and macrophage precursors, which are not derived from monocyte precursors. The latter can migrate to the brain to form microglia as well as to other embryonic tissues [143]. During the second phase (transient definitive haematopoiesis), erythro-myeloid progenitor (EMP) cells are

generated in the haemogenic endothelium of the yolk sac. They can expand and develop into yolk sac macrophages or migrate to the fetal liver. EMP-derived fetal monocytes were found to generate tissue-resident macrophages in various tissues, including the Kupffer cells, Langerhans cells or alveolar macrophages [142, 144]. In a third phase, termed definitive haematopoiesis, HSCs are formed in the aorta-gonads-mesonephros (AGM). These cells can populate the fetal liver to establish definitive haematopoiesis and settle in the bone marrow to generate HSCs in the adult [44, 144]. In the embryo, macrophages assist development and promote angiogenesis, neurodevelopment, osteogenesis, erythropoiesis and clear apoptotic cells during limb and testis development [144]. Due to their diverse origins and functions determined by their tissue environments, macrophages are highly heterogeneous. In some tissues, resident macrophage populations of different origins can co-exist, which adds additional diversity [143].

1.3.2 Macrophage phenotypes

In the early 1990s, IL-4 and IL-13 were first reported to induce “alternative macrophage activation” characterized by enhanced macrophage mannose receptor CD206 and MHCII expression as well as increased endocytic capacity and reduced pro-inflammatory cytokine production [145, 146]. This phenotype was contrasted with the classically activated macrophage phenotype observed upon IFN-γ stimulation, which enhanced pro-inflammatory mediator secretion and microbial killing [147]. In 1996, Mosman et *al.* introduced the distinction between anti-bacterial and anti-viral Th1 and anti-helminth Th2 T cell responses and the associated cytokine profiles of each response [148]. Based on this concept, Mills et *al.* introduced the idea of similar functional phenotypes in the macrophage field [149]. They had observed that macrophages derived from Th1 mouse strains could be easily induced by LPS or IFN-γ to produce nitric oxide (NO), while this was inhibited in Th2 macrophages by TGF-β-mediated suppression of iNOS. The authors also described differences in the metabolism between Th1 and Th2 macrophages and emphasized the LPS-induced increase in arginine metabolism in Th2 macrophages. Consequently, they termed these macrophage responses M1 and M2 based on the Th1/Th2 concept [149]. As other factors apart from Th2 cytokines

were discovered to induce alternative macrophage activation, Mantovani et *al.* differentiated between M1 macrophage polarization on one hand and M2 activation on the other hand as extreme states on both ends of a macrophage phenotype spectrum [150]. M1 activation is relatively easy to define based on activation by IFN-γ+LPS or TNF, which induces classical activation characterized by a Th1 response linked to pathogen killing and anti-tumor effects (Table 1.1). In contrast, the authors highlight differences in alternative macrophage activation depending on the stimulus (Table 1.1): M2a activation is induced by IL-4 or IL-13, while M2b polarization is induced by immune complexes in combination with TLR agonists or IL-1R. Both results in Th2 responses and immunoregulation. Finally, M2c activation is induced by IL-10 and glucocorticoids, causing macrophage deactivation and tissue remodeling [150]. Sometimes, M2d activation is considered separately and is described as a response to IL-6 and adenosines [151]. In classically activated M1 macrophages, iNOS mediates the production of NO from arginine, while M2 macrophages in the mouse express Arg-1, which hydrolyzes arginine to ornithine and urea [152].

It is becoming increasingly clear that a dualistic model of M1 and M2 macrophage polarization is oversimplified and has many important limitations. As described above, macrophages are extremely heterogeneous and differ significantly in their phenotype and function depending on their origin and tissue environment. Macrophage M1 and M2 stimuli and phenotypes were first described *in vitro* and thus do not take into account that such stimuli do not occur isolated in tissues *in vivo* [153]. Importantly, even macrophage polarization *in vitro* is not as clear-cut as often believed. For example, LPS, IFN-γ and GM-CSF, although often grouped together as M1 stimuli, generate different gene expression profiles and functional responses depending on the combination used for stimulation [153]. In addition, even the use of tightly regulated stimuli *in vitro* does not always result in consistent macrophage phenotypes [154]. Macrophages possess high levels of plasticity and are therefore able to re-polarize depending on their environment [155]. Murray highlights in his 2017 Annual Review that therefore, macrophage polarization should be merely considered a snapshot, which exists on a wide spectrum in

between the extremes of M1 and M2 polarized states and is highly time- and environment-dependent [154].

Table 1. 1 M1 and M2 macrophage properties
Table summarizes findings reported in [150, 152-154, 156-159].

	M1	**M2**
Stimulus	IFN-γ, LPS, TNF, GM-CSF	IL-4, IL-13 (M2a) ICs+IL-1β or LPS (M2b) IL-10, glucocorticoids (M2c) IL-6 and adenosines (M2d) M-CSF
Surface markers	MHCII, CD68, CD80, CD86, MARCO	CD206, MHCII, CD163, SR, CD200R, TGM2
Cytokines	TNF, IL-1β, IL-6, KC/IL-8, IL-12, Il-18, IL-23, IL-27	TGF-β, IL-10, IL-6
Chemokines	CCL2, CCL3, CCL4, CCL5, KC/IL-8, CXCL8, CXCL9, CXCL10, CXCL11	CCL1, CCL16, CCL17, CCL21, CCL22, CCL24, CXCL4, CXCL13
Chemotaxis towards	CCL7, CCL19, CCL21, CCL24, CCL25, CXCL8, CXCL10, XCL2	CCL7
Transcription factors	STAT1, STAT5, IRF1, IRF5, IRF8, NF-κB, AP-1	STAT6, IRF4, STAT3
Metabolism	NO, ROS (iNOS) Decreased OXPHOS	Polyamines (Arg-1) Increased OXPHOS
Function	Bacterial phagocytosis and killing	Parasite encapsulation and killing Anti-fungal response Efferocytosis Tissue repair

1.3.3 Macrophage mediators of inflammation

1.3.3.1 Cytokines

Cytokines (from Greek *cyto*= cell and *kinos*= movement) are low molecular weight proteins (around 5-25 kDa in size) and have been linked to many essential processes like development, cell proliferation, metabolism and immune effector function as well as inflammation [160-163]. They were first described as “soluble factors” and later divided into lymphokines (produced by lymphocytes) and monokines (produced by monocytes) [161]. Cytokines also include chemokines (short for chemotactic cytokines), which elicit chemotactic cell responses, as well as interleukins, that are produced by leukocytes and target other leukocytes [164]. Most cytokines signal in an autocrine or paracrine manner, but others, like TGF-β or M-CSF, can also affect distant cells in an endocrine fashion. [160, 164]. Cytokines are functionally redundant and pleiotropic, as one cytokine can target different cell types and while each cytokine binds to a specific cell surface receptor, cells can express multiple receptors that can recognize a specific cytokine [160]. The main sources of cytokines are Th cells and macrophages but PMNs, endothelial or epithelial cells, amongst others, can also contribute to their production [164].

During an immune response, macrophages secrete cytokines to activate and recruit innate and adaptive immune cells and to modulate their environment, depending on their polarization state [160, 165]. Cytokines in the macrophage environment can in turn also change macrophage polarization. Important pro-inflammatory cytokines released predominantly by classically activated macrophages are TNFα, IL-1β, IL-6, IL-8, IL-12 and IL-23 and are associated with symptoms of inflammation, such as pain or fever [160, 164]. These cytokines can increase vascular permeability and induce inflammatory cell infiltration and the production of further cytokines or chemokines during acute inflammation. When this response is dysregulated, excessive production of pro-inflammatory cytokines can cause pathologies including sepsis, IBD or severe COVID-19 [166-168]. Anti-inflammatory cytokines including IL-10 or TGF-β on the other hand are produced by alternatively activated macrophages and suppress the production of pro-inflammatory mediators. The presence of anti-inflammatory

cytokines, such as IL-4, IL-13 or IL-10, can also re-polarize classically activated macrophages to limit inflammation [160].

1.3.3.2 Chemokines

Members of the chemokine family share a conserved secondary structure and can selectively target certain immune cell populations to elicit directional migratory responses [169]. Apart from functions in immune responses, chemokines also coordinate processes like angiogenesis, haematopoiesis, immune system development and wound healing [170, 171]. Depending on their conserved cysteine residues, chemokines can be assigned to either of four classes: C-C, C-X-C, C or CX_3C chemokines [164].

Pro-inflammatory cytokines can induce chemokine production by macrophages to recruit and activate other immune cells. Chemokines CXCL1 and CXCL2 attract neutrophils as well as haematopoietic stem cells [172-174]. CCL5 (RANTES) was shown to recruit T cells, eosinophils, basophils as well as monocytes, NK cells or DCs to sites of inflammation. It can also activate NK cells [175]. Pro-inflammatory chemokine CXCL5 is mostly derived from epithelial cells but can also be produced by pro-inflammatory macrophages or macrophages in the tumor [176, 177]. It is a strong chemoattractant for neutrophils during acute inflammation [178]. CXCL8 (IL-8) produced by macrophages at the site of inflammation, but also by epithelial and endothelial cells, potently recruits neutrophils and promotes their degranulation and phagocytosis capacity in early stages of inflammation [179]. CXCL9, CXCL10 and CXCL11 production can be induced by interferons. CXCL9 and CXCL11 attract T cells, while CXCL10 recruits T cells, macrophages/monocytes, NK cells and DCs [160, 180].

Interestingly, chemokines can also act as “find-me” signals to guide phagocytes to apoptotic cells. Apoptotic cells or apoptotic blebs display anionic phosphatidylserine (PS) and other “eat-me” signals on the outer plasma membrane leaflet [181], which can be bound by chemokines such as CXCL16, CX3CL1 [182, 183], CCL2, CCL11, CCL21, CXCL9, CXCL11 and CCL20 to recruit monocytes and macrophages [184].

1.3.3.3 Nitric Oxide

In an inflammatory setting, pro-inflammatory macrophages can produce nitric oxide (NO) in addition to cytokines [185]. Besides its role in inflammation, NO was shown to be involved in the regulation of vascular tone and neurotransmission [186]. During inflammation, NO mediates pathogen killing, anti-tumoral activity, lymphocyte apoptosis and leukocyte recruitment [186, 187]. The inflammatory mediator is produced in macrophages by NO synthase (NOS), which generates NO and L-citrulline from L-arginine and O_2 [185]. While classically activated macrophages produce NO via iNOS (NOS2), alternatively activated macrophages express arginase to hydrolyze arginine to ornithine and urea [188].

1.3.4 Macrophages in inflammatory pathologies

Macrophages are key players in rheumatic disease. The joint capsule contains the synovial membrane, which consists of the intimal lining layer and the sub-lining layer (Fig. 1.4). The intimal lining layer contains fibroblast-like synoviocytes (type B synoviocytes) and macrophage-like synoviocytes (type A synoviocytes), while the sub-lining consists of interstitial macrophages and fibroblasts as well as mast cells and lymphocytes [189]. Under physiological conditions, the lining layer contains macrophages that express surface markers Trem2 and CX_3CR1, while in the interstitial synovium, vessel-adjacent macrophages can be found which are characterized by $Lyve1^+/Relm\alpha^+$ expression (Fig. 1.4) [189]. These two macrophage populations are maintained by MHCII- and CSF-1R-expressing macrophages that can be found in the interstitial synovial tissue of the mouse (Fig. 1.4) [189, 190]. All three populations of tissue-resident macrophages are of embryonic origin and are maintained independently from bone marrow-derived monocytes [190].

The Trem2-expressing synovial lining macrophage population forms tight junctions and desmosomes and has apical and basal cell poles, which are features normally found in epithelial cells (Fig. 1.4) [189]. These features allow this macrophage population to form a barrier between the synovial cavity and the synovial interstitial tissue, where they maintain synovial fluid composition and cell debris/DAMP clearance. As a consequence, these

macrophages have an anti-inflammatory phenotype and possess high capacities for phagocytosis and endocytosis while lacking pro-inflammatory mediator expression [189].

1.3.4.1 Macrophages in gout

The auto-inflammatory disease gout is characterized by joint inflammation triggered by monosodium urate (MSU) crystals. The prevalence of gout is steadily increasing and in 2020 affected <1%-6.8% globally [191]. Patients episodically develop gout flare-ups associated with severe joint pain, which typically self-resolve within 7-10 days without treatment [192]. Similarly, calcium pyrophosphate dihydrate (CPPD) crystals can cause pseudo-gout by triggering acute inflammatory arthritis in the joints of affected patients. In contrast to gout, acute CPPD crystal arthritis may not resolve within a week and may persist for up to three months [193].

Upon inflammation initiation, recruited monocyte-derived macrophages infiltrate the synovial lining and the interstitial tissue (Fig. 1.4) [189]. In the synovial fluid of patients with acute gout or pseudo-gout, recruited CCR2-expressing $CD14^+$ monocytes were found to be the source of pro-inflammatory cytokines TNFα or IL-1β and contained high levels of intracellular IL-8, demonstrating that they are the driver of inflammation [190, 193, 194]. Interestingly, they also produced more IL-10 and had higher CD163 levels than monocytes from RA patients, indicating the presence of both pro- and anti-inflammatory recruited monocytes in the gouty joint [194]. However, Lan et *al.* showed that in mice with MSU crystal-induced gout, TRPV4-mediated NLRP3 inflammasome activation in tissue-resident CX_3CR1^+ macrophages initiates and drives inflammation (Fig. 1.4) [195].

When investigating the role of macrophage polarization in gout resolution, Zhao et *al.* found that M1 macrophage infiltration in rat gouty joints correlated positively with disease severity. In the early inflammatory response, macrophages had M1-like phenotypes ($iNOS^+$), which peaked at 24 h, while at later stages of inflammation, namely between 48 h and 120 h after disease onset, alternatively activated macrophages ($Arg\text{-}1^+$) dominated [196]. Interestingly, M2-like macrophages appeared as early as 2 h after gout onset and the authors speculated

that at this time point, they may be derived from the immunoregulatory RELMα$^+$CD163$^+$CD206$^+$ resident interstitial macrophage population [197].

Inflammation resolution of MSU-induced inflammation depends on efferocytosis of apoptotic neutrophils by macrophages [198, 199]. In addition, synovial fluid macrophages can phagocytose NETs induced by MSU crystals to limit inflammation (Fig. 1.4) [200]. The capacity of monocyte-derived macrophages to take up apoptotic neutrophils is promoted by IL-1β, TNFα and TGF-β, and ingestion of apoptotic cells promotes anti-inflammatory phenotypes in macrophages, indicating a switch from the onset of inflammation to the resolution phase [201, 202]. Bone marrow-derived monocytes also display increased phagocytotic capacity during differentiation into pro-inflammatory macrophages upon MSU crystal stimulation [203].

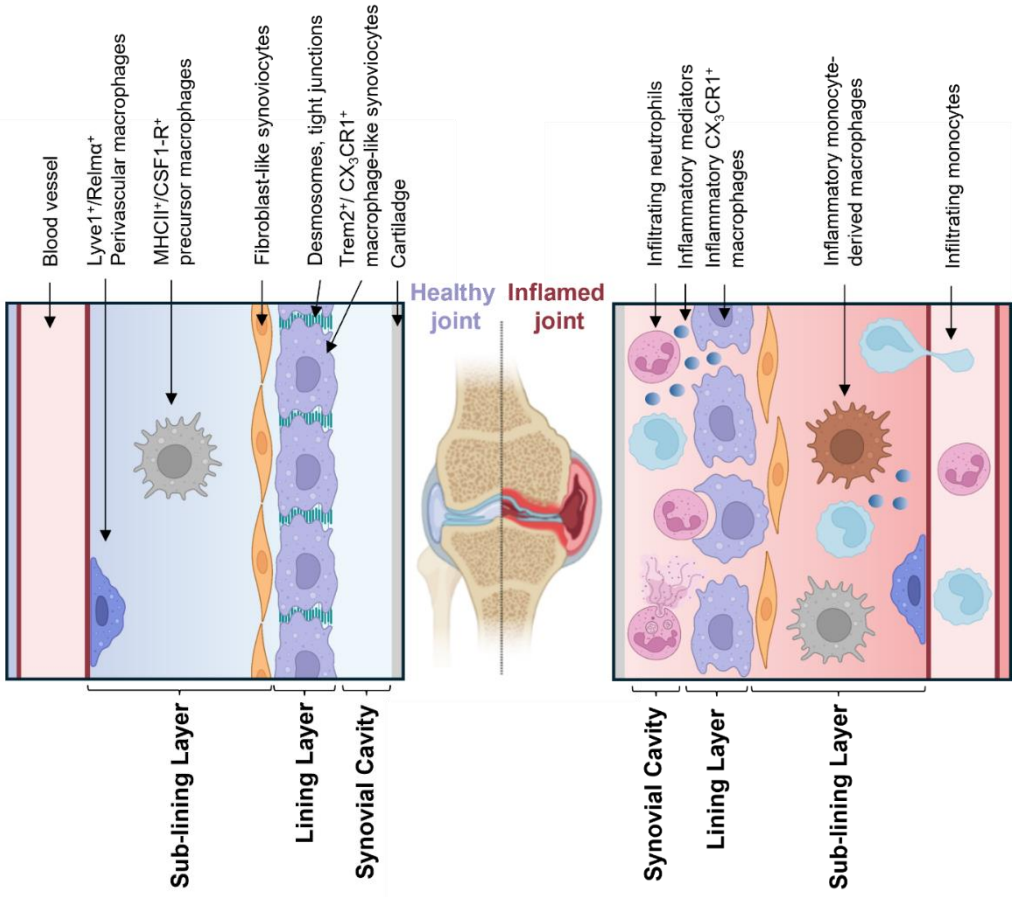


Fig. 1. 4 The role of macrophages in joint homeostasis and gouty joint inflammation. Trem2$^+$/CX$_3$CR1$^+$ macrophages in the synovial lining layer form desmosomes and tight junctions and have a defense/ maintenance function and high phagocytic capacity. Lyve1$^+$/Relmα$^+$ macrophages of the sub-lining layer are associated with blood vessels. Both populations are maintained by MHCII$^+$/CSF-1R$^+$ precursor macrophages. During gouty inflammation, inflammation is initiated by NLRP3 inflammasome activation in CX$_3$CR1$^+$ macrophages. Inflammatory monocytes and neutrophils infiltrate the synovial cavity and interstitial tissue, produce pro-inflammatory mediators and differentiate into pro-inflammatory macrophages. Resolution includes efferocytosis of apoptotic neutrophils and a switch of pro-inflammatory macrophages towards a pro-resolution phenotype. Figure created with BioRender and PowerPoint and adapted from [189, 204].

In contrast to MSU crystal-stimulated monocytes, MSU crystal phagocytosis by differentiated monocyte-derived macrophages was found to promote an anti-inflammatory phenotype and suppress endothelial activation (indicated by E-selectin expression) and subsequent neutrophil capture, thus limiting inflammation [205]. The anti-inflammatory cytokine TGF-β is increased in the synovial fluid of gout patients during inflammation resolution [206, 207] and was found to promote macrophage M2-like polarization and enhance efferocytosis of apoptotic cells [189, 208].

1.3.4.2 Macrophages in Rheumatoid Arthritis

Rheumatoid arthritis is a chronic autoimmune inflammatory disorder associated with joint inflammation causing pain, swelling and bone destruction [209].

Based on studies in MSU crystal-induced peritonitis, it was originally believed that resident macrophages initiate inflammation in arthritis [210]. However, more recent studies demonstrate immune regulatory functions of synovial macrophage populations in RA: CX_3CR1^+ barrier macrophages suppress inflammation by protecting the synovium through their barrier function, as depletion of this population or barrier disruption resulted in enhanced RA severity and PMN infiltration in mice [190]. Another study found that $MerTK^+/Trem2^{hi}$ and $MerTK^+/Lyve1^+$ synovial tissue macrophages have anti-inflammatory properties and promote inflammation resolution by producing pro-resolving lipids and enhancing tissue repair via synovial fibroblasts [211]. In addition, synovial tissue-resident macrophages were demonstrated to be essential for homeostasis and suppressing inflammation in a mouse model of RA [212].

Similarly, perivascular $Lyve1^+/Relmα^+$ macrophages of the interstitial synovium have immunomodulatory properties. They were found to produce CCL24 and CCL12 and thus regulate leukocyte recruitment. Phenotypically, they express markers of alternatively activated macrophages such as CD206 and CD163 and produce anti-inflammatory cytokines IL-10 and TGF-β. Depletion of this macrophage subset in lung and heart fibrosis models in mice resulted

in enhanced fibrosis, vascular permeability and monocyte and neutrophil recruitment [189, 213].

During inflammation, classical Ly6C^{hi} CCR2^{+} bone marrow-derived monocytes are recruited to the RA joint. They are classically activated and produce pro-inflammatory mediators, including IL-1β [214]. Classical monocytes were found to promote arthritis development and aggravate disease pathology in a mouse model of RA [215].

Non-classical Ly6C^{-} monocytes were also reported to be important drivers of joint inflammation in a mouse model of RA [216]. Misharin et *al.* found that they are recruited to the joint during onset of inflammation and differentiate into classically activated macrophages that promote disease pathology. During inflammation resolution, Ly6C^{-} monocyte-derived M1 macrophages re-polarize and become alternatively activated [216]. The authors found that tissue-resident synovial macrophage populations did not change in number and phenotype and maintained anti-inflammatory properties, demonstrating that pro-inflammatory processes are mainly mediated by monocyte-derived macrophages [216]. These findings are supported by Puchner et *al.*, who showed that in hTNFtg arthritis mice, which lack CCR2 and thus classical monocytes, the number of circulating non-classical monocytes was elevated, which correlated with increased differentiation into osteoclasts and enhanced bone destruction [217]. However, another study found that adoptive transfer of Ly6C^{lo} monocytes into arthritic NR4A1$^{-/-}$ mice lacking non-classical monocytes resulted in attenuation of joint inflammation. This was mediated by Ly6C^{lo} monocyte-dependent recruitment of Treg cells, demonstrating their immunoregulatory role in RA [215].

The role of intermediate monocytes has also been highlighted, as their numbers are elevated in the blood and the synovial fluid of RA patients and correlate with disease severity [218-222]. They produce pro-inflammatory cytokines such as TNFα, IL-1β and IL-6, activate Th17 cells and differentiate into classically activated macrophages. Similar to classical monocytes, which generate the majority of osteoclasts [223], intermediate monocytes can differentiate into osteoclasts and mediate bone resorption in RA joints [218, 220, 224-226].

Many studies highlight the important role of the NLRP3 inflammasome and classically activated monocyte-derived macrophages as drivers of arthritic inflammation. The multi-protein complex assembles upon PAMP or DAMP sensing, resulting in the release of pro-inflammatory cytokines IL-1β and IL-18 as well as in the initiation of pyroptosis, which results in a dysregulated immune response associated with bone and cartilage destruction in RA [227]. Therefore, drug development efforts have focused on targeting both the NLRP3 inflammasome as well as M1-like macrophage polarization in arthritis. Interestingly, glucocorticoids, including triamcinolone and dexamethasone, which are used to treat arthritis, promote monocyte polarization towards alternatively activated macrophages and enhance anti-inflammatory cytokine production [228]. To limit systemic adverse effects of triamcinolone, a study by Park et *al.* demonstrated that delivering the glucocorticoid in a nanoparticle complex enhanced its anti-inflammatory and pro-repair effects in collagen-induced arthritis (CIA) by promoting macrophage polarization towards an M2-like phenotype [229]. In addition, a variety of NLRP3 inflammasome inhibitors are currently being investigated in clinical trials for their potential to treat inflammatory diseases, including arthritis (see Table 4.2) [230]. Dapansutrile for example, which inhibits NLRP3 inflammasome activation and IL-1β production, was found to reduce pain in gout patients in a phase II clinical trial [231].

It is becoming increasingly clear that important differences exist in the role of macrophages in arthritis depending on their origin, with tissue-resident macrophages possessing important homeostatic and immune regulatory functions. However, conflicting reports on tissue-resident macrophages initiating gouty inflammation or on the role of Ly6C^{lo} monocytes in RA highlight the need for further research into the mechanisms underlying monocyte/macrophage infiltration and activation in the joint.

1.4 Inflammatory signaling pathways

1.4.1 Extracellular and intracellular pathogen recognition

When tissue-resident innate immune cells, including macrophages or DCs, recognize PAMPs or DAMPs via their pattern recognition receptors, they initiate inflammatory responses. The

specific receptors initiate downstream signaling cascades resulting in the nuclear translocation of transcription factors NF-κB, AP-1, CREB as well as IRF3 or IRF7, which promote the transcription and consequently protein production of pro-inflammatory and anti-viral mediators (Fig. 1.5) [232, 233]. In addition, these signaling pathways trigger the activation of adaptive immunity [234].

TLRs are transmembrane receptors and contain three domains: The N-terminal extracellular ligand recognition domain with leucine-rich-repeat motifs, the transmembrane domain and the C-terminal cytoplasmic domain, which interacts with adapter proteins via its Toll/interleukin 1 receptor (TIR) homology domain to initiate downstream pathways [235]. TLRs were first identified in *Drosophila melanogaster* in 1985, where they were found to regulate embryo polarization [236]. Later, studies demonstrated the role of Toll in the anti-fungal response and the NF-κB-dependent innate immune cell response to LPS in *Drosophila* [237, 238]. In 1997, TLR4 was discovered as the human analog to *Drosophila* Toll, which induced NF-κB-mediated expression of pro-inflammatory cytokines and iNOS in THP1 monocytes [239]. To date, 10 TLRs have been described in humans, namely TLR1-10, while mice possess three additional TLRs (TLR11-13) with TLR10 being non-functional [235]. These TLRs can be categorized based on their cellular location: cell surface TLRs (TLR1, TLR2, TLR4, TLR5 and TLR6) are localized on the cell membrane and mostly detect PAMPs such as lipoproteins, lipids or proteins. Intracellular TLRs include TLR3, TLR7, TLR8 and TLR9 and sense nucleic acids (Table 1.2) [233].

Table 1. 2 Features and ligands of Toll-like receptors
Adapted from [233, 235, 240-243].

Receptor	Cellular location	TLR dimer formation	Ligands	Ligand origin
TLR1	Cell surface	TLR2, TLR10	Triacyl lipoproteins, modulin	Bacterial
TLR2	Cell surface	TLR1, TLR2, TLR6, TLR10	Lipoproteins, Lipoteichoic acid, peptidoglycan, zymosan, porins, glycolipids	Bacterial, fungal, viral, parasitic, self
TLR3	Endosomes	TLR3	dsRNA	Viral
TLR4	Cell surface, Endosomes	TLR4/MD2, TLR6	LPS	Bacterial, fungal, parasitic, viral, self
TLR5	Cell surface	TLR5	Flagellin	Bacterial
TLR6	Cell surface	TLR2, TLR6, TLR10	Diacyl lipoprotein, modulin, zymosan	Bacterial, fungal
TLR7	Cell surface, Endosomes	TLR7	ssRNA	Viral, bacterial, self
TLR8	Endosomes	TLR8	ssRNA	Viral, bacterial
TLR9	Endosomes	TLR9	CpG-DNA	Bacteria, viral, parasitic
TLR10	Cell surface, Endosomes	TLR1, TLR2, TLR6, TLR10	HIV-gp41, Diacyl lipoprotein?	Bacterial, viral

Upon ligand binding, TLRs dimerize to induce downstream signaling (Fig. 1.5) [244]. Except for TLR3, which signals through TRIF, all TLRs signal via MyD88-dependent pathways to

promote pro-inflammatory cytokine and chemokine production. However, TLR4 can also recruit TRIF to induce downstream transcription of type I interferon genes [242].

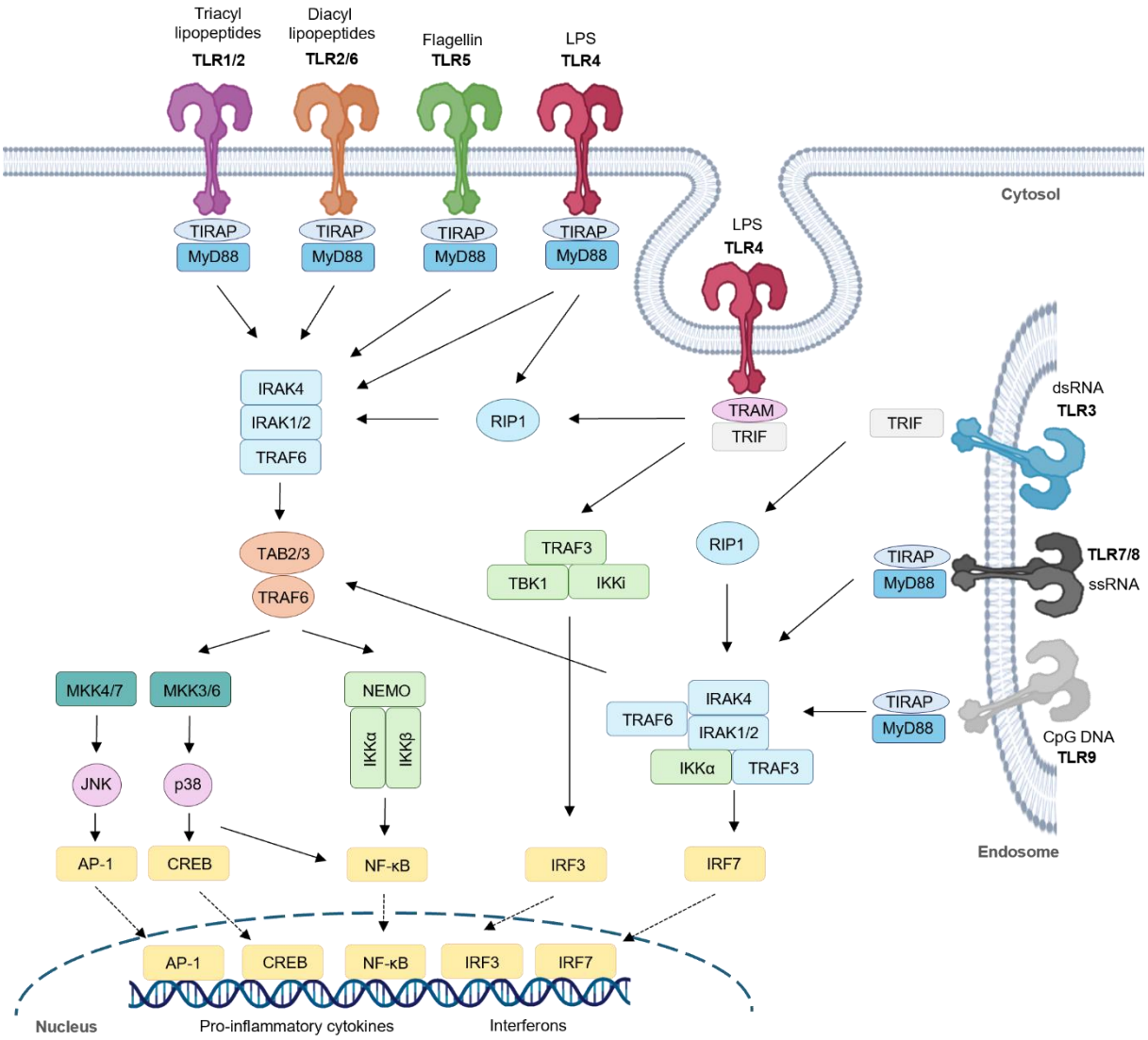


Fig. 1. 5 TLR signaling in inflammation. Upon stimulation by PAMPs or DAMPs, TLRs initiate downstream signaling cascades via TIRAP/MyD88 or the TRIF (TLR4, TLR3), resulting in the nuclear translocation of transcription factors NF-κB, AP-1, CREB as well as IRF3 or IRF7, which initiate the transcription and consequently protein production of pro-inflammatory cytokines or type I interferons. Figure created with BioRender and PowerPoint and adapted from [233, 245].

1.4.2 TLR4 signaling

TLR4 activation by LPS and its downstream signaling cascade involving NF-κB have been extensively studied in innate immune cells. LPS binding to TLR4 is mediated by LPS binding protein (LBP), which induces binding of single LPS molecules to soluble or membrane-bound CD14. CD14 then transfers LPS to MD-2, which in turn forms heterodimers with TLR4.

Subsequently, two TLR4/MD-2 complexes dimerize and form a functional signaling unit [246, 247]. In their 2020 review, Fitzgerald et *al.* highlight the advantages of this multi-step process: First, it enables even picomolar concentrations of LPS to trigger a TLR4 response. In addition, it allows thousands of macrophages to be activated by LPS derived from a single bacterium. Third, soluble CD14 can bind LPS to deliver it to cells that express TLR4 and MD-2 but not CD14, such as endothelial cells, further amplifying the local host response [246].

Upon dimerization following ligand binding, TLR4 recruits TIRAP and MyD88, which recruit IRAK4, IRAK1 and IRAK2 to form the Myddosome complex (Fig. 1.5). This results in the activation of IRAK4 through MyD88. In turn, IRAK4 activation triggers the activation and autophosphorylation of IRAK1 and IRAK2 (Fig. 1.5) [248]. Once activated, IRAK1 interacts with TRAF6, an E3 ubiquitin ligase, which polyubiquitinates itself and IRAK1. As a consequence, the TAK1 complex, consisting of TAK1 and TAB2/3 is recruited and activated [246]. Activated TAK1 phosphorylates and activates the IKK complex to initiate the NF-κB pathway. In addition, TAK1 also induces MAPK signaling through MKK4/7 and JNKs or MKK3/6 and p38, resulting in the phosphorylation and nuclear translocation of transcription factors AP-1 and CREB, respectively, where they mediate inflammatory gene transcription [233, 249].

Following endosomal internalization of TLR4-MD-2 dimers in complex with their ligand, TLR4 signaling becomes TRIF-dependent [243]. TRAM and TRIF trigger the formation of the Triffosome complex, containing TRAF6 and TRAF3. Once activated, TRAF6 recruits RIP1, causing the recruitment and activation of the TAK1 complex and the subsequent induction of NF-κB and MAPK signaling, resulting in the production of pro-inflammatory cytokines. On the other hand, TRAF3 also activates TBK1, IKKi and NEMO, which trigger the dimerization nuclear translocation of IRF3 to promote type I interferon production [243, 250, 251].

1.4.2 Inflammatory signaling pathways

1.4.2.1 NF-κB signaling

NF-κB (**N**uclear **F**actor **κ**-light-chain-enhancer of activated **B**-cells) is a transcription factor that was first described by Baltimore et *al.* 1986. It was named after the discovery that it binds to the κ-IgG light chain enhancer in B cells [252]. The transcription factor is expressed in nearly all cell types [253] and under physiological conditions regulates important processes like development, cell survival or apoptosis [254]. In addition, it is an important mediator of innate and adaptive immunity and is essential for immune responses of innate cells to pathogen infection and other stimuli such as inflammatory cytokines [255]. In innate immune cells such as monocytes and macrophages, NF-κB activation drives the transcription of cytokines, chemokines or interferon-stimulated genes (ISGs) [249]. Due to its important role in immunity, dysregulated NF-κB activity has been linked to excessive inflammatory responses underlying the pathology of inflammatory disorders including RA, gout, IBD, multiple sclerosis (MS) and atherosclerosis [256, 257]. Therefore, re-establishing appropriate of NF-κB activation is being widely investigated as a strategy to treat inflammatory diseases [258].

The mammalian NF-κB family consists of five subunits: p50 (NF-κB1), p52 (NF-κB2), p65 (RelA), c-Rel and RelB [259, 260]. These monomers can dimerize to form homo- or heterodimers, with p50/p65 being the most common dimer [261]. NF-κB activation can occur through the canonical (classical) pathway, the non-canonical (non-classical/alternative) pathway or the atypical signaling pathway [262], depending on the activating stimulus.

Canonical NF-κB signaling can be induced by cytokines (i.e. TNFα or IL-1β) or PAMPs (i.e. LPS) that are recognized by cytokine receptors or PRRs, respectively (Fig.1.6) [262]. This results in the phosphorylation of the IKK2 complex (IKKβ and NEMO (NF-κB essential modulator)) [257, 263], which in turn phosphorylates IκBα [264-266]. In the absence of stimuli, IκBα retains the p65:p50 heterodimer in the cytoplasm. Upon phosphorylation, however, IκBα is ubiquitinated and tagged for proteasomal degradation [267]. Consequently, the nuclear localization sequences are exposed and p65:p50 can translocate into the nucleus. Here, it

initiates the transcription of primary response inflammatory genes including cytokines *tnf, il-1β* and *il-6,* chemokines *il-8* and *ccl2* or other inflammatory mediators like *inos* or adhesion molecules [249, 262, 268, 269].

The non-canonical NF-κB pathway is activated by certain TNF cytokine family members [257, 270-272] (Fig.1.6). Activation is generally slower than through the classical pathway and was thus originally considered to mainly regulate B cell maturation and the development of lymphoid organs. However, emerging evidence points towards its important functions in immune responses [273].

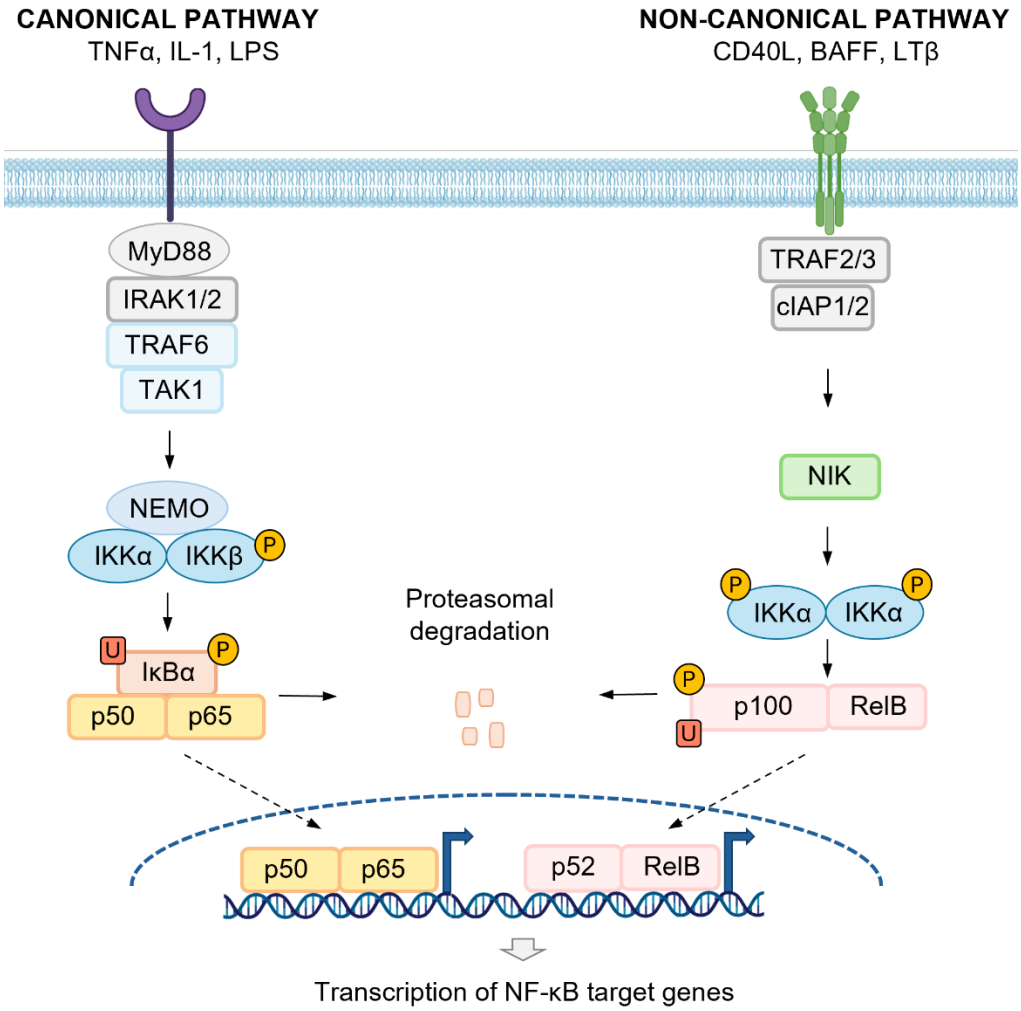


Fig. 1. 6 The canonical and non-canonical NF-κB signaling pathways. Canonical or non-canonical signaling in macrophages can be activated by various stimuli and result in the activation of a NF-κB heterodimer, which translocates into the nucleus to induce the transcription of pro-inflammatory target genes, including cytokines, chemokines, adhesion molecules and other pro-inflammatory mediators. This figure was generated with BioRender and PowerPoint and summarizes experimental findings reviewed in [249, 257, 262].

Atypical NF-κB signaling is mostly triggered by genotoxic stress including UV damage or ROS exposure. In addition, atypical NF-κB activation can also be induced by kinases, including casein kinase 2 or tyrosine kinases like EGFR [274-278].

1.4.2.2 The NLRP3 inflammasome

Inflammasomes are multi-protein complexes that mediate immune responses against PAMPs released by pathogens or sterile host- or environment-derived DAMPS (Fig. 1.7) [279].

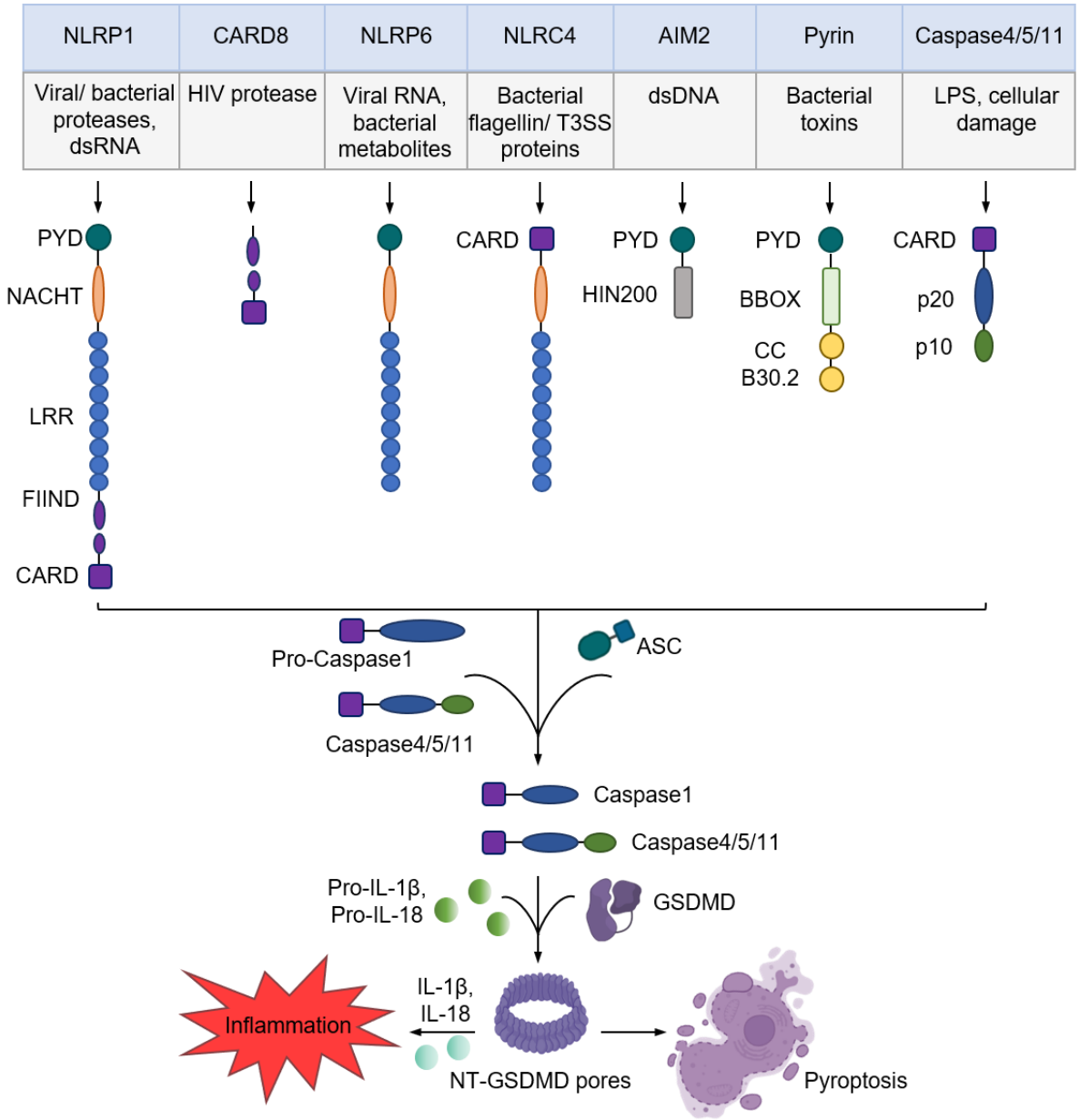


Fig. 1. 7 Overview of inflammasomes and their activators. Activation of various inflammasomes by various PAMPs or DAMPs results in the cleavage and activation of Caspase1 or activation of Caspases 4/5/11. Caspase1 and Caspases 4/5/11 cleave and activate Gasdermin D (GSDMD) to free its N-terminus (NT-GSDMD), which results in pore formation, NLRP3 inflammasome activation, pro-inflammatory IL-1β and IL-18 release, and potentially pyroptosis. Caspase1, not Caspases 4/5/11, cleaves pro-IL-1β into its mature form before its release. Figure generated with BioRender and PowerPoint. This figure summarizes findings presented in [280-284].

The NLRP3 inflammasome consists of sensor protein (PRR) NLRP3, adaptor protein ASC and effector protein pro-Caspase-1 [285]. NLRP3 inflammasome activation requires two sequential signals (Fig. 1.8): As the priming signal (signal 1), TLR agonists like LPS activate the NF-κB pathway, leading to NLRP3 transcription and post-transcriptional activation as well as pro-IL-1β and pro-IL-18 production. Various stimuli, such as extracellular ATP or MSU crystals, can act as signal 2 to trigger the assembly of the inflammasome complex. As a consequence, NLRP3 oligomerizes, resulting in ASC speck assembly and the recruitment of pro-Caspase-1. The effector self-cleaves and is now able to process pro-IL-1β and pro-IL-18 into their mature, active form. While IL-1β secretion is associated with inflammatory responses resulting in immune cell recruitment and the exacerbation of inflammation, IL-18 promotes IFN-γ production and adaptive immune responses [286, 287]. In addition, Caspase-1 also cleaves gasdermin D, which consequently forms membrane pores. This leads to the release of IL-1β and IL-18 and induces pyroptosis, a form of programmed inflammatory cell death [288]. Under steady-state conditions, NLRP3 activity in macrophages and neutrophils is low. However, pathologically elevated NF-κB activation and NLRP3 inflammasome activity are associated with many inflammatory disorders, including RA and gout [289].

Dysregulated NLRP3 inflammasome activity is a feature of many inflammatory diseases, making it an attractive target for drugs with wide-ranging therapeutic possibilities [230]. Many current drug development strategies, such as the development of anti-IL-1R agonists, involve NLRP3 inflammasome inhibitors targeting different stages of inflammasome priming and activation. However, recent studies have demonstrated that this approach may lack efficacy due to the redundancy of mediators involved in NLRP3 inflammasome activation [290, 291]. Fischer et *al.* recently identified kinases TBK1 and IKKε as important physiological off-switches of NLRP3 activation, which are counteracted by PP2A phosphatase [291]. Further research into such endogenous phosphor-switches is required, but targeting excessive NLRP3 activation by dysregulated PP2A activation could be an alternative strategy to treat inflammatory pathologies.

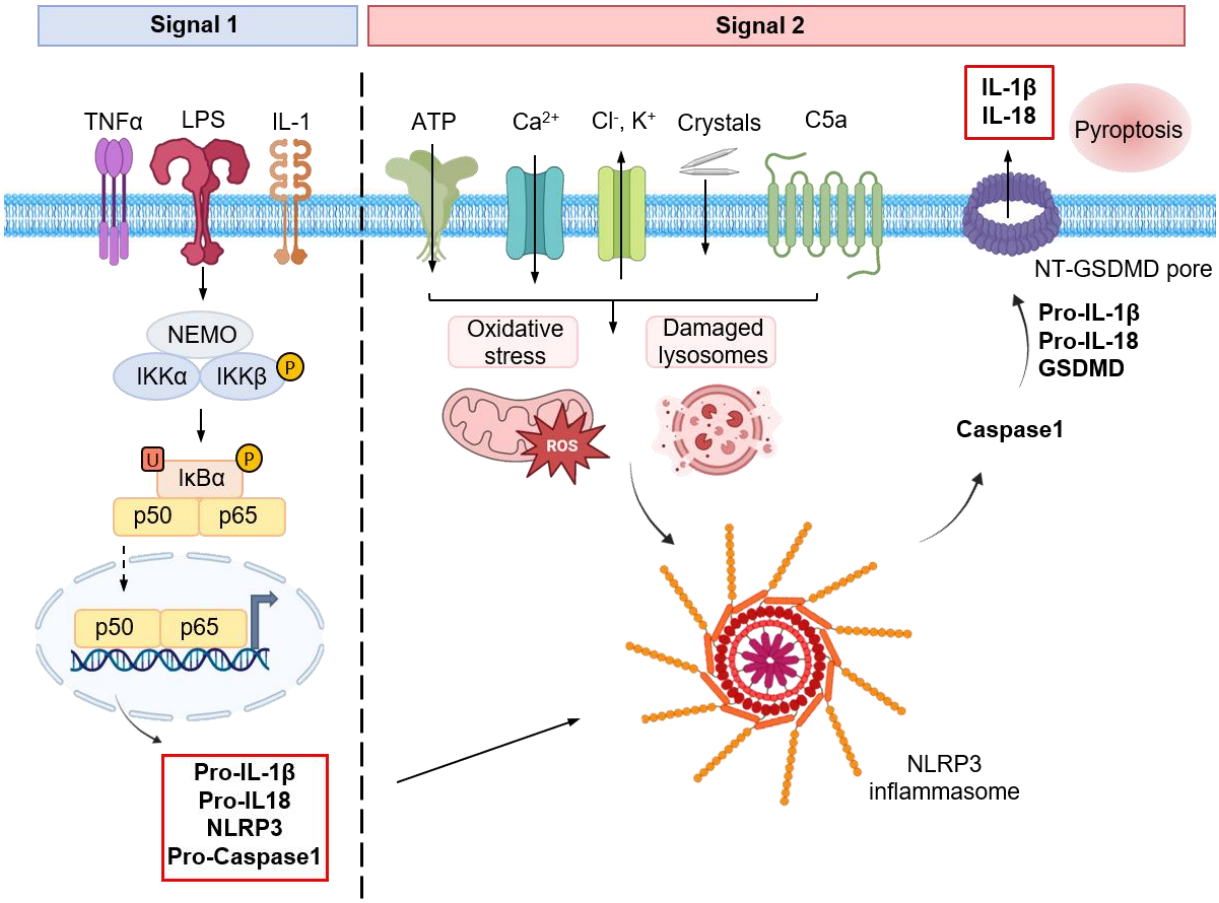


Fig. 1. 8 Priming and activation of the NLRP3 inflammasome. Signal 1 (inflammasome priming) occurs upon PRR activation, e.g. after LPS binding to TLR4, or upon binding of pro-inflammatory cytokines, such as IL-1 or TNFα, to their respective receptors. Downstream, NF-κB signaling is initiated, resulting in the transcription of pro-IL-1β, pro-IL-18, NLRP3 and pro-Caspase1. Signal 2 (inflammasome assembly) is provided by various stimuli, such as extracellular ATP, ion fluxes, crystals or complement activation. This results mitochondrial dysfunction, oxidative stress and lysosomal damage, inducing the assembly of the NLRP3 inflammasome complex. Consequently, Caspase1 is cleaved and activated, which in turn cleaves pro-IL-1β, pro-IL-18 into their mature forms and cleaves Gasdermin D (GSDMD) to free its N-terminal domain and allow it to form membrane pores. As a result, mature IL-1β and IL-18 are released and pyroptosis can be initated. Figure generated with BioRender and Powerpoint and is adapted from or contains findings summarized in [292-296].

1.5 Tyrosine kinase signaling in inflammation

In the human genome, 90 tyrosine kinases have been identified, including 58 receptor tyrosine kinases and 32 non-receptor tyrosine kinases [297]. Many inflammatory processes are modulated by tightly regulated kinase and phosphatase activity. Both surface receptor and intracellular non-receptor tyrosine kinases transduce signals during innate immune cell activation in inflammation, thus mediating the production of pro-inflammatory mediators and the recruitment and activation of leukocytes (Fig. 1.9).

1.5.1 VEGFR

Vascular endothelial growth factor receptors (VEGFRs) 1 (Flt-1), 2 (KDR/Flk-1) and 3 (Flt-4) are receptor tyrosine kinases which are important mediators of angiogenesis and vascular permeabilization and can be associated with cancer and inflammation (Fig. 1.9) [298]. Therefore, various VEGFR inhibitors have received FDA approval for the treatment of malignancies, including sorafenib, regorafenib, lenvatinib or axitinib [299].

VEGFR-1 is expressed on macrophages and its expression can be further up-regulated in response to LPS [300, 301]. VEGFR-1 can induce monocyte and macrophage chemotaxis towards VEGF [300-303] and promote neutrophil activation and migration in pathological inflammatory conditions such as preeclampsia [304]. In contrast, Wheeler et *al.* found that while decidual VEGF production is enhanced in early pregnancy and recruits macrophages, it induces alternative macrophage activation and prevents classical macrophage polarization associated with preeclampsia [305].

In cancer, VEGFR-2 mediates macrophage recruitment to tumors and promotes TAM polarization [306, 307]. In the context of inflammation, VEGFR-2 was found to contribute to the pathology of age-related macular degeneration by promoting the formation of characteristic choroidal neovascularization. VEGFR-2 inhibition by tyrosine kinase inhibitor (TKI) fruquintinib resulted in the suppression of NF-κB-mediated CCL2 expression by endothelial cells and the reduction of M1 macrophage polarization and migration [308]. In rats with CFA-induced arthritis, VEGFR-2 induced microglia infiltration to the dorsal horn and monocyte attachment to brain endothelial cells by upregulating ICAM-1 on ECs to promote chronic pain [309]. A similar up-regulation of endothelial ICAM-1 by VEGF/VEGFR-2 was observed to enhance neutrophil adhesion and disease severity in a mouse model of IBD [310].

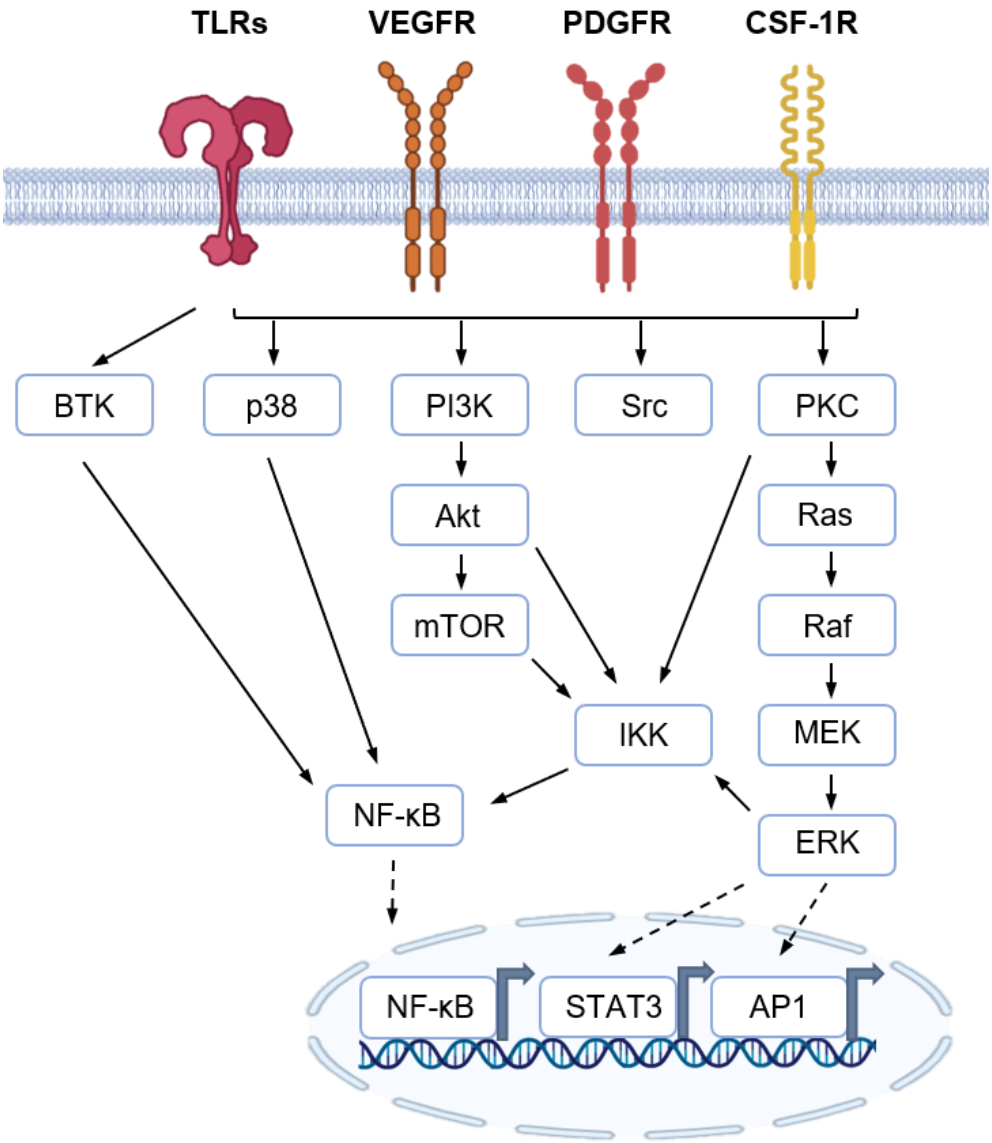


Fig. 1. 9 Tyrosine kinase signaling in inflammation. The activation of tryrosine kinase receptors VEGFR, PDGFR or CSF-1R as well as TLR activation results in the downstream activation of signaling pathways involving tyrosine kinases BTK and Src as well as PI3K/Akt and MAPK signaling pathways. Consequently, the IKK complex is activated, resulting in the nuclear translocation of transcription factors NF-kB, STAT3 and AP-1, which initiate the transcription of pro-inflammatory genes. Figure generated with BioRender and Powerpoint. Figure summarizes reports from [311-317].

1.5.2 PDGFR

Platelet-derived growth factor receptor β (PDGFR-β) is a receptor tyrosine kinase highly expressed on macrophages. It is implicated in physiological processes of embryonic development and wound healing as well as disease pathology in cancer, pulmonary fibrosis, atherosclerosis or neuroinflammation [318, 319]. Activated macrophages and vascular smooth muscle cells in atherosclerotic lesions are a source of PDGF, which induces PDGFR-β-

mediated leukocyte recruitment and enhances plaque formation [318, 320]. Lung fibrosis is associated with increased levels of lung PDGF, which is produced by epithelial cells and alveolar macrophages, leading to fibroblast proliferation [321-323].

Macrophage PDGFR-β expression has also been associated with monocyte/ macrophage chemotaxis and infiltration to sites of inflammation [318, 324]. PDGF was found to induce CCL2 production by astrocytes through induction of MAPK, JNK and PI3K/Akt signaling and downstream NF-κB activation, which promoted monocyte chemotaxis through human brain microvascular endothelial cells to mimic blood-brain barrier breakdown in neuroinflammation [325]. Similarly, studies by Yang et *al.* and Ma and colleagues showed that intracerebral hemorrhage induced PDGF overexpression, which promoted macrophage and neutrophil infiltration, microglial activation and pro-inflammatory cytokine production, possibly by disrupting the blood-brain barrier [319, 326]. PDGFR inhibition with imatinib attenuated brain injury and neuroinflammation and protected the blood brain barrier [319, 326].

1.5.3 CSF-1R

Colony stimulating factor 1 receptor (CSF-1R), also termed M-CSFR, c-FMS or CD115, is a receptor tyrosine kinase expressed on myeloid cells including monocytes and macrophages and mediates their proliferation, differentiation, survival, activation, adhesion and migration [327, 328]. The receptor recognizes agonists CSF-1 (M-CSF) and IL-34, which trigger receptor dimerization and tyrosine phosphorylation, resulting in the recruitment of SH2 domain-containing proteins, such as Src. Downstream, PI3K/Akt, MAPK, JAK-STAT and NF-κB signaling pathways are activated (Fig. 1.9) [328, 329].

CSF-1R activation is required for macrophage cytoskeletal rearrangements, cell proliferation and adhesion during chemotaxis [330]. CSF-1 and IL-34 can induce alternative activation of macrophages under homeostatic conditions [331-334] and promote phagocytosis and tissue repair [327, 335].

Increased circulating CSF-1 levels have been detected in many inflammatory diseases [327], associating CSF-1R with inflammatory pathologies such as RA, MS or atherosclerosis [328].

CSF-1R inhibition had anti-inflammatory and disease-modulating effects in animal models of MS and was even found to promote remyelination by targeting microglia and oligodendrocytes [336-338]. In RA, CSF-1R expression is enhanced and downstream signaling pathways, including NF-κB, promote the production of pro-inflammatory cytokines [328]. Pharmacological inhibition of CSF-1R was shown to attenuate inflammation and disease pathology in arthritis models *in vivo* [339, 340]. *In vitro* studies confirmed that CSF-1R activation triggers macrophage NF-κB activation and CCL2 expression, which are associated with classical macrophage activation and monocyte recruitment, while CSF-1R inhibition blocked LPS-induced pro-inflammatory cytokine production [341, 342].

These findings summarized above demonstrate that CSF-1R has both immunoregulatory as well as pro-inflammatory effects on macrophages; inhibition of CSF-1R in pathological inflammation seems to be a promising strategy to attenuate inflammation and disease pathology.

1.5.4 Src family kinases

To date, nine members of the Src kinase family have been identified, including Lyn, Fyn, Lck, Hck, Fgr, Blk, Yrk, Yes and c-Src (Src) [343]. Src activity mediates cell proliferation, survival, adhesion and migration, leukocyte recruitment, phagocytosis as well as angiogenesis and has thus been implicated in the pathogenesis of various inflammatory diseases, including cancer, rheumatoid arthritis or inflammatory skin disease [343, 344]. Due to its oncogenic function, multiple tyrosine kinase inhibitors targeting Src in cancer have been developed and have received FDA approval, including bosutinib, dasatinib and ponatinib [343, 345].

Members of the Src family share four conserved SRC homology (SH) domains (SH1-4) and a tyrosine residue (Tyr527) in the C-terminus, which, when phosphorylated, induces Src inactivation through conformational changes that prevent ATP binding [346]. Conversely, auto-phosphorylation of Tyr-416 and dephosphorylation of Tyr527 induce the active conformation of Src, which allows binding partners or substrates to bind to the SH2 or SH3 domain [343].

Src, Fyn, Yes and Frk are expressed ubiquitously, while Blk, Hck, Fgr and Lyn are expressed by myeloid cells, including macrophages [346]. A common downstream mediator of Src kinase signaling is spleen tyrosine kinase (Syk), which contains an SH2 domain and is found in many haematopoietic cells [344]. In leukocytes, Src is activated downstream of receptor tyrosine kinases such as PDGFR or CSF-1R and promotes inflammatory signaling resulting in the production of pro-inflammatory mediators [347]. In addition, Src regulates inflammatory leukocyte recruitment by inducing slow leukocyte rolling, arrest and endothelial adhesion as well as transendothelial migration and chemotaxis (see Chapter 5) [52, 348-353]. Further, Src promotes phagocytosis, as the phagocytic capacity of fibroblasts was found to be reduced in Src-deficient cells [354].

In macrophages, Src is involved in the downstream signaling cascades initiated upon TLR activation, including TLR2/6, TLR3, TLR4, TLR7/8 and TLR9 [346]. Upon lipoteichoic acid (LTA) stimulation of TLR2, Src is phosphorylated and activated by PKCδ, resulting in the activation of transcription factors AP-1 and NF-κB and the consequent induction of pro-inflammatory cytokine expression in RA synovial fibroblasts [355]. Similarly, Src activation upon LTA-induced TLR2 stimulation resulted in the initiation of pro-inflammatory signaling cascades via PDGFR transactivation, including PI3K/Akt and MAPK signaling, which induced the NF-κB pathway. This resulted in the production of pro-inflammatory mediators and enhanced migration of astrocytes [356].

Src is also involved in downstream signaling of TLR4 upon LPS stimulation. The expression of Src family kinases Src, Lyn, Fgr and Hck is up-regulated upon LPS stimulation in murine and rat macrophages [357, 358]. In human macrophages, Lyn has been shown to directly bind to CD14, which associates with TLR4 upon LPS stimulation, resulting in the downstream phosphorylation of Hck and Fgr as well as pro-inflammatory cytokine production [359]. Similarly, Hck and Lyn promote an inflammatory response upon LPS stimulation of murine macrophages *in vitro* [360-362]. These findings were validated by pharmacological inhibition of Src with PP1, which suppressed Hck phosphorylation as well as TNF and iNOS production

in LPS-stimulated RAW 264.7 macrophages [363]. TLR4-mediated Src activation in LPS-stimulated macrophages is MyD88-dependent, triggers MAPK signaling and promotes phagocytosis [364]. In contrast to these *in vitro* findings, studies using *hck*$^{-/-}$*fgr*$^{-/-}$*lyn*$^{-/-}$ triple-KO mice demonstrated that these three Src family kinases may be dispensable for the NF-κB-mediated inflammatory response of macrophages to LPS in mice *in vivo* [358].

1.5.5 BTK

Non-receptor tyrosine kinase Bruton's tyrosine kinase (BTK) is essential for B cell function and development and drives B cell proliferation and survival in leukemia. Therefore, multiple BTK inhibitors have been developed, including ibrutinib, acalabrutinib and zanubrutinib [365]. Activation of the B cell receptor or TLRs triggers Src-induced BTK activation and subsequently phosphorylates PLCγ and PI3K to induce downstream MAPK and NF-κB signaling (Fig. 1.9) [366]. BTK is highly expressed in B cells and myeloid cells, especially monocytes/macrophages and neutrophils [367]. BTK mediates TLR2 and TLR4 responses in macrophages and is required for the production of pro-inflammatory cytokines TNF and IL-1β [368-370].

Upon macrophage LPS stimulation, BTK gets phosphorylated and activated and can directly interact with TLR4 as well as adaptor proteins MyD88, MyD88-adapter like (Mal) and IRAK1 [369, 371]. It induces NF-κB signaling in monocytes and macrophages, which was demonstrated via pharmacological BTK inhibition with LFM-A13 or ibrutinib [370-372]. In addition, BTK can directly interact with NLRP3 and ASC to promote NLRP3 phosphorylation and inflammasome assembly, resulting in IL-1β secretion by macrophages [372-376].

Given its role in macrophage inflammation, Purvis et *al.* demonstrated that BTK inhibition could reduce neutrophil and monocyte recruitment as well as pro-inflammatory mediator production in zymosan-induced peritonitis (ZIP). These effects were attributed to reduced NF-κB/Akt activation as well as attenuated monocyte/macrophage chemotaxis in response to ibrutinib treatment [377]. Further studies have shown that BTK inhibition has anti-inflammatory and disease-attenuating effects in *in vivo* models of ischemic brain injury [375], arthritis [378, 379],

sepsis [380], metabolic inflammation [372], SLE [381, 382] and MS [383-385]. Therefore, clinically used BTK inhibitors may be promising drug repurposing candidates for inflammatory diseases outside of B cell leukemia. In addition to its original indications of leukemia and lymphoma treatment, ibrutinib has since been approved as the first specific therapeutic for chronic graft versus host disease [386].

1.6 Current anti-inflammatory medicines

1.6.1 NSAIDs

Non-steroidal anti-inflammatory drugs (NSAIDs) are amongst the most frequently prescribed medicines to manage fever, pain and inflammation, accounting for 5-10 % of annual prescriptions [387]. However, they can cause significant gastrointestinal (GI) and cardiovascular adverse events, with NSAIDs being responsible for the death of around 16,500 rheumatoid arthritis and osteoarthritis patients due to GI toxicity per year in the USA. Therefore, NSAIDs require close monitoring of side effects and limitation of dose and duration of administration are strongly recommended [387, 388].

NSAIDs target the two isoforms cyclooxygenase 1 and 2 (COX-1/2), which are part of the arachidonic acid pathway. The enzymes convert arachidonic acid into precursors of prostaglandins and thromboxane A_2. Bioactive prostaglandins include prostaglandin E_2 (PGE_2), prostacyclin (PGI_2), prostaglandin D_2 (PGD_2) and prostaglandin $F_{2\alpha}$ ($PGF_{2\alpha}$) [389].

COX-1 is constitutively expressed in most tissues under physiological conditions and plays important roles in gastric mucosa protection, platelet aggregation, renal function and hemostasis. However, COX-1 expression can be up-regulated on monocytes and PMNs during inflammation [390]. COX-2 expression is more restricted and is induced upon inflammatory stimulation in inflammatory cells [387, 388]. For example, COX-2 expression is increased by NF-κB activation and subsequent IL-1β production in the synovium of RA patients [391, 392]. Consequently, COX-2 activity induces inflammation, pain and fever. NSAIDs that selectively target COX-2 over COX-1 are considered safer as they have fewer adverse effects. However, COX-2 inhibitors are still associated with considerable cardiovascular toxicity [387].

Interestingly, studies have found NSAIDs to have both pro- and anti-inflammatory effects on macrophages. Targeted delivery of low dose (0.24 mg/kg) NSAID Celecoxib to monocytes was shown to reduce sciatic nerve pain in rats by reducing macrophage infiltration and pro-inflammatory COX-2 and PGE_2 levels [393]. COX-2 also induced IL-6 secretion in peritoneal macrophages by promoting PGE_2 production during LPS-induced inflammation *in vitro*, which could be inhibited by COX-2 inhibitor NS-398 [394]. However, a study by Haimerl et *al.* found that chronic NSAID–exacerbated respiratory disease is associated with increased macrophage numbers, chemokine production and pro-inflammatory macrophage phenotypes [395]. These findings are consistent with the report that constant COX inhibition drives pro-inflammatory polarization in macrophages, associated with enhanced TNFα production and NF-κB activation, both *in vitro* as well as in a mouse model of endotoxemia [396]. NSAIDs, including indomethacin, were further shown to increase TNFα production in LPS-stimulated RAW264.7 macrophages while aspirin and phenylbutazone suppressed TNFα secretion. Aspirin also enhanced macrophage phagocytotic capacity and reduced $CD4^+$ T cell proliferation while enhancing $CD8^+$ T cell proliferation [397].

1.6.2 Glucocorticoids

In 1946, Kendall was the first to isolate glucocorticoid cortisone from the adrenal gland [398], which was synthesized by Sarett in the same year [399]. Three years later, Hench described the benefits of treating RA with cortisone [399]. In 1950, Kendall and Hench were awarded the Nobel Prize for their scientific contributions regarding glucocorticoids [398].

Glucocorticoids (GCs) are cholesterol-derived steroid hormones that are produced mostly by the adrenal gland but also in local cells and tissues like epithelia or the brain [400]. Their production is controlled by the hypothalamic-pituitary-adrenal (HPA) axis and is subject to circadian regulation, with glucocorticoid production peaking between 6-8 am [401]. Under physiological conditions, glucocorticoids are involved in the regulation of metabolism, water and electrolyte balance, immune functions, development and growth, cardiovascular function, cognitive function and reproduction [400]. During inflammation, infection or trauma as well as

during emotional stress, glucocorticoid production is enhanced. They bind to the glucocorticoid receptor (GR) that belongs to the nuclear receptor family. The GR is constitutively expressed in most tissues and upon ligand binding undergoes conformational changes and translocates into the nucleus, where it initiates the transcription of anti-inflammatory genes [400, 401]. Pro-inflammatory NF-κB signaling and immunoregulatory GR activity mutually regulate each other, mostly in an antagonistic manner [402]. This cross-regulation can occur in the form of trans-repression (GR inhibits inflammatory NF-κB target genes), trans-activation (GR induces genes inhibiting NF-κB) or competition for co-factors required for transcriptional activation [402]. Interestingly, studies found that the GR increased the binding affinity of IκB to the NF-κB heterodimer, bound directly to p65, p50 and IκB and promoted IκB production and stability to facilitate trans-activation by promoting NF-κB inactivation in the cytosol [403, 404]. To inhibit inflammatory gene transcription induced by NF-κB by trans-repression, glucocorticoids can prevent NF-κB from binding to the DNA or to components of the transcription machinery as well as directly inhibit the transcription factor's transcriptional activity [405-408]. In addition, the GR was also observed to promote the export of p65 from the nucleus into the cytosol [409, 410].

Thus, GR activation inhibits the production of NF-κB-driven production of pro-inflammatory mediators, including IL-6, TNFα, GM-CSF, CCL5, CXCL8, iNOS or COX-2 as well as adhesion molecules ICAM-1 and VCAM-1 and at the same time enhances anti-inflammatory cytokine production (e.g. IL-10) [401, 411]. Therefore, glucocorticoids are frequently prescribed for the treatment of inflammatory conditions such as asthma, RA, MS, SLE, allergy or shock [400, 401].

Naturally occurring glucocorticoids have short half-lives to prevent unwanted side effects. Therefore, synthetic glucocorticoids, such as prednisone or dexamethasone, have been developed using cortisone as a scaffold to increase their half-life and enhance their anti-inflammatory properties [401]. However, long-term glucocorticoid treatment or administration of high doses are associated with serious adverse effects, including neurotoxicity,

cardiovascular toxicity, metabolic toxicity, systemic immune suppression, GI toxicity, hepatotoxicity and the development of glucocorticoid resistance [401, 412]. As a consequence, long-term use for treatment of chronic conditions as well as systemic applications are limited and require close monitoring of the patient.

1.6.3 DMARDs

Disease-modifying anti-rheumatic drugs (DMARDs) are immunomodulatory medicines employed to treat inflammatory disorders including RA, psoriatic arthritis, ankylosing spondylitis, IBD and SLE [413]. Generally, three classes of DMARDs can be distinguished: Conventional synthetic DMARDs (csDMARDs) are first-line treatments and include methotrexate, hydroxychloroquine and sulfasalazine and inhibit inflammatory processes at different stages to cause immune suppression. Biological DMARDs (bDMARDs) include antibody therapies such as infliximab, adalimumab, golimumab, certolizumab (anti-TNFα), tocilizumab (anti-IL-6), rituximab (anti-CD20) and anakinra (anti-IL-1R) or receptor-immunoglobulin fusion molecules (e.g. abatacept, CD80/CD86 co-stimulation inhibitor). They target specific cytokines, blocking their production, function or downstream signaling. Alternatively, they inhibit T cell activation or promote B cell depletion [413, 414]. Biological DMARDs are prescribed to patients that do not respond to csDMARDs, either alone or in combination with csDMARDs, e.g. methotrexate, or other bDMARDs [414]. Recently, targeted synthetic DMARDs (tsDMARS) have been developed, such as JAK/STAT inhibitor tofacitinib, that target pro-inflammatory pathways in inflammatory diseases and have safety and efficacy profiles comparable to those of bDMARDs [413, 414].

While csDMARDs can successfully limit bone damage and inflammation, they have low specificity and bioavailability and thus can cause severe GI as well as liver and kidney toxicity, which significantly limits their use to treat chronic inflammation [415]. Biological DMARDs on the other hand have a very specific mode of action and consequently have improved efficacy and safety profiles, making them more suitable for long-term treatment [415]. However, increased risk of developing infections or hypersensitivity and the development of drug

resistance are important limitations [414, 415]. In addition, bDMARDs may have limited stability and some require administration via injection, which may need to be supervised by trained professionals. Another important limitation is the high cost associated with bDMARD treatment, especially when administered regularly for the treatment of chronic inflammatory diseases [416].

1.6.5 Limitations of current anti-inflammatory medicines

Current anti-inflammatory medicines of the different classes described above have been used for decades to suppress inflammation and manage pain associated with inflammatory disorders. However, anti-inflammatory drugs used in the clinic have many, often serious, adverse events that limit their therapeutic potential (Table 1.3). One of the most important limitations is that GCs and DMARDs inhibit processes driving pathological inflammation but at the same time target mechanisms that are key for an efficient immune response to infection and tissue injury.

Some drug development strategies have focused on developing new classes of anti-inflammatories targeting matrix metalloproteases, cannabinoid receptors 1 and 2, ion channels, chemokine receptors and tyrosine or serine/threonine kinases, some of which have advanced to clinical trials [417]. Other approaches involve developing new nanotechnologies to target current anti-inflammatory drugs to specific cells or tissues and reduce adverse effects by lowering required drug doses and limiting systemic exposure [415]. Another promising approach to accelerate inflammatory drug development and to decrease risk of failure in clinical trials is drug repurposing, which aims at identifying new applications for already approved medicines besides their original indication [418].

While drug re-engineering lacks some of the benefits of drug repurposing, such approaches could be employed to specifically improve the pharmacokinetic profiles of existing drugs and to limit their off-target effects, either by strategically altering their chemical structures or by coupling them to delivery systems [419]. Many drugs currently used for clinical applications were originally selected for their efficacy in their original indication. Thus, drug re-engineering

could optimize the properties of drug repurposing candidates for new proposed indications, including inflammatory diseases.

Table 1. 3 Adverse effects of current anti-inflammatory medicines
Abbreviations: GI= gastrointestinal, CV= cardiovascular, COPD= chronic obstructive pulmonary disorder

Toxicity	NSAIDs	GCs	cDMARDs	bDMARDs
GI	•Dyspepsia •Gastroduodenal ulcers •GI bleeding and perforation	•Gastritis •Gastric ulcers •GI bleeding and perforation •Pancreatitis	•Diarrhea •Nausea •Abdominal pain •GI distress •stomatitis	•Worsening IBD •Diverticulitis •GI perforation
CV	•Edema •Hypertension •Congestive heart failure •Myocardial infarction •Stroke and other Thrombotic events •Atrial fibrillation	•Hypertension •Coronary or ischemic heart disease •Heart failure •Atherosclerosis	•Hypertension •Cardio-myopathy •Interstitial lung disease	•Worsening of congestive heart failure •Worsening COPD
Kidney	•Electrolyte imbalance •Sodium retention •Edema •Reduce glomerular filtration rate •Nephrotic syndrome •Acute interstitial nephritis •Renal papillary necrosis •Chronic kidney disease	•Adrenal insufficiency	•Renal dysfunction	
Liver	Rare •Hepatitis •Jaundice •Aminotransferase and bilirubin elevation	•Hepatic stenosis •Fatty liver	•Liver cirrhosis •Hepatitis •Hepatic fibrosis	•Elevated liver function test
Metabolic		•Hyper-glycemia •Diabetes mellitus •Dyslipidemia •Weight gain •Cushing-like syndrome •Muscular atrophy •Osteoporosis	•Folic acid deficiency •Weight loss •Rashes	•Hyper-lipidemia
Immunologic	•Thrombo-cytopenia	•Immune suppression •Predisposition to infections	•Immune suppression •Predisposition to infections	•Infections •Reactivation of latent infections •Drug-induced lupus

		•Reactivation of latent infections	•Reactivation of latent infections •Bone marrow suppression •Anemia •Leukopenia	•Exacerbation demyelinating diseases •Lymphomas, skin cancers •Pan-cytopenia •Neutropenia
References	[387, 420, 421]	[401, 412, 422]	[413, 416]	[413, 414]

Significant drug development efforts have focused on identifying anti-inflammatory compounds with improved safety and efficacy profiles. A major challenge has been the limited clinical predictivity of pre-clinical inflammatory animal models for clinical trials involving human patients. Mouse models of inflammation often only partially mimic human pathology and even if a disease manifests in a similar way in mouse models, it may be driven by different pathways [423]. Mice used in pre-clinical studies are often inbred strains and thus lack the genetic diversity found in humans and display differences in immune responses [424]. Importantly, a study conducted by Seok et *al.* reported that genomic responses of humans to acute inflammatory stimuli differed significantly from those in mice [425]. In addition, adverse events often go undetected in animal models [424]. Therefore, emerging human disease models using organoids, bioengineered tissues or organs-on-chips, which more accurately mimic pathological mechanisms and toxicology, may become increasingly important to help bridge this translational gap [424].

1.7 Original hypothesis and experimental aims

Dysregulated inflammatory responses are associated with acute and chronic inflammatory diseases, including gout and RA. Given the extensive side effect profiles of current anti-inflammatory medicines, an unmet clinical need exists for new safe and effective anti-inflammatories. Drug repurposing is an attractive approach to identify approved medicines with novel anti-inflammatory activities.

Macrophages are important regulators of homeostasis and tissue-resident macrophages are amongst the first cells to respond to infection or tissue injury. Thus, they mediate the onset of acute inflammation through initiation of NF-κB signaling and the consequent production of pro-

inflammatory adhesion molecules, cytokines, chemokines and reactive oxygen/nitrogen species, which results in the recruitment of inflammatory leukocytes. Macrophage phenotypes are highly plastic, allowing the cells to switch from a pro-inflammatory phenotype associated with enhanced NF-κB activation to a pro-resolving phenotype with reduced NF-κB signaling during inflammation resolution. Thus, prolonged pro-inflammatory macrophage activation and excessive NF-κB activation are linked to the pathology of many inflammatory diseases.

Therefore, identifying compounds that target NF-κB in macrophages to restore appropriate NF-κB activation and dampen the inflammatory response is an attractive approach to develop new anti-inflammatory medicines. In addition, a better understanding of macrophage inflammatory signaling can help identify pathways that can be targeted by new anti-inflammatory medicines.

At the start of my studies, I hypothesized that a macrophage-based drug repurposing strategy can be employed to identify FDA-approved medicines with previously unreported NF-κB inhibitory and anti-inflammatory properties both *in vitro* and *in vivo.*

Based on this original hypothesis, the experimental aims of this thesis are to

1. Identify a reliable macrophage-based assay to screen FDA-approved medicines and to identify those with novel anti-NF-κB activity.
2. Validate and characterize the anti-inflammatory effects and the underlying mechanisms of drug repurposing candidates in primary macrophages *in vitro*.
3. Investigate anti-inflammatory effects and mechanism of action of drug repurposing candidates in an NF-κB-driven model of acute inflammation *in vivo*.
4. Elucidate the mechanisms of drug repurposing candidates by studying leukocyte adhesion and migration *in vitro* and *in vivo*.
5. Explore the feasibility of repurposing approved medicines that target macrophage inflammation as new anti-inflammatory drugs by using human primary cells and investigating adverse effects in an *in vivo* model of acute inflammation.

Chapter 2: Materials and Methods

2.1 Reagents

All reagents were purchased from Sigma unless otherwise stated. The TOCRIScreen Kinase Inhibitor Library (Cat. No 6268) was purchased from TOCRIS. To confirm screening results, RO-31-8220 (Merck), ZM 306416 hydrochloride (R&D systems), p38 MAPK inhibitor VIII/ EO 1428 (Cambridge Biosciences), gefitinib hydrochloride (Cambridge Biosciences) and aminopurvalanol A (Cambridge Biosciences) were purchased. For the screening of FDA-approved tyrosine kinase inhibitors, apatinib, erlotinib hydrochloride, regorafenib hydrochloride, orantinib, ponantinib, sorafenib tosylate, pazopanib, vandetanib, nintedanib, lenvatinib, cabozantinib and tivozanib were purchased from Cambridge Biosciences and saracatinib, afatinib dimaleate and axitinib were purchased from Enzo Life Sciences. IKK-16 was purchased from Selleckchem and T-5224 (AP-1 inhibitor) was purchased from Stratech Scientific. Dulbecco's Modified Eagle Media (DMEM), RPMI 1640, penicillin plus streptomycin (P/S) and ACK lysis buffer were purchased from Gibco. Fluorophore-conjugated antibodies for flow cytometry and unconjugated CD16/32 antibody were from BioLegend. All western blot antibodies were purchased from Cell Signalling Technologies, except for the NLRP3 and ASC antibodies, which were purchased from AdipoGen and Santa Cruz Biotechnology, respectively. BSA (heat shock fraction, protease-free, fatty acid-free, globulin-free, pH7, ≥ 98%) was purchased from Merck. RAW-Blue, THP1-Dual and THP1-ASC-GFP cells, Quanti-Blue solution, blasticidin and zeocin were purchased from InvivoGen. LPS was from *E.coli* serotype O111:B4. Cell Titer Glo and Griess assay kits were purchased from Promega. ELISA DuoSet kits were purchased from R&D Systems and the albumin matched ELISA antibody pair kit was purchased from Abcam. Pierce BCA assay kit and NuPage gels were purchased from ThermoFisher Scientific. The Trans-Blot Turbo RTA Transfer kit with PVDF membranes was purchased from Bio-Rad. Cytospin staining was carried out using the Hema-Rapid staining set GURR for haematology from VWR Chemicals. RTCA CIM-16 plates (Agilent) and chemoattractants (Peprotech) were used for chemotaxis assays. For isolation of primary human leukocytes, Histopaque 1077 and Histopaque 1119 (Sigma), $CD14^+$ microbeads and

LS columns (Miltenyi Biotech) were used. For static migration assays, M199 medium (Gibco), glutaraldehyde (Sigma), endothelial cell growth MV medium (Promocell) and TNFα (R&D Systems) were purchased. ATP was purchased from Sigma and CCPD/MSU crystals for inflammasome assays were purchased from Invivogen.

2.2 Animal experiments

All animal care and experimental protocols in this study were in accordance with the Home Office guidance on Operation of Animals (Scientific Procedures Act 1986) and were approved by the Sir William Dunn School of Pathology Animal Welfare Ethics Review Board (AWERB) and the University of Oxford. The study was performed under the licenses issued by the Home Office P144E44F2 and PP0728730. I hold a personal license (I08432139) and have been authorized to perform Schedule 1 procedures, intraperitoneal injections and oral gavage. All animal experiments were designed and performed in adherence with the guidelines from the National Centre for the Replacement, Refinement & Reduction of Animal Research (NCR3s) and humane endpoints were discussed and considered in experimental designs. Group sizes for *in vivo* experiments were calculated from power calculations using data from published studies and pilot experiments (MSU crystal-induced peritonitis (4 h) with prophylactic oral drug administration).

2.2.1 Animal husbandry

Animals were purchased from Charles River or obtained from the Pathology Support Building at the University of Oxford and housed in individually ventilated cages (between 2 and 10 mice per cage) in specific pathogen-free conditions. All animals were provided with chow and water *ad libitum* and were maintained on a 12 h light, 12 h dark cycle at controlled temperature (20-22°C) and humidity.

2.2.2 MSU crystal-induced peritonitis (prophylactic model)

MSU crystal-peritonitis was used as a mouse model of acute inflammation and followed the protocol described by Spalinger et *al.* [426]. Eight to ten-week-old male or female C57BL/6J mice were randomly assigned to a treatment group to orally receive either regorafenib (10

mg/kg or 30 mg/kg, dissolved in DMSO at 20 mg/ml and diluted 20-fold in vehicle to obtain a 1 mg/ml solution), sorafenib (10 mg/kg or 30 mg/kg), indomethacin (5 mg/kg) or vehicle alone (10% (v/v) polysorbate 80, 6.5% (v/v) ethanol, 5% DMSO and 2.5% (w/v) glucose in water) at -24 h and -2 h. The vehicle and dose used were previously reported to achieve sufficient plasma concentration at the relevant time points [427]. At 0 h, mice were injected intraperitoneally (i.p.) with either phosphate-buffered saline (PBS, Sigma-Aldrich) or 1.8 mg MSU crystals (InvivoGen) in PBS. For the 16 h endpoint, mice received a third oral dose of regorafenib (30 mg/kg) at 6 h. Mice were euthanized by CO_2 asphyxiation followed by exsanguination at 4 h or 16 h, and their peritoneal cavities were lavaged with 5 ml ice-cold PBS+ 2 mM EDTA. Blood was collected from the inferior vena cava and stored in anti-coagulant tubes containing EDTA powder (Teklab) for flow cytometry or in collection tubes containing clot-activating gel (Sarstedt) for serum analysis.

Peritoneal lavage fluid was centrifuged at 400g, 4°C, 10 min to separate cells from supernatant. The cytokine and chemokine protein levels in the supernatant were measured by ELISA. The levels of IL-1β and ASC in the supernatant and pro-Caspase-1 and phospho-p65 levels in lysates of peritoneal cells were measured by Western Blot. $1x10^6$ peritoneal cells were analyzed by flow cytometry [426].

2.2.3 MSU crystal-induced peritonitis (therapeutic model)

Eight to ten-week-old male C57BL/6J mice were randomly assigned to a treatment group. At 0 h, mice were injected intraperitoneally (i.p.) with either PBS or 1.8 mg MSU crystals in PBS. At 0.5 h, mice orally or intraperitoneally received either regorafenib (30 mg/kg) or vehicle alone. Mice were euthanized by CO_2 asphyxiation followed by exsanguination at 16 h and cells and blood were processed as described above.

2.3 Cell culture

2.3.1 RAW-Blue macrophage reporter cells

The murine macrophage reporter cell line RAW Blue (InvivoGen) is derived from murine RAW 264.7 macrophages with chromosomal integration of a secreted embryonic alkaline phosphatase (SEAP) reporter construct, which is induced by NF-κB and activator protein 1 (AP-1) transcriptional activation. Cells were cultured in T-75 flasks in Dulbecco's Modified Eagle Medium (DMEM) containing 4.5 g/L glucose, 10% heat-inactivated Fetal Bovine Serum (FBS), 2 mM L-glutamine, and 100 µg/ml zeocin antibiotic (InvivoGen) at 37°C in 5% CO_2. To minimize experimental variability, only cells with fewer than seven passages were used. For experiments, cells were washed with phosphate-buffered saline, detached by aspiration, centrifuged and resuspended at desired concentrations.

2.3.2 THP1-Dual monocyte reporter cells

The human monocyte reporter cell line THP1-Dual™ (InvivoGen) is derived from the human THP1 monocyte cell line by stable integration of two inducible reporter constructs. As a result, THP1-Dual cells allow the simultaneous study of the NF-κB pathway, by monitoring the activity of SEAP, and the IRF pathway, by assessing the activity of a secreted luciferase (Lucia). Cells were cultured in T-75 flasks in RPMI 1640 medium containing 2 mM L-glutamine, 25 mM HEPES, 10% heat-inactivated FBS, 100 mg/ml Zeocin, 10 mg/ml blasticidin (InvivoGen) and pen-strep (100 U/ml-100 µg/ml) at 37°C in 5% CO_2. For differentiation into macrophage-like cells, THP1-Dual cells were treated with 20 ng/ml Phorbol 12-myristate 13-acetate (PMA) on day 1 for 24 h and used for experiments on day 4. To minimize experimental variability, only cells with fewer than seven passages were used.

2.3.3 THP1-ASC-GFP monocyte reporter cells

The human monocyte reporter cell line THP1-ASC-GFP (InvivoGen) is derived from the human THP1 monocyte cell line. It is an inflammasome reporter cell line that allows the monitoring of ASC-dependent inflammasome formation using fluorescence microscopy. Cells stably express a gene encoding an ASC:GFP fusion protein for which expression is driven by an NF-κB-

inducible promoter. Cells were cultured in T-75 flasks in RPMI 1640 medium containing 2 mM L-glutamine, 25 mM HEPES, 10% heat-inactivated FBS, 100 mg/ml zeocin and pen-strep (100 U/ml-100 µg/ml) at 37°C in 5% CO_2. To minimize experimental variability, only cells with fewer than seven passages were used.

2.3.4 Murine bone marrow-derived macrophages

Murine bone marrow-derived macrophages (BMDMs) were obtained from fresh bone marrow cells from tibiae and femurs of male C57BL/6 mice aged 8–10 weeks as previously described [428]. Bones were flushed with PBS and whole bone marrow isolates were cultured in DMEM containing 4.5 g/L glucose, 2 mM l-glutamine, penicillin/streptomycin (100 U/ml-100 µg/ml), 10% heat-inactivated FBS and 10% L929 cell-conditioned media as a source of macrophage colony-stimulating factor (M-CSF) for 6 days in 8 ml of medium in 9 cm non-tissue culture treated Petri dishes. On Day 4, 3 ml media was replaced with 5 ml fresh media. On day 6, cells were detached by gentle scraping, counted, suspended in DMEM containing 2 % FBS, plated for experiments at the desired cell concentration and were allowed to settle overnight. BMDMs were routinely characterized using flow cytometry by expression ($CD45^+$, $F4/80^+$, $CD11b^+$) (Fig. 2.1 A-B).

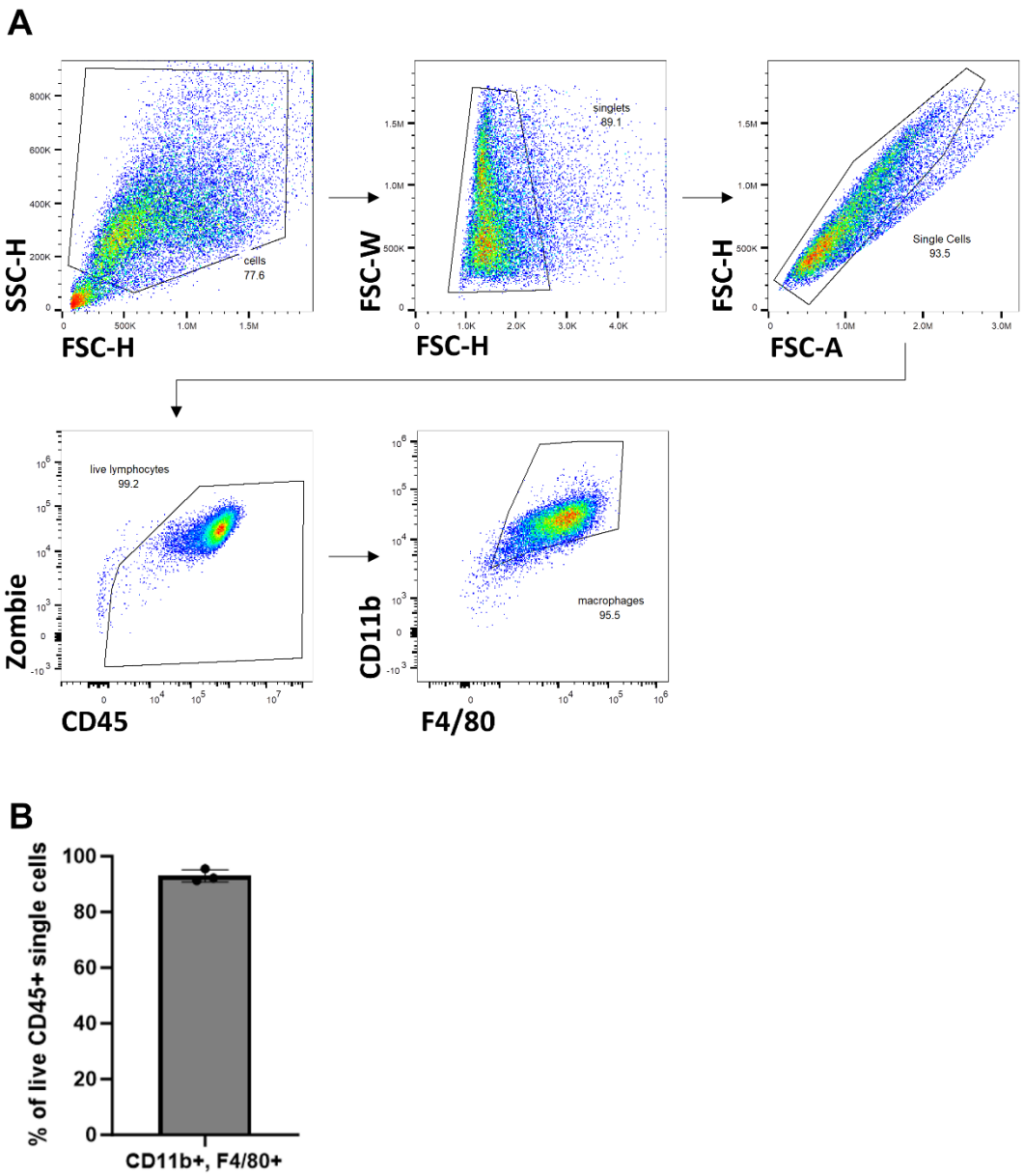


Fig. 2. 1 Characterization of day 7 BMDMs by flow cytometry. On day 7, BMDMs were detached from Petri dishes by gentle scraping and resuspended in FACS buffer without BSA (2 mM EDTA in PBS). Cells were stained with live/dead stain Zombie NIR for 15 min on ice before resuspension in FACS buffer (0.05 % BSA+ 2 mM EDTA in PBS) and blocking of FCγRIII/FCγRII by CD16/32. Subsequently, extracellular receptors were stained with primary antibodies CD45-APC, CD11b-BV421 and F4/80-PE (all 1:400 or 0.25 µl/ 100 µl) for 30 min. After washing with FACS buffer, cells were characterized by flow cytometry.

2.3.5 Human monocytes and neutrophils

Blood was collected from healthy volunteers into 10 ml EDTA-coated tubes. Written informed consent was obtained from all donors and approval was granted by the University of Birmingham Local Ethical Review Committee (ERN_18 −0382).

Monocytes and neutrophils were isolated using a double-density histopaque gradient and hypotonic lysis as described previously [429]. To generate human monocyte-derived

macrophages (MDMs), $CD14^+$ monocytes were cultured in RPMI containing 50 ng/ml M-CSF for 6 days with a media change at day 3. On day 6, media was replaced with RPMI containing 2 % FBS and experiments were performed on day 7.

2.3.6 Primary human dermal blood endothelial cells

Primary human dermal blood endothelial cells (HDBECs) were cultured in endothelial cell growth medium MV. HDBECs ($2x10^5$) were seeded into 12-well tissue culture plates, yielding confluent monolayers. HDBEC monolayers were washed in endothelial cell growth MV medium warmed to 37 °C before treatment.

2.4 NF-κB-SEAP Reporter Assay

RAW-Blue or THP1-Dual cells were plated in 96-well plates at 100,000 cells per well. Cells were pre-treated with drugs or controls at indicated concentrations for 1 h. All FDA-approved medicines were made up in DMSO to achieve a final experimental concentration of 0.1 % DMSO or 0.3 % DMSO. After pre-treatment, cells were stimulated with 100 ng/mL LPS for 6 h (RAW-Blue cells) or 24 h (THP1-Dual cells) as reported in [430]. Subsequently, 20 µl of cell supernatant was added to 180 µl of QUANTI-Blue substrate and incubated at 30°C for 2 h as per the manufacturer's protocol. The plate was then read at an OD of 620 nm on a microplate spectrophotometer (PherastarFSX, BMG Lab).

2.5 Cell viability assays

To determine cell viability, the CellTiter-Glo assay was used, which determines cellular ATP levels, indicating metabolic activity, to determine the number of viable cells. The reagent was mixed with an equal volume of cell culture medium containing cells from the wells used in the experiment. The mix was incubated for 2 min at room temperature on the shaker and incubated for 10 min at RT, followed by luminescence measurement with a microplate spectrophotometer (PherastarFSX, BMG Lab).

Alternatively, the CytoTox 96 Non-Radioactive Cytotoxicity Assay was used to evaluate macrophage cell death by detecting the release of LDH into the medium.

2.6 RT-qPCR

Cells were harvested into TRIzol reagent (Life Technologies) and the total RNA was extracted. RNA concentration and quality were determined with an ND-1000 spectrophotometer (NanoDrop Technologies). cDNA was synthesized from 1,000 ng RNA using the QuantiTect Reverse Transcription kit (Qiagen) according to the manufacturer's instructions. Real-time quantitative PCR was performed using Sybr Select gene expression master mix (Life Technologies) in the StepOnePlus™ thermal cycler (Applied Biosystems). Primers were purchased from Qiagen. Cycle threshold values were determined by the StepOne software, and target gene expression was normalized to (18S).

Table 2. 1 List of mouse primers

Gene	**Supplier**	**ID**
18s	Qiagen	QT02448075
tnf	Qiagen	QT00104006
il-6	Qiagen	QT00098875
il-1β	Qiagen	QT01048355
ccl2	Qiagen	QT00167832
inos	Qiagen	QT01547980
cxcl1	Qiagen	QT00115647

2.7 Cytokine quantification

Murine BMDMs (100,000 cells/well) were seeded in 96-well plates and pre-treated with drugs or controls for 1 h before stimulation with LPS (100 ng/mL) for 7 h. For IL-1β secretion, 5 mM ATP or 150 µg/ml MSU crystals/ 100 µg/ml CPPD crystals were added in the last 1 hour or 5 hours, respectively. Measurement of the protein levels of IL-1β, TNFα and IL-6, IL-10, CCL2, CXCL5 or KC secreted into cell supernatants was performed by ELISA (R&D Systems) according to the manufacturer's instructions.

2.8 Western Blotting

Protein concentration was determined by using a BCA protein assay kit. Total cell protein was added to 4× Laemmli buffer (250 mM Tris–HCl, pH 6.8, 8% SDS, 40% glycerol, 0.004% bromophenol blue, 20% β-mercaptoethanol) and heated at 95°C for 5 min. Samples were then resolved on SDS-PAGE gels and transferred onto 0.2 µm PV membranes using the Trans-Blot Turbo Transfer System. Membranes were blocked with 5% BSA in TBS-Tween for 1 h at RT and then incubated with the primary antibodies (Table 2.2) diluted 1:1000 in 5% BSA/TBS-Tween overnight at 4°C. Next, membranes were incubated with goat anti-rabbit (DyLight800, SA5-10036, Invitrogen) or goat anti-mouse (Alexa Flour 680, A-21057, Thermo Scientific) cross-absorbed secondary antibody diluted 1:5000 in 5% milk for 1 h at RT. Fluorescent detection was performed using the Odyssey SA imaging system (Li-cor Biosciences). Rabbit anti-GAPDH was used as a loading control. For successive antibody incubations using the same membrane, bound antibodies were removed with stripping buffer (Thermo Scientific, Cat. No. 62300).

Table 2. 2 List of primary antibodies used in this study

Antibody	**Source/Isotype**	**Supplier**	**Catalog No.**
Src	Mouse IgG1	Cell Signaling Technology	2110
Tyr^{416}-Src	Rabbit IgG	Cell Signaling Technology	59548
ERK	Mouse IgG1	Cell Signaling Technology	9107
Thr^{202}/Tyr^{204}-ERK	Rabbit	Cell Signaling Technology	9101
Akt	Mouse IgG1	Cell Signaling Technology	2920
Ser^{473}-Akt	Rabbit IgG	Cell Signaling Technology	5012
p38	Rabbit IgG	Cell Signaling Technology	2387
Thr^{180}/Tyr^{182}-p38	Mouse IgG1	Cell Signaling Technology	9216
STAT3	Rabbit IgG	Cell Signaling Technology	4904
Ser^{727}-STAT3	Mouse IgM	Cell Signaling Technology	9136
p65	Rabbit IgG	Cell Signaling Technology	30656

Ser^{536}-p65	Rabbit IgG	Cell Signaling Technology	3033
CSF-1R	Rabbit	Cell Signaling Technology	3152
Tyr^{798}-CSF-1R	Rabbit	Cell Signaling Technology	3080
NLRP3	Mouse IgG2b	Caltag Medsystems	AG-20B-0014-C100
ASC	Mouse IgG1 k	Santa Cruz Biotechnology	sc-514414
GAPDH	Rabbit IgG	Cell Signaling Technology	8884

2.9 Flow cytometry

For flow cytometry of the spleen, the tissue was disrupted mechanically and flushed through a 70 µM cell strainer with 10 ml PBS to obtain a single-cell suspension. 200 µl were used for flow cytometry. 50 µl blood was mixed with ACK lysis buffer (1:10, 5 min) to remove erythrocytes. Cells were pelleted and resuspended in PBS+ 2 mM EDTA.

Cells were incubated on ice for 5 min in PBS+ 2 mM EDTA before staining with cell viability dye for 15 min. Subsequently, cells were resuspended in FACS buffer (0.05% BSA, 2 mM EDTA in PBS, pH 7.4) and blocked using anti-CD16/32 (1 µg; BioLegend) for 15 mins at 4°C, followed by 30 min antibody staining for surface markers with isotype controls. Cells were washed twice with FACS buffer and fixed with 100 µl 4 % PFA in PBS for 10 min at RT. After washing twice with FACS buffer, cells were resuspended in 200 µl of FACS buffer before data acquisition. Antibodies used are listed in Table 2.3, all from BioLegend.

Table 2. 3 List of fluorophores used in this study

Marker	**Flourophore**	**Isotype**	**Clone**	**Catalog No.**
B220	PE	Rat IgG2a, κ	RA3-6B2	103207
CD3ε	PerCP	Armenian Hamster IgG	145-2C11	100326
CD11b	BV421	Rat IgG2b, κ	M1/70	101235
CD45	APC	Mouse IgG21, κ	2D1	368512
CD115	PE	Rat IgG1, κ	9-4D2-1E4	347304
CD206	PE-Cy7	Rat IgG2a, κ	C068C2	141720

F4/80	PE-Cy7	Rat IgG2a, κ	BM8	123114
F4/80	APC	Rat IgG2a, κ	BM8	123116
Ly6C	FITC	Rat IgG2c, κ	HK1.4	128006
Ly6G	BV510	Rat IgG2a, κ	1A8	127633
MHCII	FITC	Rat IgG2b, κ	M5/114.15.2	107606

To determine cell viability, 7-AAD viability staining (BioLegend) or the Zombie NIR (BioLegend) fixable viability kit was used.

Data were acquired using BD Fortessa X20 cytometer and Diva software (BD Biosciences) or using the CytoFLEX LX flow cytometer and then analyzed using FlowJo (Tree Star Inc.) software. Fluorescence minus one (FMO) controls were used for gating and single stains for compensation were obtained using UltraComp eBeads™ Compensation Beads (Invitrogen) for peritoneal lavage panels and single-stained cell samples for BMDMs. To count blood and spleen cells, CountBright absolute counting beads (Invitrogen) were used.

2.10 xCELLigence Chemotaxis assay

Chemotaxis assays were carried out with CIM-16 well plates and an xCELLigence RTCA-DP instrument (Roche Diagnostics) as described in [431]. Briefly, human CCL2 or murine M-CSF was made up to desired concentrations (final volume of 160 µl) in chemotaxis buffer (RPMI-1640 completed with 25 mM HEPES and 0.5 % BSA) and added to the lower wells of the plate. Following upper chamber attachment, the upper wells were filled with 50 µl pre-warmed chemotaxis buffer and the plate was incubated for 30 mins at RT to pre-equilibrate to allow the formation of a stable gradient. Subsequently, the background was measured in the RTCA-DP analyzer. THP1-Dual monocytes or BMDMs were resuspended to 2×10^6 cells/ml in chemotaxis buffer and 50 µl cell suspension (1×10^5 cells) was transferred to the top wells. After 10 min incubation at 37°C, the assembled plate was transferred to the RTCA-DP machine and data was collected every 40 s throughout 900 sweeps. Electrical impedance caused by cell migration is reflected in the cell index (CI) [432]. Rising cell impedance correlates to increasing

numbers of migrated macrophages adhering to the underside of the filter. Data were normalized to wells that contained media only and analysis for the area under the curve (AUC) was carried out with the RTCA Software 2.0 and provides a combined measure for both migration and adhesion [433].

2.11 Static migration assay

Static migration assays were performed as described in [434]. Briefly, 2×10^5 HDBECs were seeded and pre-treated with 3 µM regorafenib, sorafenib or DMSO vehicle for 1 h before stimulation with TNFα (100 U/ml) for 4 h. Monocytes and neutrophils were isolated from the blood of healthy volunteers as described above. Cells were diluted to 1×10^6 cells/ml in M199 media and incubated with or without 3 µM regorafenib, sorafenib or vehicle for 30 min before addition to activated HDBEC for 7 min at 37 °C. Wells were washed twice with PBS to remove non-adhered cells and fixed with 2% glutaraldehyde for 10 min at RT. Glutaraldehyde was removed with two 1 ml washes of PBS containing Ca^{2+} and Mg^{2+}. Images were taken at six different fields in the center of each well, and quantification was performed using Image-pro 6.0 software.

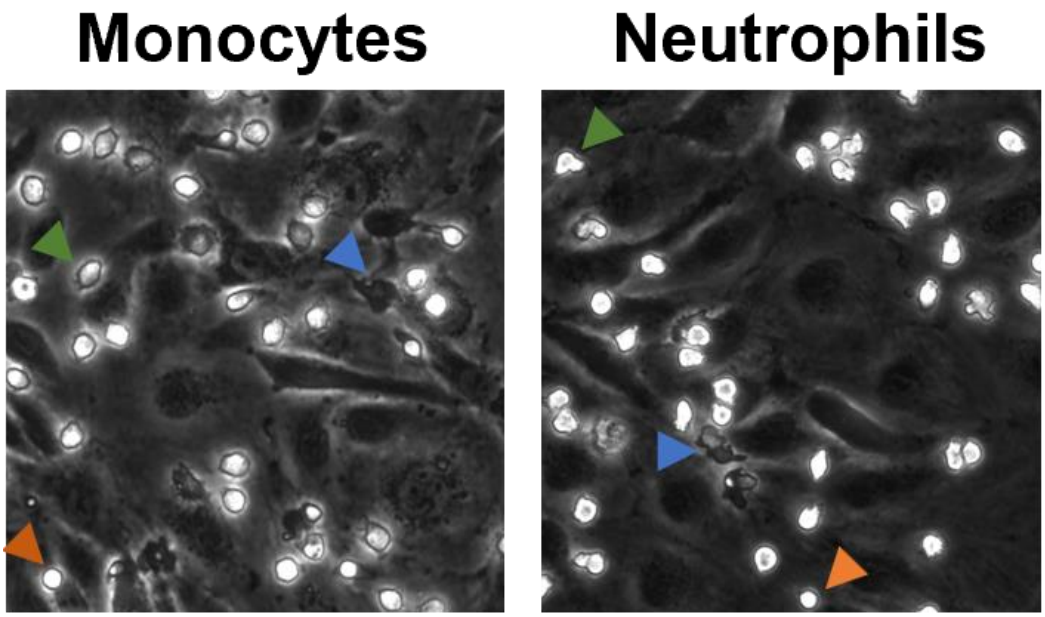


Fig. 2. 2 Quantification of leukocyte adhesion, activation and migration in static migration assays. Surface adhered phase bright leukocytes (orange arrow), phase bright/grey activated leukocytes with protrusions (green arrow) and transmigrated, phase dark leukocytes (blue arrow) were counted in six imaging fields.

2.12 Imagestream

RAW-Blue cells ($1x10^6$) were seeded into 6-well plates and pre-treated with 3 µM drugs or controls for 1 h before stimulation with 100 ng/mL LPS for 10 min. Cells were scraped and centrifuged at 4 °C for 5 min at 300 g. Cells were blocked with anti-mouse CD16/32 (1:50 dilution) in FACS buffer for 10 min on ice. After centrifugation, cells were fixed in 2 % PFA in PBS for 15 min at RT. To permeabilize the cells, they were incubated in permeabilization buffer for 15 min at RT prior to staining with anti-NF-κB/p65-PE (1:50 dilution) for 1 h at RT. Cells were stored in FACS buffer at 4 °C and DAPI was added immediately before imaging. 8000 events were collected for all samples on an ImageStream IS100 using 561 nm laser excitation. Cell populations were hierarchically gated for single cells that were in focus and were positive for p65. After the gates were applied, 70–80% of the total number of acquired images were incorporated into the final analysis. Following data acquisition, the spatial relationship between the NF-κB and nuclear images was measured using the 'Co-localization' feature in the IDEAS^R software package [435], which provides a measure of the degree of nuclear localization of NF-κB/p65 by measuring the co-localization between the anti- NF-κB/p65-PE and DAPI images.

THP1-Dual and THP1-ASC-GFP cells ($1x10^6$) were seeded into 6-well plates and differentiated with 20 ng/mL PMA for 24 h. Cells were then washed twice with PBS and incubated in RPMI 1640. On day 3 after PMA treatment, cells were washed with PBS again before pre-treatment with 3 µM drugs or controls for 1 h. Cells were stimulated with 100 ng/mL LPS (signal 1) for 6 h to allow NF-κB expression. Culture medium was adjusted to 5 mM ATP in the last 60 min to induce ASC-speck formation (signal 2). Cells were scraped and centrifuged at 4 °C for 5 min at 300 g. Then, cells were fixed in 2 % PFA in PBS for 15 min at RT before they were stored in FACS buffer at 4 °C for imaging. DAPI was added immediately before imaging. 8000 events were collected for all samples on an ImageStream IS100 using 488 nm laser excitation. Cell populations were hierarchically gated for single cells that were in focus and were positive for GFP. After the gates were applied, 80–90% of the total number of acquired images were incorporated into the final analysis. Following data acquisition, the number of ASC-GFP specks was measured using the 'Spot' feature in the IDEAS^R software package [435].

2.13 Inflammasome activation and priming

BMDMs, THP1-Dual and THP1-ASC cells were cultured as described. Priming was provided by addition of 100 ng/mL LPS and step 2 activation by ATP (5 mM) or by MSU crystals (150 µg/ml)/ CPPD crystals (100 µg/ml).

2.14 Nitric oxide quantification

BMDMs were plated, treated and stimulated as described above. Following 22 hours of LPS (100 ng/ml) +IFN-γ (20 ng/ml) stimulation, supernatants were collected and NO concentrations were measured by Griess assay following the manufacturer's instructions as previously reported [428].

2.15 Cytospin and staining

Total PEC numbers were determined and 200,000 cells were resuspended in 150 µl PBS+ 2 mM EDTA and centrifuged onto slides at 400 rpm for 10 min with a Shandon Cytospin 3. Cells were fixed and stained with eosin and methylene blue using the Hema-Rapid staining set GURR for haematology (VWR Chemicals) following the manufacturer's instructions, and images were taken using the EVOS light microscope (20x magnification).

2.16 Statistical analysis

Graphs were generated and statistical analysis was performed using the GraphPad Prism 10.2.2 software. Data are shown as mean ±S.E.M values. Statistical significance between groups was assessed by ANOVA with Dunnet's multiple comparisons test or unpaired Student t-test as indicated in the legends. P values <0.05 were considered statistically significant. For all figures in this thesis, the following significance levels were used: *p<0.05, **p<0.01, ***p<0.001, ****<p0.0001.

Chapter 3: Screen of FDA-approved medicines in NF-κB reporter assay identifies drug repurposing candidates with anti-inflammatory properties

3.1 Introduction

3.1.1 Drug repurposing vs. *de novo* drug development

Drug repurposing, also referred to as drug repositioning, is the process of identifying new indications for commercially used medicines or drugs rejected in clinical trials for novel applications. *De novo* drug development is a costly and time-consuming process with a high failure rate. In contrast, drug repurposing has significantly lower development costs due to the well-known efficacy and pharmacokinetic profiles of drugs that have already undergone extensive testing in clinical trials (Table 3.1) [436, 437].

Table 3. 1 Comparison of time, success rate and cost of drug repurposing versus *de novo* drug development strategies. Table adapted from [436, 437].

	Drug repurposing	***De novo* drug development**
Time	6 years	13-15 years
Success rate	30-75%	2 %
Cost	$300 million	$2-3 billion

Another downside of *de novo* drug development is that it has small profit margins when developing new medicines to treat rare diseases due to low demand. Drug repurposing may make the discovery of such treatments more financially appealing.

Another concern with *de novo* drug development is that the number of new drugs reaching the market per billion US dollars spent on research has been observed to halve every 9 years on average in the past 70 years, a phenomenon that is referred to as “Eroom’s law” [438]. Drug repurposing is a promising strategy to counter-act this trend by decreasing the development costs for new treatments and receiving approval in less than half the time.

Anti-inflammatory agents have a market share of 39 % of the drug market in North America. The market size is steadily increasing due to an aging population and is estimated to reach $ 234 billion by 2032, with arthritis medications making up the largest segment of over 70 billion

USD [439]. However, current anti-inflammatory medicines have many serious adverse effects, such as increased risk of infection due to broad immune suppression, increased risk of bleeding, gastric, hepatic or renal toxicity as well as cardiovascular side effects [421]. This has created an unmet need for new classes of anti-inflammatory medicines that are both safe and effective. So far, *de novo* drug development has not been able to solve this urgent problem.

Drug repurposing has proven to be a promising alternative to discover medicines with potent anti-inflammatory properties. In the COVID-19 pandemic, the RECOVERY trial made systematic drug repurposing efforts and identified FDA-approved drugs that possess novel anti-inflammatory effects. It led to the successful repurposing of dexamethasone as well as anti-IL-6 receptor monoclonal antibody tocilizumab for the treatment of hospitalized COVID-19 patients with systemic inflammation. Dexamethasone is estimated to have saved the lives of one million patients in the nine months following its identification alone [419, 440].

3.1.2 Experimental drug repurposing strategies

Different strategies to identify drug repurposing candidates can be employed, including experimental, computational or serendipitous approaches (Fig. 3.1).

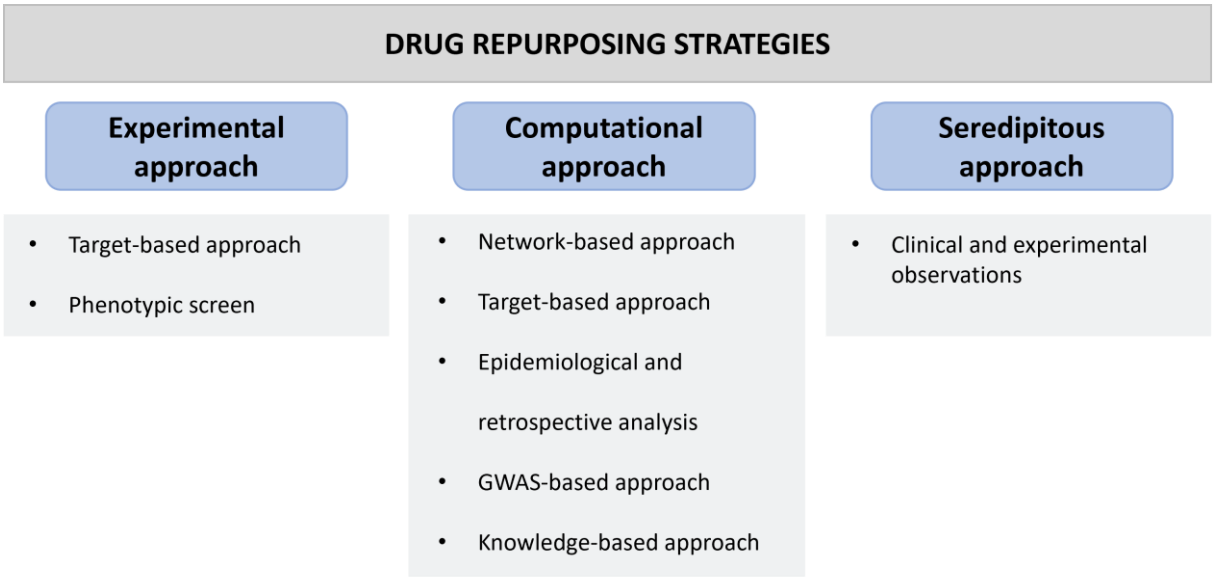


Fig. 3. 1: Drug repurposing approaches. Experimental, computational and serendipitous drug repurposing strategies can be utilized to identify drug repurposing candidates from libraries of existing medicines. Figure adapted from [441].

Experimental approaches can be categorized into target-based strategies and phenotypic screens. Target-based approaches require information about the molecular target of repurposing candidates or the disease of interest, while phenotypic screens do not require explicit knowledge of the drug mode of action or a complete understanding of the mechanism underlying disease pathology. Both experimental approaches rely heavily on cell-based assays to reliably screen and identify promising candidates and validate their effectiveness to minimize failure rates before entering costly clinical trials.

3.1.2.1 Target-based drug repurposing strategies

Target-based drug repurposing approaches rely on knowledge of drug mode of action or identification of promising targets underlying disease pathology. Pro-inflammatory MAPK, Syk, JAK/STAT, PI3K or NF-κB signaling pathways are the main pathways initiating and perpetuating pathologic inflammation in RA and depend on tyrosine kinase activation [442-445]. Therefore, many studies have investigated the effect of tyrosine kinase inhibitors in arthritis models. One such example is dasatinib, an anti-cancer medicine used for the treatment of Philadelphia chromosome-positive acute lymphoblastic leukemia. The multi-tyrosine kinase inhibitor targets BCR/ABL, c-Kit, PDGFR and Src as well as collagen receptor tyrosine kinases discoidin domain receptors 1 and 2, all of which are important drivers of RA pathology [444, 446]. Thus, Guo et *al.* investigated the effect of dasatinib in mice with CIA. They showed that the TKI significantly reduced disease severity by inhibiting the production of pro-inflammatory cytokines and anti-collagen type II-specific antibodies while simultaneously increasing repair-enhancing IL-10 levels [447]. In addition, the drug repurposing candidate reduced the migration and proliferation of primary human fibroblast-like synoviocytes (FLS) of RA patients that produce receptor activator of nuclear factor κB ligand (RANKL), which drives osteoclastogenesis and bone destruction [448]. This target-based approach identified dasatinib as a promising repurposing candidate with anti-inflammatory effects in a preclinical model of RA, which justifies its further investigation as a potential therapeutic for RA.

3.1.2.2 *In vitro* phenotypic drug repurposing strategies

In contrast, phenotypic drug repurposing approaches are not based on explicit knowledge about molecular mechanisms underlying the drug's mode of action or the disease pathology. Using cell-based *in vitro* assays to assess the effect of repurposing candidates on disease-relevant phenotypic readouts allows for screening of large compound libraries at different concentrations [449]. Here, immortalized cell lines offer the advantage of being cost-effective and readily available in numbers required for high-throughput screens and provide reproducible results [450].

In atherosclerosis, phagocytosis of oxidized low-density lipoprotein (oxLDL) by macrophages results in the formation of foam cells, which accumulate in the necrotic core of atherosclerotic lesions, reducing plaque stability and increasing the risk of rupture and thrombosis [451]. Therefore, Etzion et *al.* used the J774 macrophage cell line to develop a fluorescence-based high-throughput phenotypic screen to identify compounds from a library of bioactive molecules that reduce oxLDL uptake [452]. After excluding cytotoxic compounds, they identified 7 agents that decreased macrophage oxLDL uptake, including NF-κB inhibitor Bay11-7082. Considering that cell lines are immortalized, the findings were subsequently tested in primary peritoneal macrophages, which retain characteristics of the tissue of origin and are thought to be a more accurate model for testing potential therapeutics. They were able to confirm their previous findings and subsequently successfully validated the effect of Bay11-7082 on thioglycolate-elicited macrophages from mice *in vivo*. A similar phenotype-based drug repurposing approach was recently reported by Hoeffner et *al.*, who used BMDM-derived foam cells to identify FDA-approved drug repurposing candidates that reduced oxLDL uptake [453].

In multiple sclerosis (MS), autoimmune inflammation results in the loss of myelin sheaths and consequently in axonal and neuronal degeneration leading to behavioral decline. Medicines currently used to treat MS patients are immunosuppressive but do not promote re-myelination by oligodendrocytes. Many promising pre-clinical candidates have failed in clinical trials due to a lack of efficiency in enhancing re-myelination, possibly due to the complex mechanism

underlying the process. Thus, drug candidates targeting single pathways or cell populations may lack efficacy in human patients [454].

To identify FDA-approved drugs that enhance the process of oligodendrocyte remyelination, Mei et *al.* established a sophisticated phenotypic high-throughput functional screening assay using micropillars to measure and quantify primary oligodendrocyte differentiation and myelination [455]. They found that clemastine fumarate, a H_1 histamine antagonist used to treat allergic rhinitis, promoted oligodendrocyte differentiation and remyelination. This effect has since been validated in animal models and human cells [455-461] and the mechanism was specifically linked to enhanced oligodendrocyte differentiation [457]. In addition, the drug repurposing candidate reduced inflammation, microglial M1-like polarization and astrocyte loss in mouse models of depression and ALS [462, 463]. This anti-inflammatory activity was linked to its inhibitory effect on NF-κB signaling [464, 465]. Recently, a phase II clinical study in patients with relapsing MS found that clemastine promoted myelin repair, resulting in improved nerve impulse speed [466]. Another phase II trial currently in process aims to investigate the effect of clemastine on remyelination and neuroprotection in patients with acute demyelinating optic neuritis (trial number: NCT02521311). The progression of clemastine from phenotypical drug repurposing screens through pre-clinical animal models to phase II clinical trials demonstrates the power of phenotypical drug repurposing approaches.

3.1.2.3 *In vivo* phenotypic drug repurposing strategies

Medium and high-throughput phenotypic drug repurposing screens have been developed using *Danio rerio* zebrafish, *Drosophila melanogaster* or *Caenorhabditis elegans* as model organisms to assess the effect of candidate compounds *in vivo* [467-470].

Zebrafish are becoming an increasingly popular model organism [471]. The animal model allows for real-time cell migration assessment, has increased throughput screening capacity compared to mice and their immune system shares many features with that of humans [472, 473]. Several zebrafish models have been successfully employed to identify and investigate anti-inflammatory compounds [471]. Zebrafish embryos only develop a functional blood-brain

barrier 3-10 days after fertilization. Therefore, Rihel et *al.* used early zebrafish embryos to classify drugs added to the water by analyzing their effect on the rest/wake cycle of the fish [474]. Anti-inflammatory drugs, including compounds with previously unknown anti-inflammatory effects, were found to co-cluster by inducing a unique behavioral pattern. Therefore, this whole animal behavioral assay has the potential to identify further drug repurposing candidates with novel anti-inflammatory properties.

Another zebrafish *in vivo* drug repurposing assay measured neutrophil migration to screen for FDA-approved medicines with novel anti-inflammatory properties. The assay assessed neutrophil recruitment in acute inflammation induced by tail fin injury and the anti-inflammatory properties of the 10 most potent hit compounds were successfully validated in mouse models of atopic dermatitis [475].

3.1.2.4 Organoid-based phenotypic drug repurposing strategies

Despite their many advantages, zebrafish are more remotely related to humans than other animal models and thus, results obtained in zebrafish assays may not be translatable into human studies. To achieve higher disease relevance and translatability, patient-derived organoids can be used for drug repurposing screens. They have proven valuable resources for drug repurposing in cancer [476, 477] as well as cystic fibrosis [478, 479] and present a promising tool for further drug repurposing studies to identify novel anti-inflammatories.

3.1.3 Repurposing NF-κB inhibitors to treat inflammation

While no specific NF-κB inhibitors have progressed to the therapeutic market yet, many FDA-approved drugs mediate their anti-inflammatory effects in part by inhibiting the NF-κB signaling pathway at different stages [480, 481]. Therefore, identifying FDA-approved repurposing candidates that target NF-κB activation presents a promising strategy to identify new therapeutic options (Table 3.2).

TKI imatinib mesylate, which targets Bcr-Abl and is approved for the treatment of chronic myeloid leukemia (CML), was identified as a potent inhibitor of NF-κB signaling and

inflammation *in vivo* and *in vitro* (Table 3.2) [482, 483]. The anti-inflammatory mode of action of imatinib was linked to suppression of IκB phosphorylation and DNA binding of NF-κB and thus inhibition of NF-κB-mediated pro-inflammatory cytokine production [484, 485]. A phase II clinical trial is currently investigating whether imatinib can provide better outcomes than standard treatment for relapsing multiple sclerosis patients (Trial number NCT03674099).

Instead of directly inhibiting NF-κB signaling, the proteasome can be targeted to stabilize phosphorylated IκBα, preventing NF-κB activation. Bortezomib is a proteasome inhibitor and is used to treat multiple myeloma and mantle cell lymphoma [486]. It covalently binds to the active site of the 26 S proteasome and has proven its potential to be repurposed as an anti-inflammatory drug by reducing inflammation in models of autoantibody-mediated immune diseases such as MS, RA or colitis (Table 3.2) [487-491]. In these disorders, bortezomib selectively triggers apoptosis of plasma cells and lymphocytes, which drive disease pathology. Multiple myeloma patients receiving bortezomib were reported to have significantly reduced RA severity [490, 492]. This effect may be mediated by the reduction of NF-κB-induced pro-inflammatory cytokine production and enhanced apoptosis of T effector cells that was observed in RA patients after bortezomib treatment [493].

Table 3. 2 Drug repurposing candidates for inflammatory diseases targeting NF-κB signaling. Table from my review [441].

New Indication	Drug	Original Implication	Effect on NF-κB Signaling	Effect on Inflammation	References
MS	Imatinib mesylate	Cancer (CML, ALL, GIST, HES, CEL)	Inhibits IκB phosphorylation and DNA binding of NF-κB	Attenuates inflammation and enhances BBB integrity in EAE, Phase II clinical trial for MS	[482-484]
	Clemastine	Relief of allergy symptoms	Decreases NF-κB activity and TLR4 expression	Promotes oligodendrocyte differentiation and re-myelination in EAE/MS, inhibits inflammation and microglial M1-like activation	[455-461, 466]

	Ibudilast	Asthma, stroke	Inhibits NF-κB activity (possibly by preventing nuclear translocation)	Reduces inflammation in rats with chronic cerebral reperfusion and MS patients, Phase II clinical trial for MS	[494-497]
	Topotecan	Cancer (ovarian cancer, lung cancer, SCLC)	Inhibits IKKβ and thus IκBα degradation	Attenuates inflammation in EAE	[498]
RA	Ibrutinib	Cancer (MCL, CLL, WM)	Inhibits NF-κB nuclear translocation	Anti-inflammatory effects in models of RA, sepsis and diabetes	[380, 499-501]
	Bortezomib	Cancer (MM, MCL)	Proteasome inhibitor, prevents degradation of IκBα	Anti-inflammatory effects in models of MS, RA, SLE and colitis; promotes osteoblast activation and RA pathogenesis, Phase II clinical trial for RA	[493, 502] [487-492] [493, 502]
	TDZ	Schizophrenia, psychosis	Inhibits IKKβ phosphorylation and IκBα degradation	Attenuates inflammation in endotoxemia model	[503]
	Dasatinib	Cancer (CML, ALL)	Inhibits phosphorylation of IKKα, p65/p100/p105 and c-Rel	Inhibits inflammation and bone erosion in CIA and human FLS, increases IL-10 in CIA	[447, 504-506]
COVID-19	Dexamethasone	Inflammatory conditions (RA, asthma, allergies etc.)	Induces the expression of IκBα	Reduces mortality in later-stage COVID-19 patients	[440, 507-509]
	Anakinra	Relief of RA symptoms	Prevents activation of IL-1R	Reduces hyper-inflammation and mortality and improves clinical signs of COVID-19	[510-515]

Abbreviations: CML= Chronic myelogenous leukemia, ALL= Acute lymphoblastic leukemia, GIST= Gastrointestinal stromal tumor, HES= Hypereosinophilic syndrome, CEL= Chronic eosinophilic leukemia, SCLC= Small cell lung cancer, BBB= blood brain barrier, EAE= Experimental autoimmune encephalitis, MCL= Mantle cell lymphoma, CLL= Chronic lymphocytic leukemia, WM= Waldenström macroglobulinaemia, ALL= Acute lymphoblastic leukemia, SLE= systemic lupus erythematosus.

Imatinib and bortezomib demonstrate that drug repurposing strategies can be employed to identify new modes of action and applications for FDA-approved medicines to treat inflammatory diseases linked to dysregulated NF-κB activation and successfully progress to clinical trials for new indications.

3.2 Rationale and experimental aims of the chapter

The steady increase in the prevalence of inflammatory conditions and the limitations of current anti-inflammatory drugs mean that there is an urgent unmet need for the development of new anti-inflammatory medicines. Ideally, new anti-inflammatories should have high target specificity to reduce the incidence of broad immune suppression and toxicity due to off-target adverse events. Drug repurposing offers a cost- and time-effective alternative to *de novo* drug development with higher success rates.

Macrophages play a key role in inflammation. NF-κB polarizes them towards an inflammatory phenotype and drives the expression of pro-inflammatory genes. Therefore, dysregulated macrophage NF-κB signaling is a key feature of inflammatory disease pathology and re-establishing its appropriate regulation by repurposing FDA-approved medicines that have novel anti-NF-κB activity is a promising strategy to identify new classes of anti-inflammatory drugs.

The experimental aims of this chapter were to:

- Establish assays to reliably detect macrophage/monocyte NF-κB activity and determine the Z‘-factor as an indication for assay quality.
- Identify kinases that drive macrophage NF-κB activation in inflammation.
- Screen a library of FDA-approved medicines targeting those kinases to identify drugs with novel anti-inflammatory properties in murine and human macrophages in phenotypic cell-based NF-κB reporter assay.
- Validate anti-inflammatory properties of selected candidates in primary murine and human macrophages by measuring pro-inflammatory mediator expression and secretion as well as macrophage polarization.

- Determine mechanism of drug action by investigating the effects on tyrosine kinase signaling and the NF-κB pathway.
- Confirm anti-inflammatory activity on inflammation mediated by different PAMPs and DAMPs.

Isolation of primary human monocytes to generate monocyte-derived macrophages (Fig. 3.8C) was assisted by Jenefa Begum and Areeba Fatima at the University of Birmingham.

3.3 Results:

3.3.1 Screen of tyrosine kinase inhibitor library for NF-κB inhibition in RAW-Blue and THP1-Dual reporter cell lines

To identify small molecules that inhibit macrophage NF-κB activity, a blind screen of the Tocriscreen Kinase Inhibitor Library containing 80 commercially available small molecule kinase inhibitors (Table 3.3) using a quantitative cell-based NF-κB SEAP reporter gene assay was performed using human THP1-Dual monocytes and murine RAW-Blue macrophages.

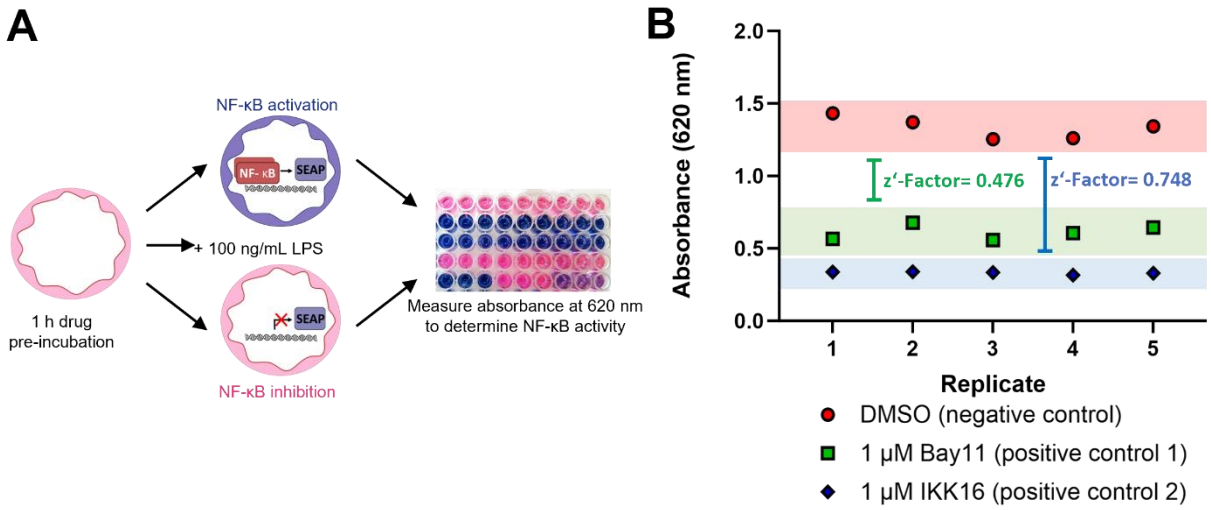


Fig. 3. 2 Reproducible and reliable cell-based screen to identify compounds with unknown NF-κB inhibitory activity. (A) Set-up of QuantiBlue screening assay. RAW-Blue or THP1-Dual cells were pre-treated with drugs or controls 1 h before stimulation with 100 ng/mL LPS for 6 h or 24 h, respectively. 20 µl of cell supernatant was added to 180 µl of QuantiBlue substrate and incubated at 37°C for 2 h. Cells treated with drugs inhibiting NF-κB signaling secrete less SEAP reporter construct, causing the supernatant to remain pink after addition of QB solution. If NF-κB is activated, the secreted SEAP construct causes the supernatant to appear dark blue. To determine NF-κB activity, absorbance at 620 nm was measured. **(B)** Assay quality and reproducibility indicated by the Z'-score. Red= negative control (LPS + DMSO), green= positive control 1 (LPS + 1 µM Bay11-7082) and blue= positive control 2 (LPS+ 1 µM IKK16).

Cells were pre-treated with 1 or 3 µM of small molecule inhibitors or DMSO vehicle for 1 h and subsequently stimulated with LPS, resulting in NF-κB activation and thus SEAP secretion (Fig.

3.2A). 1 µM Bay11-7082 and 1 µM IKK16, both known NF-κB inhibitors, and 1 µM dexamethasone, a glucocorticoid with well-established anti-inflammatory effects, were used as positive controls. The library also included compounds that are known to specifically inhibit NF-κB signaling, such as IKK16 or IMD 0354, which both target IKK and thereby inhibit IκBa phosphorylation. To ensure high quality and reproducibility of the assay, the Z'-factor was determined. In drug development, it is considered a standard measurement of assay quality on each plate and indicates the suitability of a specific assay for high throughput screening [516, 517]. The Z'-factor demonstrates how well positive and negative controls are separated in the screen and thus for the likelihood of false negative or positive results. A Z'-prime factor between 0 and 0.5 indicates acceptable assay quality, whereas a Z'-factor of 0.5-1 suggests excellent reproducibility. Following calculations described in [518], a Z'-factor of 0.476 or 0.748, respectively, was calculated for the Quanti-Blue assay with LPS-stimulated THP1-Dual monocytes using Bay11-7082 or IKK16 as positive controls and DMSO as the negative control. This suggests acceptable assay quality when using positive control Bay11-7082 and excellent assay quality when using IKK16 (Fig. 3.2B).

Table 3. 3 Compounds with anti-inflammatory activity identified with NF-κB reporter assay Screening of Tocriscreen Kinase Inhibitor Library in NF-κB reporter assay using RAW-Blue and THP1-Dual cells. Table is color coded: green= drugs with promising anti-NF-κB activity in screen, yellow= drugs with some anti-NF-κB activity in screen, grey= specific NF-κB inhibitor (positive controls). nt= not tested. Data presented are from n=2/3 independent cell preparations.

Compound	Targets	IC_{50} THP1-Dual (µM)	IC_{50} RAW Blue (µM)	Cytotoxicity (µM) in THP1-Dual	Comments	Reported anti-inflammatory activity?	Reported anti-NF-κB activity in macrophages?	References
SB 202190	p38	nt	nt	No	Reduces IL-6 and NF-κB levels in rats with flap ischemia-reperfusion injury Does not affect the LPS-induced nuclear translocation of either RelA/p65 or c-Rel in BMDMs Induces NF-κB translocation to the nucleus in human bladder transitional cancer cells (T24)	Yes	Yes/ No	[519-521]
RO-31-8220 mesylate	PKC	0.905	5.111	31.25-1.15	Inhibits acidification in human osteoclasts and thereby bone resorption	Yes?	No	[522]
Amino-purvalanol A	CDK1, CDK2, CKD5, ERK1/2	0.526	2.113	31.25	Inhibits NF-κB in HTLV-1 infected T cell lines Blocks leukocyte adhesion and migration	Yes?	No	[523, 524]
ZM 306416 hydrochloride	VEGFR1, Flt, EGFR, Abl, Src	5.169	-	31.25	-	No	No	-

IKK 16	IKK	nt	nt	31.25	Inhibits IKK and attenuates organ injury dysfunction in sepsis model Inhibits M1 macrophage activation to contribute to the resolution of inflammation	Yes	Yes	[525, 526]
SB 218078	Chk1	nt	nt	No	-	No	No	-
Ryuvidine	KMT5A, SETD8, PrSET7	nt	nt	31.25-1.15	-	No	No	-
IMD 0354	IKKβ	nt	nt	31.25-1.15	Inhibits IKKβ activation and IL1β production and reduces pathological features of airway remodeling in mouse model of chronic asthma Reduces inflammation in mouse model of allergic inflammation NF-κB inhibition by IMD 0354 reduces macrophage accumulation	Yes	Yes	[527-529]
EO 1428	p38	-	30.88	31.25	Inhibits production of inflammatory cytokines including IL-8, TNFα, IL-6 and IL-1β in PBMCs after LPS stimulation. Has anti-inflammatory activity in murine models of acute and chronic dermatitis	Yes	No	[530]
NH 125	eEF-2K	nt	nt	31.25-10.41	Reduces ROS production in SHR and the induction of inflammatory molecules in rats with hypertension Reduces TNFα production, p65 phosphorylation and ROS production in HUVECs Reduces neuroinflammation in LPS-induced depression mouse model	Yes	No	[531, 532]

SB 203580 hydrochloride	p38	nt	nt	No	Enhances NF-κB transcriptional activity in TF-1 cells, independent of p65 phosphorylation Reduces IL-1, IL-6 and TNFα production in hypothalamus of sheep during prolonged inflammation induced by LPS.	Yes	No	[533, 534]
SB 239063	p38	nt	nt	No	Inhibits NF-κB/AP-1 DNA-binding activity in rats exposed to cold stress Inhibits NF-κB transcription but does not reduce its binding capacity or IκBα phosphorylation in A549 cells Inhibits IL-1 and TNFα production in LPS-stimulated human PBMs and inhibits inflammation in mice with inhaled ovalbumin (OA)-induced airway eosinophilia Suppresses TNFα and IL-1β in rats with stress-induced gastric mucosal injury	Yes	Yes	[535-538]
PQ 401	IGF-R1	nt	nt	31.25	Reduces inflammatory monocytes/macrophages in colon and bone marrow of WT mice treated with DSS	Yes	No	[539]
Gefitinib	EGFR	12.52	nt	No	Up-regulates IKKβ/NF-κB in HNSCC cells Promotes inflammation by upregulating IL-1β, stimulates NLRP3 inflammasome formation in BMDMs and THP1 cells Increases immune cell infiltration and secretion pro-inflammatory cytokines in lungs of irradiated rats but inhibits lung fibrosis	No	No	[540-542]

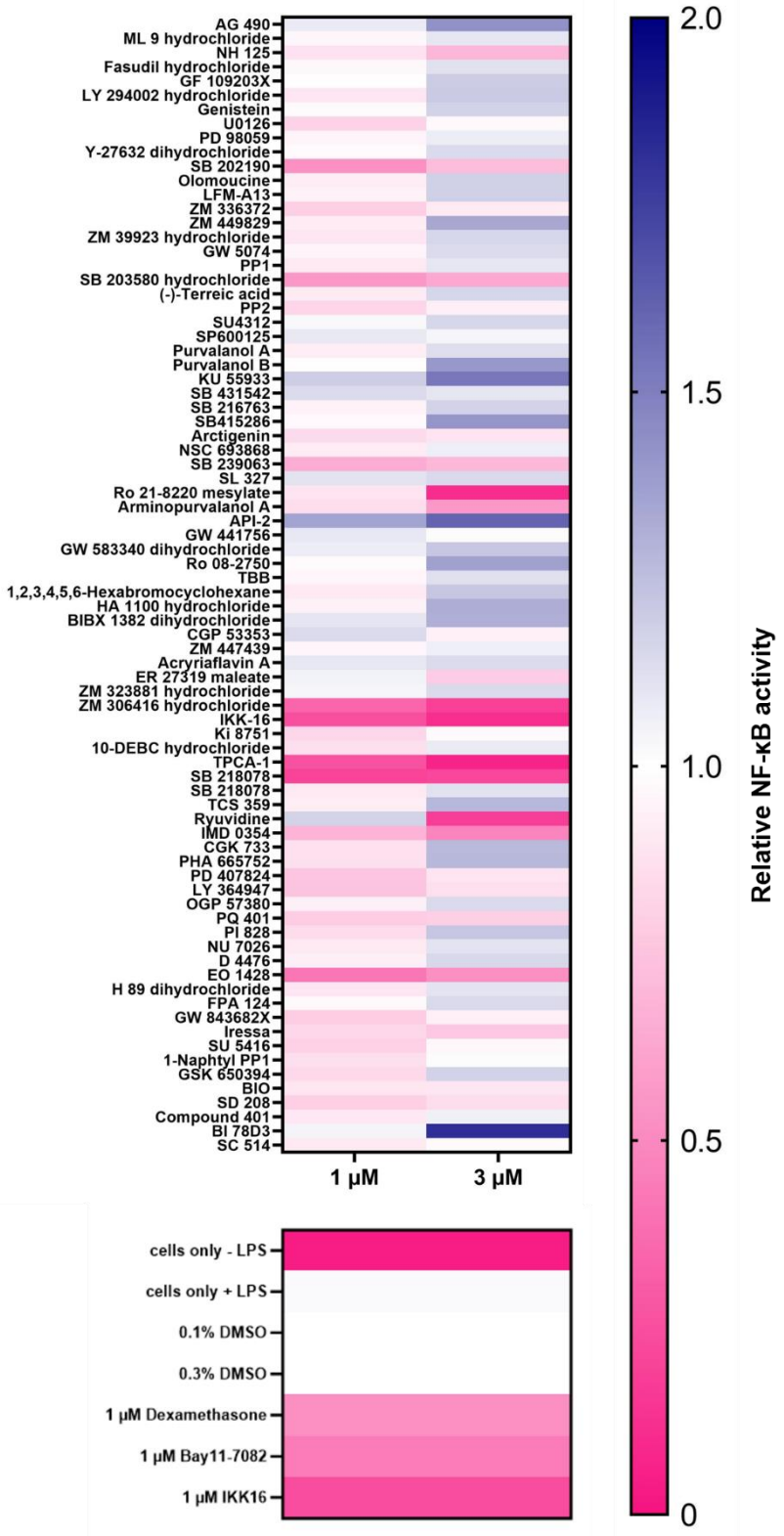
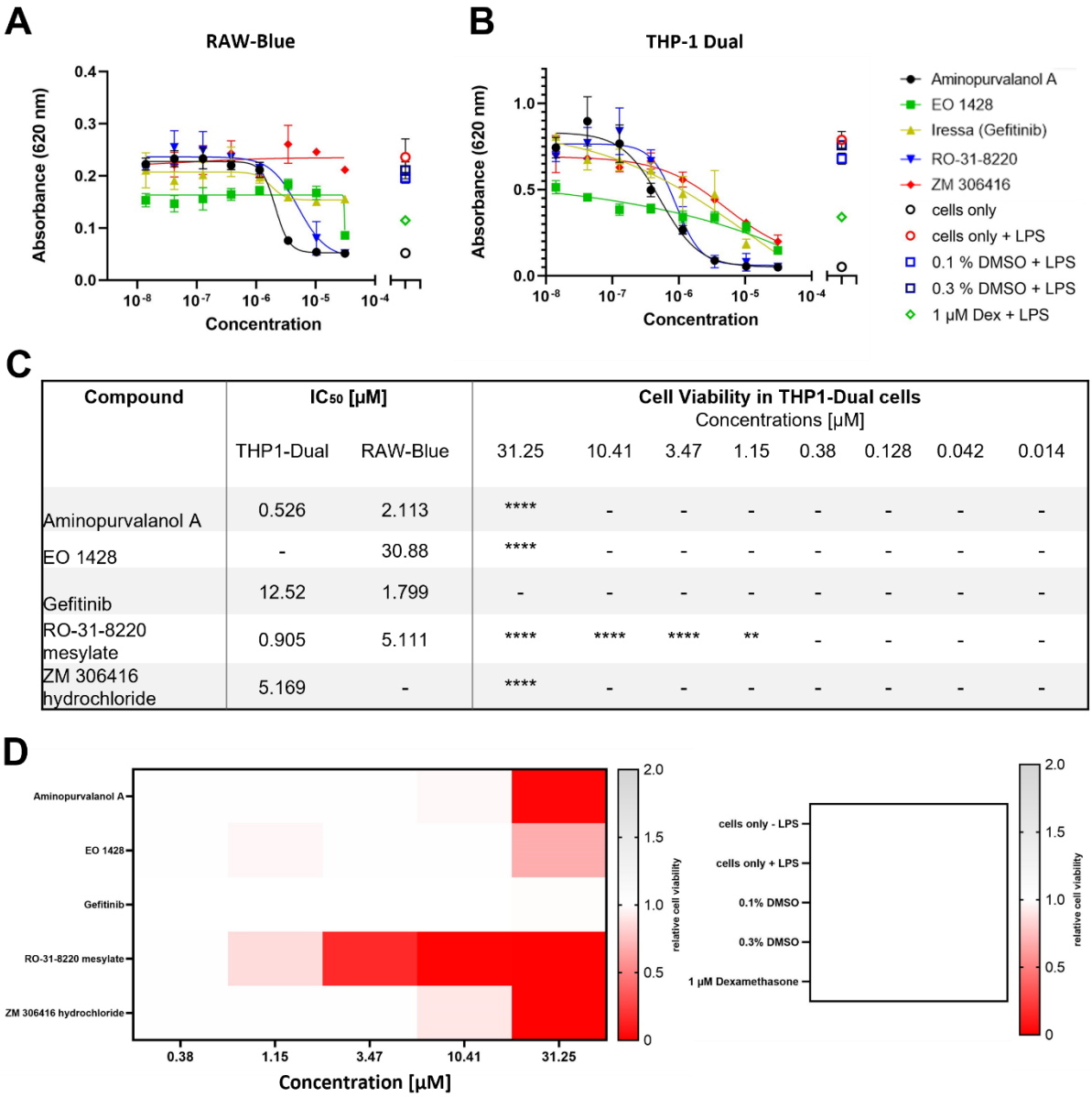


Fig. 3. 3 Drug repurposing screen identifies kinase inhibitors with unknown NF-κB inhibitory activity. Screen of 80 tool compounds from the TocriScreen Kinase Inhibitor Library for NF-κB inhibition. THP-1 Dual cells were pre-treated with compounds at 1 or 3 µM for 1 h before 24 h stimulation with 100 ng/mL LPS. Relative NF-κB activity was assessed by measuring the absorbance at 620 nm and normalization to DMSO + LPS. White indicates no change in NF-κB activity, while blue indicates an increase and pink indicates a decrease in NF-κB activity. Mean ±SEM, n=3-5 independent experiments.

The screen of the Tocriscreen Kinase Inhibitor Library identified compounds that significantly reduce NF-κB signaling in human and murine macrophages at both 1 µM and 3 µM compared

to DMSO-treated cells (Fig. 3.3). Based on potency and novelty of mechanism, aminopurvalanol A (CDK inhibitor), ZM 306416 hydrochloride (VEGFR1/EGFR/Abl/Src inhibitor), EO 1428 (p38 inhibitor), RO-31-8220 mesylate (PKC inhibitor) and gefitinib (EGFR inhibitor) were selected for further investigation, and the compounds were purchased from commercial vendors. Of these compounds, the dose-response was measured at 8 concentrations in RAW-Blue (Fig. 3.4A) and THP1-Dual cells (Fig. 3.4B) in the NF-κB SEAP reporter assay, with aminopurvalanol A and RO-31-8220 mesylate being the most potent inhibitors of NF-κB activity in both reporter cell lines with IC_{50} values in the high nanomolar to low micromolar range (Fig. 3.4C). Gefitinib potently reduced NF-κB activity in murine RAW-Blue cells (IC_{50}= 1.80 µM) but had weaker activity in THP1-Dual cells (IC_{50}= 12.52 µM). ZM 306416 hydrochloride was potent in inhibiting NF-κB activity in THP1-Dual cells but did not show any effect in RAW-Blue cells. EO 1428 did not show any effect in THP1-Dual cells and only mildly inhibited NF-κB activity in RAW-Blue cells with an IC_{50} of 30.88 µM, which is why it was excluded. To confirm that the observed effect was solely due to NF-κB inhibition and not cytotoxicity, cell viability was determined after drug treatment (Fig. 3.4C and D). RO-31-8220 mesylate was shown to significantly inhibit cell viability at concentrations as low as 1.15 µM and was therefore excluded from further studies.



Compound	IC50 [µM]		Cell Viability in THP1-Dual cells Concentrations [µM]							
	THP1-Dual	RAW-Blue	31.25	10.41	3.47	1.15	0.38	0.128	0.042	0.014
Aminopurvalanol A	0.526	2.113	****	-	-	-	-	-	-	-
EO 1428	-	30.88	****	-	-	-	-	-	-	-
Gefitinib	12.52	1.799	-	-	-	-	-	-	-	-
RO-31-8220 mesylate	0.905	5.111	****	****	****	**	-	-	-	-
ZM 306416 hydrochloride	5.169	-	****	-	-	-	-	-	-	-

Fig. 3. 4 Tool compound screen in NF-κB reporter assay identifies potential drug repurposing targets. Dose-response of THP1-Dual **(A)** or RAW-Blue **(B)** cells pre-treated with aminopurvalanol A (black), EO 1428 (green), gefitinib (yellow), RO-31-8220 (blue) and ZM 306416 (red) from Tocriscreen Kinase Inhibitor Library screen at 8 concentrations for 1 h prior to stimulation with LPS (100 ng/mL) for 24 h or 6 h, respectively. Controls were untreated cells (black circle), LPS only (red circle), 0.1 % DMSO + LPS (light blue square), 0.3 % DMSO + LPS (dark blue square) and 1 µM dexamethasone + LPS (green square). Mean ±SEM, n=3 independent cell preparations, normalization to DMSO + LPS. **(C)** IC_{50}s of NF-κB inhibition and cell viability of selected compounds tested at 8 concentrations. Mean ±SEM, n=3 independent cell preparations, normalization to DMSO + LPS. **(D)** Cell viability of THP1-Dual cells pre-treated with 8 concentrations of selected compounds or indicated controls measured in CellTiter-Glo assay. Relative cell viability was assessed by measuring the luminescence after the addition of CellTiter-Glo solution and normalization to DMSO + LPS. White indicates no change in cell viability, gray indicates an increase and red indicates a decrease in viability. Mean ±SEM, n=3 independent experiments.

3.3.2 Screen of FDA-approved tyrosine kinase inhibitors for NF-κB inhibition in RAW-Blue and THP1-Dual reporter cell lines

In the Tocriscreen Kinase Inhibitor Library screen we identified kinase inhibitors which target kinases that, when inhibited, reduce NF-κB signaling in human and murine macrophages. These kinases were VEGFR receptors, EGFR, Abl and Src. Based on these findings, selected FDA-approved tyrosine kinase inhibitors (TKIs) sharing those targets were included in a screening library that I designed based on bibliographic searches (Table 3.4).

All TKIs were screened at 8 concentrations in both THP1-Dual (Fig. 3.5A) and RAW-Blue cells (Fig. 3.5C) using the NF-κB SEAP reporter assay. To exclude effects due to cell cytotoxicity, cell viability was determined at the same time (Fig. 3.5B and 3.5D).

Compound	IC_{50} THP1-Dual (μM)	IC_{50} RAW Blue (μM)	Targets	Reported anti-inflammatory activity?	Reported anti-NF-κB activity in macrophages?	Current indication	Comments	References
Ponatinib	0.251	2.415	VEGFR2, Abl, Src, PDGFR	Yes	No	Leukemia	Increased NF-κB activity in HAEC cells Reduces IL-8 and MCP-1 in influenza A infection model Inhibits NF-κB activity in HEK Blue and USO2 cells	[543, 544]
Tivozanib	6.897	6.946	VEGFR1-3	No	No	Renal cell carcinoma	Inhibits NF-κB activity in OVCAR3 and A2780CP cells	[545]
Orantinib	-	10.19	VEGFR2, PDGFR, FGFR	No	No	Lung/ liver cancer*	-	-
Erlotinib	-	-	EGFR	Yes	Yes	Lung cancer, pancreatic cancer	Inhibits TNFα, case reports of inhibiting psoriasis, inflammatory bowel disease, rheumatoid arthritis, and other nonautoimmune inflammatory disorders Decreases LPS-induced TLR4 expression on macrophages Reduces NF-κB activity and both cytokine expression and endotoxicity in response to LPS Increases RelA translocation in HCC827 and 11-18 cells and tumors Inhibits NF-κB in lung cancer trials	[546-550]

Nintedanib	-	-	Lck, Lyn, Src, PDGFR, FGFR, VEGFR1-3, FLT3	Yes	Yes?	Lung cancer, pulmonary fibrosis	Attenuates activation of renal fibrosis and partially reverses established renal fibrosis by inhibiting STAT3 and NF-κB activation and thus inflammation and macrophage infiltration Ameliorates imiquimod-induced psoriasis by inhibiting NF-κB and VEGFR2 signaling Reduces experimental lung fibrosis by inhibiting inflammation	[551-555]
Vandetanib	1.203	104	VEGFR2, EGFR, Src	Yes	No	Thyroid gland tumour	Reduces Inflammation and ameliorates COVID-19 in mice	[556]
Apatinib	19.98	59.30	VEGFR2	Yes	No	Gastric cancer	Apatinib inhibits NF-κB activation in doxorubicin-stimulated MDA-MB-231/ADR cells and human liver cancer cell lines Resolvied psoriasis leasions in cancer patient treated with Apatinib (one case report)	[557-560]
Regorafenib	3.568	7.403	VEGFR1-3	Yes	No	Colorectal/ gastrointestinal/ hepatocellular cancer	Inhibits NF-κB activation in vivo in mice with hepatocellular carcinoma and lung cancer and in vitro in SK-HEP-1 and HEK-Blue cells Inhibits inflammatory cytokine production in SK-Hep-1 cells Reduces neuroinflammation and AD pathology in mice with AD and BV2 microglia via Akt/STAT3 inhibition	[561-567]
Pazopanib	5.446	791	VEGFR2	Yes	No	Renal cell/ soft tissue carcinoma	Reduces NF-κB activity in patients with renal cell carcinoma Decreases expression of NF-κB in patients with kidney cancer	[568, 569]
Sorafenib	3.043	18.67	VEGFR, PDGFR, RAF kinases	Yes	No	Kidney/ thyroid/ liver cancer, leukemia	Reduces neuroinflammation and AD pathology in mice with AD and in BV2 microglia by inhibiting AKT/p38-linked STAT3/NF-κB signaling	[570-577]

							Inhibits TNF-dependent necroptosis and protects mice from inflammation and tissue injury, did not affect TNF-induced NF-κB activation Reduces inflammation in models of liver and breast cancer Inhibits NF-κB in HEK293 GFP-IκBα GripTite , OS U-2 and HCCLM3 Acctivates NF-κB in HCT116 cells	
Axitinib	-	5.674	VEGFR1-3, PDGFR, c-Kit	Yes/No	No	Renal cell carcinoma	Reduces NF-κB and TNFα levels in corneal neovascularization rat model Reduces LPS-induced monocyte-derived human DC activation by reducing nuclear expression of cRel and inhibiting p38/STAT3 signaling Increases immune cell infiltration and reduces supressive capacity of monocytic MDSCs in mouse melanoma model	[578-580]
Saracatinib	2.295	12.19	Src, Abl	Yes	No	Alzheimer‘s disease*	Reduces osteoclast differentiation, polarization and resorptive function *in vitro* and in mice with multiple myeloma Reduces microgliosis, astrogliosis, neurodegeneration, neuroinflammation and nitro-oxidative stressors in rats treated with DFP (epilepsy model) and rat KA-model of TLE	[581-583]
Afitinib	3.679	4.789	EGFR	Yes/No	No	Lung cancer	Activates NF-κB in HCC827 cells Reduces astrocyte activation, proliferation, NO production and inflammasome activvation in OGD-induced neuroinflammation in primary cultured astrocytes Case reports of fatal afatinib-induced interstitial pneumonia	[549, 584, 585]

Lenvatinib	1.321	23.58	VEGFR1-3, FGFR1-4, PDGFRα/β, c-Kit, RET	Yes	Yes	Thyroid cancer	Decreases the proportion of monocytes and macrophages population and increased that of $CD8^+$ T cell populations in Hepa1-6 hepatocellular carcinoma model Decreases Treg infiltration and TGFβ signaling in HCC patients Inhibits NF-κB/Akt signaling in NSCLC *in vivo* and *in vitro* Inhibits NF-κB in hepatocellular carcinoma *in vivo* and *in vitro*	[586-590]
Pexidartinib	-	-	CSF-1R	Yes	Yes	Tenosynovial giant cell tumor	Suppresses inflammation in endometriosis Reduces microglia expression of *il-1β*	[591, 592]

Table 3. 4 Drugs with anti-inflammatory effect identified with NF-κB reporter assay. Screening of FDA-approved tyrosine kinase inhibitors in NF-κB reporter assay using RAW-Blue and THP1-Dual cells. Table is color coded: green= drugs with promising anti-NF-κB activity in screen and shown anti-inflammatory activity in macrophages, yellow= drugs with promising anti-NF-κB activity in screen, anti-inflammatory activity in macrophages still under investigation. * = in clinical trials. Data are presented as mean ±SEM, n=2/3 independent cell preparations.

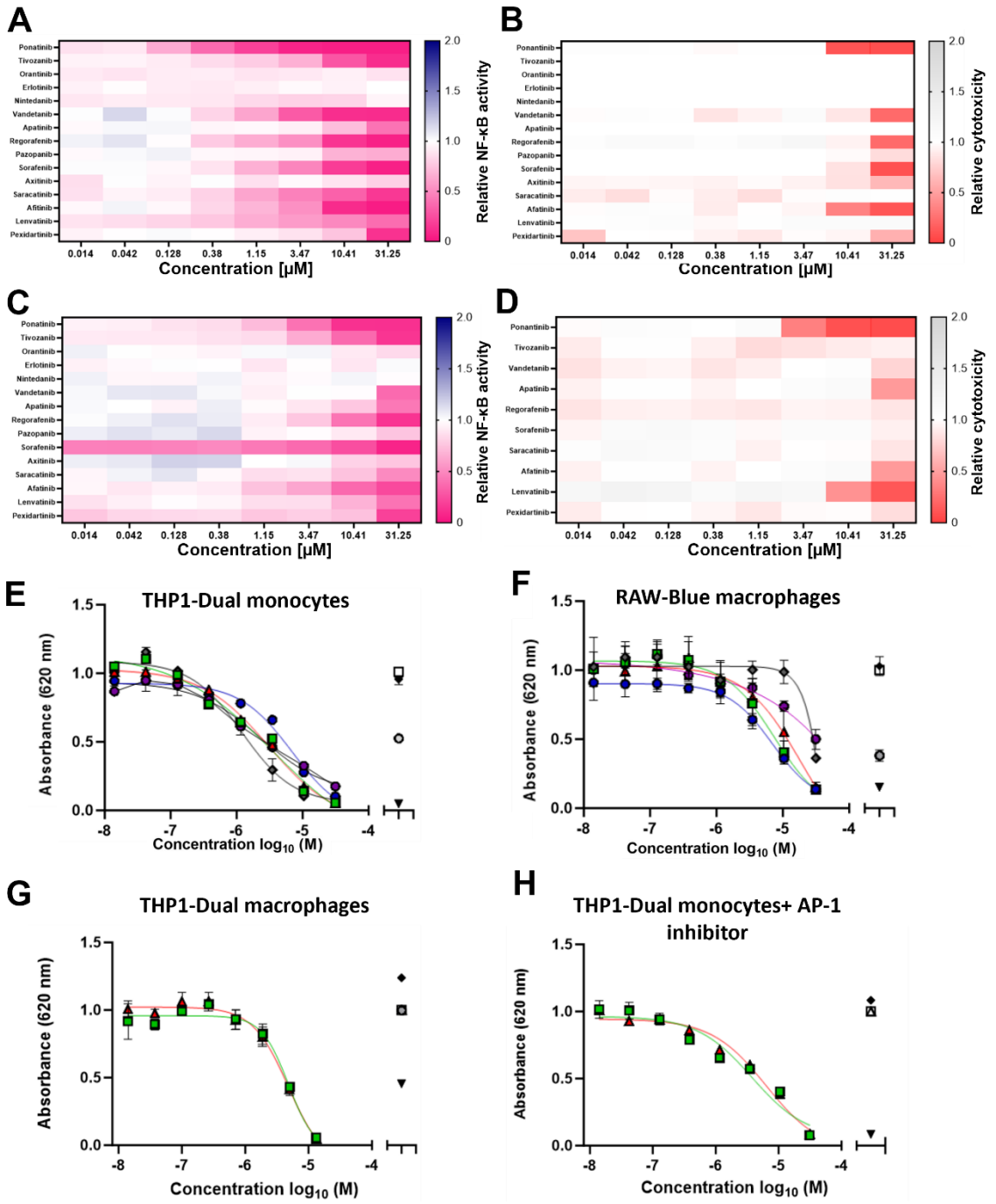


Fig. 3. 5 Screen of FDA-approved medicines in NF-κB reporter assay identifies drug repurposing candidates. (A) THP1-Dual monocytes or **(B)** RAW-Blue macrophages were pre-treated with FDA-approved tyrosine kinase inhibitors at 8 concentrations for 1 h before 24 h or 6 h stimulation with LPS, respectively. Relative NF-κB activity was assessed by measuring the absorbance at 620 nm after the addition of QB solution and normalization to DMSO + LPS. White indicates no change in NF-κB activity, blue indicates an increase and pink indicates a decrease in NF-κB activity. Mean ±SEM, n=3-6 independent experiments. Cell viability of THP1-Dual monocytes **(C)** or RAW-Blue macrophages **(D)** pre-treated with 8 concentrations of selected FDA-approved medicines measured in CellTiter-Glo assay. Relative cell viability was assessed by measuring the luminescence after the addition of CellTiter-Glo solution and normalization to DMSO + LPS. White indicates no change in cell viability, grey indicates an increase and red indicates a decrease in viability. Mean ±SEM, n=3 independent experiments. Relative NF-κB activity in THP1-Dual monocytes **(E)** or RAW-Blue macrophages **(F)** pre-treated with regorafenib

(green square), sorafenib (red triangle), tivozanib (blue circle), vandetanib (purple diamond) or saracatinib (purple circle) at 8 concentrations for 1 h before stimulation with LPS for 24 h (THP1-Dual) or 6 h (RAW-Blue). Normalization to DMSO+ LPS. Mean ±SEM, n=3 independent cell preparations. Controls on the right: untreated cells (filled black triangle), untreated cells + LPS (filled black diamond), 0.1 % DMSO + LPS (black square), 0.3 % DMSO (black triangle) and 1 µM dexamethasone + LPS (grey circle). **(G)** NF-κB activity of THP1-Dual macrophages pre-treated with regorafenib (green) or sorafenib (red) 24 h post LPS stimulation measured by QuantiBlue assay and normalized to DMSO+ LPS. **(H)** Relative NF-κB activity in THP1-Dual monocytes pre-treated with 10 µM AP-1 inhibitor T-5224 for 1 h before 1 h pre-treatment with regorafenib (green) and sorafenib (red) or indicated controls at 8 concentrations and subsequent with LPS stimulation for 24 h normalized to DMSO+ LPS. Mean ±SEM, n=3 independent cell preparations.

Based on their potency of inhibiting NF-κB activation, 5 medicines were selected for further studies: tivozanib (VEGFR1-3 inhibitor), vandetanib (VEGFR2/EGFR/Src inhibitor), saracatinib (Src/Abl inhibitor), regorafenib and sorafenib (VEGFR/PDGFR/FGFR/Tie2/c-Kit/Ret/CSF-1R/Raf inhibitors).

Table 3. 5: IC_{50} values of inhibition of NF-κB activity in Quanti-Blue assay in reporter cell lines. nt= not tested.

Drug	**IC_{50} (µM)**		
	RAW-Blue macrophages	**THP1-Dual monocytes**	**THP1-Dual macrophages**
Tivozanib	6.95	6.90	19.35
Vandetanib	-	1.20	-
Regorafenib	7.40	3.57	9.90
Sorafenib	18.67	3.04	9.88
Saracatinib	12.19	2.30	nt

Their IC_{50} values of inhibiting NF-κB in THP-1 Dual monocytes (Fig. 3.5E), RAW-Blue cells (Fig. 3.5F) and PMA-treated THP1-Dual macrophages (Fig. 3.5G) were in the low micromolar range and they generally seemed more potent in human THP1-Dual cells than in murine RAW-Blue cells (Table 3.5). Since the SEAP reporter construct in the reporter cell lines used to determine NF-κB inhibition reports on both NF-κB as well as AP-1 activity, we sought to exclude that AP-1 inhibition was responsible for the effect of

the tyrosine kinases observed in the screen. Therefore, THP1-Dual cells were pre-treated with 10 µM AP-1 inhibitor T-5224 prior to treatment with regorafenib or sorafenib and stimulation with LPS. Importantly, dose-response curves (Fig. 3.5H) and IC_{50} values (regorafenib: IC_{50}=3.74 µM, sorafenib: IC_{50}= 6.31 µM) determined in the QUANTI-Blue assay were comparable to those observed in the absence of T-5224.

3.3.3 Validation of the anti-inflammatory activity of repurposing candidates in primary murine macrophages

Upon NF-κB activation, macrophages initiate the production of pro-inflammatory cytokines and chemokines. To confirm the anti-inflammatory activity of our drug repurposing candidates identified as NF-κB inhibitors in the initial screen, their effect on LPS-induced gene expression and protein production of pro-inflammatory mediators in primary murine macrophages and human THP1-Dual macrophages was investigated.

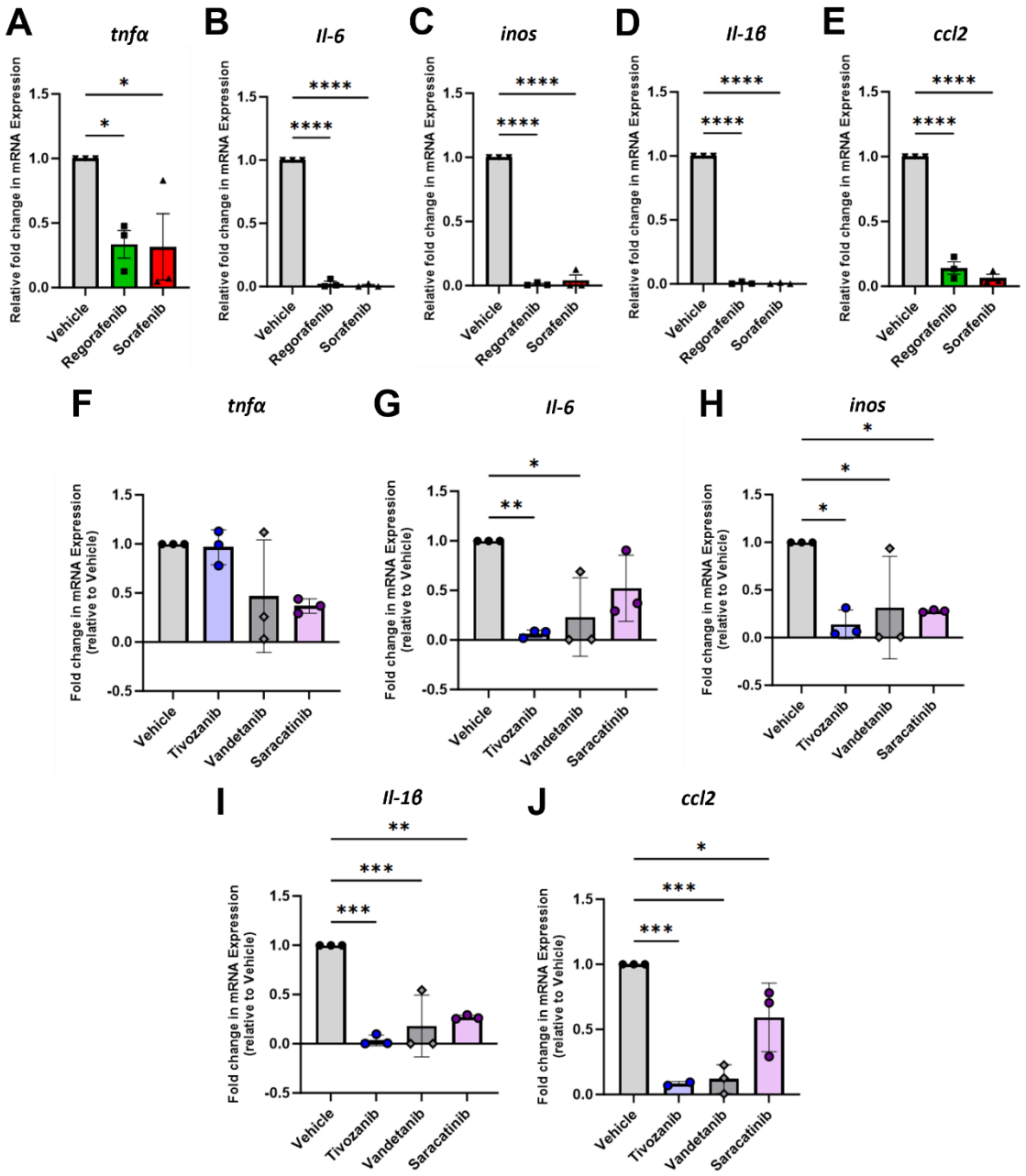


Fig. 3. 6 Regorafenib and sorafenib reduce inflammatory gene expression in primary murine macrophages. Relative gene expression of *tnfα, il-6, il-1β, ccl2* and *inos* was assessed by qPCR and normalized to 18S in BMDMs after pre-treatment with 3 µM of regorafenib (green) and sorafenib (red) **(A-E)** or 3 µM tivozanib (blue), vandetanib (dark grey) and saracatinib (purple) **(F-J)** or 0.1 % DMSO (light grey) for 1 h before LPS stimulation for 2 h. Mean ±SEM, n=3 independent cell preparations. One-way ANOVA with Dunnett's multiple comparisons test against LPS + DMSO.

Pre-treatment of BMDMs with 3 µM regorafenib or sorafenib prior to LPS stimulation for 2 h potently reduced mRNA levels of pro-inflammatory mediators *tnfα* (Fig. 3.6A), *il-6* (Fig. 3.6B), *inos* (Fig. 3.6C), *il-1β* (Fig. 3.6D) and *ccl2* (Fig. 3.6E).

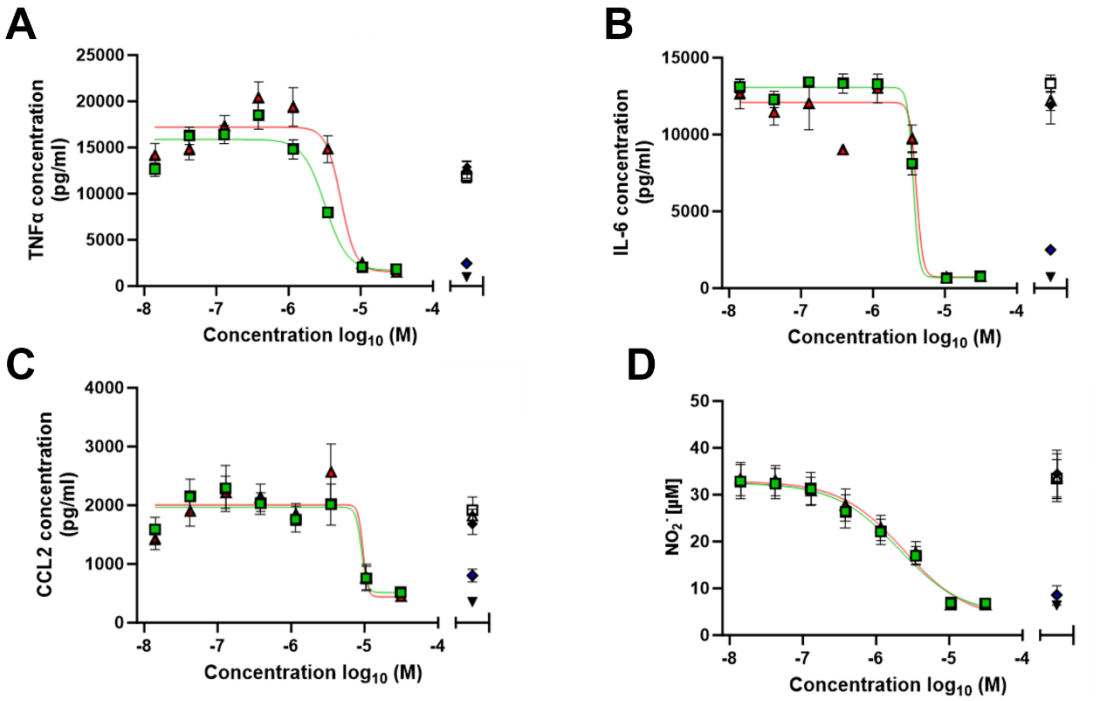


Fig. 3. 7 Regorafenib and sorafenib reduce inflammatory mediator production in primary murine macrophages. (A-C) Dose-response of pro-inflammatory mediator secretion by BMDMs measured by ELISA after pre-treatment with regorafenib, sorafenib or vehicle for 1 h and subsequent LPS stimulation for 7 h. Mean ±SEM, n=3 independent cell preparations**. (D)** Nitrite production by BMDMs was measured by Griess assay after pre-treatment with regorafenib, sorafenib or vehicle for 1 h and subsequent LPS + IFN-γ stimulation for 22 h. Mean ±SEM, n=3 independent cell preparations.

Correspondingly, regorafenib and sorafenib dose-dependently suppressed protein production of pro-inflammatory cytokines TNFα (Fig. 3.7A), IL-6 (Fig. 3.7B) as well as chemokine CCL2 (Fig. 3.7C) in BMDMs 7 h after LPS stimulation (Table 3.6). Both TKIs also effectively reduced nitric oxide levels (Fig. 3.7D) induced by LPS+IFN-γ stimulation (Table 3.6).

Table 3. 6 IC_{50} values for inhibition of pro-inflammatory mediator production in BMDMs

Drug	IC_{50} (µM)			
	TNFα	IL-6	CCL2	NO
Regorafenib	3.17	3.60	9.00	2.06
Sorafenib	5.26	3.98	9.43	2.39

At this point, the decision was made to exclude tivozanib, vandetanib and saracatinib as they did not inhibit *tnfα* expression and had overall weaker anti-inflammatory effects in LPS-stimulated BMDMs (Fig. 3.6F-J). Throughout this thesis, regorafenib-treated samples are depicted in green and sorafenib-treated samples are shown in red.

3.3.4 Anti-inflammatory activity of regorafenib and sorafenib on human MDMs

As regorafenib and sorafenib have potent anti-inflammatory activity in primary murine macrophages, I investigated whether this effect translates into human THP1-Dual macrophages. We observed that regorafenib and sorafenib dose-dependently inhibited LPS-induced TNFα (IC_{50}s= 0.67 µM and 1.07 µM, respectively, Fig. 3.8A) and IL-6 production (IC_{50}s= 1.07 µM and 1.90 µM, respectively, Fig. 3.8B).

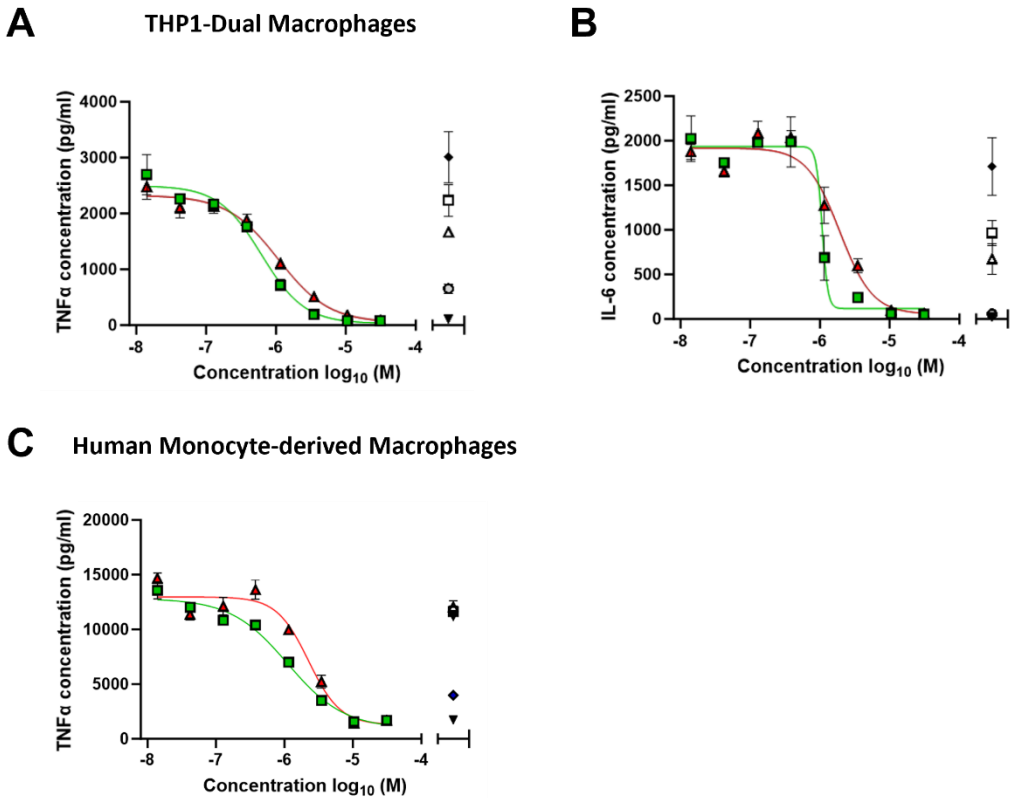


Fig. 3. 8 Regorafenib and sorafenib reduce inflammation in human macrophages. Dose-response of TNFα **(A)** and IL-6 **(B)** protein production by THP1-Dual macrophages measured by ELISA after pre-treatment with regorafenib (green), sorafenib (red) or vehicle for 1 h and subsequent LPS stimulation for 24 h. Mean ±SEM, n=3 independent cell preparations. **(C)** Dose-response of TNFα secretion by primary human monocyte-derived macrophages pre-treated with regorafenib, sorafenib or vehicle for 1 h and subsequent LPS stimulation for 7 h. Mean ±SEM, n=3 independent cell preparations.

To confirm the clinical relevance of the observed anti-inflammatory properties in human macrophages, the effect of both TKIs was tested in human primary monocyte-derived macrophages. We found that in human MDMs, regorafenib and sorafenib dose-dependently suppressed LPS-induced TNFα production more effectively than in primary murine macrophages, with IC_{50}s= 1.12 µM and 2.26 µM, respectively (Fig. 3.8C).

3.3.5 Effect of regorafenib and sorafenib on NF-κB signaling in macrophages

In murine RAW-Blue macrophages and human THP1-Dual monocyte reporter cells, Regorafenib potently inhibited NF-κB induced SEAP reporter production. Therefore, I sought to confirm that these drug repurposing candidates directly reduce NF-κB phosphorylation as well as its subsequent translocation into the nucleus. RAW-Blue macrophages were pre-treated with 3 µM regorafenib, sorafenib or DMSO vehicle before LPS stimulation for 0, 5, 15, 30 or 60 min (Fig. 3.9A). While regorafenib significantly reduced p65 phosphorylation at 5, 30 and 60 minutes post-stimulation, sorafenib inhibited p65 phosphorylation already at 0 min and continued to suppress phosphorylation at 5 min and 30 min compared to Vehicle.

Once the NF-κB heterodimer is phosphorylated, it translocates from the cytosol into the nucleus, where the transcription factor induces the transcription of pro-inflammatory target genes. Thus, I next investigated whether regorafenib and sorafenib inhibit p65 nuclear translocation following their inhibition of p65 phosphorylation. RAW-Blue macrophages were pre-treated with 3 µM regorafenib, 3 µM sorafenib, 1 µM IKK16 or DMSO vehicle before stimulation with LPS for 10 min. Localization of p65 was analyzed using ImageStream flow cytometry (Fig. 3.9B).

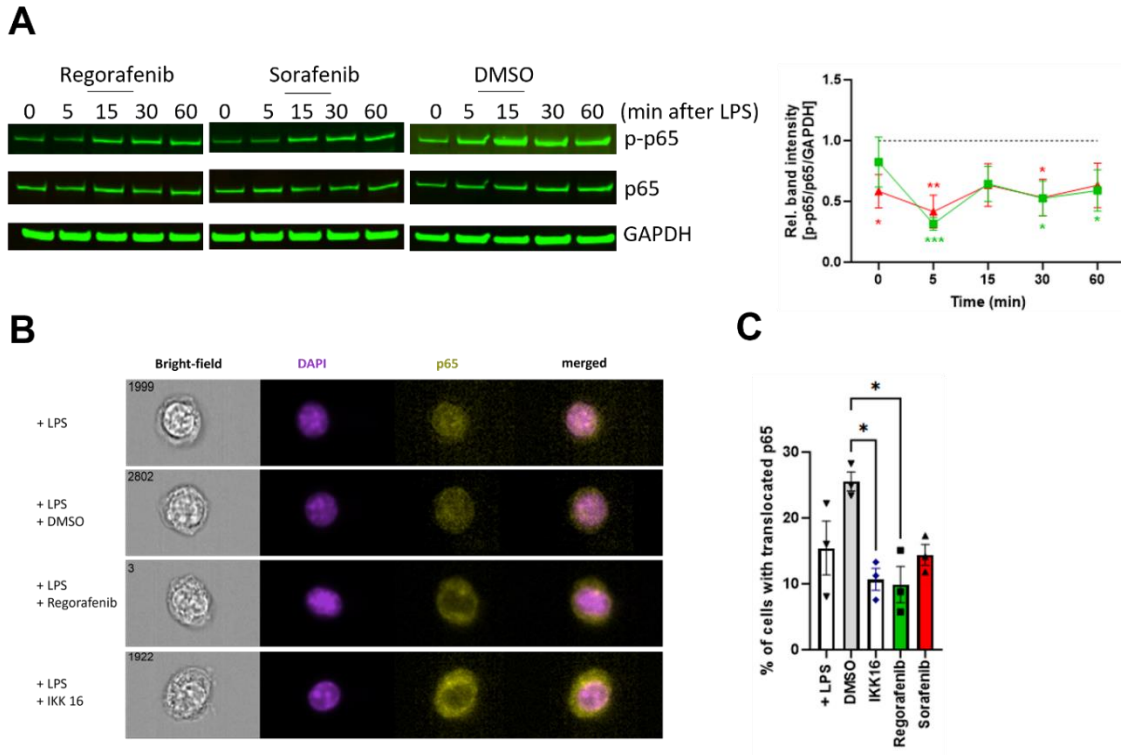


Fig. 3. 9 Regorafenib and sorafenib reduce NF-κB signaling in macrophages. (A) Representative Western Blots for phosphorylation of Ser^{536} on p65 in RAW-Blue cells and normalized to total p65 and GAPDH. Quantification using densitometry. Cells were treated with 3 µM regorafenib (green) or 3 µM sorafenib (red) for indicated time points. Data shown on the right are individual values with means ±SEM, n=3-5 per group; Two-way ANOVA with Dunnett's multiple comparisons test. **(B)** ImageStream images are illustrative of 3 separate experiments (60x magnification). RAW-Blue cells were pre-treated with 3 µM regorafenib or sorafenib or indicated controls for 1 h before LPS stimulation for 10 min. **(C)** Quantification of ImageStream data indicating the percentage of cells in which p65 nuclear translocation has occurred. One-Way ANOVA with Dunnett's multiple comparisons test.

As expected, in unstimulated cells or LPS-stimulated cells that were pre-treated with IKK16, p65 was localized in the cytosol. In contrast, p65 had translocated into the nucleus in cells treated with LPS or LPS+DMSO Vehicle. Regorafenib significantly reduced the number of cells in which p65 nuclear translocation had occurred compared to Vehicle by 61 %, whereas the effect of sorafenib on p65 nuclear translocation (43 % decrease in cells with p65 translocation) was not significant (Fig. 3.9C).

3.3.6 Effect of regorafenib and sorafenib on tyrosine kinase phosphorylation in macrophages

In cancer cells, regorafenib and sorafenib have been reported to inhibit receptor tyrosine kinases VEGFR1-3, TIE-2, PDGFR-β, FGFR, CSF-1R, c-Kit and Ret as well as intracellular kinases Src and Raf, the latter of which induces STAT3 activation through the MEK/ERK signaling pathway. Downstream signaling of these tyrosine kinases results in the activation of NF-κB. Therefore, I investigated the effects of regorafenib and sorafenib on these signaling cascades in macrophages.

RAW-Blue macrophages were pre-treated with 3 µM regorafenib, sorafenib or DMSO vehicle before LPS stimulation for 5, 10 or 15 min. Both regorafenib and sorafenib significantly suppressed p38 phosphorylation at all time points by around 50 % compared to vehicle (Fig. 3.10A). Src phosphorylation was significantly inhibited by the TKIs at 5 min post LPS stimulation (Fig. 3.10B). Importantly, phosphorylation of CSF-1R, which is highly expressed on the surface of monocytes and macrophages and is linked to pathological inflammation, was inhibited by regorafenib and sorafenib (Fig. 3.10C). Notably, ERK (Fig. 3.10D), AKT and STAT3 (Fig. 3.10E) phosphorylation, which occurs downstream of RTK activation, was not affected.

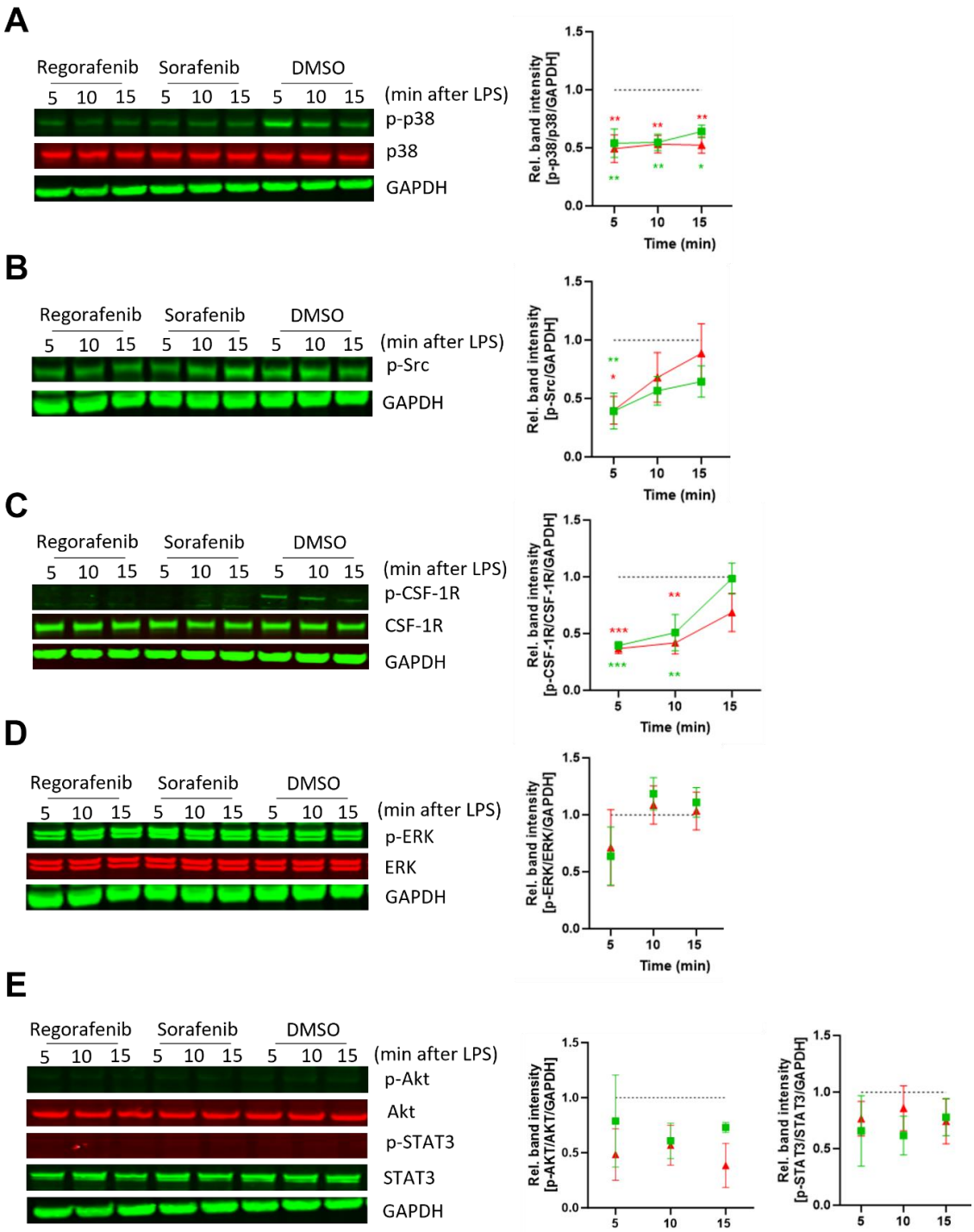


Fig. 3. 10 Regorafenib and sorafenib reduce pro-inflammatory signaling in macrophages. **(A)** Representative Western Blots for phosphorylation of Thr180/Tyr182 on p38 in RAW-Blue cells and normalized to total p38 and GAPDH; **(B)** for phosphorylation of Tyr416 on Src in RAW-Blue cells and normalized to GAPDH; **(C)** for phosphorylation of Tyr723 on CSF-1R and normalized to total CSF-1R and GAPDH; **(D)** for phosphorylation of Thr^{202}/Tyr^{204} on ERK and normalized to total ERK and GAPDH and **(E)** for phosphorylation of Ser^{473} on Akt or Ser^{727} on STAT3 and normalization to total AKT or STAT3 and GAPDH. Quantification using densitometry. Cells were treated with 3 µM regorafenib (green) or 3 µM sorafenib (red) or DMSO vehicle (black line) before LPS stimulation for indicated time points. Mean ±SEM, n=3; One-way ANOVA with Dunnett's multiple comparisons test.

3.3.7 Effect of regorafenib on macrophage polarization

NF-κB activation and subsequent pro-inflammatory mediator production are linked to classical activation (M1-like state) of macrophages. Therefore, shifting macrophage polarization from an M1-like state to alternative activation (M2-like state) has been explored to treat pathological inflammation and enhance tissue repair. FDA-approved anti-cancer medicine ibrutinib, which targets BTK, was shown to not only inhibit NF-κB signaling but to also to induce a shift of macrophage polarization towards an M2-like phenotype, characterized by increased surface levels of CD206 and metabolic reprogramming [372, 593, 594].

Given regorafenib's ability to reduce NF-κB signaling, I aimed to investigate the effect of regorafenib on BMDM polarization. Unpolarized BMDMs (M0) were pre-treated with 3 µM regorafenib or vehicle for 1 h before polarization towards a classically activated M1-like phenotype (100 ng/ml LPS + 20 ng/ml IFN-γ) or an alternatively activated M2-like phenotype (20 ng/ml IL-4) for 16 h as described in [595]. After polarization, the expression of M1 marker MHCII and M2 marker CD206 on the cell surface were determined by flow cytometry as described in [430]. As shown in the gating strategy for BMDM polarization analysis (Fig. 3.11A), cells were first gated by size (forward scatter, FSC) *vs*. granularity (side scatter, SSC) before single cells were identified by excluding cell aggregates in FSC height/FSC area and FSC height/ FSC width plots. From all single $F4/80^+$ cells, population sizes of M1 macrophages ($F4/80^+$, $MHCII^+$) and M2 macrophages ($F4/80^+$, $CD206^+$) were determined. Analysis of polarization marker expression confirmed that BMDMs were successfully polarized, with 66 % of M1-like macrophages expressing MHCII on their surface (Fig. 3.11B).

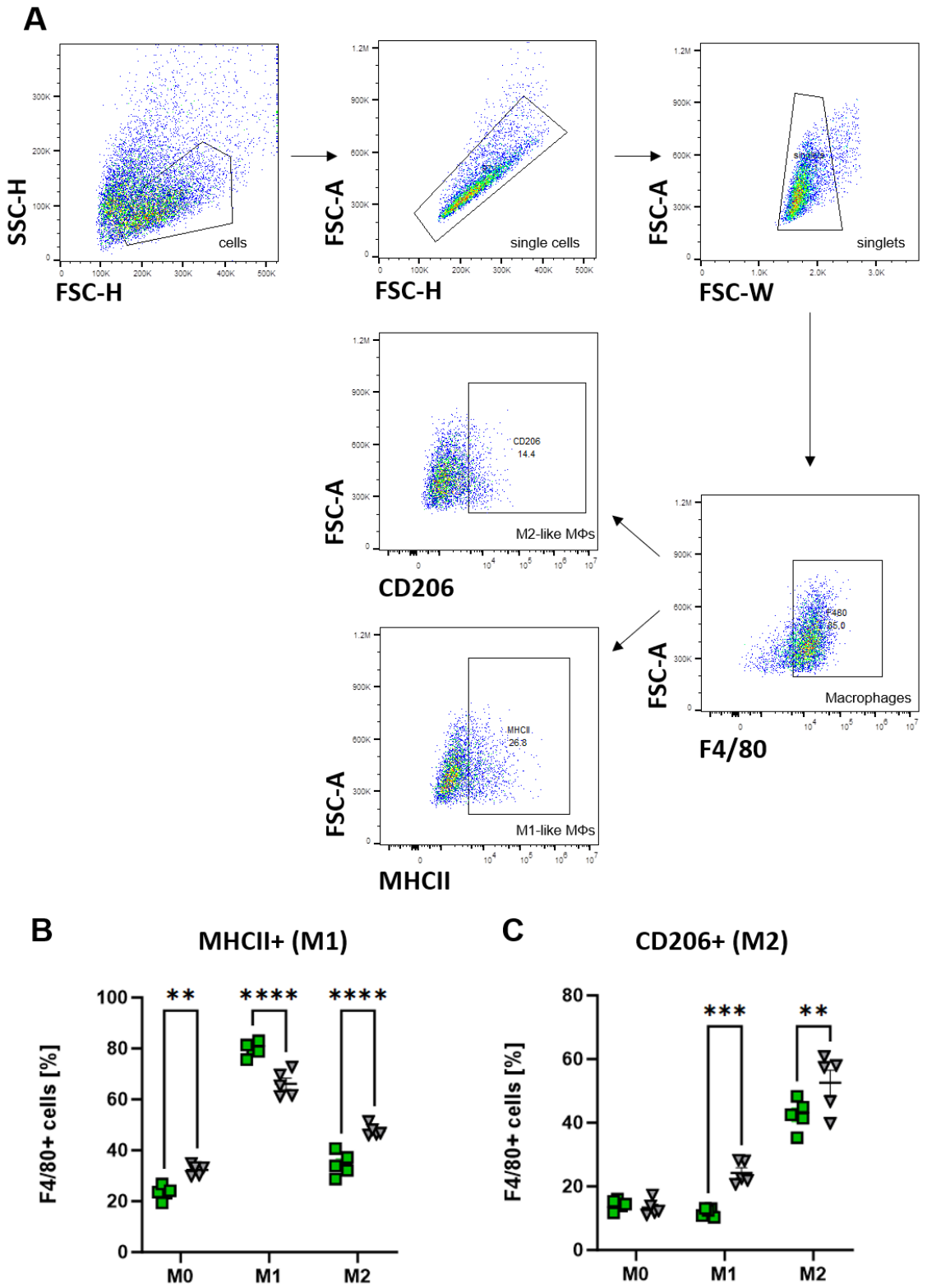


Fig. 3. 11 Regorafenib and sorafenib modulate macrophage polarization in vitro. A) Gating strategy for flow cytometry analysis of BMDM polarization. BMDMs were pre-treated with 3 µM regorafenib (green) or DMSO vehicle (grey) for 1 h before M1, M2 or M0 (control) macrophage (MΦ) polarization, and MHCII **(B)** and CD206 **(C)** surface expression was assessed using flow cytometry. One-Way ANOVA with Dunnett's multiple comparisons test. Mean ±SEM, n=5 biological replicates.

Expression was significantly lower in M0 (32 %) and M2-like (47 %) BMDMs. Regorafenib further decreased MHCII surface levels on M0 and M2-like BMDMs by 27.5 % and 27.7 %, respectively, while increasing MHCII expression on M1-like macrophages to 80 % (20.5 % increase).

IL-4 treatment of BMDMs increased CD206 surface levels from 13 % in non-polarized macrophages to 53 % in M2-like BMDMs, confirming successful polarization (Fig. 3.11C). In contrast, only 24 % of classically activated macrophages expressed CD206 on their surface. Regorafenib had no effect on CD206 expression on M0 macrophages but significantly decreased CD206 levels on the surface of both M1-like macrophages as well as M2-like macrophages (50.9 % and 19.1 % decrease, respectively).

Here, we found that regorafenib modulates macrophage polarization. The TKI increased MCHII expression on M1-polarized macrophages and decreased MHCII surface levels on M0 and M2-like macrophages. CD206 levels were reduced on both classically and alternatively activated macrophages.

3.3.8 Effect of regorafenib and sorafenib on TLR4 surface expression

Considering the strong anti-inflammatory properties of regorafenib on LPS-stimulated primary macrophages, I sought to investigate whether this effect is mediated by targeting the TIRAP/MyD88 signaling cascade or TRIF-dependent LPS-induced internalization of TLR4 [596].

Regorafenib has been reported to down-regulate *tlr4* gene expression in Huh7 cells [597] and sorafenib was shown to decrease TLR4 surface expression on LPS-stimulated BMDMs [598]. Therefore, I determined mRNA levels of *tlr2* and *tlr4*, both of which are targeted by LPS, in RAW-Blue macrophages pre-treated with 3 µM regorafenib, sorafenib or vehicle after 2 h LPS stimulation (Fig. 3.12A). Neither regorafenib nor

sorafenib treatment significantly affected *tlr2* or *tlr4* expression in RAW-Blue macrophages at this time point.

Given regorafenib and sorafenib did not alter *tlr4* expression at the mRNA level, flow cytometry was used to assess receptor internalization of TLR4 in BMDMs following LPS stimulation, which serves as an indicator of LPS-dependent TRIF activation, as described by Richard *et al.* [599]. BMDMs were pre-treated with 3 µM regorafenib or vehicle for 1 h before stimulation with LPS for 0, 10, 30 or 60 min. The gating strategy of the flow cytometry experiment is shown in Fig. 3.12B. Cell debris was excluded, single cells were selected and TLR4 levels were visualized in a histogram for geometric mean fluorescence intensity (gMFI) in F4/80^{+} macrophages (Fig. 3.12C). As expected, TLR4 surface levels decreased post-LPS stimulation, with significantly reduced TLR4 detection at the 30- and 60-min time points. However, regorafenib did not affect TLR4 levels on BMDMs compared to vehicle. From my experiments, I concluded that regorafenib's inhibition of NF-κB activation in response to LPS is likely not mediated by a direct effect on TLR2/4 expression or TLR4 endocytosis.

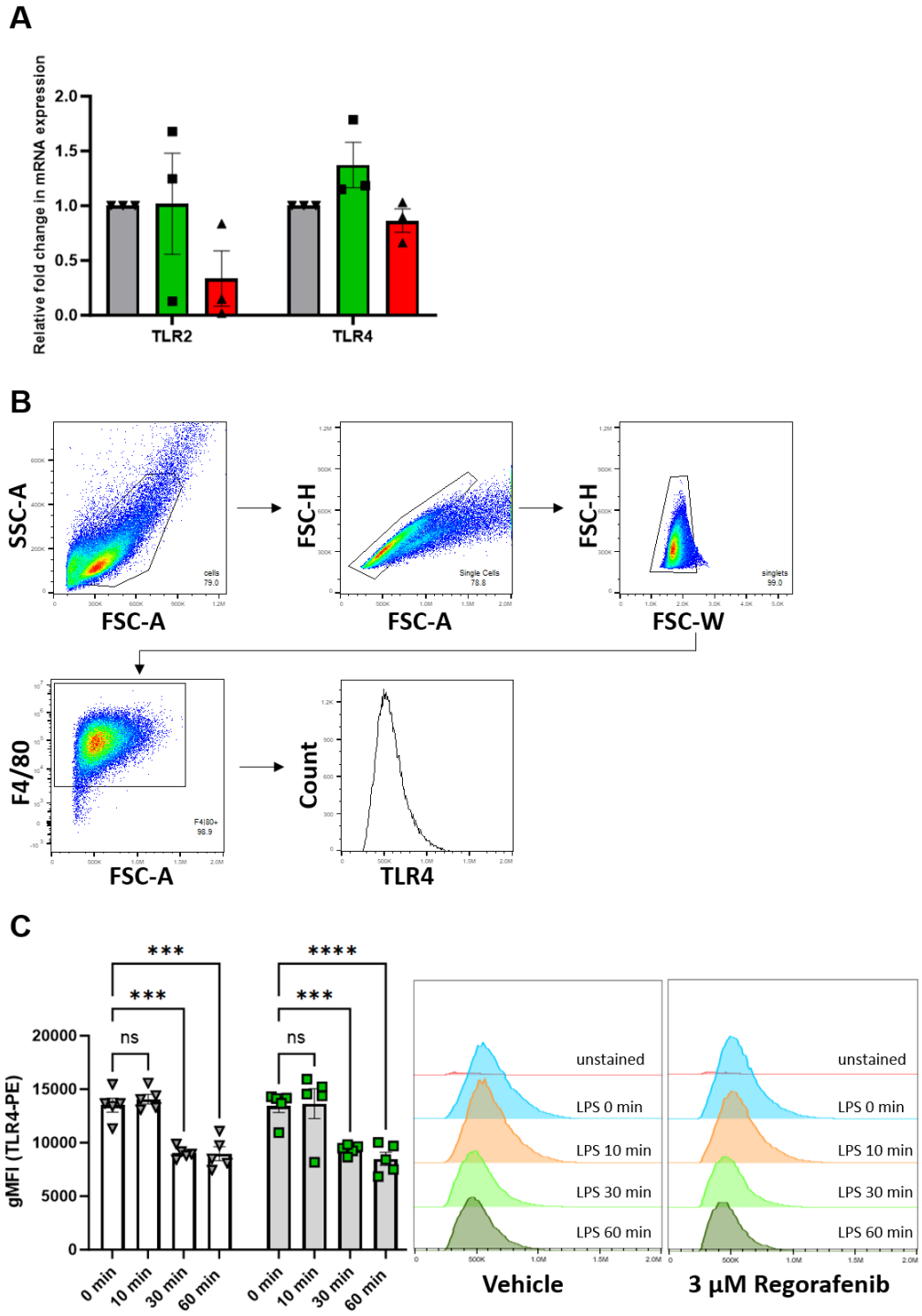


Fig. 3. 12 Regorafenib and sorafenib do not affect TLR2/4 expression or TLR4 internalization in BMDMs. (A) Relative gene expression of *tlr2* and *tlr4* was assessed by qPCR and normalized to 18S in RAW-Blue macrophages after pre-treatment with 3 µM regorafenib (green), sorafenib (red) or DMSO vehicle (grey) for 1 h before LPS stimulation for 2 h. Mean ±SEM, n=3 independent cell preparations; One-way ANOVA with Dunnett's multiple comparisons test against LPS + DMSO. **(B)** Gating strategy of flow cytometry analysis of TLR4 surface levels on BMDMs. **(C)** BMDMs were pre-treated with 3 µM regorafenib (green squares) or DMSO vehicle (grey triangles) for 1 h before LPS stimulation and quantification of geometric mean fluorescence intensity (gMFI) of surface TLR4 by flow cytometry at indicated time points. Representative histograms are shown. Mean ±SEM, n=5 biological replicates; Two-way ANOVA with Dunnett's multiple comparisons test.

3.3.9 Effect of regorafenib and sorafenib on DAMP- and PAMP-induced inflammation in cell lines and primary macrophages

In the previous section of this chapter, I showed that regorafenib and sorafenib inhibit pro-inflammatory signaling in macrophages stimulated with bacterial outer membrane component LPS. Therefore, I aimed to investigate whether this anti-inflammatory activity can be observed when macrophages are stimulated with other pro-inflammatory stimuli recognized by different receptors. THP-1 Dual macrophages (Fig. 3.13A) and BMDMs (Fig. 3.13B) were pre-treated with 3 µM regorafenib or sorafenib, 1 µM IKK16 or DMSO vehicle and subsequently stimulated with heat-killed listeria (HLKM, TLR2), Pam3CSK4 (TLR1/2) and R848 (TLR7/8) for 24 h or 7 h, respectively.

In THP1-Dual cells, both regorafenib and sorafenib as well as positive control IKK16 effectively inhibited TNFα production in response to all three stimuli. In contrast, in BMDMs, only IKK16 and regorafenib significantly reduced TNFα secretion in response to stimulation with all three TLR ligands.

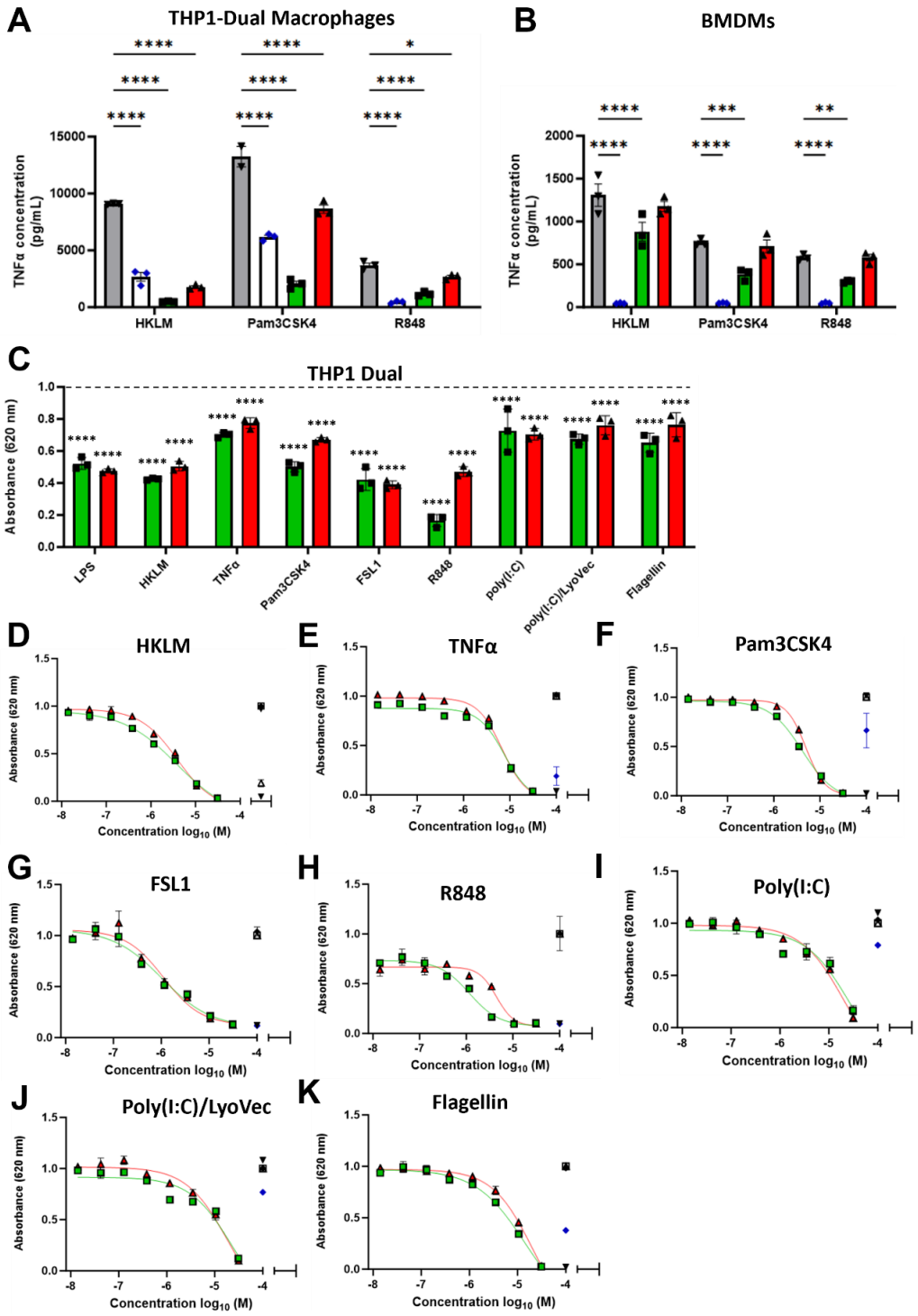


Fig. 3. 13 Regorafenib and sorafenib reduce macrophage inflammation in response to a wide variety of stimuli. (A) THP1-Dual macrophages or BMDMs **(B)** were pre-treated with 3.47 µM regorafenib (green), sorafenib (red), 1 µM IKK16 (bue) or DMSO vehicle (grey) for 1 h prior to stimulation with LPS (100 ng/ml), HKLM (3x 10^7 cells/ml), Pam3CSK4 (1 ng/ml) or R848 (300 ng/ml) for 24 h or 7 h, respectively. TNFα secretion was measured by ELISA. Mean ±SEM, n=3-6 independent experiments. Relative NF-κB activity in THP1-Dual monocytes pre-treated with **(C)** 3.47 µM regorafenib, sorafenib or DMSO vehicle or **(D-K)** 8 concentrations of regorafenib, sorafenib or vehicle for 1 h before stimulation with LPS (100 ng/ml), HKLM (3x 10^7 cells/ml), human TNFα (10 ng/ml), Pam3CSK4 (300 ng/ml), FSL1 (1 ng/ml), R848 (10 µg/ml), poly(I:C) (10 µg/ml), poly(I:C)/ LyoVec (100 ng/ml) or Flagellin (100 ng/ml) for 24 h. Mean ±SEM, n=3 independent experiments.

To investigate whether this anti-inflammatory effect of regorafenib and sorafenib was due to their ability to inhibit NF-κB, THP1-Dual monocytes were pre-treated with 3 µM regorafenib, sorafenib or DMSO vehicle before stimulation with different PAMPs and DAMPs for 24 h (Fig. 3.13C-K). NF-κB activity was assessed by determining SEAP levels in the supernatant (Table 3.7).

Table 3. 7 IC_{50} values of NF-κB inhibition in THP1-Dual monocytes stimulated with different PAMPs and DAMPs

IC_{50} (µM)	**Regorafenib**	**Sorafenib**
HKLM	3.802	3.835
hTNFα	7.556	6.714
Pam3CSK4	4.110	4.932
FSL1	1.036	1.109
R848	1.158	4.393
Poly(I:C)	21.75	18.74
Poly(I:C)/ LyoVec	11.18	11.49
Flagellin	14.24	20.51

Both drug repurposing candidates showed the highest potency in inhibiting FSL1-induced TLR2/6-mediated NF-κB activation (Fig. 3.13G) with IC_{50} values of 1.036 µM or 1.109 µM, respectively (Table 3.7). They also significantly suppressed TLR7/8-mediated NF-κB activation by R848 (IC_{50}= 1.158 µM and IC_{50}= 4.393 µM, respectively) (Fig. 3.11H), HKLM-induced TLR2-mediated NF-κB activation (IC_{50}= 3.802 µM and IC_{50}= 3.835 µM) (Fig. 3.11D) as well as TLR1/2-mediated Pam3CSK4-induced NF-κB signaling (IC_{50}= 4.11 µM and IC_{50}= 4.932 µM) (Fig. 3.11F). NF-κB activation in response to TNF-R activation by human TNFα was also dose-dependently decreased with slightly higher IC_{50}s of 7.556 µM and 6.714 µM, respectively (Fig. 3.11E). Interestingly, both TKIs only weakly inhibited NF-κB activation by transfected poly(I:C)/LyoVec through RIG-1/

MDA-5 (Fig. 3.11J) and Flagellin through TLR5 (Fig. 3.11K). No effect on TLR3-mediated NF-κB activation was observed (Fig. 3.11I).

In addition, the effect of regorafenib and sorafenib on IRF pathway activation in THP1-Dual cells stimulated with untransfected poly(I:C) or transfected poly(I:C)/LyoVec was assessed via the secreted Lucia luciferase reporter gene, which is under the control of an ISG54 minimal promoter in conjunction with five IFN-stimulated response elements. IFN pathway activation was assessed by measuring Lucia luciferase activity in the supernatant (Appendix 2). Neither regorafenib nor sorafenib inhibited IRF pathway activation in response to poly(I:C)/LyoVec. Weak inhibition of IRF activation in response to poly(I:C) was observed after pre-treatment with regorafenib or sorafenib (IC_{50}= 13.02 µM and IC_{50}= 20.57 µM, respectively). However, this inhibition was most likely due to reduced cell viability of THP1-Dual at 24 h at these TKI concentrations.

3.4 Discussion

In this chapter, I set out to use reliable and reproducible cell-based assays to identify kinases that drive NF-κB activation in macrophages by screening a commercially available TocriScreen library of small molecule kinase inhibitors. The Z'-prime score determined using positive control IKK16 (1 µM) indicated excellent assay reliability and reproducibility (Fig. 3.2). Based on these results, I designed a library of selected FDA-approved tyrosine kinase inhibitors and identified vandetanib, tivozanib, regorafenib, sorafenib and saracatinib as drug repurposing candidates with underexplored anti-inflammatory effects in both human and murine macrophages (Fig. 3.5). Subsequent experiments investigating the anti-inflammatory effects of the TKIs on the inflammatory response in primary murine macrophages revealed that regorafenib and sorafenib were the most potent candidates and generally exhibited higher potencies in human than in murine macrophages. Both TKIs significantly inhibited LPS- or LPS+INF-γ-induced pro-inflammatory mediator expression and protein production (Fig. 3.6 and 3.7). Importantly,

the anti-inflammatory properties of the TKIs translated to human primary macrophages, in which both drugs dose-dependently inhibited LPS-induced TNFα production (Fig. 3.8C). Their effect on NF-κB activation and pro-inflammatory cytokine production was confirmed in THP1-Dual macrophages and BMDMs stimulated with a variety of PAMPs and DAMPs, with regorafenib exhibiting higher potency than sorafenib. Finally, I sought to determine the mechanism of action through which the TKIs inhibit NF-κB activation and inflammation. Regorafenib and to a lesser extent sorafenib reduced p65 phosphorylation and translocation (Fig. 3.9) by attenuating upstream activation of CSF-1R, p38 and Src (Fig. 3.10).

3.4.1 Cell-based reporter screens for anti-NF-κB and anti-inflammatory activity

Macrophages are a promising target for anti-inflammatory agents as they are implicated in disease progression of many acute and chronic inflammatory diseases [600]. Their central role in disease pathology has been verified by macrophage depletion in animal models of inflammatory disorders including RA, obesity or endometriosis [600]. After the inflammatory insult, tissue-resident cells like macrophages are the first to respond by secreting chemokines, cytokines, reactive oxygen and nitrogen species as well as lipid mediators to recruit neutrophils and initiate the differentiation and expansion of Th1 and Th17 cells [601, 602]. Macrophage phenotypes are highly plastic, which allows them to switch from a pro-inflammatory phenotype in early inflammation to a pro-repair phenotype during inflammation resolution [154]. This plasticity can be exploited by promoting M2-like polarization. Many well-established anti-inflammatory drugs like dexamethasone or metformin were shown to target NF-κB activation, which induces M1-like polarization, thereby promoting the switch to an M2-like state [603-607].

While human cell lines might have more clinical relevance, considering the repurposing candidates are targeted for use in humans, I decided to evaluate NF-κB inhibition in both human and murine cell lines because further experiments to validate drug repurposing

candidates will be strengthened by the use of murine primary cells and mouse models. Therefore, I chose to prioritize drug repurposing candidates that efficiently inhibit NF-κB signaling in both human and murine cells. Even though immortalized cell lines are less physiologically relevant compared to primary cells, they are easier to obtain in the required numbers and thus compatible with high-throughput screens. These cell lines have been validated and are commercially available (Invivogen). As they secrete SEAP, which can be easily detected with Quanti-Blue solution, screens using THP-1 Dual or RAW-Blue cells are cheaper and more time-efficient than screens measuring cytokine secretion (by ELISA or LUMINEX) or phenotypic changes (by microscopy, qPCR, ImageStream or flow cytometry). Further, assays using commercially available reporter cell lines were found to be more robust with higher Z'-factors [608]. To validate our findings from initial screens, we chose to use primary murine and human MDMs as they are representative of monocyte-derived macrophages recruited to sites of inflammation. Candidates having the desired effects in BMDMs can therefore be further investigated in *in vivo* mouse models of inflammation.

When establishing a high-throughput assay, it is important to determine the Z'-factor as an indicator of assay quality to avoid a high number of false positives or negatives. Only a fraction of papers reporting new screening methods for anti-inflammatories report the Z'-factor [577, 609, 610], even though it is important for determining the reproducibility and suitability of a screening method for a high-throughput screen. To our knowledge, no Z'-score has been reported so far for a drug screening assay using RAW-Blue or THP1-Dual cells to identify changes in NF-κB activity by measuring the OD_{620} in a Quanti-Blue assay.

The decision was made to use LPS as the inflammatory stimulus of choice in our initial cell-based drug repurposing screen. Other physiologically relevant inflammatory stimuli include TNFα or MSU crystals, which drive inflammation in cardiovascular disease or

gout [611, 612]. However, LPS is one of the most well-studied inflammatory stimuli and the signaling cascades initiated in monocytes and macrophages upon LPS binding to the receptor complex consisting of CD14, TLR4 and MD2 are well established [613]. They initiate NF-κB activation and thus the production of pro-inflammatory cytokines including TNFα, IL-6 and IL-1β, inflammatory mediators such as NO or ROS as well as chemokines like CCL2 [614]. Even though LPS has been most widely investigated in the context of endotoxemia and sepsis, its signaling pathways are involved in the pathology of many other inflammatory diseases like Parkinson's and Alzheimer's disease, cardiovascular disease, diabetes and chronic gut inflammation [615, 616]. Since the development of new therapies depends on the understanding of molecular mechanisms of the disease in appropriate cell types and of potential therapeutic agents, we decided that LPS-induced macrophage inflammation is a useful tool to identify and validate anti-inflammatory medicines in our initial screens.

To validate the anti-inflammatory effect of our drug repurposing candidates, I decided to use a variety of physiologically relevant PAMPs and DAMPs targeting other macrophage receptors that initiate the downstream activation of NF-κB, such as Pam3CSK4 (TLR1/2), HKLM (TLR2), Flagellin (TLR5), FSL1 (TLR2/6), R848 (TLR7/8), non-transfected poly(I:C) (TLR3) and poly(I:C)/LyoVec (RIG-I and MDA-5) as well as TNFα (TNF-R) (Fig. 3.13).

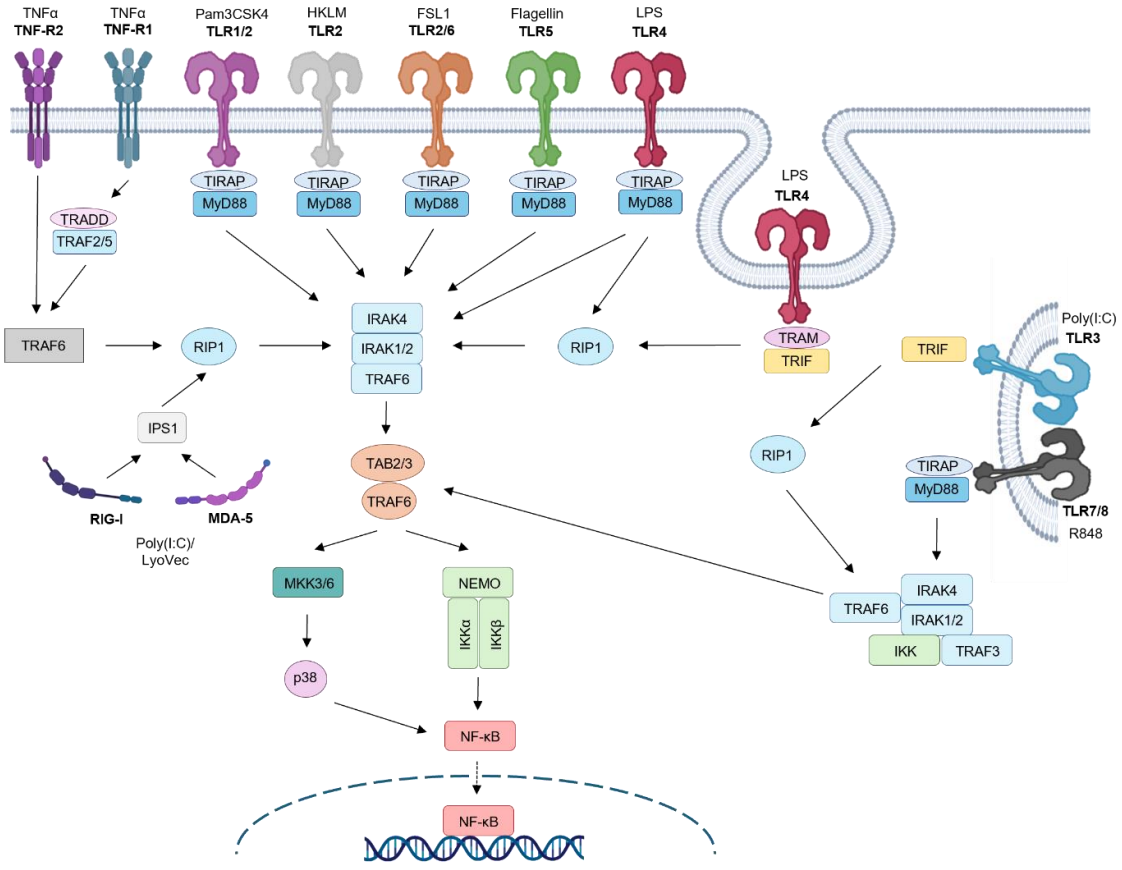


Fig. 3. 14 NF-κB activation by TLR and TNF-R signaling pathways in innate immune cells. The recognition of different PAMPs and DAMPs by specific TLRs or the TNF receptor triggers the initiation of signaling pathways, resulting in downstream NF-κB activation. Constructed from [233, 617, 618] using BioRender and PowerPoint.

3.4.2 Identification of regorafenib and sorafenib as inhibitors of macrophage NF-κB

Sorafenib, marketed by Bayer as NEXAVAR, was first FDA-approved in 2005 for the treatment of hepatocellular carcinoma (HCC), followed by approval for the treatment of advanced renal cell carcinoma (RCC) and differentiated thyroid carcinoma (DTC) [619]. Sorafenib's ability to reduce inflammation has been reported *in vivo* models of liver and breast cancer [572, 573]. A cell-based screen identified sorafenib as an inhibitor of TNF-dependent necroptosis, which protected mice from inflammation and tissue injury in models of systemic inflammatory response syndrome and renal ischemia-reperfusion injury [571]. The ability of sorafenib to inhibit NF-κB signaling through STAT3, MAPK and

AP-1 was observed in various cell lines, including TNF-stimulated GFP-IκBα GripTite cells (HEK-293-derived), U-2 OS cells, LPS-stimulated hepatoma HepG2 and HCCLM3 cells and LPS-stimulated RAW 264.7 macrophages. In addition, the TKI inhibited NF-κB activation in primary HCC patient samples as and *in vivo* in a mouse model of LPS- and Aβ-induced neuroinflammation, in which sorafenib reduced neuroinflammatory responses [570, 574-577, 620]. This study also observed a decrease in pro-inflammatory cytokines and Akt/p38-linked STAT3/NF-κB inhibition in LPS-stimulated BV2 microglia upon sorafenib treatment.

Regorafenib was developed in a drug discovery program by Bayer after they developed sorafenib [621, 622]. In 2012, regorafenib received approval for the treatment of metastatic colon or rectal cancer (mCRC) and was later also approved to treat patients with HCC and gastrointestinal stromal tumors (GIST). It targets receptor tyrosine kinases VEGFR1-3, Tie2, FGFR1-2, PDGFR, Kit, Ret and CSF-1R as well as intracellular kinase Raf [623]. Previous studies have described the ability of regorafenib to inhibit NF-κB activation in cancer models [561, 562, 624] *in vivo* and in hepatoma cells *in vitro.* In the cell lines, its anti-cancer effect was mediated by inhibition of ERK/NF-κB signaling and pro-inflammatory cytokine production [563, 564]. In an inflammatory setting, regorafenib was reported to inhibit NF-κB signaling in HEK-Blue cells stimulated with NOD2 agonist L18-MDP [566] and in LPS-stimulated BV-2 microglia, in which it also attenuated the production of pro-inflammatory cytokines by inhibiting Akt/STAT3 signaling. Further, the study found that in BV2 microglia, regorafenib reduced LPS- and Aβ-induced neuroinflammation and AD pathology in mice [567]. In a recent paper, Grünewald et *al.* report the inhibition of CSF-1R after CSF-1 stimulation by regorafenib in RAW 264.7 macrophages. They also observed a reduction in $F4/80^+$ TAMs in tumors as well as decreased CCL2 levels in the peripheral blood in mice with subcutaneous CT26 tumors [625]. In contrast, another study reported that regorafenib was observed to promote M1

macrophage polarization in TAMs in a mouse model of HCC and in BMDMs by inhibiting p38 [626].

3.4.2.1 Novel anti-inflammatory effects of regorafenib and sorafenib in macrophage inflammation

Here, we add to the existing knowledge around regorafenib and sorafenib and report that both drugs dose-dependently inhibit NF-κB activity in human THP1-Dual monocyte and murine RAW-Blue macrophage reporter cell lines (Fig. 3.5). We found that this translates to anti-inflammatory effects in primary BMDMs in which both drugs dose-dependently reduce the gene expression and protein production *tnfα*/TNFα, *il-6*/IL-6, *ccl2*/CCL2 and *inos*/NO upon LPS-stimulation or LPS+IFN-γ stimulation (Fig. 3.6 and 3.7). Further, we confirmed the anti-inflammatory activity of the drug repurposing candidates in LPS-stimulated primary human MDMs (Fig. 3.8), which has not been previously reported. Other studies have demonstrated the inhibitory effect of regorafenib and sorafenib on NF-κB signaling but to our knowledge, this has not been reported in LPS-stimulated primary macrophages.

Here, we confirm that in LPS-stimulated RAW-Blue macrophages, regorafenib and to a lesser extent sorafenib reduce the phosphorylation and translocation of p65 as well as the phosphorylation of TKIs CSF-1R, p38 and Src. In contrast to published findings in cancer models or BV2 microglia, we did not observe an effect on Akt, ERK or STAT3 phosphorylation at 5, 10 or 15 min post LPS stimulation. However, the antibodies we used against p-Akt and p-STAT3 did not produce a strong signal, so it is possible that a potential effect might not be observed using these antibodies.

CSF-1R as a target of regorafenib and sorafenib is especially intriguing, as it is highly expressed on the surface of monocytes and macrophages. Besides regulating later stages of macrophage development, dysregulation of CSF-1R signaling has been linked to cancer, neurodegeneration in MS or AD and other inflammatory diseases like RA, gout

or diabetes [627]. In RA, CSF-1R signaling enhances disease progression by promoting the accumulation of macrophages in the synovium as well as the stimulation of fibroblast-like synoviocytes and also enhances bone destruction directly [340, 628, 629]. In patients with severe gout, an increase in circulating M-CSF was reported and patient PBMCs and synovial fluid mononuclear cells showed increased osteoclastogenesis upon M-CSF stimulation [630]. In addition, the receptor plays a key role in the development of pain after nerve injury in bone cancer and RA. The development of inflammatory pain in RA models was successfully inhibited by anti-CSF-1R mABs [627, 631]. Therefore, targeting CSF-1R signaling in macrophages in pathologic inflammation is an intriguing strategy to reduce disease progression and pain.

Previous studies have reported that sorafenib reduced TLR4 mRNA expression and protein levels in HCCLM3 cells both in the presence and absence of LPS after treatment with 10 µM sorafenib for 24 h [576]. In addition. Li et *al.* observed a reduction of surface TLR4 levels on LPS-stimulated BMDMs 12 and 24 h after treatment with 10 µM sorafenib [620]. I found that neither 3 µM regorafenib nor sorafenib affected *tlr2* or *tlr4* expression at 2 h after LPS stimulation in BMDMs (Fig. 3.12A). I further investigated the effect of 3 µM regorafenib on TLR4 internalization in BMDMs treated with LPS for 0, 10, 30 and 60 min (Fig. 3.12C). The TKI did not affect TLR4 internalization compared to vehicle at these time points. Previous studies used high concentrations of sorafenib and treated cells with drug and LPS for 12 and 24 h (10 µM compared to 3 µM in our study). Therefore, the reported effect may be due to cytotoxicity, as neither study measured cell viability. In addition, TLR4 internalization in macrophages in response to LPS stimulation occurs rapidly with a decrease of surface TLR4 reported as early as 5 min post-stimulation, and at the 30 min time point, a significant amount of TLR4 is internalized [599, 632, 633]. As LPS stays present in the media, TLR4 surface levels continue to stay low even 4 h after

stimulation [634, 635]. Therefore, most studies researching modulators of TLR4 endocytosis investigate early events up to 90 or 120 min [599, 632, 633, 636-640].

3.4.2.2 Regorafenib affects primary murine macrophage polarization

Reprogramming of macrophages towards a more M2-like phenotype is an intriguing strategy to treat pathologic inflammation. Therefore, I investigated the effect of regorafenib on BMDM polarization. As reported previously, regorafenib increased surface levels of M1 polarization marker on M1-polarized BMDMs and decreased surface expression of M2-phenotype marker CD206 on M2-macrophages [626]. Interestingly, however, regorafenib at the same time decreased MHCII surface levels on non-polarized M0 and M2-polarized macrophages. In their study, Ou et *al.* used LPS-induced mRNA expression and protein levels of TNFα and IL-6 as additional markers of M1 polarization [626]. NF-κB activation is considered another main mediator of M1 polarization [262]. We observed a decrease in both NF-κB signaling as well as pro-inflammatory cytokine production in macrophages treated with regorafenib, therefore indicating a less classically activated state of the cells.

However, the concept of clearly distinguished M1 and M2 macrophage phenotypes is becoming increasingly controversial, with macrophages exhibiting high levels of plasticity. As stated by Murray in his 2017 Annual Review on macrophage polarization, a dualistic model lacks scientific evidence since even highly regulated *in vitro* experiments with LPS-stimulated macrophages are not able to produce consistent phenotypes. Therefore, expecting clear M1 and M2 macrophage phenotypes in complex environments like tissues and whole organisms is unrealistic [154]. Instead, macrophage phenotypes can be considered a spectrum with what is commonly referred to as M1 and M2 polarization being the most extreme states. They do however not represent functionally and phenotypically diverse macrophage populations that can exist in many intermediate polarization states [641].

3.4.3.3 Regorafenib and sorafenib inhibit NF-κB-driven macrophage inflammation in response to a wide variety of stimuli

Unlike previous published studies, we used a variety of stimuli to induce inflammation in BMDMs and THP1-Dual macrophages to verify the anti-inflammatory activity observed in LPS-stimulated macrophages. Interestingly, regorafenib and sorafenib inhibited NF-κB activation mediated by TLR1, TLR2, TLR4, TLR6, TLR7/8 and TNF-R agonists and had mild anti-inflammatory effects on TLR5 or RIG ligand-induced NF-κB activation in THP1 monocytes, while they did not inhibit NF-κB activation through TLR3 (Fig. 3.13). These findings indicate that the TKIs probably do not exert their anti-inflammatory effects by acting directly on TLR receptors or Myddosome (MyD88-IRAK4-IRAK1/2), since these signaling molecules are not shared between the TNF receptors and the TLRs (Fig. 3.14). Therefore, regorafenib and sorafenib likely inhibit NF-κB signaling by acting on shared tyrosine kinases downstream of the receptors that ultimately result in NF-κB activation.

I observed slight differences in the potency of regorafenib and sorafenib in inhibiting NF-κB activation and translocation as well as pro-inflammatory mediator production, with regorafenib generally being more potent. Structurally, the only difference between sorafenib (Fig. 3.15A) and regorafenib (Fig.3.15B) is the addition of a fluorine atom in the central phenyl ring in regorafenib.

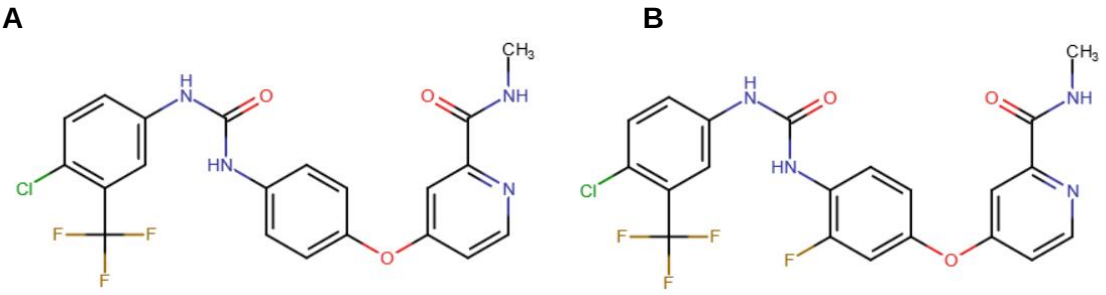


Fig. 3. 15 Chemical structures of sorafenib and regorafenib. Chemical structures were generated with the Chemical Sketch tool by the PDB (**(A)** sorafenib CID: 216239, **(B)** regorafenib CID: 11167602).

Regorafenib was developed in a discovery program that sought to enhance the efficacy of sorafenib. The additional fluorine might cause a higher potency due to differences in

target inhibition [311, 642]. The underlying mechanism has not been elucidated fully, but it was shown that besides inhibiting most of the targets inhibited by sorafenib more effectively, regorafenib also blocks Tie-2 signaling (Table. 3.8) [311, 621].

Table 3. 8 Target profiles of regorafenib and sorafenib. IC_{50} values were determined in *in vitro* biochemical kinase inhibition assays. Table was adapted from [621].

Target	IC_{50} (nM/L)	
	Regorafenib	**Sorafenib**
VEGFR-1	13	N/A
VEGFR-2	4.2	15
VEGFR-3	46	20
Tie-2	311	N/A
PDGFR-β	22	57
FGFR1	202	580

In addition, introducing fluorine atoms was shown to increase cell permeability and solubility and reduce *in vivo* clearance, which results in increased oral exposure, while not interfering with target potency [643]. However, studies have shown that the pharmacokinetic profiles of both drugs are very similar in mice [644] and that the metabolism of the drugs in mice resembles that in humans [644-646]. When investigating the pharmacodynamic properties of regorafenib and sorafenib in patient-derived HCC xenografts, Kissel et *al*. reported that while the effect of the drugs was similar, they did observe some differences in the regulation of protein expression [644-646]. Both drugs are lipophilic and were shown to insert into the lipid-water interface of membranes, which increases membrane permeability [647]. High lipophilicity (cLogP) may enhance target binding but also increase adverse effects. Regorafenib has a higher lipophilicity (cLogP= 4.8) than sorafenib (cLogP=3.2). This may explain the higher promiscuity and more potent anti-inflammatory effects of regorafenib, but also its more severe side effects compared to sorafenib [648].

3.4.3 Limitations of the studies reported in this chapter

An important limitation of this study is that the initial drug repurposing screens relied on LPS as the sole inflammatory stimulus of macrophage reporter cell lines. As discussed above, using LPS offers many advantages when investigating inflammatory signaling and especially NF-κB-mediated inflammation in macrophages. Therefore, other TKIs that were excluded after the initial screen may have exhibited stronger anti-inflammatory properties upon inflammation initiation through other stimuli inducing different inflammatory pathways. However, we did confirm the effect of the selected TKIs regorafenib and sorafenib on macrophage NF-κB activation and inflammation induced by a variety of PAMPs and DAMPs targeting different macrophage receptors.

Another limitation is that only 15 selected TKIs were included in the screen of FDA-approved medicines. These were selected based on results from the screen of commercially available small molecule kinase inhibitors. By determining the Z'-factor, we demonstrated the reproducibility and reliability of this screen. Therefore, it could be used as a platform to screen a larger library of kinase inhibitors and/or FDA-approved medicines from different chemical classes. With computational drug repurposing approaches becoming more powerful, our *in vitro* screening approach could be coupled with computational methods to identify other anti-inflammatory drug repurposing candidates.

3.4.4 Summary

In this chapter I identified kinases that, when inhibited, prevent NF-κB activation in macrophages. Based on these findings, I used our reliable and reproducible cell-based screen to identify regorafenib and sorafenib as potent NF-κB inhibitors in human and murine macrophages which dose-dependently suppress pro-inflammatory mediator production. Their anti-inflammatory activity is likely mediated in part by their ability to inhibit p38, Src and CSF-1R phosphorylation, which results in downstream NF-κB

activation. Their anti-inflammatory effect applies to inflammation initiated by a variety of stimuli and the TKIs are therefore likely not targeting the TLRs or the Myddosome directly.

Chapter 4: Regorafenib reduces acute inflammation in MSU crystal-induced peritonitis by inhibiting NF-κB-dependent NLRP3 inflammasome priming

4.1 Introduction

To understand pathways and processes underlying acute inflammation, a variety of mouse models have been established and are valuable tools to investigate inflammatory mediator production and leukocyte recruitment in a controlled setting.

4.1.1 Mouse models of acute inflammation

4.1.1.1 Experimental endotoxemia

Endotoxemia is initiated by intraperitoneal or intravenous injection of LPS, which triggers the activation of resident macrophages and causes rapid and systemic TNFα, IL-6, IL-1β and KC production that can be detected in the serum [649]. While this model was developed to research the inflammatory response in sepsis, it does not closely mirror events of septic shock in human patients. The model depends on purified LPS as the sole inflammatory stimulus and does not rely on complex host-pathogen interactions found in polymicrobial sepsis. In addition, studies comparing endotoxemia with sepsis in humans have found that serum cytokine levels are higher, peak earlier and resolve faster in mice [650-652]. However, this simple model is widely used to study the systemic immune response and underlying signaling pathways in a controlled inflammatory setting and can be applied to determine anti-inflammatory effects of compounds *in vivo* [649, 650, 653].

4.1.1.2 Subcutaneous air pouch models

First described by Selye in 1953 as the “granuloma pouch”, subcutaneous air pouch models can be used to study acute inflammation and identify anti-inflammatory agents *in vivo* [654]. Read-outs include exudate volumes, inflammatory cell recruitment and the production of pro-inflammatory mediators. This model requires the generation of a subcutaneous air pouch by repeated injection of sterile air into the back of the mouse or

rat, which can subsequently be injected with an inflammatory stimulus of choice [655]. Common irritants used to induce air pouch inflammation include carrageenan, zymosan, LPS, inflammatory chemokines like CCL2 or cytokines like IL-17 as well as crystals [655-658]. The air pouch lining has a structure similar to the synovium and contains fibroblasts and mononuclear cells [659]. To initiate acute inflammatory responses that resemble those in gout, MSU crystals can be injected into the air pouch. This results in rapid leukocyte recruitment peaking at 9 h before returning to baseline within two days [660]. Pro-inflammatory cytokines IL-1β, IL-18, and TNFα peak at 8 h post-MSU crystal injection [661]. This inflammatory response to MSU crystals in the air pouch seems to be mediated by MyD88 and TLR2/4 activation [662].

4.1.1.3 Peritonitis models

Peritonitis models induced by the intraperitoneal injection of pathogenic or sterile inflammatory agents are commonly used to investigate and characterize acute inflammatory processes like leukocyte recruitment or pro-inflammatory mediator production [663]. The peritoneal cavity is easily accessible and sterile peritonitis models allow for controlled inflammation initiation and quantification of cell recruitment and inflammatory mediators [664, 665]. Therefore, they are a useful tool to identify and study new anti-inflammatory treatments [664]. Sterile peritoneal irritants include thioglycolate, zymosan, MSU crystals or calcium pyrophosphate dihydrate (CPPD) crystals as well as specific cytokines or chemokines and cause rapid acute inflammatory responses [656, 664, 666].

4.1.1.3.1 MSU crystal-induced peritonitis

The intraperitoneal injection of MSU crystals, the causative agent of gouty inflammation, triggers acute inflammatory responses including the production of pro-inflammatory cytokines and chemokines and the infiltration of polymorphonuclear leukocytes, especially neutrophils and monocytes [666].

The initiation of inflammation in response to MSU crystals is mediated by resident peritoneal macrophages, which make up 60-70 % of peritoneal cells in naïve mice [210]. Upon MSU crystal challenge, resident macrophages are responsible for the production of large amounts of pro-inflammatory cytokines, including IL-6 and IL-1β, as well as chemokines, such as KC/IL-8 or CXCL1, to recruit neutrophils and monocytes [667, 668]. The key role of resident macrophages in MSU crystal-induced peritonitis was demonstrated by macrophage depletion studies, which reported the abrogation of early inflammation as well as significantly decreased neutrophil recruitment and IL-6 and IL-1β production. However, TNFα production and monocyte recruitment were not affected by macrophage depletion [210, 669]. Cells of the peritoneal mesothelium were shown to be the source of monocyte chemoattractant CCL2 and mediate monocyte recruitment in MSU crystal peritonitis [669].

MSU crystals initiate acute inflammation through NLRP3 inflammasome activation and the resulting secretion of mature IL-1β [666, 670]. The crystals are likely not recognized by direct binding to the inflammasome but instead trigger cell stress and the production of reactive oxygen species, which indirectly activate the NLRP3 inflammasome [668, 671].

In addition, resident peritoneal macrophages attempt to take up MSU crystals, which results in “frustrated phagocytosis” and the generation of further inflammatory signals activating the NLRP3 inflammasome [671]. The role of macrophage TLR2 and TLR4 in MSU crystal-induced peritonitis is under debate, as Chen et *al.* showed they were dispensable for MSU crystal-induced inflammation [672]. However, other studies reported that macrophage CD14-mediated TLR4 signaling and the presence of TLR2/4 on macrophages were important for MSU crystal phagocytosis, IL-1β production and neutrophil recruitment in MSU crystal-induced inflammation [662, 673]. MSU-mediated TLR2 activation and consequent initiation of NF-κB signaling were confirmed in models

of joint inflammation [674, 675]. Therefore, TLR-mediated NF-κB activation in resident macrophages in MSU crystal-induced peritonitis likely results in NLRP3 inflammasome priming and pro-IL-1β production as well as the secretion of other inflammatory cytokines [668]. ROS and other cell stress signals then trigger NLRP3 inflammasome assembly through recruitment of ASC and pro-Caspase1, resulting in the maturation and secretion of IL-1β (Fig. 4.1) [671].

The cytokine then stimulates IL-1R on nonhaematopoietic cells, resulting in MyD88-dependent production of CXCL1/KC, TNFα, IL-6 and more IL-1β. This triggers the recruitment of neutrophils and the exacerbation of inflammation [672]. Interestingly, peritoneal neutrophil infiltration directly correlates with the amount of IL-1β produced in the peritoneum and therefore with the extent of NLRP3 inflammasome activation [426]. MSU crystals also stimulate endothelial cells directly and induce the production of CCL2, which recruits monocytes to the peritoneum [669]. In contrast to endothelial cells, IL-1R and MyD88 in macrophages are dispensable for MSU crystal-induced inflammation [672].

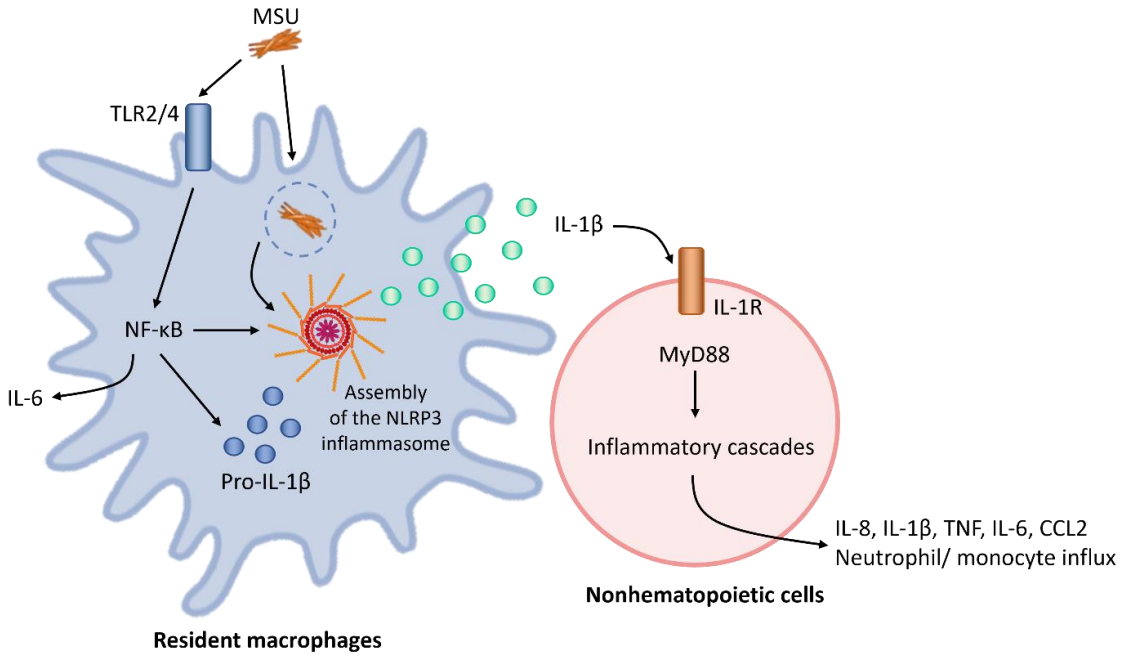


Fig. 4. 1 Initiation of inflammation in MSU crystal-induced peritonitis. Resident peritoneal macrophages (blue) detect MSU crystals, which induce NF-κB-mediated NLRP3 inflammasome priming and IL-6 secretion through the TLR2/4 signaling pathway. Cell stress mediators produced in response to "frustrated phagocytosis" of MSU crystals by macrophages result in the assembly of the NLRP3 inflammasome and the release of mature IL-1β. IL-1β initiates inflammatory signaling in nonhaematopoietic cells (pink) in the peritoneum and promotes pro-inflammatory mediator production and the recruitment of neutrophils and monocytes to the site of inflammation. Figure was adapted from [671] and [676] and generated with BioRender and PowerPoint.

Monocyte and neutrophil numbers are increased at 4 h post-MSU crystal injection and peak at 16 h, with neutrophil infiltration being greater and faster than monocyte recruitment [210]. Resident peritoneal macrophages disappear from the peritoneum within the first 2 hours of inflammation, a phenomenon called "macrophage disappearance reaction". They adhere to the peritoneal membrane, undergo apoptosis and emigrate to draining lymph nodes [210, 602, 677, 678]. Cytokine levels of IL-6, IL-1β and TNFα peak at 4 h. Interestingly, infiltrating neutrophils and monocytes do not produce IL-6, IL-1β and TNFα in the presence of MSU crystals in the peritoneum. Both leukocyte numbers and cytokine concentrations return to baseline within 48 h of inflammation initiation [210].

4.1.2 Repurposing tyrosine kinase inhibitors in acute inflammation

The activation of tyrosine kinases initiates pathways involved in inflammation, including TLR signaling and resulting cytokine production (see Chapter 1.5) [679]. Therefore, repurposing existing tyrosine kinase inhibitors has been investigated as a strategy to identify new therapeutics for acute inflammatory diseases.

The activation of tyrosine kinase Src for example has been linked to the LPS-induced NF-κB-mediated inflammatory response of monocytes, macrophages and neutrophils, which could be suppressed by the use of Src inhibitors. Similarly, Src family kinases are important for neutrophil adhesion, migration and degranulation in acute inflammation [680]. Thus, Src inhibitors dasatinib and reserveratrol attenuated neutrophil degranulation in *in vivo* models of acute lung inflammation [681, 682].

Tyrosine kinase BTK mediates TLR-induced NF-κB and NLRP3 inflammasome activation in macrophages in acute inflammation, which results in the increased production of pro-inflammatory cytokines [372]. Ibrutinib is a BTK inhibitor used for the treatment of lymphocytic lymphoma and GVHD. The TKI is known to reduce NF-κB and NLRP3 inflammasome activation and M1 macrophage polarization in mouse models of polymicrobial sepsis and ischemic brain injury [372, 375, 594]. Further studies showed that ibrutinib attenuates recruitment of neutrophils and monocytes as well as peritoneal neutrophil activation and inflammatory cytokine production in mice with zymosan-induced peritonitis [377, 683-685].

Acute inflammatory gout flares are driven by NLRP3 inflammasome activation and IL-1β production in response to MSU crystals [686]. Recently, imatinib, a tyrosine kinase inhibitor targeting CSF-1R, Abl, c-Kit and PDGFR-β and approved for anti-cancer treatment, was demonstrated to have promising anti-inflammatory effects in MSU crystal-induced inflammation in the air pouch and joints of mice [687]. Similarly, PP121, which inhibits tyrosine kinases PDGFR, VEGFR2, Src and Abl, effectively decreased NLRP3

inflammasome activation and subsequent inflammatory cell recruitment and tissue damage triggered by intra-articular MSU crystal injection in the ankle joint [688]. In addition, Src and Abl inhibitor dasatinib potently suppressed MSU crystal-induced acute joint inflammation by reducing neutrophil infiltration and activation as well as IL-1β production in the joint [689].

These findings demonstrate that tyrosine kinase inhibitors have potent anti-inflammatory properties in pre-clinical models of acute inflammation and have the potential to be repurposed as a new class of anti-inflammatory medicines.

4.1.3 MSU crystal-induced peritonitis in drug repurposing studies

The initiation of sterile peritoneal inflammation by MSU crystals is a useful tool to study the effects of drug repurposing candidates on processes driving acute inflammation [426]. The model has led to the identification of various drug repurposing candidates with promising anti-inflammatory properties.

One example is β-blocker carvedilol, which was originally approved for hypertension treatment. After *in vitro* studies had shown its ability to inhibit NF-κB and NLRP3 inflammasome activation in macrophages [690, 691], MSU crystal-induced peritonitis experiments revealed that peritoneal neutrophil recruitment and pro-inflammatory mediator production as well as NLRP3 inflammasome activation in the peritoneum and PECs could be reduced by carvedilol treatment at 4 h *in vivo* [691].

Another anti-hypertension medicine, angiotensin II type 1 receptor antagonist candesartan, was found to similarly inhibit NF-κB-mediated NLRP3 inflammasome activation and thus decrease IL-1β production in macrophages *in vitro*. In MSU crystal-induced peritonitis *in vivo*, candesartan reduced peritoneal neutrophil influx as well as pro-inflammatory cytokine and chemokine production. It further suppressed NLRP3 inflammasome activation in PECs 4 h after MSU challenge [692].

Tyrosine kinase inhibitors have proven to be promising drug repurposing candidates to treat acute inflammation in MSU crystal-induced peritonitis. Tivantinib, which inhibits c-Met and is in phase III clinical trials for the treatment of lung and liver cancers, reduced peritoneal IL-1β and IL-18 production as well as neutrophil recruitment in mice 6 h after MSU crystal challenge [693]. PF-562271 inhibits tyrosine kinases FAK and Pyk2 and was found to have good safety profiles in cancer patients in a phase I clinical trial [694, 695]. In MSU crystal-induced peritonitis, the TKI effectively inhibited recruitment of neutrophils and monocytes to the peritoneum as well as peritoneal IL-1β production 6 h after MSU crystal challenge [696].

These reports demonstrate that MSU crystal-induced peritonitis is a useful model of acute inflammation to identify and characterize anti-inflammatory drug repurposing candidates. Consequently, studies employing this model have resulted in the identification of tyrosine kinase inhibitors with promising anti-inflammatory activities *in vivo*.

4.2 Original hypothesis and experimental aims of this chapter

My findings discussed in the previous chapter identified regorafenib and sorafenib as potent inhibitors of NF-κB signaling and inflammatory mediator production in macrophages *in vitro*. NF-κB activation induces priming of the NLRP3 inflammasome, which is a promising target for the treatment of many human inflammatory diseases [257]. Therefore, I hypothesized that regorafenib and sorafenib can inhibit NF-κB-dependent NLRP3 inflammasome priming and that their anti-inflammatory properties will translate from macrophages into *in vivo* models of acute inflammation.

The experimental aims of this chapter were to:

- Investigate the effect of regorafenib and sorafenib on NF-κB-mediated NLRP3 inflammasome activation in macrophages *in vitro.*

- Validate the effect of oral regorafenib and sorafenib administration in a mouse model of acute inflammation that is driven by NF-κB-dependent NLRP3 inflammasome activation.
- Investigate dose dependency of the TKI's anti-inflammatory effects *in vivo.*
- Compare anti-inflammatory effects of the drug repurposing candidates to those of a clinical gold standard anti-inflammatory medicine.
- Explore the molecular mechanism of anti-inflammatory activities of regorafenib *in vivo.*

My *in vitro* and *in vivo* experiments involving MSU crystal-induced inflammation were informed by discussions with Prof. Jelena Bezbradica Mirkovic and Dr. Fabian Fischer.

4.3 Results

4.3.1 Effect of regorafenib and sorafenib on NLRP3 inflammasome activation in macrophages

NF-κB activation is a critical step of NLRP3 inflammasome priming, which induces the transcription and production of inflammasome components NLRP3, ASC and pro-Caspase1 as well as pro-IL-1β [257, 296, 697]. Therefore, I hypothesized that since regorafenib and sorafenib inhibit LPS-induced NF-κB activation in macrophages, the drug repurposing candidates may consequently reduce NLRP3 inflammasome priming and thus the secretion of mature IL-1β. To investigate the effect of the TKIs on NLRP3 inflammasome priming, BMDMs were pre-treated with 8 concentrations of regorafenib or sorafenib, DMSO vehicle or 1 µM of positive control dexamethasone for 1 h before LPS stimulation (signal 1). After 7 h, NLRP3 inflammasome assembly was induced by addition of ATP (signal 2) for 60 min (Fig. 4.2A) and IL-1β production was measured by ELISA. Regorafenib and sorafenib dose-dependently reduced the secretion of mature IL-1β (IC_{50}=2.041 µM and IC_{50}=2.913 µM, respectively). As expected, pre-treatment with the anti-inflammatory drug dexamethasone also decreased IL-1β production. To

investigate whether the drugs could also directly inhibit NLRP3 inflammasome assembly, BMDMs were primed with LPS before addition of ATP and regorafenib or sorafenib, DMSO vehicle or 1 µM dexamethasone at the same time (Fig. 4.2B).

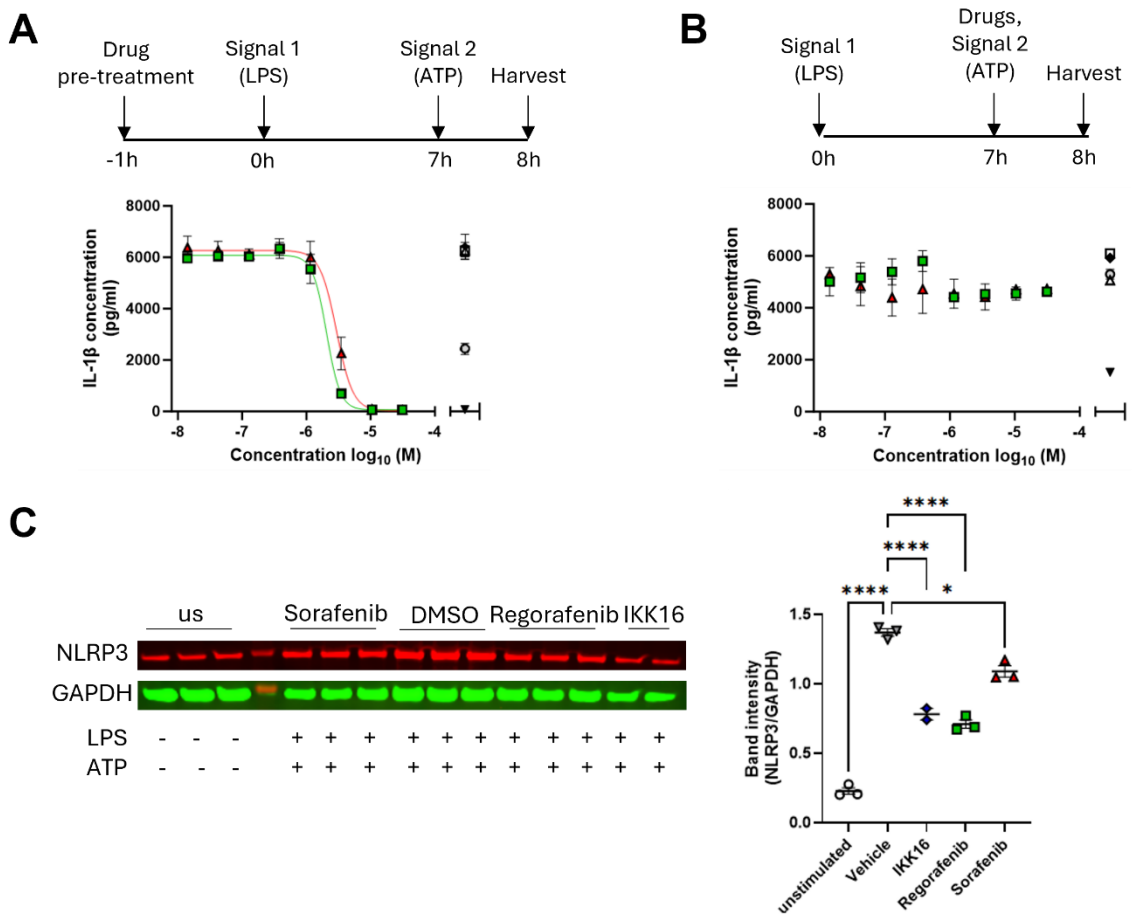


Fig. 4. 2 Regorafenib and sorafenib inhibit NF-κB-mediated NLRP3 inflammasome priming in macrophages. (A) Dose-response of IL-1β secretion as an indication for inflammasome priming measured by ELISA in BMDMs after pre-treatment with 8 concentrations of regorafenib (green squares) or sorafenib (red triangles) for 1 h and subsequent 7 h LPS stimulation. For the last 60 min, 5 mM ATP was added. Controls: untreated cells (black triangle), LPS+ATP (black diamond), 0.1 % DMSO+LPS+ATP (white square), 0.3 % DMSO+LPS+ATP (white triangle) or 1 µM dexamethasone+LPS (grey circle). **(B)** Dose-response of IL-1β secretion as an indication for inflammasome activation measured by ELISA in BMDMs after LPS stimulation for 7 h. For the last 60 min, 5 mM ATP and regorafenib or sorafenib were added. Mean ±SEM, n=3 independent cell preparations. **(C)** Western Blot for NLRP3 (red) in RAW-Blue cells and normalized to GAPDH (green) after pre-treatment with 3 µM regorafenib or sorafenib before addition of signal 1 (LPS). 4 h later, signal 2 (ATP) was added for 60 min. One-way ANOVA with Dunnett's multiple comparisons test. All data are shown as mean ±SEM, n=3 independent cell preparations.

Here, we observed no change in mature IL-1β production in response to TKI treatment, indicating that regorafenib and sorafenib suppress NLRP3 inflammasome activation by inhibiting the NF-κB-dependent priming step but do not directly affect its assembly. Notably, dexamethasone did not affect NLRP3 inflammasome assembly either.

To validate these findings, I investigated the effect of our drug repurposing candidates on NLRP3 production, which is driven by NF-κB in LPS-treated macrophages [257]. RAW-Blue macrophages were pre-treated with 3 µM regorafenib, sorafenib, 1 µM IKK16 or vehicle before LPS and ATP stimulation (Fig. 4.2C). As detected by western blotting, LPS+ATP stimulation increased NRLP3 production, which was significantly reduced by regorafenib, sorafenib and positive control IKK16.

Using THP1-ASC:GFP reporter monocytes allows for visualization of NF-κB activity and NLRP3 inflammasome activation. Upon inflammasome priming with LPS, an NF-κB-inducible promoter drives the expression of the ASC:GFP fusion protein, which can be detected throughout the cytoplasm. When a second stimulus induces NLRP3 inflammasome activation, ASC:GFP polymerization can be observed in the form of large specks, which were detected by ImageStream analysis. We confirmed that in resting cells, no GFP signal was detected (Fig. 4.3). Upon LPS-mediated priming and inflammasome activation by ATP, the fluorescent reporter construct was visible in the cytoplasm and polymerized to form bright ASC specks, indicating the assembly of the NLRP3 inflammasome. The percentage of cells containing an ASC speck was significantly reduced by pre-treatment with 3 µM regorafenib or 1 µM IKK16, while sorafenib did not have a significant effect on ASC speck formation. However, both regorafenib and sorafenib as well as positive control IKK16 significantly decreased the mean GFP intensity inside the cells, which correlates with NF-κB activation (Fig. 4.3).

So far, we only investigated the anti-inflammatory activity of the drug repurposing candidates on NLRP3 inflammasome activation induced by LPS priming and ATP-mediated assembly. I aimed to validate these findings using CPPD or MSU crystals as the second activation signal (Fig. 4.4). The crystals deposit in the joints of pseudo-gout and gout patients, respectively, and act as DAMPs triggering cell stress-induced NLRP3 inflammasome activation and thus joint and peri-articular inflammation [698, 699]. As a

result, macrophages produce IL-1β and neutrophil recruiting chemokine IL-8 (KC in mice) [700, 701].

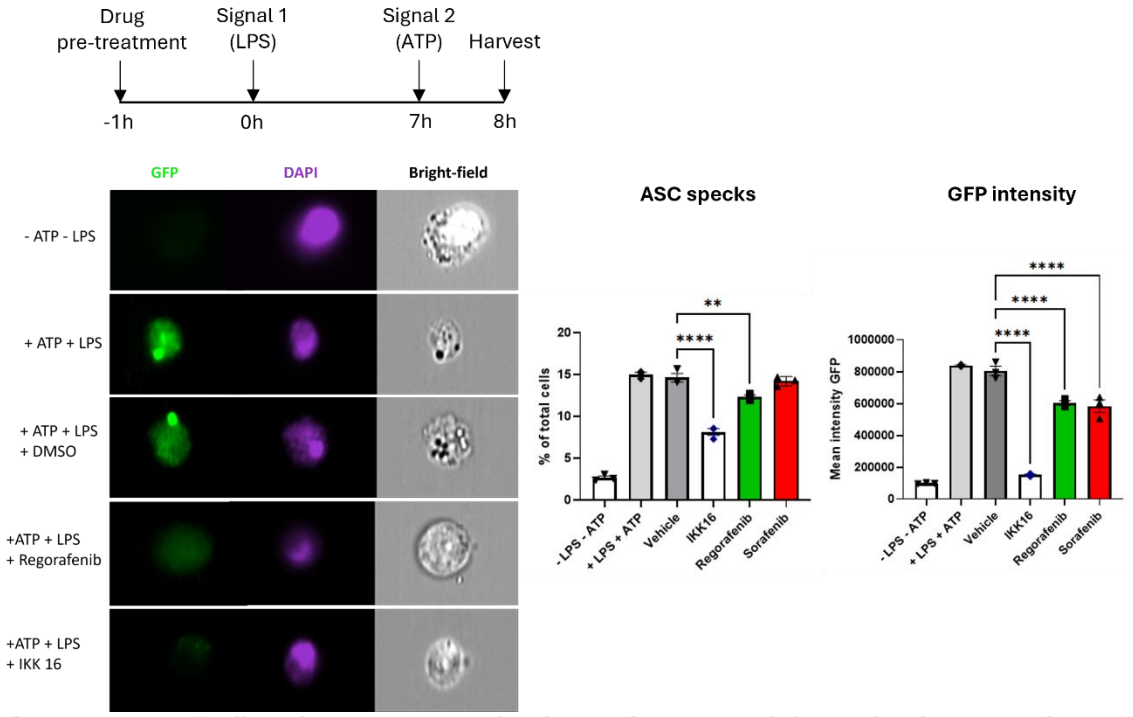


Fig. 4. 3 Regorafenib reduces NF-κB activation and ASC speck formation in macrophages. Representative ImageStream images, captured at magnification 40×. THP1-ASC-GFP reporter cells were pre-treated with 3 µM regorafenib (green) or sorafenib (red) or indicated controls for 1h before 7 h LPS stimulation. For the last 60 min, 5 mM ATP was added. Percentage of THP1-ASC-GFP cells with ASC-GFP specks or mean intensity of NF-κB-dependent GFP production in THP1-ASC-GFP cells treated with regorafenib, sorafenib or indicated controls. Mean ±SEM, n=3 independent cell preparations; one-way ANOVA with Dunnett's multiple comparisons test, significantly different from Vehicle+LPS+ATP.

THP1-Dual macrophages were pre-treated with regorafenib and sorafenib prior to LPS-induced priming followed by CPPD (100 µg/ml) crystal activation. To detect IL-8 production, supernatants were collected 1.5 h post-CPPD stimulation (Fig. 4.4A), as the chemokine is produced by macrophages early in the inflammatory response [702-704].

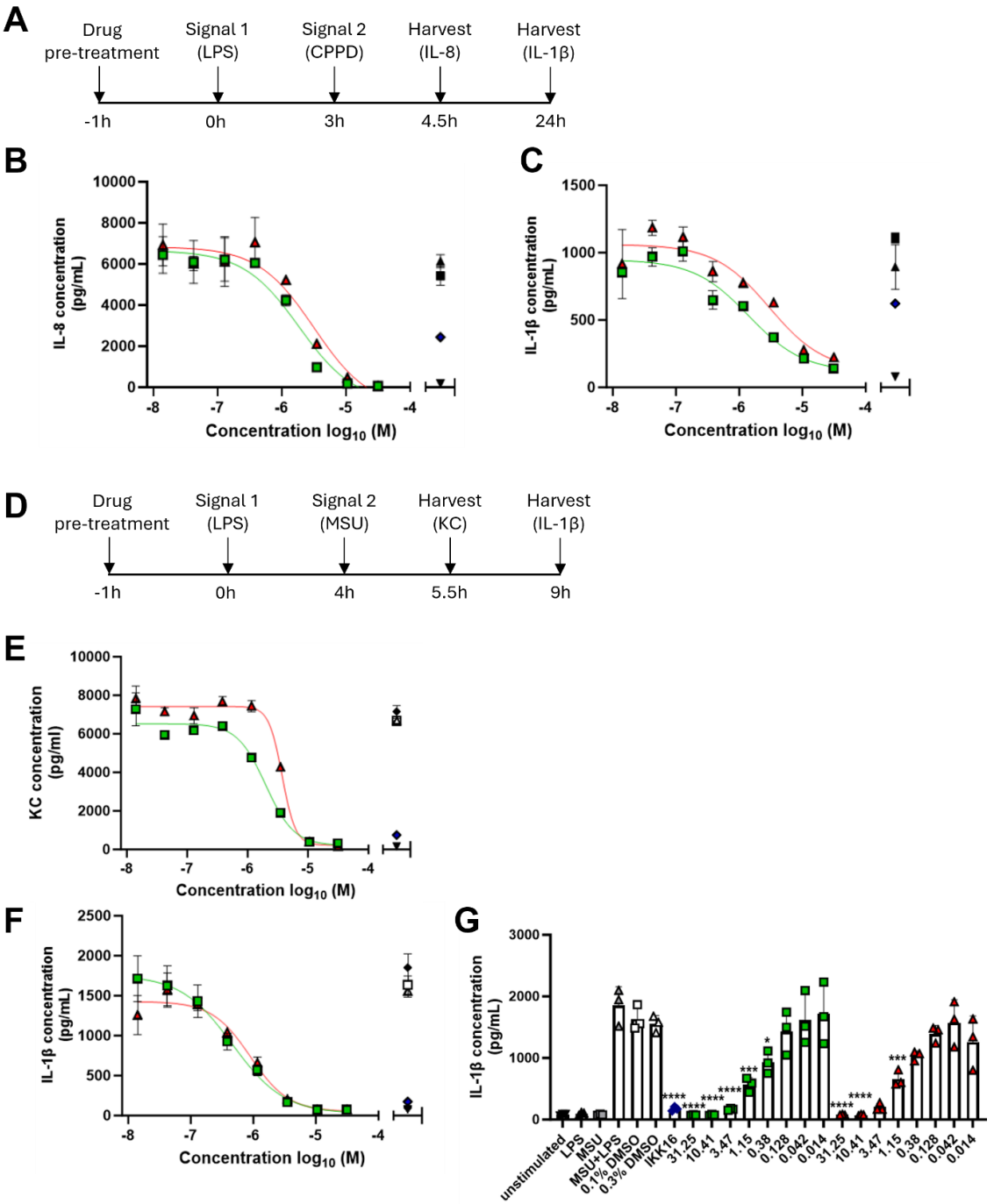


Fig. 4. 4 Regorafenib and sorafenib inhibit crystal-induced NLRP3 inflammasome activation in macrophages. (A) NLRP3 inflammasome activation in THP1-Dual macrophages by LPS+CPPD crystals. Concentration-response curve of regorafenib (green) and sorafenib (red) on IL-8 **(B)** or IL-1β **(C)** secretion by THP1-Dual cells pre-treated with drugs for 1 h before addition of signal 1 (LPS) and signal 2 (100 µg/ml CPPD crystals). Protein levels of IL-1β (at 24 h) or KC (at 4.5 h) were determined by ELISA. Controls are shown on the right: untreated cells (black downward triangle), LPS+CPPD (black upward triangle), DMSO+LPS+CPPD (black square), or IKK16+ LPS+CPPD (blue diamond). **(D)** NLRP3 inflammasome activation in BMDMs by LPS+MSU crystals. Concentration-response curve of regorafenib and sorafenib on KC **(E)** or IL-1β **(F-G)** secretion by BMDMs pre-treated with drugs for 1 h before addition of signal 1 (LPS) and signal 2 (150 µg/ml MSU crystals). Protein levels of IL-1β (at 9 h) or KC (at 1.5 h) were determined by ELISA. Controls are shown on the right: untreated cells (black downwards triangle), LPS+MSU (black upwards triangle), DMSO+LPS+MSU (black square) or IKK16+LPS+MSU (blue diamond).

Supernatants for IL-1β detection were collected 24 h after addition of signal 2, as IL-1β levels were reported to increase gradually and to peak at 24 h in THP1 cells in response to crystal stimulation (Fig. 4.4A) [705]. Regorafenib and sorafenib effectively decreased IL-8 levels at 1.5 h (IC_{50}s= 1.579 µM and 2.353 µM, respectively) and IL-1β production at 24 h (IC_{50}s= 1.402 µM and 2.995 µM, respectively) post CPPD crystal stimulation (Fig. 4.4B-C).

Similarly, BMDMs were pre-treated with regorafenib and sorafenib and primed with LPS for 4 h before MSU crystal stimulation (150 µg/ml) for 1.5 h (KC) or 24 h (IL-1β) (Fig. 4.4D). Regorafenib and sorafenib potently reduced KC production (IC_{50}= 1.966 µM and IC_{50}= 3.705 µM) in the initial stages of inflammation in primary murine macrophages (Fig. 4.4E). Both drugs also effectively suppressed IL-1β production with IC_{50}s in the sub-micromolar range (IC_{50}s= 0.460 µM and 0.890 µM) at 24 h post-MSU stimulation (Fig. 4.4F). Sorafenib significantly inhibited IL-1β secretion down to a concentration of 1.15 µM, while regorafenib was more potent and had significant effects on IL-1β secretion at concentrations as low as 0.38 µM (Fig. 4.4G).

These findings demonstrate that regorafenib and sorafenib are inhibitors of NF-κB-dependent NLRP3 inflammasome priming and the consequent production of IL-1β and IL-8/KC, both in response to ATP- as well as CPPD/MSU crystal-mediated inflammasome activation.

4.3.2 Selection of an appropriate *in vivo* model of acute inflammation

Given the potent anti-inflammatory activity of regorafenib and sorafenib in macrophages *in vitro*, we aimed to explore the drugs' efficacy in a model of acute inflammation *in vivo*. To allow for the determination of an effective *in vivo* drug dose as well as the early detection of any possible adverse effects of drug administration, we decided to test the TKIs in a short-term model of acute inflammation. Considering that their anti-inflammatory effects are mediated by NF-κB inhibition in macrophages, an appropriate

model should be driven by NF-κB activation in macrophages and allow for the measurement of NF-κB-induced pro-inflammatory mediator production and the resulting inflammatory cell influx, while causing minimal harm to the animals.

We observed that *in vitro*, regorafenib and sorafenib inhibit LPS+MSU crystal-induced IL-1β production in primary murine macrophages with sub-micromolar IC_{50} values and effectively reduce neutrophil-recruiting KC levels. Mechanistically, this effect was based on their ability to suppress NF-κB-dependent NLRP3 inflammasome priming. Therefore, we decided to test the drug repurposing candidates in MSU crystal-induced peritonitis *in vivo*. In this sterile peritonitis model, NF-κB-driven NLRP3 inflammasome activation, inflammatory cell influx and pro-inflammatory mediator production can be studied at different time points, with peritoneal neutrophil recruitment correlating to inflammasome activation and IL-1β levels [426]. Following the protocol of Spalinger et *al.* [426], we decided to orally administer mice with regorafenib and sorafenib 24 h and 2 h before intraperitoneal (i.p.) injection of MSU crystals (1.8 mg) (Fig. 4.5A).

At 4 h or 16 h post-MSU stimulation, blood and peritoneal lavage were to be collected to obtain serum, peritoneal exudate cells (PECs) and lavage supernatant. As read-outs, cytokine and chemokine protein levels can be determined in the peritoneal lavage supernatant as well as in the serum. The latter can also be analyzed to provide information about toxicology based on clinical biomarkers. PEC composition can be analyzed by flow cytometry and the mRNA expression of pro-inflammatory genes or protein levels of phospho-p65 or NLRP3 inflammasome components can be determined by RT-qPCR or western blotting, respectively (Fig. 4.5A).

The dosing regimen was selected based on the bioavailability of regorafenib and sorafenib *in vivo*. As both drugs are FDA-approved, their pharmacokinetics have been extensively studied and reported in the literature. A single oral dose of 10 mg/kg

regorafenib in male WT FVB mice causes plasma levels to peak at 2 h post-administration at 12 µM (Fig. 4.5B), which is similar to maximal plasma concentrations in humans after a single dose of regorafenib [427]. Then, regorafenib gets metabolized quickly and the plasma concentration declines rapidly. Similar pharmacokinetic data has been published for sorafenib in female WT mice on a DBA1/lacJ background that were orally administered with 10 mg/kg sorafenib [706].

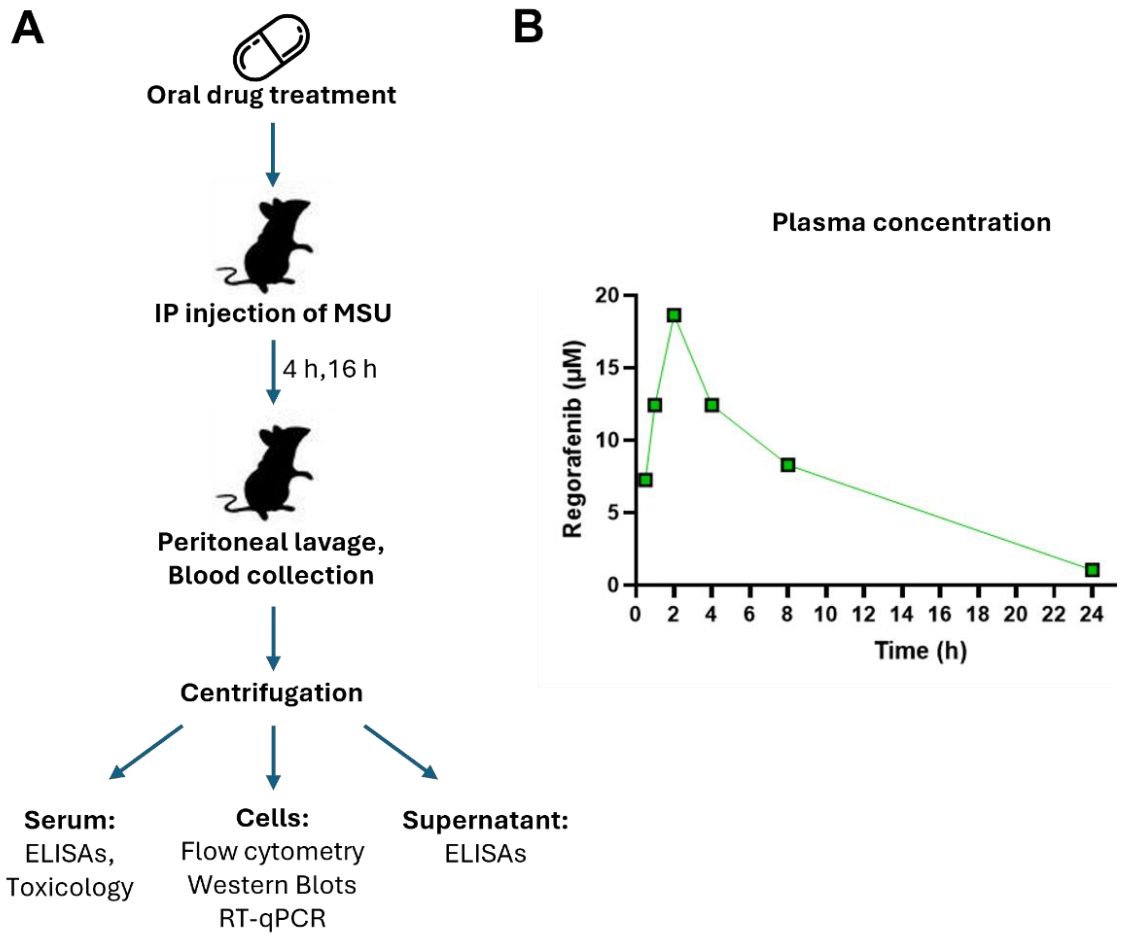


Fig. 4. 5 Design of MSU crystal-induced peritonitis study. *(***A)** Steps of MSU crystal-induced peritonitis protocol to study the effect of TKIs on acute inflammation *in vivo*. Adapted from [426]. **(B)** Previously reported plasma concentration after a single oral dose of 10 mg/kg regorafenib from [427].

The plasma concentrations of regorafenib and sorafenib reach pre-administration concentrations around 8 h post-oral gavage [706, 707]. Therefore, cancer patients are required to take four regorafenib tablets or two tablets of sorafenib per day to maintain elevated plasma levels [619, 708].

Based on these data, I decided to orally administer 10 mg/kg and 30 mg/kg regorafenib or sorafenib prophylactically 24 h and 2 h before MSU crystal injection to study the dose-dependent effects of the TKIs. This dosing regimen was designed considering published data by Reber et *al*., who used a similar prophylactic regimen to administer TKI imatinib to C57BL/6J WT mice before intra-articular MSU crystal injection [687]. In a drug repurposing study in the Greaves lab, Chaffey et *al.* pre-dosed C57BL/6J WT mice with TKI sunitinib to maximize target inhibition at the time of inflammatory stimulation [430].

4.3.3 Effect of prophylactic oral regorafenib and sorafenib administration on MSU crystal-induced peritonitis at 4 h

To assess the anti-inflammatory activity of regorafenib and sorafenib *in vivo*, male C57BL/6J WT mice received oral doses of 10 mg/kg or 30 mg/kg both 24 h and 2 h before i.p. injection with MSU crystals (Fig. 4.6A). After 4 h, serum and peritoneal cells were harvested for analysis. Following the flow cytometry gating strategy shown in Fig. 4.6B, we analyzed total PEC numbers as well as PEC populations of single live $CD45^+$ T cells ($CD3\varepsilon^+$/ $B220^-$), B cells ($CD3\varepsilon^-$/$B220^+$), monocytes ($CD3\varepsilon^-$/$B220^-$/ $Ly6C^{+/-}$/ $Ly6G^-$), neutrophils ($CD3\varepsilon^-$/ $B220^-$/ $Ly6C^+$/ $Ly6G^+$) and macrophages ($CD3\varepsilon^-$/ $B220^-$/ $Ly6C^-$/ $Ly6G^-$ / $CD11b^+$/ $F4\text{-}80^+$). The gating strategy was based on previous publications investigating peritoneal immune cell populations [709, 710] and the protocol for MSU crystal-peritonitis from Spalinger et *al.* [426].

To confirm successful initiation of MSU crystal-induced peritonitis, Cytospin preparations of 200,000 PECs per treatment group were stained and imaged (Fig.4.6C). We found that in sham mice that had received vehicle and were i.p. injected with PBS, the majority of PECs were macrophages/monocytes. Upon i.p. injection with MSU, a large number of neutrophils as well as some monocytes were detected.

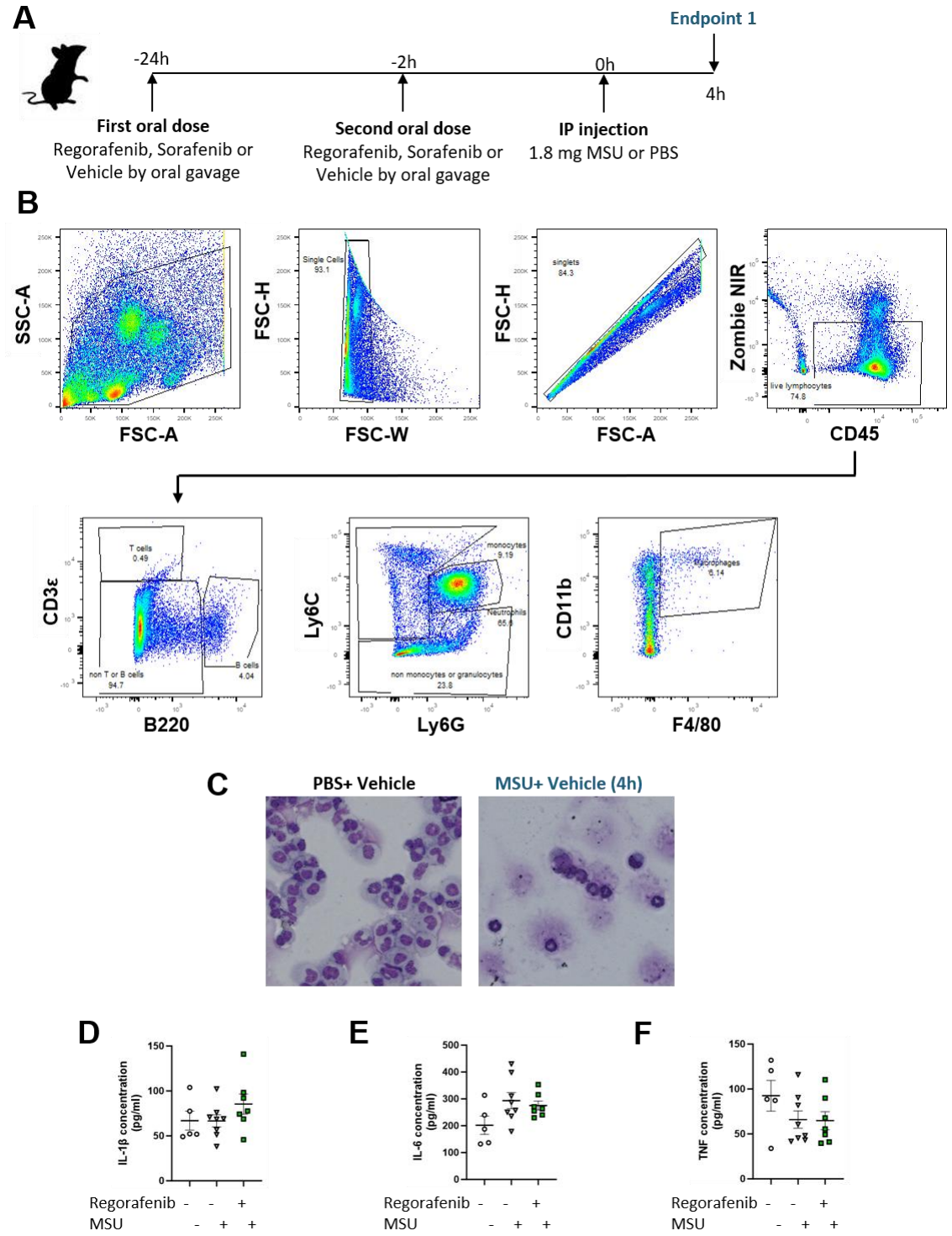


Fig. 4. 6 Intraperitoneal MSU crystal injection causes acute local inflammation. **A)** Experimental outline. Mice were orally administered with regorafenib or sorafenib (10 mg/kg or 30 mg/kg) or vehicle 24 h and 2 h prior to intraperitoneal (i.p.) injection of MSU-crystals (1.8 µg) and peritoneal exudate cells were harvested at 4 h. **(B)** Gating strategy for analysis of PEC composition (from MSU+vehicle mouse). **(C)** Representative images of Cytospin preparations of PECs after injection of PBS or MSU crystals. The levels of pro-inflammatory cytokines IL-1β **(D)**, IL-6 **(E)** and TNFα **(F)** in the serum after treatment with vehicle (grey) or 10 mg/kg regorafenib (green) were determined by ELISA 4 h after MSU/PBS injection. Mean ±SEM of n=5-8 mice per group. One-way ANOVA with Dunnett's multiple comparisons test.

Serum protein levels of pro-inflammatory cytokines IL-1β (Fig. 4.6D), IL-6 (Fig. 4.6E) and TNFα (Fig. 4.6F) were analyzed to determine whether peritoneal MSU administration had systemic inflammatory effects or whether inflammation was contained to the site of insult. Pro-inflammatory cytokine levels were not significantly increased in regorafenib or vehicle-treated mice stimulated with MSU crystals compared to sham mice. Therefore, i.p. MSU crystal injection seemed to cause local inflammation in the peritoneum.

4.3.3.1 Effect on peritoneal cell recruitment

At 4 h post-MSU injection (Fig. 4.7A), we did not observe a statistically significant increase in total PEC numbers in any treatment group compared to sham mice (Fig. 4.7B). Sham mice had an average of $5.7x10^6$ PECs and this increased to $7.2x10^6$ upon MSU crystal injection in vehicle-treated mice, but the increase was not significant. However, as reported by Spalinger et *al*. [426], the composition of PECs changed, with a significant 3138 % increase in peritoneal neutrophil numbers in vehicle-treated mice ($4.3x10^6$ neutrophils) compared to sham mice ($1.3x10^5$ neutrophils). This increase was significantly and dose-dependently attenuated by regorafenib, while only the higher 30 mg/kg sorafenib dose significantly reduced neutrophil influx (Fig. 4.7C). 10 mg/kg regorafenib reduced neutrophil numbers by 43 %, while 30 mg/kg caused a 60 % decrease in peritoneal neutrophil numbers. 10 mg/kg sorafenib mildly but not significantly inhibited neutrophil influx by 34 %, whereas 30 mg/kg sorafenib had comparable effects to 30 mg/kg regorafenib and decreased neutrophil recruitment by 57 % compared to vehicle-treated mice. At the 4 h time point, no significant increase in monocyte numbers was detected in any group upon MSU stimulation (Fig. 4.7D).

4.3.3.2 Effect on peritoneal cytokine and chemokine production

MSU crystal injection induced a significant increase in peritoneal protein levels of pro-inflammatory cytokines and chemokines (Fig. 4.7E-I).

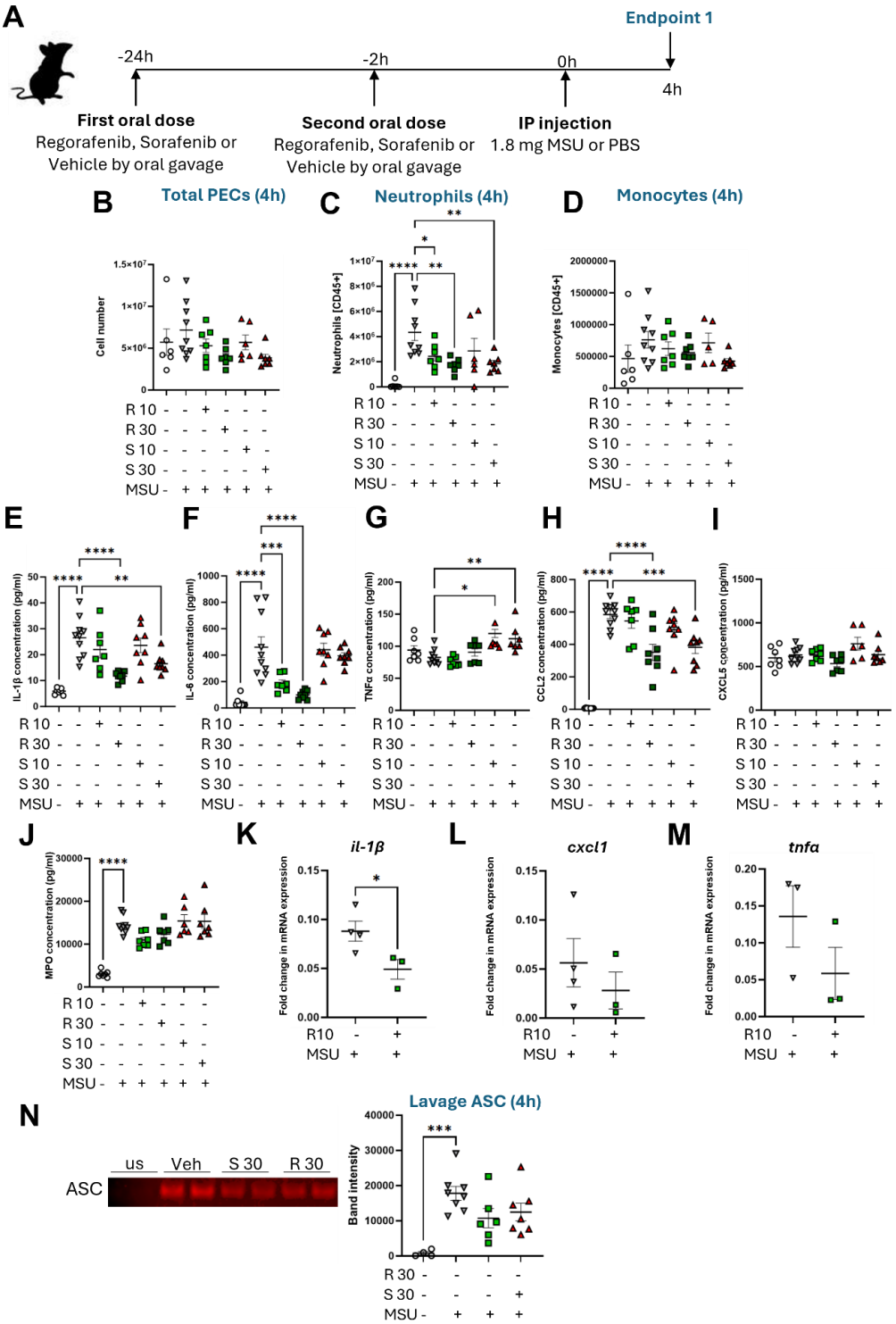


Fig. 4. 7 Prophylactic regorafenib or sorafenib administration reduces inflammation in MSU crystal-induced peritonitis at 4 h. (A) Experimental outline. Mice were orally administered with regorafenib (R, green squares) or sorafenib (S, red triangles) (10 mg/kg or 30 mg/kg) or vehicle (grey triangles) 24 h and 2 h before intraperitoneal (i.p.) injection of MSU crystals (1.8 µg) and peritoneal exudate cells were harvested at 4 h. Total peritoneal exudate cells **(B)**, neutrophils **(C)** and monocytes **(D)** were quantified in the peritoneal lavage fluid. **(E-J)** The levels of pro-inflammatory mediators in the peritoneal lavage fluid were determined by ELISA. Mean ±SEM of n=6-9 mice per group. PEC mRNA levels of *il-1β* **(K)**, *cxcl1* **(L)** and *tnfα* **(M)** after treatment with vehicle or 10 mg/kg regorafenib at 4 h after MSU/PBS injection. **(N)** Representative Western Blots for ASC in the peritoneal lavage at 4 h. Quantification using densitometry. us=sham.

IL-1β production was significantly up-regulated in vehicle-treated mice upon MSU stimulation, which was attenuated by prophylactic treatment with 30 mg/kg regorafenib (56 % decrease) or sorafenib (38 % decrease), but not 10 mg/kg of regorafenib or sorafenib (Fig. 4.7E).

While regorafenib dose-dependently reduced IL-6 levels by 59 % (10 mg/kg regorafenib) and 79 % (30 mg/kg regorafenib), sorafenib did not affect IL-6 production at either concentration (Fig. 4.7F). Peritoneal TNFα concentrations were not significantly altered in vehicle-treated mice upon MSU crystal injection and were not affected by regorafenib administration (Fig. 4.7G). However, oral administration with sorafenib dose-dependently increased peritoneal TNFα production compared to vehicle (Fig. 4.7G). Upon MSU crystal injection, we observed a large increase in peritoneal secretion of monocyte chemoattractant CCL2 from an average of 7 pg/ml to 584 pg/ml in vehicle-treated mice (Fig. 4.7H). The higher dose of both regorafenib and sorafenib significantly reduced CCL2 production by 40 % and 35 %, respectively. CXCL5 is a neutrophil chemoattractant produced in response to MSU crystal challenge and is associated with gouty inflammation and pain [711]. At 4 h post-MSU stimulation, no change in CXCL5 production was observed in vehicle-treated mice or any other treatment group (Fig. 4.7I). Myeloperoxidase (MPO) is released by activated neutrophils and is linked to tissue damage and exacerbation of inflammation [712]. We found that 4 h post-MSU crystal challenge, MPO protein levels were significantly increased in vehicle-treated mice compared to sham. Neither regorafenib nor sorafenib treatment attenuated MPO levels and thus neutrophil activation in the peritoneum (Fig. 4.7J).

4.3.3.3 Effect on PEC cytokine gene expression

In addition, we found that in PECs, mRNA levels of *il-1β* were significantly reduced in mice treated with 10 mg/kg regorafenib compared to vehicle (Fig. 4.7K). The expression of pro-inflammatory mediators *cxcl1* (Fig. 4.7L) and *tnfα* (Fig. 4.7M) was not significantly

decreased. Notably, PEC mRNA levels could only be determined in some mice due to low numbers of PECs and thus low amounts of purified RNA at 4 h post MSU crystal stimulation.

4.3.3.4 Effect on NLRP3 inflammasome markers in the peritoneum

In Fig. 4.2-4.4, we showed that TKI inhibition by regorafenib and sorafenib suppresses NLRP3 inflammasome priming and consequently the production of NLRP3 and the secretion of mature IL-1β in macrophages *in vitro*. To investigate the mechanism behind the observed anti-inflammatory effects of regorafenib and sorafenib *in vivo*, protein levels of NLRP3 inflammasome adapter ASC were determined in the peritoneal lavage as an indicator of inflammasome assembly (Fig. 4.7N). Western blot analysis revealed that while ASC levels were trending down in regorafenib-treated mice (40 % decrease), neither 30 mg/kg regorafenib nor 30 mg/kg sorafenib significantly reduced ASC levels in the peritoneum compared to Vehicle at 4 h.

Taken together, these findings demonstrate that the anti-inflammatory effects of regorafenib and sorafenib *in vitro* translate to a model of acute inflammation *in vivo*. Overall, regorafenib had more prominent anti-inflammatory effects than sorafenib, which is why only the 30 mg/kg regorafenib treatment group was included in further *in vivo* experiments.

4.3.4 Effect of prophylactic oral regorafenib administration on MSU crystal-induced peritonitis at 16 h

Since regorafenib attenuates the early inflammatory response in our model of acute inflammation at 4 h, I next aimed to investigate whether the TKI had similar anti-inflammatory effects on cell recruitment and pro-inflammatory mediator production at 16 h post-MSU crystal challenge. Therefore, male C57BL/6J WT mice were orally dosed with 30 mg/kg regorafenib or vehicle at 24 h and 2 h before i.p. injection with MSU

crystals. Peritoneal cell influx and inflammatory mediator production were analyzed at 16 h post-MSU crystal stimulation (Fig. 4.8A).

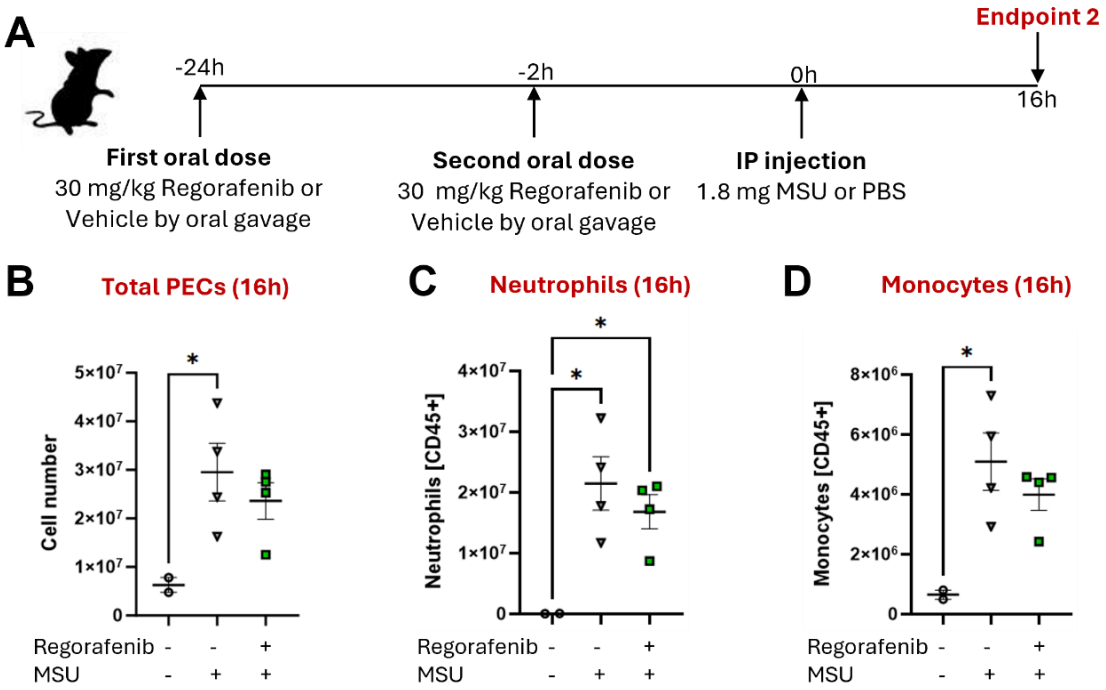


Fig. 4. 8 Prophylactic regorafenib administration does not affect inflammation in MSU crystal-induced peritonitis at 16 h. (A) Experimental outline. Mice were orally administered with regorafenib (30 mg/kg, green squares) or vehicle (grey triangles) 24 h and 2 h before i.p. injection of MSU crystals (1.8 µg) and peritoneal exudate cells were harvested at 16 h. Total peritoneal exudate cells **(B)**, neutrophils **(C)** and monocytes **(D)** were quantified in the peritoneal lavage fluid. Mean ±SEM of n=2-4 mice per group. One-way ANOVA with Dunnett's multiple comparisons test.

4.3.4.1 Effect on peritoneal cell recruitment

At 16 hours, the total number of peritoneal cells had significantly increased in vehicle-treated mice that were injected with MSU crystals compared to the sham group (Fig. 4.8B). This was due to a significant increase of neutrophils in the peritoneum from $7.9x10^4$ in sham mice to $2.2x10^7$ in vehicle-treated MSU-challenged mice (Fig. 4.8C). Peritoneal monocytes (Fig. 4.8D) increased from $8.2x10^5$ in sham mice to $5.2x10^6$ in mice that had received vehicle and MSU crystal injection. However, neither the total number of PECs nor neutrophil or monocyte influx was reduced by prophylactic administration of 30 mg/kg regorafenib. Considering the rapid metabolization of regorafenib after its plasma concentration peaks at 2 h post-oral gavage [427], we re-assessed the dosing

regimen. To maintain a sufficient plasma concentration to achieve therapeutic effects, cancer patients need to take four oral doses of regorafenib per day [619, 708]. A similar approach had been reported by Reber et *al.,* who prophylactically administered mice with TKI imatinib prior to intra-articular MSU injection. Before assessing the therapeutic effect of the drug repurposing candidate at 24 h, they administered mice with an additional therapeutic drug dose 6 h post-MSU crystal stimulation [687]. Taking this into consideration, I decided to change the dosing regimen accordingly to guarantee efficacious plasma concentrations of regorafenib for the entire duration of the experiment.

4.3.5 Effect of prophylactic and therapeutic oral regorafenib administration on MSU crystal-induced peritonitis at 16 h

Based on our previous findings, mice received two prophylactic oral doses of 30 mg/kg regorafenib or vehicle 24 h and 2 h before i.p. injection with MSU crystals for 16 h. Due to the pharmacokinetics of regorafenib, mice received a third oral dose of regorafenib or vehicle 6 h after MSU crystal stimulation (Fig. 4.9A).

4.3.5.1 Effect on peritoneal cell recruitment

Changes in PEC composition were qualitatively assessed by staining and imaging of Cytospin preparations containing 200,000 cells per treatment group (Fig. 4.9B). After the disappearance of resident peritoneal macrophages and an influx of neutrophils following MSU crystal challenge for 4 h, we observed an increasing number of monocytes in addition to neutrophils at the 16 h time point. This was confirmed by quantitative PEC analysis by flow cytometry (Fig. 4.9C-G). The numbers of total PECs (Fig. 4.9C) as well as neutrophils (Fig. 4.9D) and monocytes (Fig. 4.9E) were significantly increased 16 h post-MSU crystal injection compared to sham mice. Neutrophil numbers increased from $2.5x10^4$ to $2.5x10^7$ and monocytes from $5.1x10^5$ to $5.0x10^6$. Regorafenib suppressed the recruitment of both neutrophils and monocytes by 50 % and 36 %, respectively, thereby

significantly reducing total PEC numbers by 47 % compared to vehicle. Considering the kinetics of the inflammatory process initiated by intraperitoneal MSU crystal injection, we detected a continuous increase in peritoneal neutrophil (Fig. 4.9F) and later monocyte (Fig. 4.9G) numbers up to 16 h post-inflammatory insult. While sham mice had an average of $6x10^6$ PECs, this number steadily increased from $7x10^6$ PECs at 4 h to $3.4x10^7$ in MSU crystal-stimulated vehicle-treated mice. Importantly, inflammatory cell recruitment was successfully attenuated by regorafenib treatment.

4.3.5.2 Effect on peritoneal cytokine and chemokine production

At 16 h after MSU stimulation, pro-inflammatory mediator levels in the peritoneum had generally decreased compared to the 4 h time-point (Fig. 4.9H-M). Nevertheless, peritoneal IL-1β, IL-6, CCL2 and MPO protein levels were still significantly increased in MSU-challenged vehicle-treated mice compared to sham mice. At 16 h, TNFα and CXCL5 levels had remained at similar levels to the 4 h time point and were not significantly altered in any experimental group (Fig. 4.9J and L).

4.3.5.3 Effect on NLRP3 inflammasome activation in PECs

To investigate the molecular mechanism underlying the anti-inflammatory effects of regorafenib at 16 h post-MSU crystal challenge, we assessed ASC levels in the peritoneal lavage and pro-Caspase1 production in PECs (Fig. 4.9N). NF-κB activation drives the transcription and consequently protein production of pro-Caspase1 and ASC in inflammation [257, 296, 697].

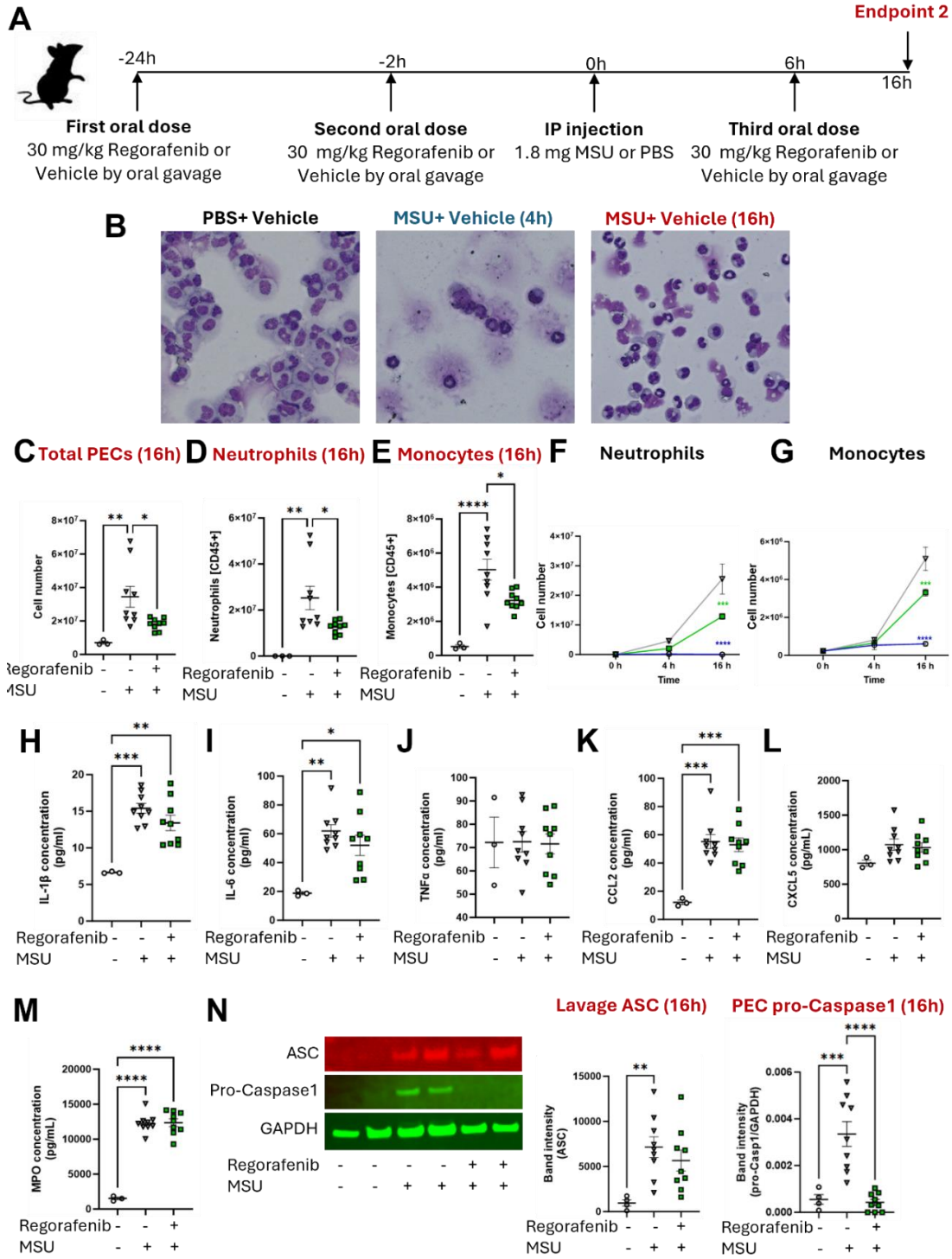


Fig. 4. 9 Prophylactic and therapeutic regorafenib administration reduces inflammation in MSU crystal-induced peritonitis at 16 h. (A) Mice were orally administered with regorafenib (30 mg/kg, green squares) or vehicle (grey triangles) 24 h and 2 h before i.p. injection of MSU crystals (1.8 µg). At 6 h, mice received a third oral dose of regorafenib or vehicle and PECs were harvested at 16 h. **(B)** Representative images of Cytospin preparations of PECs after injection of PBS or MSU crystals at 4 h and 16 h. Total PECs **(C)**, neutrophils **(D)** and monocytes **(E)** were quantified in the peritoneal lavage fluid. The number of neutrophils **(F)** and monocytes **(G)** in the peritoneum in the different treatment groups over time. **(H-M)** Levels of pro-inflammatory mediators in the peritoneal lavage fluid were determined by ELISA. **(N)** Representative Western Blot for pro-Caspase 1 and normalized to GAPDH in PECs at 16 h. Quantification using densitometry. Mean ±SEM of n=3-9 mice per group. One-way ANOVA with Dunnett's multiple comparisons test.

Densitometry western blot analysis revealed that the band mean fluorescence intensity (MFI) of ASC in the peritoneal lavage in sham mice was around 800-1000, which increased to around 18000 in vehicle-treated mice 4 h post-MSU injection. At 16 h, the mean ASC band intensity had decreased to approx. 7000 in the vehicle-treated group but was still significantly elevated compared to sham mice (Fig. 4.9N). Similar to the 4 h time point, regorafenib did not significantly attenuate peritoneal ASC levels at 16 h.

Pro-Caspase1 protein production in PECs of vehicle-treated mice significantly increased upon MSU stimulation for 16 h. Regorafenib administration substantially reduced pro-Caspase1 protein concentration by 87 % to levels comparable to those in sham mice (Fig. 4.9N).

These findings demonstrate that regorafenib inhibits inflammatory cell influx following MSU crystal challenge at 4 h and 16 h. This anti-inflammatory effect is mediated by suppression of NLRP3 inflammasome priming.

4.3.6 Effect of prophylactic oral regorafenib administration on MSU crystal-induced peritonitis in female mice at 4 h

We demonstrated that prophylactic regorafenib administration has anti-inflammatory effects in male mice with MSU crystal-induced peritonitis. Next, we sought to assess whether a similar anti-inflammatory effect can be observed in female C57BL/6J WT mice receiving regorafenib. Following the dosing regimen used in male mice (Fig. 4.7A), female mice were orally administered 30 mg/kg regorafenib 24 h and 2 h before intraperitoneal challenge with MSU crystals or PBS for 4 h (Fig. 4.10A).

4.3.6.1 Effect on peritoneal cell recruitment

Similar to male mice, we did not observe a significant increase in peritoneal exudate cells in vehicle-treated female mice compared to sham mice at 4 h after the onset of inflammation (Fig. 4.10B). Again, the composition of PECs changed, with a significant 5641 % increase in peritoneal neutrophil numbers in vehicle-treated mice ($7.3x10^6$

neutrophils) compared to sham mice ($1.3x10^5$ neutrophils) (Fig. 4.10C). This increase was significantly attenuated by regorafenib ($4.3x10^6$ neutrophils). Similar to male mice, no significant change in monocyte numbers was detected in any group upon MSU stimulation at 4 h in female mice (Fig. 4.10D).

4.3.6.2 Effect on peritoneal cytokine and chemokine production

Peritoneal MSU crystal challenge induced pro-inflammatory mediator production in the peritoneum of vehicle-treated female mice compared to the sham group at 4 h (Fig. 4.10E-J). Similar to male mice, regorafenib had an anti-inflammatory effect in female mice, effectively reducing IL-1β (Fig. 4.10E), IL-6 (Fig. 4.10F) and CCL2 (Fig. 4.10H) protein levels in the peritoneal lavage compared to vehicle. CXCL5 and MPO levels in the peritoneal lavage were not significantly reduced by regorafenib compared to vehicle (Fig. 4.10I-J). However, CXCL5 and MPO production in the regorafenib group were not significantly increased compared to sham mice either. At 4 h post-MSU crystal injection, TNFα levels in the peritoneum were not significantly elevated compared to sham mice in either treatment group (Fig. 4.10G).

4.3.6.3 Effect on NLRP3 inflammasome activation in the peritoneum

To investigate the mechanism of these anti-inflammatory effects in female mice at 4 h post-MSU crystal challenge, we assessed NF-κB-mediated ASC protein production in the peritoneal lavage (Fig. 4.10K). Regorafenib significantly reduced peritoneal protein levels of ASC (59 % decrease) compared to vehicle in female mice at 4 h. Interestingly, we observed a similar trend in male mice (Fig. 4.7N), indicating that the effect on ASC levels follows a similar pattern. However, the reduction of ASC protein levels in regorafenib-treated mice only reached statistical significance in female mice.

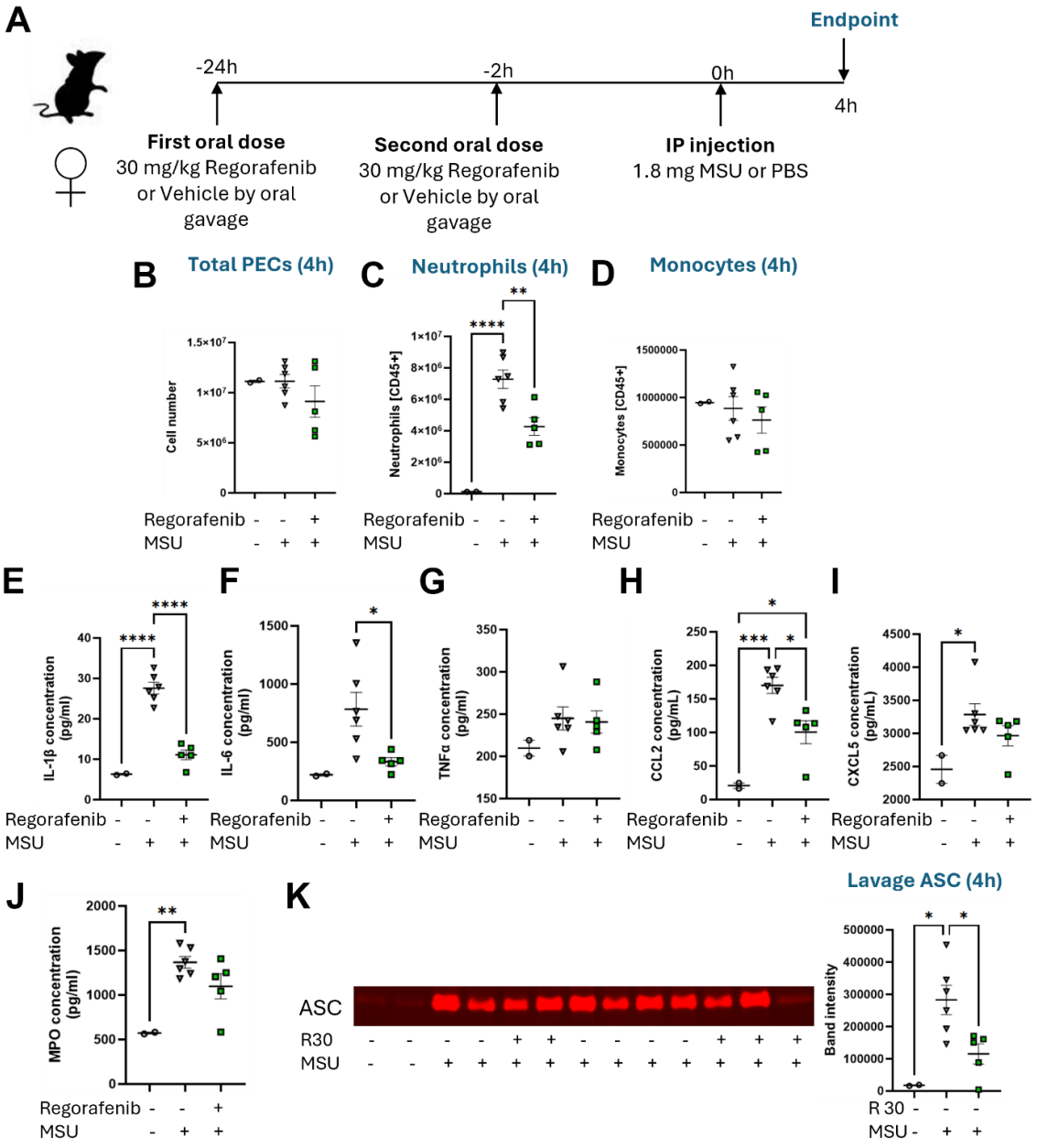


Fig. 4. 10 Prophylactic regorafenib treatment reduces inflammation in MSU crystal-induced peritonitis in female mice. (A) Experimental outline. Female mice were orally administered with regorafenib (30 mg/kg, green squares) or vehicle (grey triangles) 24 h and 2 h before i.p. injection of MSU crystals (1.8 µg) and peritoneal exudate cells were harvested at 4 h. Total peritoneal exudate cells **(B)**, neutrophils **(C)** and monocytes **(D)** were quantified in the peritoneal lavage fluid. **(E-J)** The levels of pro-inflammatory mediators in the peritoneal lavage fluid were determined by ELISA. **(K)** Representative Western Blot for ASC in the peritoneal lavage at 4 h. Quantification using densitometry. us=sham, Veh=vehicle+MSU, R30= regorafenib+MSU. Mean ±SEM of n=2-6 mice per group. One-way ANOVA with Dunnett's multiple comparisons test.

Our results indicate that the anti-inflammatory activity of TKI regorafenib in MSU crystal-induced peritonitis as a mouse model of acute inflammation is not sex-specific, as our previous findings in male mice translate into female mice.

4.3.7 Comparison of effects of regorafenib and NSAID indomethacin on MSU-crystal-induced peritonitis at 16 h

The NSAID indomethacin is widely used to treat patients suffering from arthritis or gout. The COX inhibitor alleviates symptoms such as fever, pain and joint swelling [713, 714]. Therefore, indomethacin was chosen as an appropriate control to assess how the anti-inflammatory effects of regorafenib compare to those of a commonly used NSAID in our model of acute inflammation driven by gout crystals.

Following the dosing regimen used for regorafenib (Fig. 4.9), mice received two prophylactic oral doses of 5 mg/kg indomethacin or vehicle before i.p. challenge with MSU crystals for 16 h. 6 h after initiation of inflammation, mice were administered with a third oral indomethacin dose (Fig. 4.11A).

4.3.7.1 Effects on peritoneal cell recruitment

As observed previously (Fig. 4.9), the number of total PECs (Fig. 4.11B) as well as neutrophils (Fig. 4.11C) and monocytes (Fig. 4.11D) increased significantly in vehicle-treated mice 16 h after MSU injection compared to sham mice. Similar to regorafenib, indomethacin significantly suppressed this inflammatory cell influx. The NSAID reduced total peritoneal neutrophil numbers by 34 % and monocyte numbers by 45 %. However, it did not significantly reduce total PEC numbers, even though numbers were trending down (32 % decrease) and they were less elevated in indomethacin-treated mice compared to sham (Fig. 4.11B). Compared to regorafenib, the effect of indomethacin on neutrophil infiltration was slightly weaker, while the NSAID more effectively inhibited monocyte influx.

While it is difficult to directly compare the effect of both drugs due to the different concentrations used, we chose not to increase the indomethacin dose due to ethical and animal welfare considerations about reported adverse effects of higher indomethacin concentrations in mice [715-717].

4.3.7.2 Effects on peritoneal cytokine and chemokine production

MSU crystal injection caused a significant increase in peritoneal protein levels of pro-inflammatory mediators IL-1β, IL-6, CXCL5 and MPO in vehicle-treated mice at 16 h (Fig. 4.11E-J), while TNFα levels remained unchanged between experimental groups (Fig. 4.11G). Similar to regorafenib, indomethacin did not affect IL-1β (Fig. 4.11E), CXCL5 (Fig. 4.11I) or MPO (Fig. 4.11J) production in the peritoneum at 16 h. However, the NSAID significantly reduced IL-6 levels by 37 % (Fig. 4.11F). While IL-6 levels were less increased in regorafenib-treated mice, they were not significantly reduced compared to vehicle at 16 h (16 % decrease, Fig. 4.9I). Notably, indomethacin significantly increased pro-inflammatory monocyte chemoattractant CCL2 at 16 h (1161 % increase compared to sham and 78 % increase compared to vehicle, Fig. 4.11H), while regorafenib did not affect CCL2 levels at this time point (Fig. 4.9K).

4.3.7.3 Effects on NF-κB and NLRP3 inflammasome activation in PECs

Phosphorylation levels of p65 and pro-Caspase1 protein concentrations were measured in PECs to compare the mechanism mediating the anti-inflammatory effects of regorafenib and indomethacin (Fig. 4.11K). At 16 h after MSU crystal challenge, p65 phosphorylation had significantly increased in vehicle-treated mice. Phosphorylation was not significantly reduced by regorafenib at 16 h, while indomethacin significantly inhibited p65 phosphorylation in PECs at this time point by 50 % (Fig. 4.11K). However, regorafenib decreased NF-κB-dependent pro-Caspase1 production in PECs (97 % reduction), which was elevated in vehicle-treated MSU crystal-challenged mice compared to sham mice. This brought pro-Caspase1 protein concentrations down to similar levels as in sham mice. In contrast, indomethacin significantly increased pro-Caspase1 levels by 169 % in peritoneal exudate cells compared to vehicle (Fig. 4.11K).

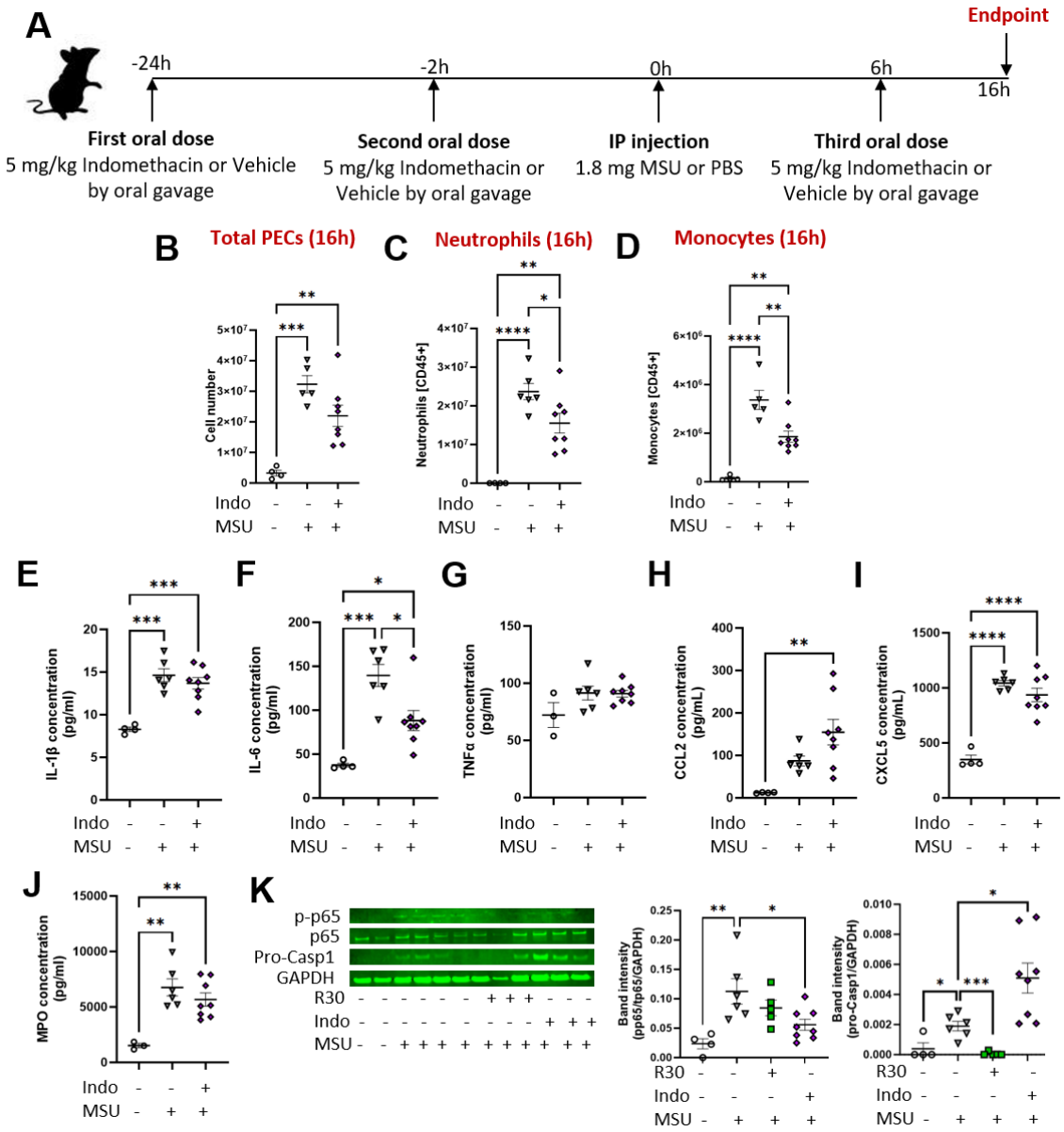


Fig. 4. 11 Regorafenib and indomethacin both have anti-inflammatory effects in MSU crystal-induced peritonitis. A) Experimental outline. Mice were orally administered with 5 mg/kg indomethacin (Indo, purple diamonds) or vehicle (grey triangles) 24 h and 2 h before i.p. injection of MSU crystals (1.8 µg). At 6 h, mice received a third oral dose of indomethacin or vehicle and peritoneal exudate cells were harvested at 16 h. Total peritoneal exudate cells **(B)**, neutrophils **(C)** and monocytes **(D)** were quantified in the peritoneal lavage fluid. **(E-J)** The levels of pro-inflammatory mediators in the peritoneal lavage fluid were determined by ELISA. **(K)** Representative Western Blots for phospho-p65, total p65, pro-Caspase1 and GAPDH in PECs at 16 h. Mean ±SEM of n=4-7 mice per group. One-way ANOVA with Dunnett's multiple comparisons test or unpaired student's t-test.

4.3.7.4 Toxicity of oral regorafenib and indomethacin administration

As an anti-cancer drug used to treat HCC, cases of hepatotoxicity have been reported in patients treated with regorafenib [708]. Similarly, indomethacin can impair liver function and induce liver damage [714]. Therefore, we investigated whether three oral doses of regorafenib or indomethacin impair liver function or cause liver damage in mice with MSU crystal-induced peritonitis at 16 h.

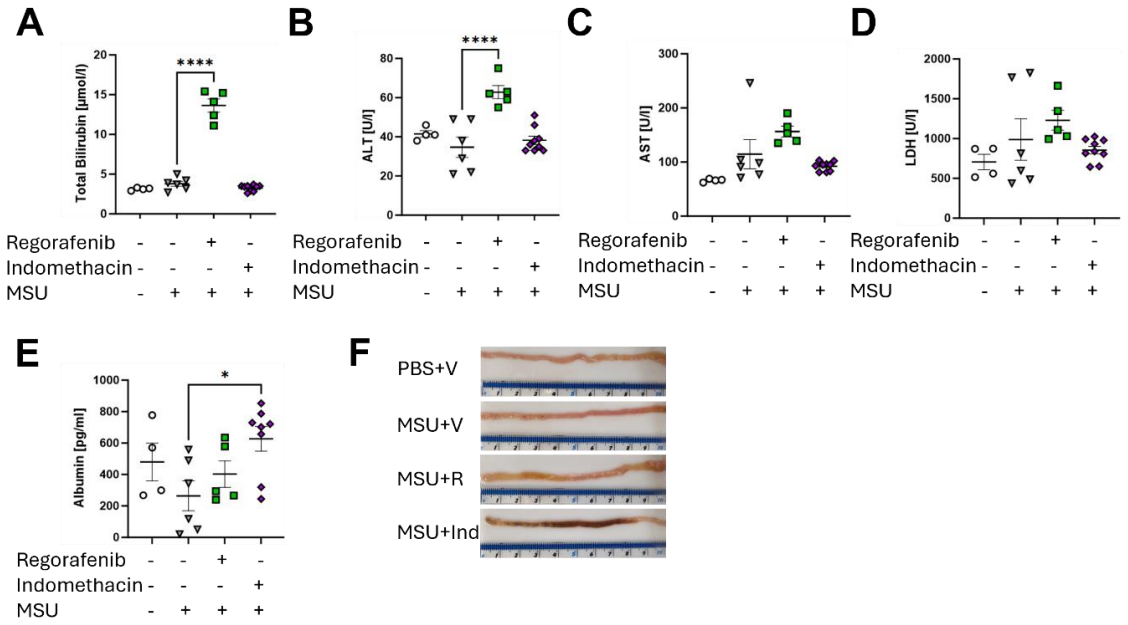


Fig. 4. 12 Liver and gastrointestinal toxicity of regorafenib and indomethacin in MSU crystal-induced peritonitis. (A-D) Liver function and cell damage markers in the serum collected from mice 16 h after i.p. MSU or PBS injection. **(E)** Blood albumin in stool at 16 h post-MSU/PBS challenge quantified by ELISA. **(F)** Representative images of the small intestines retrieved 16 h post-MSU/PBS injection. Mean ±SEM of n=4-7 mice per group; one-way ANOVA with Dunnett's multiple comparisons test. V=vehicle (grey triangles), R=regorafenib (green squares), Ind=indomethacin (purple diamonds).

We assessed serum levels of bilirubin as a marker of liver function, total alanine aminotransferase (ALT) and total aspartate aminotransferase (AST) concentrations as read-outs for hepatocellular injury as well as total lactate dehydrogenase (LDH) levels indicating general cell death and tissue damage (Fig. 4.12A-D). Neither indomethacin nor vehicle treatment alone or in combination with MSU crystal injection impaired liver function or induced liver or cell damage. Regorafenib significantly increased total bilirubin (Fig. 4.12A) and ALT (Fig. 4.12B) levels in the serum and caused an increase in serum

AST levels (Fig. 4.12C), even though this was not statistically significant. However, ALT and AST levels were still within the physiological range reported for 8- 10-week-old male C57BL/6 mice (Table 4.1). The TKI did not affect serum LDH concentrations (Fig. 4.12D).

Table 4. 1 Reference values for liver toxicity and cell death markers in the serum
Values were obtained from [718, 719].

Analyte	Min.	Max.	Median (50 %)
Total ALT	13.2	124.4	45.2
Total AST	31.7	331.7	54.2
Total Bilirubin	5.1	11.9	7.2
Total LDH	1590	2610	1888

These findings suggest that three oral doses of 5 mg/kg indomethacin do not cause hepatotoxicity or cell death in mice. However, regorafenib decreases liver function and may induce mild liver damage but does not cause a significant amount of general cell death.

4.3.7.5 Gastrointestinal toxicity of indomethacin compared to regorafenib

Considering that indomethacin treatment has been linked to an increased risk of serious gastrointestinal (GI) adverse effects, such as GI perforation and bleeding [720-722], I investigated fecal albumin protein concentrations as an indicator for GI bleeding as described in [720] (Fig. 4.12E). Neither regorafenib nor vehicle treatment alone or in combination with i.p. MSU crystal challenge affected fecal albumin levels. However, we detected significantly elevated fecal albumin levels in indomethacin-treated mice compared to vehicle, indicating an increased amount of blood in the stool. In agreement with these results, we observed altered physiology and color in the small intestine of mice that had received indomethacin (Fig. 4.12F). These changes were absent in sham mice and in MSU crystal-injected mice treated with vehicle or regorafenib.

Taking into account the drug concentrations used in this study, our results show that both regorafenib and NSAID indomethacin have anti-inflammatory effects in MSU crystal-induced peritonitis. Both drugs inhibit inflammatory cell recruitment and indomethacin additionally reduces peritoneal IL-6 levels but enhances CCL2 production at 16 h. Further, indomethacin significantly reduced PEC p65 phosphorylation, while this effect was not significant in the regorafenib group at 16 h. However, regorafenib additionally reduced NLRP3 inflammasome activation while indomethacin increased inflammasome activity. Importantly, regorafenib lacked indomethacin's gastrointestinal toxicity, which limits the NSAID's applications in gout treatment. However, 30 mg/kg regorafenib administration caused significant hepatotoxicity, which was absent in indomethacin-treated mice. Taken together, we show here that while both drugs have limitations due to adverse effects, they inhibit gouty peritoneal inflammation through different mechanisms.

4.3.8 Effect of therapeutic oral regorafenib administration on MSU crystal-induced peritonitis at 16 h

In the *in vivo* experiments described in this chapter so far, mice were prophylactically administered with regorafenib before initiation of inflammation. To investigate whether therapeutic intervention with regorafenib can be used to treat acute inflammation, mice received a single oral therapeutic dose of 30 mg/kg regorafenib or vehicle 0.5 h after i.p. injection with MSU crystals for 16 h (Fig. 4.13A).

4.3.8.1 Effect of peritoneal cell recruitment

The increase in total PECs (Fig. 4.13B), peritoneal neutrophils (Fig. 4.13C) and monocytes (Fig. 4.13D) after MSU crystal challenge was not significantly reduced by therapeutic oral intervention with regorafenib compared to vehicle.

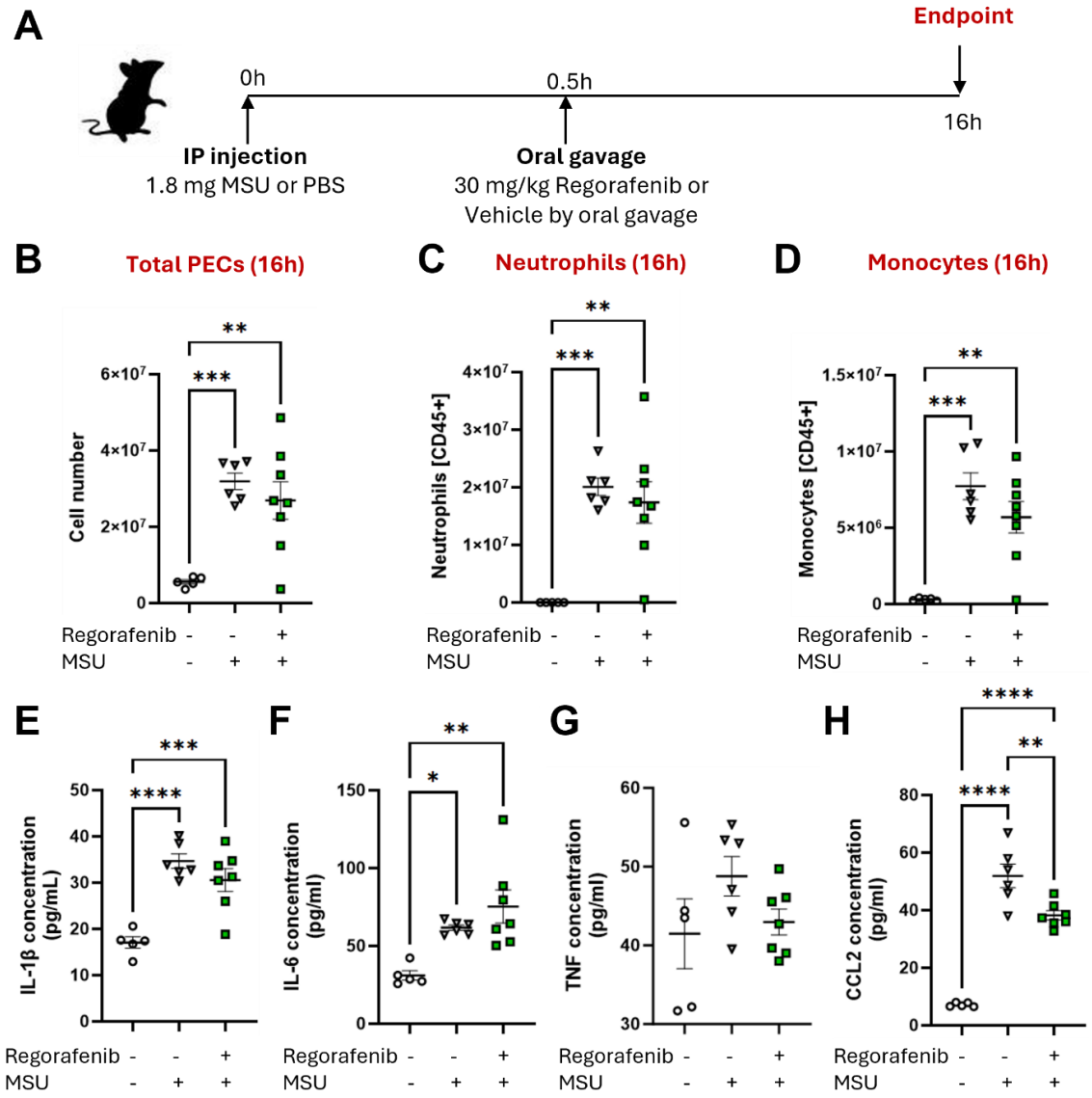


Fig. 4. 13 Therapeutic oral regorafenib administration has mild anti-inflammatory effects in MSU crystal-induced peritonitis. (A) Experimental outline. Mice were injected i.p. with MSU crystals (1.8 µg). At 0.5 h, mice received 30 mg/kg regorafenib (green squares) or vehicle (grey triangles) via oral gavage and peritoneal exudate cells were harvested at 16 h. Total peritoneal exudate cells **(B)**, neutrophils **(C)** and monocytes **(D)** were quantified in the peritoneal lavage fluid. **(E-H)** The levels of pro-inflammatory mediators in the peritoneal lavage fluid were determined by ELISA. Means ±SEM of n=5-7 mice per group. One-way ANOVA with Dunnett's multiple comparisons test.

4.3.8.2 Effect on peritoneal cytokine and chemokine production

At 16 h post-MSU crystal challenge, peritoneal IL-1β, IL-6 and CCL2 protein levels were significantly elevated compared to sham mice, while TNFα levels were not significantly increased (Fig. 4.13E-H). A single therapeutic oral dose of regorafenib was sufficient to mildly but significantly reduce CCL2 (Fig. 4.13H) production in the peritoneum compared

to vehicle. However, CCL2 levels were still similarly elevated compared to sham mice. IL-1β or IL-6 levels were not reduced by drug treatment at 16 h (Fig. 4.13E-F).

4.3.9 Effect of therapeutic intraperitoneal regorafenib administration on MSU crystal-induced peritonitis at 16 h

Considering the pharmacodynamics of regorafenib, one oral dose of the TKI may not be sufficient to maintain efficacious plasma concentrations up to the 16 h endpoint. Consequently, we decided to intraperitoneally administer the therapeutic regorafenib dose instead to ensure high concentrations of the drug at the site of inflammation. Therefore, mice were intraperitoneally administered with a therapeutic regorafenib dose 0.5 h after i.p. MSU crystal challenge (Fig. 4.14A).

4.3.9.1 Effect on peritoneal cell recruitment

Therapeutic intraperitoneal regorafenib administration did not significantly reduce total peritoneal exudate cell numbers 16 h post-MSU crystal injection compared to vehicle (Fig. 4.14B). Peritoneal neutrophil (Fig. 4.14C) and monocyte (Fig. 4.14D) recruitment was also not significantly inhibited by therapeutic i.p. regorafenib treatment. However, peritoneal neutrophil numbers in regorafenib-treated mice were not significantly increased compared to sham, as the TKI mildly reduced neutrophil infiltration by 37 % compared to vehicle.

4.3.9.2 Effect on peritoneal cytokine and chemokine production

As observed previously, peritoneal IL-1β, IL-6 and CCL2 levels were significantly elevated in the vehicle group compared to sham mice at 16 h after MSU crystal challenge, while TNFα levels remained unchanged across all three experimental groups (Fig. 4.14E-H). Therapeutic i.p. regorafenib intervention did not inhibit peritoneal pro-inflammatory mediator production compared to vehicle, similar to prophylactic oral regorafenib administration at 16 h (Fig. 4.9).

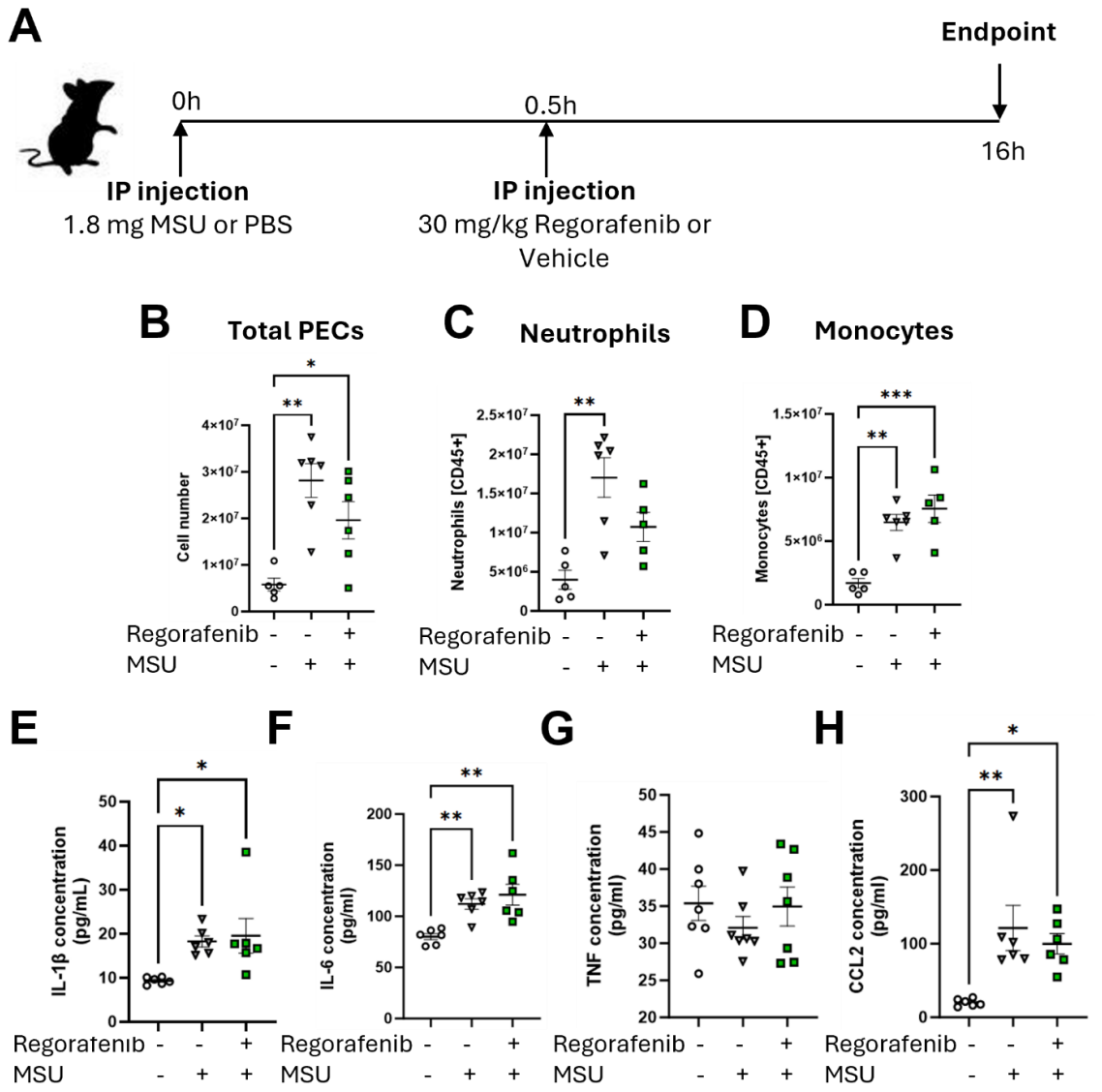


Fig. 4. 14 Therapeutic i.p. regorafenib administration has mild anti-inflammatory effects in MSU crystal-induced peritonitis. (A) Experimental outline. Mice were injected i.p. with MSU crystals (1.8 µg). At 0.5 h, mice received 30 mg/kg regorafenib (green squares) or vehicle (grey triangles) i.p. and peritoneal exudate cells were harvested at 16 h. Total peritoneal exudate cells **(B)**, neutrophils **(C)** and monocytes **(D)** were quantified in the peritoneal lavage fluid. **(E-H)** The levels of pro-inflammatory mediators in the peritoneal lavage fluid were determined by ELISA. Means ±SEM of n=5-9 mice per group. One-way ANOVA with Dunnett's multiple comparisons test.

Therapeutic i.p. administration of regorafenib did not reduce total PEC numbers or monocyte recruitment. However, I noticed that even in sham mice that had been i.p. injected with PBS and vehicle, the number of total peritoneal cells and neutrophils was unusually high. In previous experiments in which drug and vehicle had been delivered

via oral gavage, we counted an average of $2.5x10^4$ peritoneal neutrophils in sham mice at 16 h (Fig.4.9D). In comparison, the peritoneum of sham mice i.p. injected with PBS+vehicle in this experiment contained $4x10^6$ neutrophils. Therefore, we hypothesized that the vehicle itself, which was optimized for drug delivery per oral gavage, may promote neutrophil influx upon injection into the peritoneum.

4.3.10 Identification of a non-inflammatory vehicle for intraperitoneal drug delivery

A vehicle suitable for the intraperitoneal delivery of regorafenib must not in itself induce neutrophil recruitment and allow regorafenib to dissolve. Therefore, we tested a range of vehicle formulations that were used in previous studies to intraperitoneally deliver anti-inflammatory drugs. We tested PBS containing 30 % or 15 % cyclodextrin (CD) and 5 % DMSO, PBS containing 2 % Tween-80 and 5 % DMSO as well as PBS with 2 % Tween-80, 5 % DMSO and 10 % Polyethylene glycol (PEG). The effects of i.p. injection of these vehicles on peritoneal cell composition were compared to both a single injection of the vehicle used for oral gavage or a single injection of PBS alone as well as to two sequential injections of either PBS+PBS or PBS+vehicle used for oral gavage. This was to test whether the increased number of peritoneal neutrophils in sham mice was due to the inflammatory nature of the vehicle used for oral gavage, due to the two subsequent i.p. injections themselves or due to the PBS that MSU crystals were delivered in. Mice were i.p. injected with PBS followed by injection with either PBS or the selected vehicles where appropriate (Fig. 4.15A). Flow cytometry analysis of PEC populations in the different groups revealed that neither treatment significantly affected peritoneal B cell, monocyte or T cell numbers at 16 h compared to PBS+PBS injections (Fig. 4.15B). Two subsequent injections of PBS alone did not increase peritoneal neutrophil numbers, indicating that it was neither the PBS nor the injections themselves that caused inflammatory cell recruitment. Injections with the vehicle used for oral gavage alone or in combination with PBS injection however significantly increased neutrophil numbers in

the peritoneum at 16 h post injection, validating our hypothesis that it was indeed the vehicle itself that was pro-inflammatory.

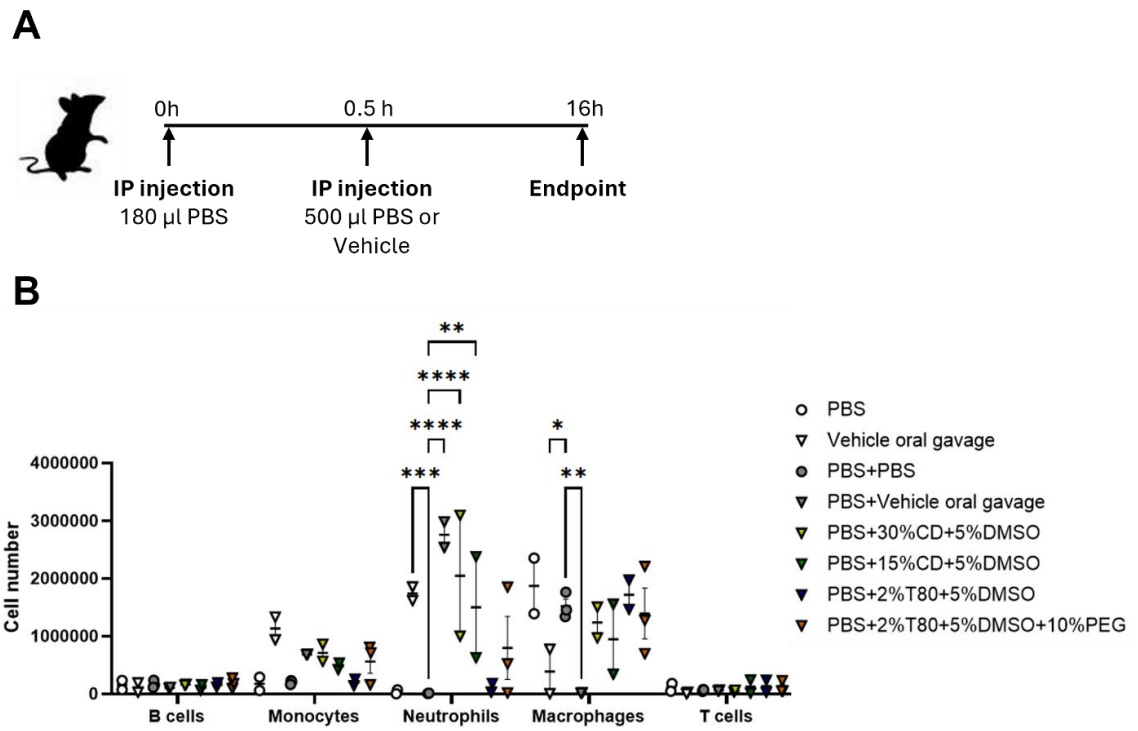


Fig. 4. 15 Vehicle optimization for i.p. regorafenib delivery. (A) Experimental outline. Mice were injected i.p. with PBS (180 µl). At 0.5 h, mice received PBS or the respective vehicle i.p. and peritoneal exudate cells were harvested at 16 h. **(B)** Numbers of B cells, monocytes, neutrophils, macrophages and T cells were quantified to determine an anti-inflammatory Vehicle for i.p. drug delivery. n=2-3 mice per group. Two-way ANOVA with Dunnett's multiple comparisons test. CD= cyclodextrin, T80= Tween-80, PEG= polyethylene glycol.

Compared to two consecutive PBS injections, this vehicle also caused the disappearance of resident peritoneal macrophages, which we also observed upon inflammatory challenge with MSU crystals and which is well documented in the literature as the "macrophage disappearance reaction" in peritoneal inflammation [210, 602, 677, 678]. Vehicles containing cyclodextrin triggered significant peritoneal neutrophil recruitment but did not affect the number of resident peritoneal macrophages. The vehicle consisting of PBS with 2 % Tween-80 and 5 % DMSO caused the least neutrophil recruitment, however, we found that it did not allow regorafenib to dissolve fully.

Therefore, we selected PBS +2 % Tween-80 +5 % DMSO +10 % PEG as the new vehicle to deliver regorafenib intraperitoneally in further experiments.

4.3.11 Effect of therapeutic intraperitoneal regorafenib administration on MSU crystal-induced peritonitis at 16 h (new vehicle)

Following the vehicle optimization for i.p. drug delivery, we aimed to test whether regorafenib could inhibit both inflammatory cell recruitment and pro-inflammatory mediator production in the peritoneum when administered therapeutically in a non-inflammatory vehicle. Following the dosing regimen of the previous study (Fig. 4.14A), regorafenib was injected at 0.5 h after the initiation of inflammation by MSU crystal challenge (Fig. 4.16A).

4.3.11.1 Effect on peritoneal cell recruitment

As expected, the total numbers of PECs (Fig. 4.16B) as well as the numbers of peritoneal neutrophils (Fig. 4.16C) and monocytes (Fig. 4.16D) were significantly increased in vehicle-treated mice compared to sham mice at 16 h post-MSU crystal injection. Total PEC numbers increased from $4.8x10^6$ to $4x10^7$ and peritoneal monocyte numbers rose from $7.8x10^5$ to $9.5x10^6$ in vehicle-treated mice. Unlike the vehicle previously used for oral gavage, however, i.p. injection with the new vehicle caused less neutrophil influx, with only $2.3x10^5$ neutrophils counted in the peritoneum in sham mice. This was comparable to mice that had received PBS i.p. ($3.9x10^5$ peritoneal neutrophils). As a consequence, regorafenib therapeutically delivered in a non-inflammatory vehicle significantly reduced peritoneal neutrophil influx by 43 % compared to vehicle (Fig. 4.16C). In addition, we observed a smaller increase in monocyte numbers in the peritoneum of regorafenib-treated mice compared to vehicle mice (Fig. 4.16D). Monocyte numbers were not statistically decreased after therapeutic regorafenib i.p. injection compared to vehicle.

4.3.11.2 Effect on peritoneal cytokine and chemokine production

At 16 h post-MSU crystal injection, the peritoneal levels of IL-1β, IL-6, CCL2 and CXCL5 were significantly elevated in vehicle-treated mice compared to sham mice, while TNFα levels remained unchanged across all three experimental groups (Fig. 4.16E-I).

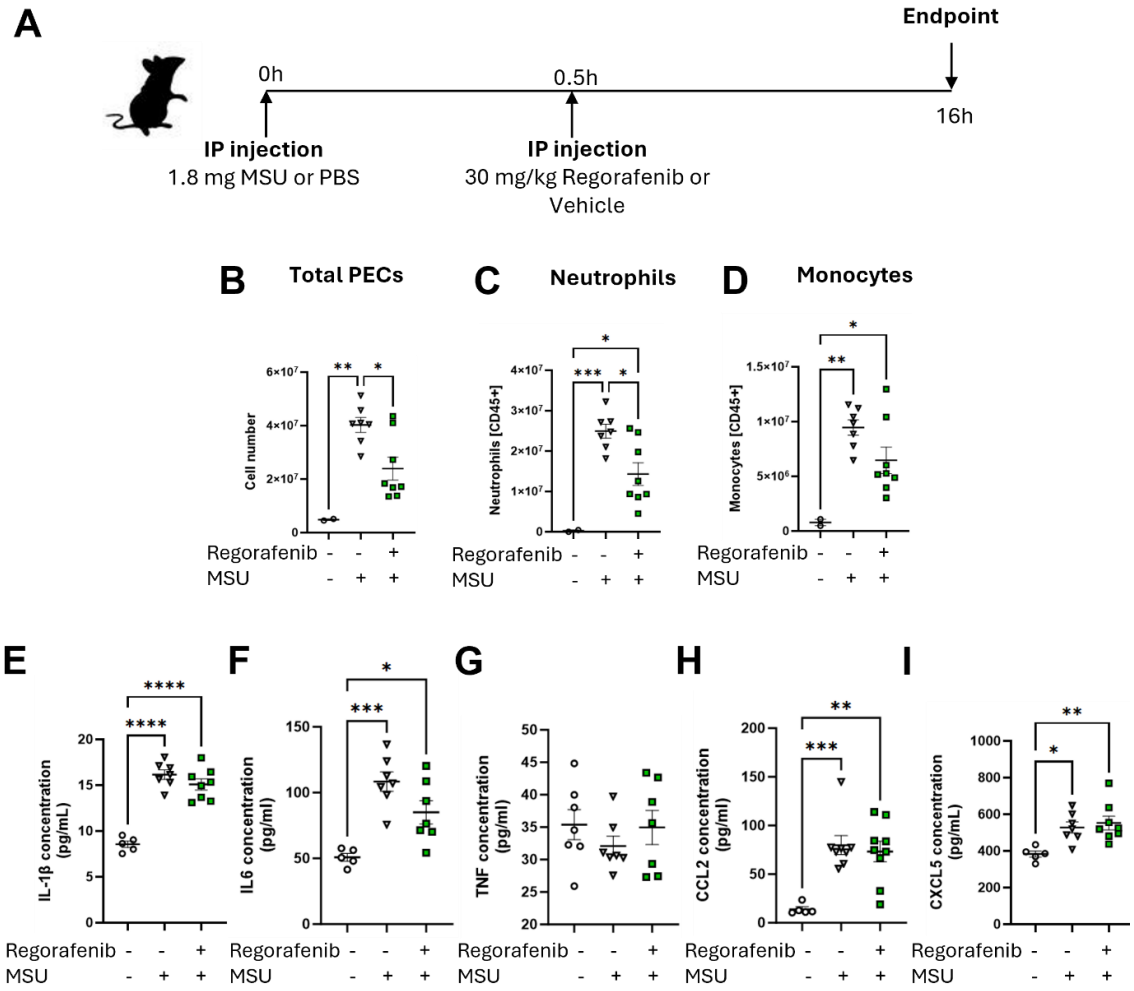


Fig. 4. 16 Therapeutic regorafenib administration reduces inflammation in MSU crystal-induced peritonitis (new vehicle). (A) Experimental outline. Mice were injected i.p. with MSU crystals (1.8 µg). At 0.5 h, mice received 30 mg/kg regorafenib (green squares) or new vehicle (grey triangles) i.p. and peritoneal exudate cells were harvested at 16 h. Total peritoneal exudate cells **(B)**, neutrophils **(C)** and monocytes **(D)** were quantified in the peritoneal lavage fluid. **(E-I)** The levels of pro-inflammatory mediators in the peritoneal lavage fluid were determined by ELISA. Means ±SEM of n=2-8 mice per group. One-way ANOVA with Dunnett's multiple comparisons test.

Therapeutic regorafenib administration in a non-inflammatory vehicle did not significantly reduce pro-inflammatory mediator production in the peritoneum at 16 h, similar to prophylactic oral regorafenib treatment (Fig. 4.9).

Taken together, these results demonstrate that therapeutic intraperitoneal intervention with a single dose of regorafenib in a non-inflammatory vehicle can reduce peritoneal neutrophil recruitment at 16 h post-MSU crystal challenge.

4.4 Discussion

In this chapter, I set out to investigate the effects of regorafenib and sorafenib on NF-κB-dependent NLRP3 inflammasome priming in macrophages. Further, I aimed to explore the anti-inflammatory properties of our drug repurposing candidates in an *in vivo* model of acute inflammation, compare their efficacy to a clinically used anti-inflammatory and determine the molecular mechanism of anti-inflammatory activities *in vivo*.

4.4.1 Regorafenib and sorafenib reduce inflammation in a mouse model of acute inflammation

Here, I report for the first time that both regorafenib and sorafenib are inhibitors of NLRP3 inflammasome activation in macrophages through attenuation of NF-κB-mediated inflammasome priming. Both drugs effectively reduced NF-κB-dependent NLRP3 and IL-1β protein production in BMDMs in response to LPS+ATP stimulation (Fig. 4.2) and inhibited KC and IL-1β secretion by BMDMs upon stimulation with LPS+MSU crystals, with regorafenib exhibiting higher potency (Fig. 4.4). In MSU crystal-induced peritonitis, an *in vivo* model of acute inflammation, regorafenib and sorafenib dose-dependently inhibited peritoneal neutrophil influx and pro-inflammatory mediator production at 4 h (Fig. 4.7). Prophylactic regorafenib administration also reduced neutrophil and monocyte recruitment to the peritoneum at 16 h post-MSU crystal challenge (Fig. 4.9). We validated regorafenib's anti-inflammatory activity in MSU crystal-induced peritonitis by comparing its effects to those of commonly used NSAID indomethacin. We found that both drug repurposing candidate regorafenib as well as established NSAID indomethacin had anti-inflammatory effects in MSU crystal-induced peritonitis at 16 h, which may be mediated by different mechanisms (Fig. 4.11). Regorafenib lacked the NSAID's gastrointestinal

toxicity and general toxicity in mice, which limited the indomethacin dose in our *in vivo* experiments. However, mice administered with regorafenib showed signs of the TKI's well-reported hepatotoxicity (Fig. 4.12). The anti-inflammatory properties of regorafenib were not sex-specific as we observed similar effects in female mice at 4 h (Fig. 4.10). Importantly, we found that therapeutic intervention with regorafenib after MSU crystal injection could similarly reduce peritoneal neutrophil influx at 16 h (Fig. 4.16).

Mechanistically, we found that early in the inflammatory process (4 h), regorafenib and to a lesser extent sorafenib suppressed the peritoneal production of monocyte chemoattractant CCL2 and of IL-1β, which has been shown to induce neutrophil migration to the peritoneum during inflammation [723] (Fig. 4.7). This may explain reduced monocyte and neutrophil numbers at 16 h post MSU crystal stimulation (Fig. 4.9). Further, a reduction in peritoneal IL-1β and ASC (in female mice) at 4 h suggests that TK inhibition by regorafenib reduces NF-κB-dependent NLRP3 inflammasome priming and activation early in the inflammatory process (Fig. 4.7 and 4.10), which is known to drive inflammation in MSU crystal-induced peritonitis. As inflammation progresses, regorafenib reduces NF-κB-driven pro-Caspase1 levels in PECs, indicating that the drug continues to inhibit NLRP3 inflammasome priming (Fig. 4.11).

4.4.2 *In vivo* mechanism of regorafenib in acute inflammation

Here, we investigated the effect of regorafenib on different stages of the acute inflammatory response in MSU crystal-induced peritonitis. Our findings revealed that early in the inflammatory process at 4 h post-MSU crystal challenge, regorafenib inhibited the recruitment of neutrophils to the peritoneum, which is known to be elevated at 4 h, as it is faster than monocyte influx. Further, regorafenib inhibited early peritoneal production of cytokines IL-1β and IL-6, which peak at 4 h in this model. Spalinger et *al.* observed the concentration of IL-1β production to directly correlate with infiltrating neutrophil numbers in MSU crystal-induced peritonitis [426]. Here, we detect a significant

reduction of both IL-1β, a key player in gouty inflammation, and neutrophil recruitment in the peritoneum post-regorafenib treatment. This indicates a reduction of NF-κB-mediated inflammasome priming and activation.

At 4 h, regorafenib inhibited peritoneal CCL2 and IL-1β secretion. This may explain its potent inhibition of peritoneal neutrophil and monocyte recruitment at 16 h post-MSU crystal challenge, which is when inflammatory cell influx peaks in this model. Mechanistically, we found that regorafenib attenuated NF-κB-dependent pro-Caspase1 levels in PECs, indicating sustained inhibition of the NLRP3 inflammasome.

While we did not directly assess the effect of regorafenib on peritoneal macrophages in MSU crystal-induced peritonitis due to the “macrophage disappearance reaction”, we found that it reduced IL-1β and IL-6 production as well as neutrophil recruitment in the peritoneum at 4 h, which are attributed to resident peritoneal macrophages and are lost upon macrophage depletion [210, 669]. However, the anti-inflammatory effects of regorafenib *in vivo* are likely not specific to macrophages. The TKI inhibited CCL2 production and monocyte recruitment, which are mediated by non-haematopoietic cells of the peritoneal membrane [669].

4.4.4 Targeting NF-κB and the NLRP3 inflammasome in acute inflammation

Inflammation mediated by MSU crystals is driven by NLRP3 inflammasome activation [671]. MSU crystals in the joint initiate TLR2/4 signaling and NF-κB activation, resulting in the production of pro-IL-1β, NLRP3, pro-Caspase1 and ASC. Cell stress caused by the crystals triggers NLRP3 inflammasome assembly and IL-1β maturation, which drives gout pathology [724]. Therefore, the NLRP3 inflammasome is a key therapeutic target to treat pain and inflammation in gout flares and its activation can be regulated at different stages. Currently, anti-inflammatory medicines like NSAIDs, glucocorticoids and colchicine are used to treat acute inflammation in gout [725]. However, they can have serious side effects like broad immunosuppression, gastrointestinal, cardiovascular,

nephro- or hepatotoxicity [724]. While many NLRP3 inflammasome inhibitors have been developed and tested in clinical trials, none have received FDA approval yet (Table 4.2) [726, 727].

Table 4. 2 NLRP3 inflammasome inhibitors in clinical trials
Table adapted from [726].

Compound	Targets	Clinical effects	Clinical trial	References
RRx-001	NLRP3, Nrf2 (antioxidant), TAK1 (NF-κB inhibition)	Reduces oral mucosis in chemoradiotherapy patients; investigated for cancer, PD and ALS treatment	Phase 3	[230, 728-730] NCT03699956
Dapansutrile (OLT1177)	ATPase activity of NLRP3	Reduces pain in knee osteoarthritis and improves exercise time and ventricular ejection fraction in systemic heart failure; improves gout pain; investigated for treatment for Schnitzer's syndrome and COVID-19	Phase 2	[230, 231, 731, 732] NCT03595371 NCT04540120
ZYIL1	ASC	Reduces IL-1β and IL-18 levels in healthy volunteers; reduces IL-6, C-reactive protein and WBC counts in CAPS patients; in phase 2 trial for ALS and PD	Phase 2	[733, 734] NCT05981040
HT-6184	NEK7 (NLRP3 inflammasome assembly)	Safe and tolerated, Phase 2 trial for myelodysplastic syndromes	Phase 2	[735, 736]
VTX2735	NLRP3	Safe and tolerated, reduces IL-1β and C-reactive protein; in phase 2 trial for FCAS	Phase 2	[737]
IFM2427/ DFV890	NLRP3	Safe and tolerated; in Phase 2 trials for CAPS and knee osteoarthritis	Phase 2	NCT06031844, NCT04886258, [738]
NT-0796 and NT-0249	NLRP3	Safe and tolerated. NT-0796 is CNS-penetrant, reduces neurodegenerative markers, inhibits neuroinflammation in CSF of Parkinson's	Phase 1/2	[739, 740]

		patients. NT-0249 is peripherally restricted		
VTX3232	NLRP3	CNS-penetrant	Phase 1	[737]
Inzomelid (IZD174)	NLRP3	Safe, tolerated and effective in CAPS	Phase 1	[741]
Somalix (IZD334)	NLRP3	Safe and tolerated	Phase 1	[742]
Selnoflast (RG6418/ IZD334)	NLRP3	In Phase 1 trial for PD and coronary artery disease; safe and well-tolerated in active ulcerative colitis	Phase 1	NCT05924243, GC43343, [743]

Abbreviations: PD- Parkinson's Disease, ALS- Amyotrophic lateral sclerosis, CAPS- Cryopyrin-associated periodic syndrome, WBC- White blood cell count, FCAS- Familial cold autoinflammatory syndrome, CSF- cerebrospinal fluid.

As gout pathology is driven by IL-1β production, IL-1β inhibitors like anakinra or canakinumab are used to treat gout patients who do not respond to or do not tolerate first-line treatments [725]. However, canakinumab was also reported to cause significant adverse effects like serious infections [744].

Even though multiple NLRP3 inflammasome inhibitors are currently under investigation in late-stage clinical trials (Table 4.2), none have received FDA approval so far. This may be due to the molecular mechanisms underlying NLRP3 inflammasome activation in disease still being under investigation. Only recently, crystal structures of the NLRP3 inflammasome have provided insights into its activation, assembly and interaction with inhibitors [290]. Further, only few data are available from specific NLRP3 inflammasome inhibitors in late-stage clinical trials [745]. Given its essential role in a wide range of pathologies, drug repurposing is a promising strategy to identify existing medicines with good safety and efficacy profiles that can inhibit NLRP3 inflammasome activation.

4.4.5 TKIs - a new class of anti-inflammatory medicines?

Acute gout flare-ups are managed with early treatment with NSAIDs, low doses of colchicine and corticosteroids to reduce the severity of inflammation and pain. NSAIDs can have serious side effects like gastrointestinal bleeding as well as allergies, hepatotoxicity, nephrotoxicity or cardiotoxicity and they can affect the central nervous system [746]. In addition, they do not affect disease progression but only relieve

symptoms [747]. Colchicine reduces phagocytosis of MSU crystals by immune cells as well as the production of pro-inflammatory cytokines and chemokines [748]. Treatment often causes severe gastrointestinal side effects and can lead to cardiotoxicity, hepatotoxicity, myotoxicity and bone marrow toxicity and is not suitable for pregnant patients, patients with impaired liver or kidney function as well as patients on ABCB1 or CYP3A4 inhibitors [724, 746, 749].

In cases where both NSAIDs and colchicine are not well tolerated or contraindicated, patients receive oral or intra-articular glucocorticoids or joint aspiration [746]. However, glucocorticoid administration can result in hyperglycemia, hypertension or mood changes, which is why frequent glucocorticoid treatments must be avoided. In addition, patients with co-morbidities such as diabetes or infections are not suitable to receive glucocorticoids [749]. After first-line treatments are exhausted, IL-1β antagonists anakinra or canakinumab can be prescribed. These treatments reduce excess immune cell infiltration but long-term use results in the development of resistance or serious infections due to immune suppression [724, 747]. In addition, anakinra and canakinumab are significantly more expensive than conventional therapies, which may further limit their suitability as long-term treatments for a large population of gout patients [750, 751].

Here, we compared the anti-inflammatory effects of regorafenib to indomethacin, an NSAID commonly used to treat acute gout flares. The clinically relevant dose of indomethacin used to treat acute gout flare-ups in patients corresponds to approx. 23 mg/kg in mice [714, 752]. However, we were not able to directly compare the effects of 30 mg/kg regorafenib administration to those of a corresponding dose of indomethacin, due to the NSAID's low oral LD_{50} in mice [753]. Indomethacin plasma concentrations peak in the first 5 hours post-administration but remain high in rodents up until 35 h, with a serum half-life of 10 h in rats and 6-10 h in mice [754-757]. Animals repeatedly treated with lower doses (5 mg/kg, 7 mg/kg or 10 mg/kg) were observed to die from

complications within a few days [715-717]. Given our dosing regimen required three oral doses within a 40-hour period, we decided on a dose of 5 mg/kg indomethacin to prevent serious adverse effects in mice.

We found that both regorafenib and indomethacin had anti-inflammatory effects in MSU crystal-induced peritonitis, as they both suppressed peritoneal neutrophil and monocyte recruitment at 16 h. While regorafenib did not affect pro-inflammatory mediator levels in the peritoneum at 16 h, indomethacin significantly reduced peritoneal IL-6 production (Fig. 4.11F). This observation is in line with reports in the literature, highlighting indomethacin's ability to suppress IL-6 production in inflammation [758, 759]. Indomethacin has previously been shown to reduce NF-κB phosphorylation [760]. Here, we report that indomethacin significantly inhibited p65 phosphorylation in PECs 16 h after MSU crystal challenge, possibly mediating the drug's anti-inflammatory effects. However, indomethacin significantly increased pro-inflammatory NF-κB-dependent pro-Caspase1 levels in PECs while regorafenib potently suppressed pro-Caspase1 production. In addition, indomethacin also enhanced the production of pro-inflammatory chemokine CCL2 in the peritoneum.

Regorafenib significantly increased serum bilirubin and ALT levels, while AST was mildly increased and LDH levels remained unchanged. However, ALT and AST levels were still within the physiological range. Therefore, regorafenib seems to impair liver function and induce mild liver damage, which is in line with its reported hepatotoxicity in patients. Medications or toxins are known causes for predominant ALT elevation over AST elevation [761]. As AST is expressed across many tissues, including the liver, heart, kidney, lungs or muscles, ALT, which is predominantly found in the liver, is considered a more specific and sensitive marker for liver function. Therefore, it is common to find higher ALT than AST levels in liver disease [761]. Serum bilirubin is frequently used as a marker to diagnose liver disease. However, it is not a sensitive or specific indicator of

liver function. Therefore, it needs to be assessed in combination with other markers. In combination with pathological ALT elevation, pathologically elevated total bilirubin levels can indicate impaired liver function in drug-induced liver injury [762, 763]. In contrast to regorafenib, indomethacin did not affect liver function, but increased blood levels in the stool, as indicated by elevated stool albumin levels, and changed the structure and color of the small intestine. Indomethacin's gastrointestinal toxicity is well documented [714] and the drug is frequently used to induce gastric ulcers or intestinal bleeding in animal studies [720, 721, 764-766].

Considering the anti-inflammatory effect of tyrosine kinase inhibition mediated by inhibition of NF-κB-dependent NLRP3 inflammasome activation, TKIs may present a promising alternative to classic NSAIDs. Indeed, tyrosine kinases are known to play an important role in the regulation of NLRP3 inflammasome activation [767]. For instance, tyrosine kinase inhibitor AG126 targeting JAK/STAT and serine/threonine kinases ERK1/2 suppressed LPS+ATP-induced Caspase1 activation and consequent IL-β production in human monocytes [768, 769]. Similarly, BTK inhibition with ibrutinib reduced NLRP3 inflammasome activation in neutrophils and macrophages. BTK interacts directly with NLRP3 and ASC and promotes NLRP3 inflammasome activation through phosphorylation of ASC [373, 375]. Tyrosine kinase Syk has also been linked to NLRP3 inflammasome activation, possibly by phosphorylating ASC and thus modulating ASC speck formation [770-772]. Therefore, TKIs may present a new class of anti-inflammatory drugs that mediate their effects in part by inhibiting the activation of the NLRP3 inflammasome, which is a driver of inflammatory disease pathology.

4.4.6 Challenges of TKIs as therapeutics for inflammatory diseases

Kinases are amongst the most common targets for the development of new therapies, with 1/3 of drug discovery efforts targeted at the development of novel kinase inhibitors [773]. As of January 2024, a total of 80 kinase inhibitors had received FDA approval. Out

of those, 63 (78%) target receptor or non-receptor tyrosine kinases [774]. However, many kinases have catalytic sites with similar structures and possess a certain degree of structural or sequence homology. Therefore, many tyrosine kinase inhibitors target multiple kinase inhibitors target multiple kinases. Based on their binding mode, six types of tyrosine kinase inhibitors can be distinguished [773, 775, 776]:

- Type I: bind to or close to the adenine pocket of active kinases
- Type I½: bind to inactive kinases in DFG-in conformation
- Type IIA: bind to an inactive DFG-out protein kinase (in the front cleft, the back cleft, and near the gatekeeper residue)
- Type IIB: bind to an inactive DFG-out protein kinase (in the front cleft and gate area but not to back cleft)
- Type III: bind to allosteric site in cleft between N- and C-terminal lobes of ATP binding pocket
- Type IV: bind to allosteric site outside of cleft
- Type V: bind to two regions of the kinase
- Type VI: bind covalently to the kinase

Sorafenib and regorafenib fall into the type IIA category [775]. Type II kinase inhibitors are considered more selective than type I inhibitors, as they bind to regions adjacent to the ATP binding site which are less conserved amongst other kinases [777] Therefore, type II kinase inhibitors are also referred to as “allosteric inhibitors” [778]. Co-crystal structures of sorafenib in complex with its targets p38α, VEGFR or b-Raf showed that the TKI binds to DGF-out forms of its targets and promotes their inactive conformation (Fig.4.17) [778-780]. In p38α, sorafenib binding triggered a conformational change in the activation loop and the DFG motif (named after the amino acid sequence Asp-Phe-Gly) of the target, which prevented ATP binding and disrupted the catalytic group, resulting in kinase inactivation [778]. Namboodiri et *al.* compared the p38 binding mode of sorafenib

to imatinib, which, in contrast to sorafenib, does not inhibit p38 activation. They found that sorafenib had a binding rate of 9.5×10^4 M^{-1} s^{-1} and an off rate of 0.018 s^{-1} with a binding constant (K_D) of 0.18 µM. In comparison, imatinib had an on rate of 1.1×10^4 M^{-1} s^{-1} and an off rate of 0.38 s^{-1} with a K_D of 34 µM [778]. This revealed that sorafenib's binding to the target kinase is mediated by its slower dissociation and consequently the formation of a more stable complex. In addition, the study showed an inverse correlation between the solvent-accessible surface area (SASA) of a TKI bound to its target and its activity. Sorafenib had a smaller SASA (44.8 Å) than imatinib (89.6 Å), indicating that a smaller SASA and thus larger surface area of the compound interacting with the target leads to increased binding [778]. This can be taken into account when potentially re-engineering TKIs to improve their anti-inflammatory effects and side effect profiles.

Mao et *al.* investigated the binding mode of sorafenib to tyrosine kinases Ret and VEGFR2 as well as serine/threonine kinase c-Raf in a cell-free system [781]. They demonstrated that sorafenib inhibits VEGFR2 in an ATP-competitive manner, while Raf was inhibited in a non-ATP competitive way. Ret inhibition was mediated by a mix between the ATP-competitive and non-ATP-competitive modes [781]. Many kinases share structural homology of their kinase domain. ATP-competitive inhibition of VEGFR2 may therefore explain the lack of selectivity of sorafenib amongst other tyrosine kinases.

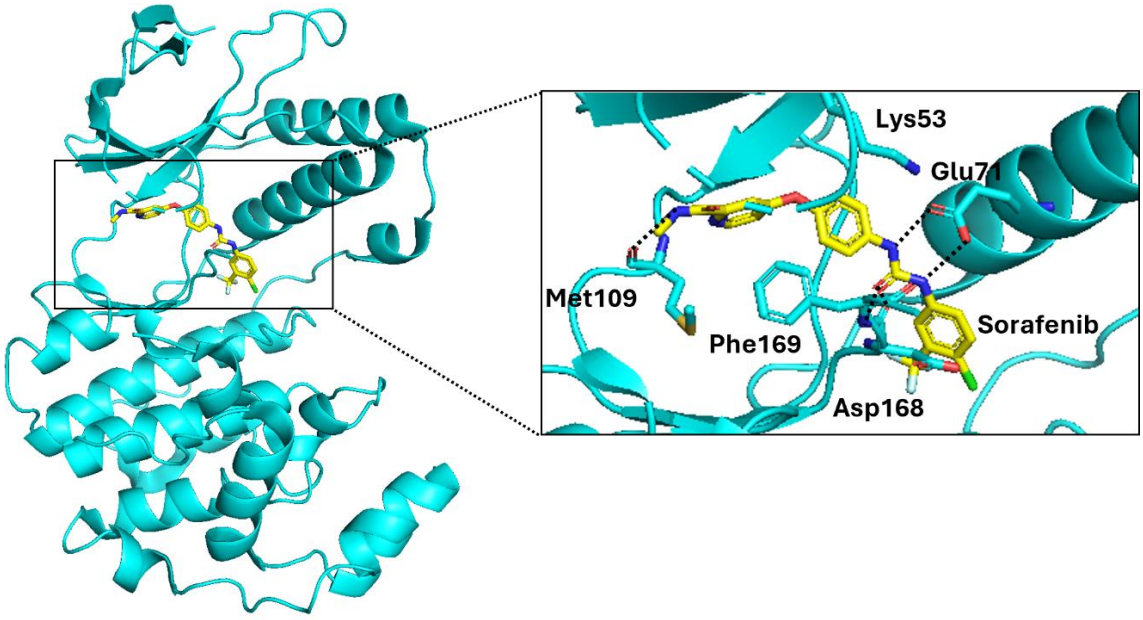


Fig. 4. 17 Sorafenib in complex with its target p38α. Interaction of sorafenib (yellow, stick representation) with p38α kinase (cyan, cartoon representation). The close-up shows hydrogen bonds formed between sorafenib and amino acids of p38α. Phe169 and Asp168 are part of the DFG loop. Adapted from [778] and generated with PyMOL. PDB: 3HEG.

Kinase inhibitors can have side effects depending on the affinity to other kinases and their role in cell signaling pathways [773]. These off-target effects may have beneficial outcomes when a disease-relevant pathway is inhibited at different stages. In addition, the inhibition of multiple targets involved in disease pathology may enhance the efficacy of the kinase inhibitor. This may in part explain the more pronounced anti-inflammatory effects of regorafenib compared to sorafenib, since regorafenib is more promiscuous [621]. However, low selectivity of tyrosine kinase inhibitors can be associated with significant adverse effects. 24 % of off-target effects of tyrosine kinase inhibitors were found to be due to the inhibition of serine/threonine kinases [773, 782]. Common adverse events of tyrosine kinase inhibitor treatment include cardiotoxicity, hepatotoxicity and haematotoxicity, which are the most prevalent reasons for discontinuation of treatment and failure of inhibitor development programs [773].

VEGF is known to promote hypertension, which is why VEGFR inhibitors are often associated with cardiotoxic events like left ventricular dysfunction and congestive heart

failure [773, 783]. In addition, VEGF is involved in haematopoiesis [784]. Regorafenib and sorafenib also target FLT3, which is important for haematopoiesis [785]. Many reports have highlighted the haematotoxicity of sorafenib and regorafenib, which can induce anemia, neutropenia and lymphopenia in cancer patients [786, 787]. The TKIs are metabolized via liver cytochrome p450 enzyme 3A4 and are hepatotoxic [788, 789]. Hepatotoxicity may be caused by mitochondrial toxicity, resulting in oxidative stress and inhibition of glycolysis, as was shown to be the case for other Type II tyrosine kinase inhibitors [790, 791]. Sorafenib can cause low rates of hepatotoxicity as indicated by elevated serum aminotransferase levels, although severe cases have been reported [788, 792]. However, regorafenib frequently causes serum aminotransferase and bilirubin elevation and can cause severe and even fatal liver damage [789, 793].

As many of these adverse events are mediated by off-target effects of tyrosine kinase inhibitors, studies have set out to quantify and compare the selectivity of FDA-approved TKIs. Karaman et *al.* established the selectivity score (S) as a quantitative measurement of selectivity. They divided the number of kinases that bind to a TKI with a dissociation constant below 3 µM (S(3)) or 100 nM (S(100)) by the total number of kinases included in the assay. Amongst the tested TKIs, sunitinib was the least selective with S(3)= 0.57 and S(100)= 0.18. Sorafenib was more selective and its S(100) was 0.048, similar to that of most other tested TKIs. They also compared the affinity of sorafenib to its main target VEGFR2 with its affinity to other kinases. Unlike most other TKIs in the assay, sorafenib bound approx. 10 % of kinases with an affinity in the 10-fold range of that of VEGFR2 (Fig. 4.18A) [794]. Most off-target kinases were closely related to VEGFR, which supports the hypothesis that its ATP-competitive inhibition of VEGFR2 may cause similar effects in closely related kinases that have a similar catalytic site structure. However, it is worth noting that sorafenib was specifically developed as a multi-tyrosine kinase inhibitor to target Raf and VEGFR in tumors [795].

Another score to quantify kinase inhibitor selectivity is the entropy score [796]. In contrast to the selectivity score S, it does not depend on which reference kinases are used in the assay. Instead, it depends on IC_{50} data and is therefore considered a more robust measurement of selectivity. A high entropy score indicates lower specificity of a kinase inhibitor. Sorafenib was shown to have an entropy score of 2.15, compared to more specific kinase inhibitors like gefitinib (Fig. 4.18B), which had an entropy score of 0.44 [796].

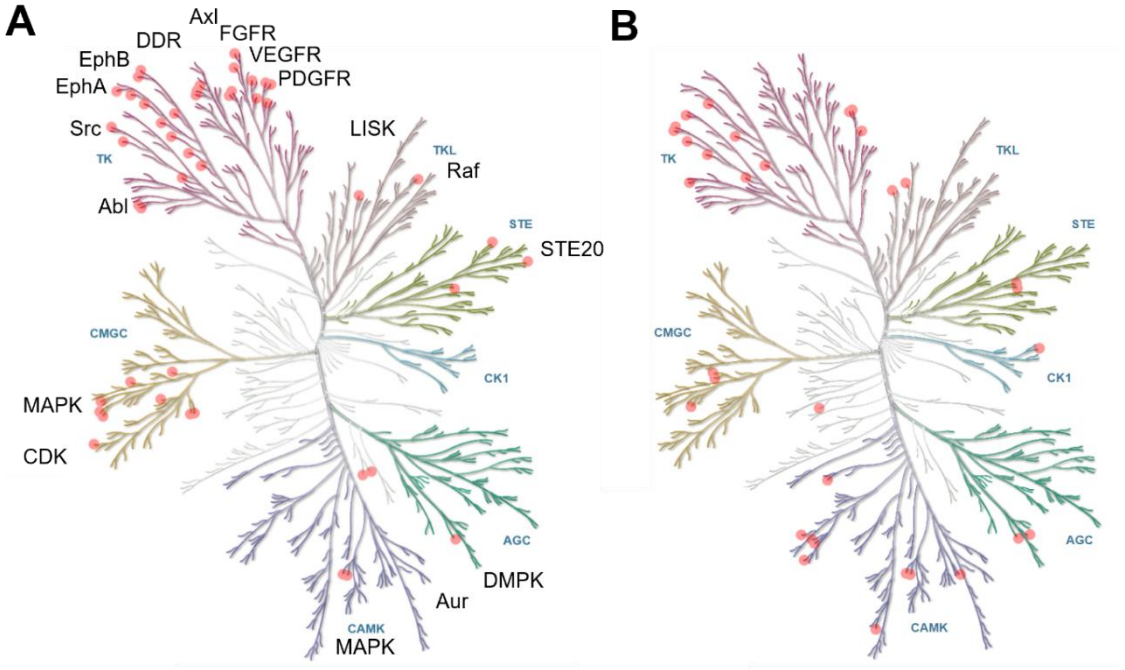


Fig. 4. 18 Inhibition profiles of sorafenib and gefitinib. Kinases inhibited by **(A)** sorafenib and **(B)** gefitinib are shown as red circles. Kinase families targeted by sorafenib are indicated on the kinome tree. Kinome trees were created with KinMap and include data from Karaman et al. [794].

The adverse effects of sorafenib and regorafenib (including the hepatotoxicity we observed in mice, which is also a well-known complication in human patients) are likely linked to the TKI's low target selectivity. While this may be tolerable for the treatment of life-threatening cancers, this may not be justifiable for the treatment of anti-inflammatory diseases.

The intensity of gout flare-ups peaks in the first 12-24 h. Early intervention and modulation of NLRP3 inflammasome activity and IL-1β production is an effective

treatment strategy [724, 797]. Considering the side effects of anti-cancer TKIs such as regorafenib, we propose their use in the early phases of gout flares to dampen acute inflammatory processes and alleviate symptoms. However, regorafenib may have to be re-engineered or delivered in a targeted manner to inflammatory cells to prevent its well-documented hepatotoxic effects. Alternatively, our drug repurposing strategy could be employed to screen and identify other anti-inflammatory TKIs with improved side effect profiles.

4.4.7 Limitations of the studies reported in this chapter

In this chapter, we investigated the effect of oral prophylactic and intraperitoneal therapeutic regorafenib administration on mice with MSU crystal-induced peritonitis. Therapeutic intervention with a single oral dose of regorafenib had minimal anti-inflammatory effects by mildly decreasing peritoneal CCL2 production. However, it would be interesting to investigate the effect of intervention with oral regorafenib administration at 0.5 h and 6 h after MSU crystal challenge, given the rapid metabolization of regorafenib. Further, therapeutic oral or i.p. regorafenib administration occurred at 0.5 h after initiation of inflammation. Future experiments could explore whether the time between MSU crystal challenge and drug intervention can be extended and whether this would affect the anti-inflammatory effects observed in regorafenib-treated mice at 16 h.

In Chapter 3 and Fig. 4.2-4.4 in Chapter 4, we demonstrated that regorafenib has potent anti-inflammatory effects in macrophages by suppressing NF-κB signaling as well as NLRP3 inflammasome priming and activation. Due to the “macrophage disappearance reaction”, we were not able to investigate the macrophage-specific effect of regorafenib on macrophages in MSU crystal-induced peritonitis directly. We observed inhibition of pro-Caspase1 production in PECs upon regorafenib administration, however, the cells in the peritoneal lavage mostly consist of neutrophils and monocytes at 4 h and 16 h post MSU crystal challenge and do not contain many macrophages. However, we detected a

regorafenib-mediated decrease in neutrophil recruitment and IL-6 production in MSU crystal-challenged mice, which have been attributed to resident peritoneal macrophages. In addition, we were not able to investigate p65 phosphorylation in PECs at 4 h due to the smaller number of PECs in the peritoneum at this early time point. Given regorafenib inhibits the production of NF-κB-dependent pro-inflammatory mediators in the peritoneum at 4 h, its effect on p65 phosphorylation may be more pronounced at 4 h than at 16 h.

An *in vivo* macrophage depletion model could be employed to elucidate the effects of regorafenib on resident peritoneal macrophages, as they were shown to drive the initial inflammatory response to MSU crystals [210]. Clodronate liposome administration is a common strategy for depletion of resident peritoneal macrophages. However, Culeman et *al.* recently showed that the anti-inflammatory effects of clodronate liposomes are mediated by neutrophil and not macrophage depletion [798]. Instead, genetic macrophage depletion models like CSF-1R-KO mice or CD11b-DTR mice could be used. However, while CSF-1R-KO mice have significantly decreased macrophage populations, their lymphocyte numbers are also decreased while granulocyte numbers were found to increase by 100-135% [799]. CD11b-DTR mice allow for controlled depletion of $F4/80^+$ macrophage populations but this is accompanied by increased neutrophil levels [799]. Due to the presence of macrophage receptors on other cell types, truly specific depletion of macrophages is difficult *in vivo*.

Alternatively, macrophage-specific effects of regorafenib could be studied by targeting the drug to specific macrophage populations using nanobodies. Nanoparticles can be engineered to deliver drugs to specific macrophage populations, e.g. by targeting phagocytosis-related macrophage receptors [800].

Zhao et *al.* developed liposomes coated with lactoferrin, which targets low-density lipoprotein receptor protein 1 (LRP1) on macrophages in the colon. They used these

liposomes to deliver the compound patchoulol to inflammatory macrophages in the colon to treat DSS-induced colitis in mice. Lactoferrin-liposomes were confirmed to preferentially target M1-like macrophages and to accumulate in the abdominal region of colitis mice. Patchoulol delivered in lactoferrin-liposomes reduced ROS and inflammatory cytokine production, NF-κB signaling and NLRP3 inflammasome activation [801].

Similarly, existing anti-inflammatory drugs can be re-engineered to target macrophages. Dexamethasone is a corticosteroid with well-described anti-inflammatory effects. However, its systemic effects can cause adverse events such as immune suppression, diabetes, osteoporosis or gastrointestinal symptoms, which limits its use for long-term treatment [802]. Ma et *al.* developed nanocarrier-dexamethasone (ND) by conjugating dexamethasone to a dextran moiety. Dextran binds specifically to macrophages expressing high amounts of mannose receptor and class A scavenger receptor. The authors confirmed that 90 % of ND was targeted to $CD11b^+$ cells in the adipose tissue upon i.p. delivery and could reduce adipose tissue inflammation in a mouse model of obesity [803]. Direct comparison to free dexamethasone revealed that ND but not free dexamethasone reduced inflammation and metabolic dysfunction and led to weight loss and lipolysis in the adipose tissue of obese mice [804].

A similar strategy was employed by Han et *al.,* who developed dextran sulfate-cisaconitic anhydride-dexamethasone micelles to deliver dexamethasone to activated macrophages in the joint of rats with adjuvant-induced arthritis (AIA). They confirmed that the micelles containing dexamethasone accumulated in the inflamed joints and found that targeted dexamethasone delivery decreased disease severity and the production of pro-inflammatory cytokines in the joint tissue more effectively than free dexamethasone. In addition, nanoparticle-mediated delivery of dexamethasone was well tolerated by rats and did not affect body weight, blood glucose levels or liver and kidney

function [805]. Therefore, regorafenib could be re-engineered or delivered in nanoparticles to specifically target macrophages to confirm its anti-inflammatory effect on macrophages *in vivo.*

Intra-articular treatment of mice with MSU crystal-induced acute arthritis with PLGA nanoparticles containing TKI imatinib significantly reduced disease severity and allowed for the use of lower therapeutic doses by prolonging the drug's half-life [687]. This demonstrates that the anti-inflammatory activity of TKIs in crystal-induced inflammation persists and is even improved by delivery in nanoparticles. This strategy could help reduce rapid metabolization and unwanted side effects of regorafenib.

In Chapter 4, I explored the anti-inflammatory effects of regorafenib administration on mice with MSU crystal-induced peritonitis at 4 h and 16 h post-inflammation initiation. These time points were chosen considering that peritoneal neutrophil and monocyte influx as well as in acute MSU crystal-induced inflammation peak at 16 h and pro-inflammatory mediator production in the peritoneum peaks at 4 h [210]. In this study, we aimed to investigate the effects of regorafenib on processes driving acute inflammation, as it targets NF-κB and NLRP3 inflammasome activation, which drive the initiation of the inflammatory response. In MSU crystal-induced peritonitis, inflammation resolves 48-72 h post MSU crystal challenge [210]. Therefore, future studies could investigate the effect of regorafenib on inflammation resolution at 24 h, 48 h or 72 h post-MSU crystal injection. After clearance of MSU crystals and during the resolution phase of inflammation, neutrophils undergo apoptosis and macrophages switch to a pro-resolution phenotype and produce pro-resolving mediators to limit inflammation and promote tissue repair [196, 806]. By investigating later time points in the acute inflammatory process, we could determine the effects of regorafenib and TK inhibition on crucial events required for inflammation resolution, such as macrophage re-programming and the secretion of pro-resolving factors.

While both the peritoneal cavity and the synovial cavity are sterile sites, their architecture and macrophage populations differ significantly. As described in Chapter 1.3.4, the joint contains Trem2$^+$/CX$_3$CR1$^+$ macrophages in the lining layer and perivascular Lyve1$^+$/Relmα$^+$ macrophages in the interstitial synovium. Both macrophage populations are maintained by embryonic MHCII$^+$/CSF-1R$^+$ interstitial macrophages. While they do have immunoregulatory functions, Trem2$^+$/CX$_3$CR1$^+$ macrophages are thought to initiate inflammation in gout upon NLRP3 inflammasome activation and recruited monocytes and monocyte-derived macrophages contribute to pro-inflammatory mediator production [197]. In the peritoneum, resident macrophages can be divided into long-lived large peritoneal macrophages (LPMs) and small peritoneal macrophages (SPMs), which both have immune-regulatory and defense functions. While LPMs are of embryonic origin, SPMs are gradually replaced by shorter-lived monocyte-derived macrophages [807]. Similar to the joint, MSU crystal challenge results in NLRP3 inflammasome activation in resident peritoneal macrophages, which initiate inflammation by secreting pro-inflammatory mediators. However, TNFα production and monocyte recruitment are mediated by peritoneal mesothelial cells [210, 668, 669]. While resident macrophages in the joint persist during gouty inflammation, resident peritoneal macrophages disappear within the first 2 hours of inflammation [210, 602, 677, 678]. In addition, the timeline of the inflammatory process differs between the peritoneum and the joint. MSU crystal-induced inflammatory mediator production peaks at 4 h while inflammatory cell influx peaks at 16 h and inflammation self-resolves 48-72 h post MSU crystal challenge [210]. In rat gouty joints, inflammatory *inos* expression and thus the number of M1-like macrophages were found to peak at 24 h and resolution, characterized by a peak in alternatively activated Arg1$^+$ macrophages, peaked at 48 h. M1-like macrophage numbers only returned to baseline between 168 and 240 h post-MSU crystal injection [196].

Here, we decided to study the effects of tyrosine kinase inhibition by regorafenib and sorafenib in MSU crystal-induced peritonitis, a simple model of acute gouty inflammation. However, important differences in peritoneal and joint macrophage populations and inflammatory processes limit the translatability of our findings. Therefore, future studies could explore the role of tyrosine kinases and the effect of their inhibition by drug repurposing candidates in intra-articular MSU crystal-induced gouty joint inflammation models, which would additionally allow the assessment of important clinical symptoms such as joint swelling, pain and joint damage.

4.4.8 Summary

In this chapter, I have shown that regorafenib and sorafenib suppress NF-κB-mediated NLRP3 inflammasome priming in macrophages *in vitro*. I further demonstrated the anti-inflammatory effects of both prophylactic and therapeutic regorafenib administrations in MSU crystal-induced peritonitis, an *in vivo* model of acute inflammation. The anti-inflammatory effect can be detected at both early and later stages in the inflammatory process and translates into female mice. Mechanistically, I have shown that TK inhibition suppresses NLRP3 inflammasome activation *in vivo*, mediating the anti-inflammatory effects of regorafenib. Importantly, regorafenib and NSAID indomethacin both have anti-inflammatory effects in MSU crystal-induced peritonitis. While regorafenib is lacking the NSAID's gastrointestinal toxicity, it induces hepatotoxicity. Our findings in this chapter demonstrate that our macrophage-based drug repurposing approach can identify FDA-approved medicines with anti-inflammatory properties *in vitro* and *in vivo,* and that targeting TKs may present a promising approach to treat inflammation.

Chapter 5: Regorafenib modulates leukocyte mobilization, transendothelial migration and chemotaxis

5.1 Introduction

5.1.1 Assays to measure immune cell adhesion, transendothelial migration and chemotaxis

Upon inflammatory insult, the recruitment of neutrophils and monocytes is essential to effectively control and eliminate the threat, but recruited leukocytes can also exacerbate inflammation, resulting in the development of pathological inflammation. Over the years, various assays have been developed to study leukocyte adhesion, endothelial transmigration and chemotaxis *in vitro*. In 1953/54, Henry Harris defined the criteria of a suitable assay to study leukocyte migration:

1. Any cell movement must be due to directional chemotaxis, which must be clearly distinguishable from random chemokinetic cell movement.
2. If the effect of soluble compounds on chemotaxis is measured, these compounds must be sufficiently present in the experimental chamber.
3. Concentration gradients of chemokinetic agents must be controllable and the presence of convection currents disturbing the gradient must be eliminated.
4. The assay must include a homogenous matrix that allows leukocytes to move towards or away from a chemokinetic agent.
5. The assay must allow observation of cell migration of a sufficient cell number to avoid sampling errors [64, 65, 808, 809].

As Rumianek et *al.* pointed out in their 2020 review, established *in vitro* chemotaxis assays do not fulfill all of Harris' criteria. Nonetheless, many common chemotaxis assays can reliably detect inhibitors or enhancers of leukocyte chemotaxis but may fall short in distinguishing between different forms of chemotaxis [64]. In addition, the potential of an assay to be used for high- or medium-throughput compound screening needs to be considered [65].

5.1.1.1 Chemotaxis assays

Trans-well chemotaxis assays

The Boyden chamber, which allows measurement of chemotaxis towards soluble chemoattractants, was described by Boyden in 1962 [810]. The Boyden chamber consists of a bottom well filled with medium containing the chemotactic agent, and a top well containing cells, which is inserted into the bottom well. The chemoattractant gradient is established through diffusion and cells may migrate towards the gradient through a porous membrane, which separates the top from the bottom well (Fig. 5.1A) [64]. However, chemokine gradients are unstable and cannot be tightly controlled. In addition, the Boyden chamber chemotaxis assay requires high numbers of cells and chemoattractant volumes [64, 811, 812].

Based on the Boyden chamber, Falk et *al.* developed a 48-well chemotaxis chamber to reduce cell numbers and chemoattractant volumes [813]. The set-up includes plates that are covered with a porous membrane to replace individual inserts found in the Boyden chamber assay (Fig. 5.1B) [64, 813]. However, these assays are limited to single time point analysis.

Following the same principle, the xCELLigence assay measures real-time cell chemotaxis based on electrical impedance that correlates to cell migration from the top well to the bottom well through a porous membrane with gold electrodes on the bottom (Fig. 5.1C) [433]. Using this assay, Iqbal et *al.* compared the chemotactic profiles of different mouse macrophage populations [433]. To count the total number of migrated cells and investigate the phenotype of migrating cells at the same time, trans-well migration assays can be combined with flow cytometry [814]. However, trans-well migration assays do not allow for live tracking of single cell movement and the fixed membrane pore size limits the investigation of mixed cell population migration [64].

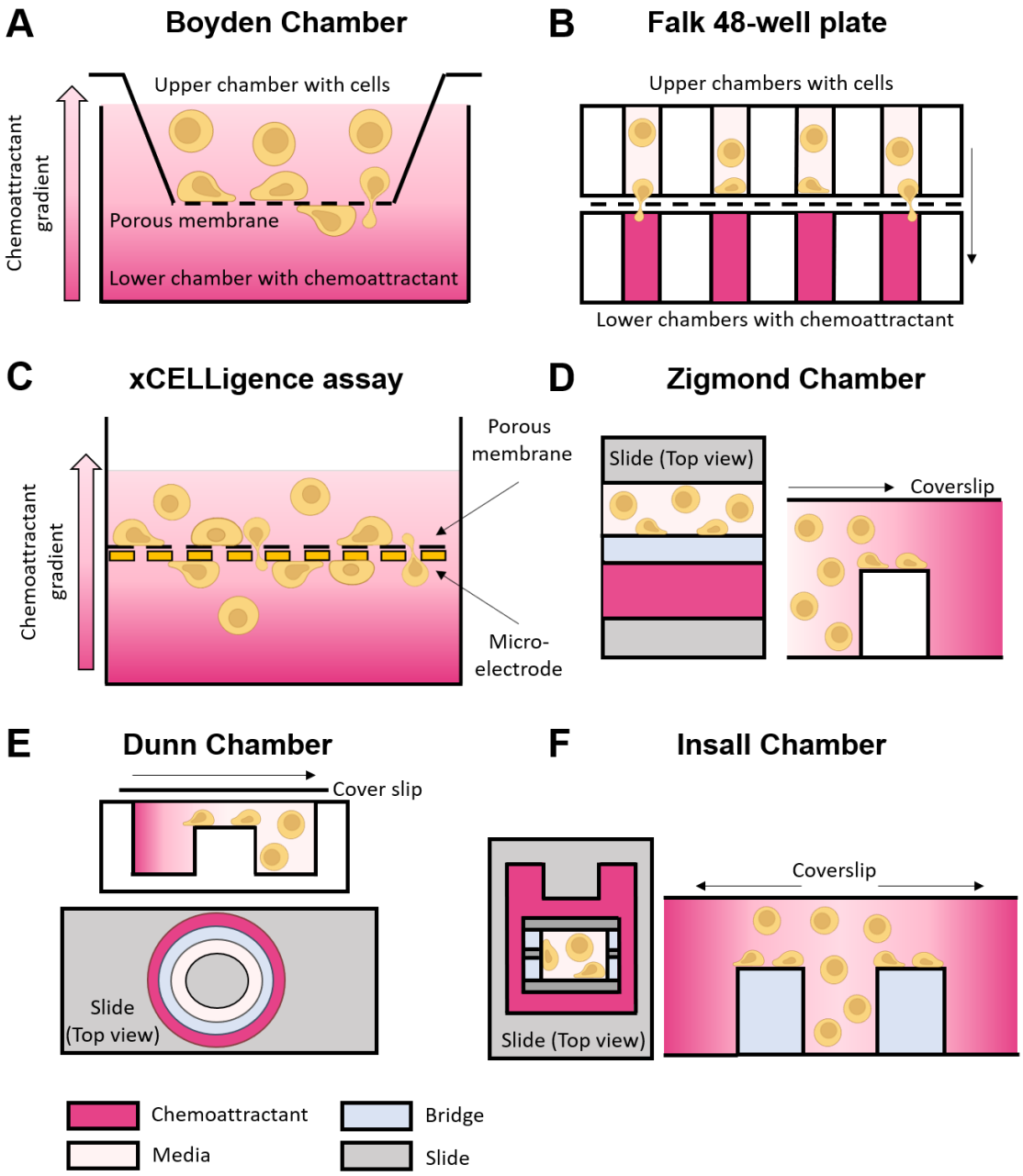


Fig. 5. 1 Chemotaxis assays 1. Setup of **(A)** the Boyden Chamber, **(B)** the Falk 48-well chemotaxis plate, **(C)** the xCELLigence real-time chemotaxis assay, **(D)** the Zigmond Chamber, **(E)** the Dunn Chamber and **(F)** the Insall Chamber. Black arrows indicate the direction of leukocyte (yellow) migration. Figure generated with BioRender and Powerpoint and illustrations adapted from [64, 815, 816].

Chemotaxis tracking chambers

Zigmond developed an assay in which cell migration towards a controlled chemokine gradient can be tracked using phase microscopy [817]. The Zigmond chamber contains two channels on a slide, which are separated by a barrier. Adding media containing a soluble chemoattractant to one channel establishes a concentration gradient across the

barrier. A cover slip is then added which contains cells and allows them to migrate once exposed to the chemokinetic agent (Fig. 5.1D) [64, 817]. Limitations of this assay are the short stability of the gradients, which evaporate quickly, as well as convection gradients that occur [811]. To overcome this problem and to improve resolution and precision, Zicha et *al.* developed the Dunn chamber, which can be described as the first microfluidic chemotaxis device [811, 818]. Here, the chambers are replaced by concentric rings on a slide and are sealed to prevent evaporation, but this does not allow for modification of the gradient during the experiment (Fig. 5.1E) [811].

The Insall chamber is also based on the Zigmond chamber but consists of a square central medium-containing well, which is separated by bridges of different widths from a surrounding well containing the chemoattractant. The assay uses thin coverslips and high numerical aperture objectives to improve cell visualization (Fig. 5.1F). In addition, stable chemokine gradients were reported for 24 h or more, and different gradients can be measured during a single experiment [816]. However, Insall chamber assembly results in cell crushing, which may interfere with chemotaxis towards defined chemotactic gradients [811, 816] In addition, assays using the Dunn and Insall chambers are low-throughput compared to trans-well assays [64].

Based on early cell tracking systems, different microfluidic systems have been developed to monitor and manipulate leukocyte chemotaxis. However, most systems include solid surrounding walls, which make it difficult to isolate specific cell populations for further analysis. Therefore, Deroy et *al*. developed a microfluidic device with fluid walls, which provides easy access to cells of interest. A chemoattractant gradient is established by a pump creating laminar streams and chemotaxis can be recorded using real-time imaging (Fig. 5.2A) [819].

Migration under agarose chemotaxis assay

To study the migration of cell populations or single cells, the “under agarose” migration assay can be employed. The assay set-up includes an agarose gel located on top of a glass slide and a row of three wells is cut out of the gel. Cells are seeded into the middle well and the other wells are filled with a chemoattractant solution or medium. Consequently, diffusion generates a chemokine gradient, and as cells cannot migrate through the agarose gel, they migrate on the slide underneath the gel towards the chemoattractant (Fig. 5.2B). At an appropriate time point, the gel is removed and cells can be fixed and imaged on the slide to determine the distance they have migrated compared to cells exposed to a control buffer [812]. Due to single time-point analysis, live cell tracking or high-throughput screening are difficult in this assay.

3D chemotaxis assays

Ibidi µ-Slides are commercially available and can be used for 2D and 3D real-time chemotaxis assays. Three independent experiments can be carried out in parallel using the same plate and cell migration, morphology and interactions can be visualized using life, high-resolution microscopy. Controlled chemokine gradients can be established that are stable for over 48 hours [820]. Chambers on the slide consist of two triangular reservoirs that are joined by an observation area (Fig. 5.2C). Cells are seeded into a channel before the chamber is filled with culture medium and chemoattractant, quickly establishing a gradient that allows measurement of early migration responses. Cells can be seeded into a matrix to investigate 3D cell chemotaxis [64, 820]. However, the assay depends on passive diffusion to establish the chemoattractant gradient and the slides and the required equipment are costly.

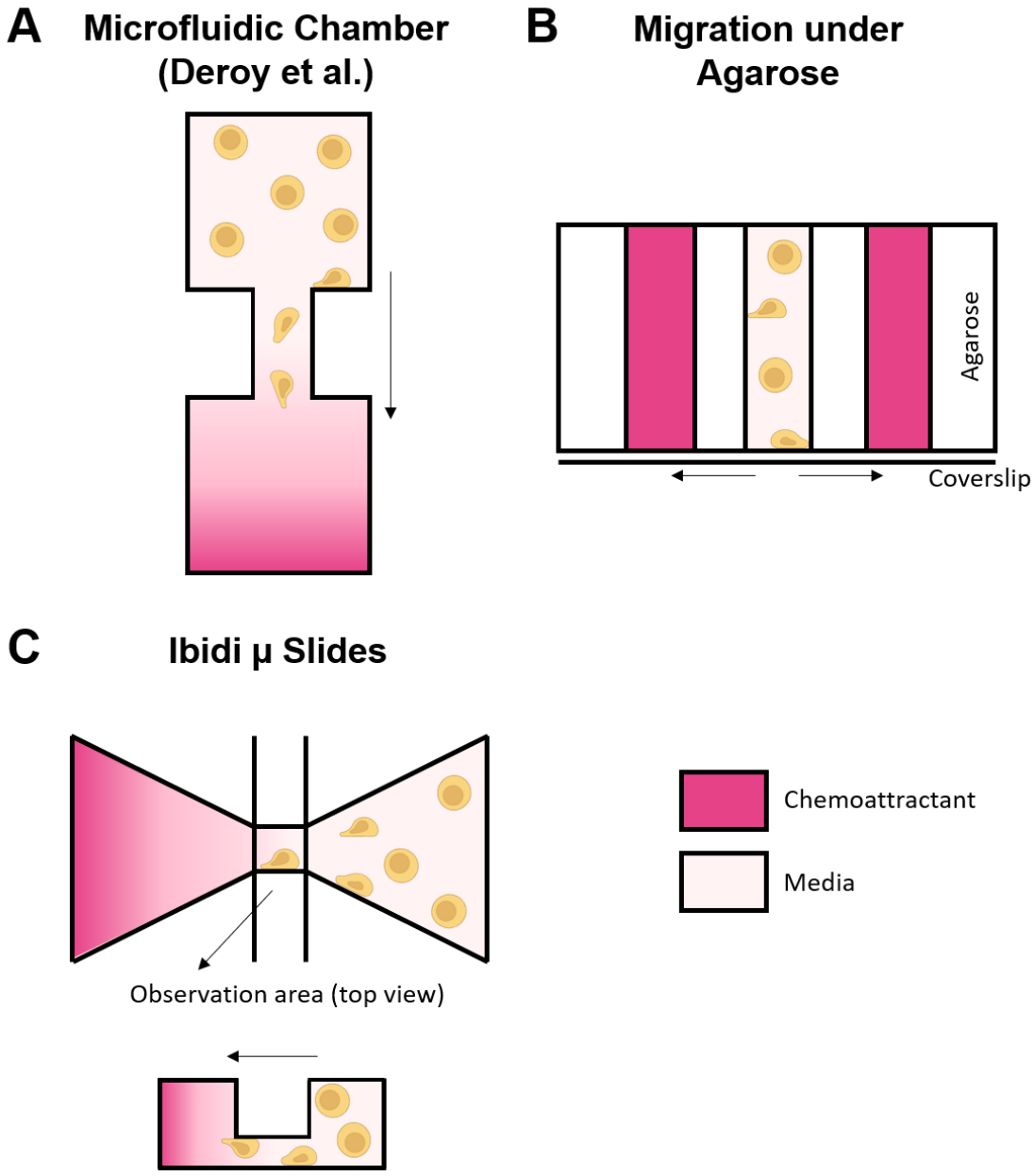


Fig. 5. 2 Chemotaxis assays 2. Setup of **(A)** the microfluidic device with fluid walls developed by Deroy et al., of **(B)** the migration under agarose chemtoaxis assay and of **(C)** a 3D chemotaxis assay using Ibidi µ-Slides. The direction of leukocyte (yellow) migration is indicated by black arrows. Figure generated with BioRender and PowerPoint and illustrations adapted from [819, 821, 822].

To mimic the physiological 3D structure of tissues through which cells migrate *in vivo*, 3D gel invasion assays can be utilized. The matrix can consist of collagen, fibrin or matrigel and may have different pore sizes and stiffness. The chemoattractant can either

be added to a well following the trans-well setup, be injected into a gel or added to an adjacent gel for diffusion [64, 65, 823]. Real-time imaging can track the migration path, speed and directionality as well as shape change or cell-cell interactions during migration towards a chemotactic agent. Alternatively, cells can be fixed, imaged and counted at a chosen time point. Even though automated procedures have been developed, such assays can require costly equipment, time-consuming analysis and are low throughput [823, 824].

5.1.1.2 Adhesion and transmigration assays

To migrate to sites of inflammation, neutrophils and monocytes need to adhere to endothelial cells of the vasculature before transmigrating through the vessel wall into the surrounding tissue.

Static migration assays

To investigate leukocyte adhesion and endothelial transmigration, monolayers of endothelial cells, such as human umbilical vein endothelial cells (HUVECs) or primary human dermal blood endothelial cells (HDBECs), can be seeded on tissue culture plates, porous membranes or collagen gels (Fig. 5.3A) [434, 825-827]. Leukocyte adhesion to activated endothelial cells or migration towards chemoattractants underneath the EC layer can be measured [65, 434].

Static migration assays using human primary endothelial cells and human primary monocytes or neutrophils can be used to characterize inhibitors or enhancers of leukocyte adhesion or transmigration in a medium throughput format. ECs are activated using pro-inflammatory cytokine TNFα, which promotes leukocyte adhesion [828]. ECs and monocytes/neutrophils can be treated separately with selected compounds to assess their effect on leukocyte adhesion and migration and attached (phase bright) and

transmigrated (phase dark) leukocytes can be easily counted using phase contrast microscopy [434].

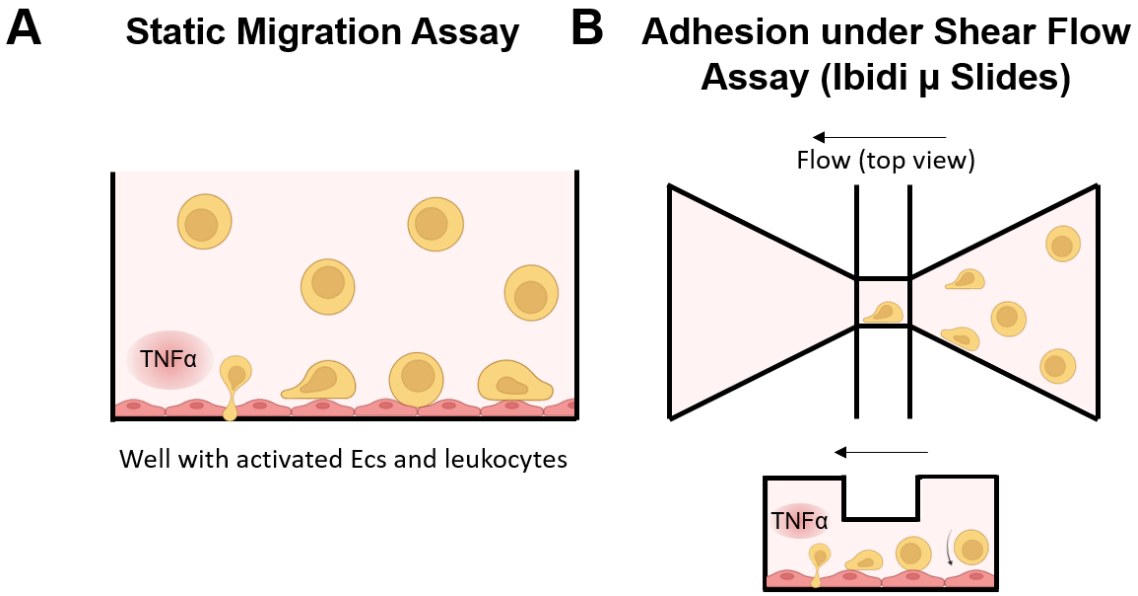


Fig. 5. 3 Adhesion and transmigration assays. Setup of **(A)** static migration assay with leukocytes (yellow) and endothelial cells (ECs, red) activated with TNFα and of **(B)** adhesion under shear flow assay with TNFα-activated Ecs and leukocytes in top and side view. Arrow indicates the direction of shear flow. Figure generated with BioRender and PowerPoint. Panel B adapted from illustrations from [822].

Adhesion under shear flow assays

As described in Chapter 1.2.2.1, forces acting on L-selectin trigger LFA-1 activation and deceleration of leukocyte rolling. This results in their arrest by firm interaction of ICAM-1 and VCAM-1 on ECs with leukocyte LFA-1, Mac-1 and VLA-4 [57, 58]. In addition, shear stress promotes coordinated neutrophil intraluminal migration in the direction of flow [829].

Therefore, studies investigating processes involved in leukocyte capture, rolling and endothelial adhesion use shear flow assays to mimic conditions under blood flow. Such assays use a flow chamber that allows fine regulation of shear stress and flow direction and can be coupled with live imaging techniques [830]. Monolayers of ECs can be grown on tissue culture plates or shear flow chambers and are activated by cytokines or chemokines [65]. Similarly, Ibidi µ-slides can be coated with selected concentrations of

chemoattractants or seeded with endothelial cells [831]. Leukocytes flow through the chamber and their rolling velocity can be measured as a read-out for the strength of adhesion molecule interactions on leukocytes and endothelial cells as well as their binding kinetics (Fig. 5.3B). The density of adhered cells can be detected as an indicator of adhesion strength [832]. Thus, shear flow adhesion assays can detect inhibitors or enhancers of adhesion or transmigration. However, it is difficult to establish a controlled chemokine gradient under shear flow and some chemokines are not well captured and presented by ECs [833]. Therefore, adhesion under flow assays are more appropriate for investigating haptotaxis rather than chemotaxis. Further, live cell imaging and analysis are time-consuming and require specialized equipment, making this assay unsuitable for high-throughput screening [65].

5.1.2 Targeting leukocyte recruitment in inflammation

5.1.2.1 Targeting tyrosine kinases in leukocyte adhesion and chemotaxis

Tyrosine kinases, especially Src family kinases (SFKs), play an important role in leukocyte adhesion and endothelial transmigration as well as in chemotaxis during inflammation (Fig. 5.4).

Leukocyte capture and rolling induced by endothelial L-selectin binding to PSGL-1 on leukocytes triggers the activation of SFKs Fgr, Hck and Lyn, which phosphorylate the ITAM sequence on adapter protein DAP12. Unlike the other two SFKs, Fgr can bind directly to L-selectin. SFK activation causes the binding of Syk via its SH2 domain. Syk initiates SLP-76 and ADAP-dependent BTK recruitment to the plasma membrane, where it gets activated. BTK activates PI3K, resulting in PIP_3 production and Vav1-dependent actin polymerization, causing the formation of L-selectin clusters. In addition, BTK also activates PLCγ2, which triggers p38 signaling, resulting in the unfolding of Talin-1 and its recruitment to PIP_3. This results in conformational change and activation of LFA-1 and the slowing of leukocyte rolling [53, 834]. After chemokines induce leukocyte arrest,

outside-in signaling activates SFKs Hck and Fgr, which induce Syk recruitment via DAP12. Syk in turn phosphorylates and activates Vav1/3 and Slp76, which are required for neutrophil ROS production and degranulation as well as the formation of firm adhesions, leukocyte polarization and migration. In addition, integrin-dependent neutrophil activation and adhesion also depend on Src-mediated activation of TK Pyk2, which activates PI3K as well as Akt and p38 signaling to induce ROS production and actin remodeling required for adhesion [353, 834]. Endothelial transmigration is mediated by tyrosine kinase-dependent signaling cascades.

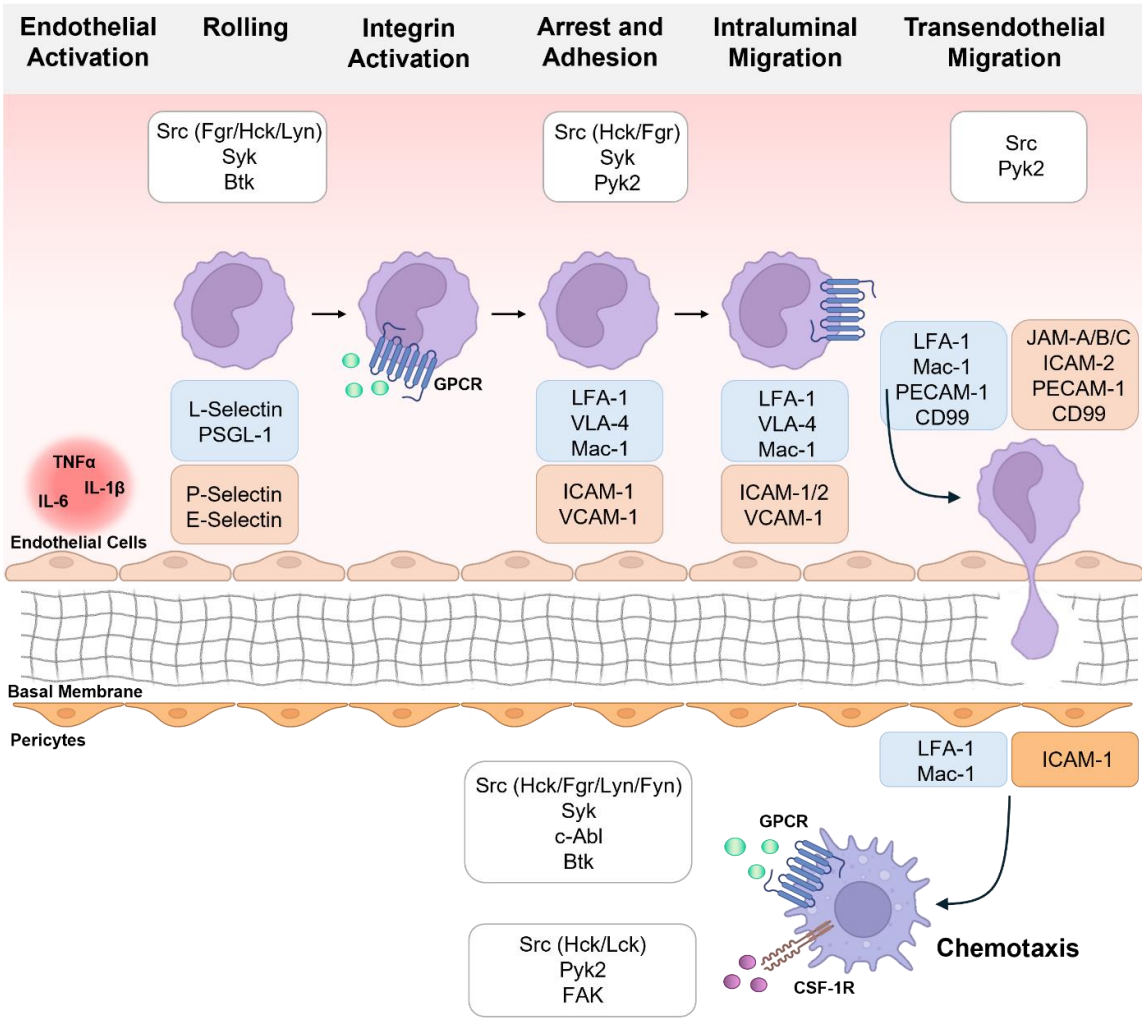


Fig. 5. 4 Tyrosine kinases in leukocyte extravasation and chemotaxis. Tyrosine kinases, especially SFKs, mediate important processes during leukocyte extravasation and chemotaxis. After leukocyte capture by the activated endothelium, TKs promote slow rolling, adhesion, cell polarization and directional intraluminal migration. Src and Pyk2 also are key for transendothelial migration by mediating VE-cadherin dissociation. In leukocyte chemotaxis, TKs induce adhesion, polarization, directional cell migration and ECM remodeling required for macrophage chemotaxis. Figure adapted from [59] and includes findings described in [348-353]. Created with BioRender and PowerPoint.

During paracellular transmigration, endothelial VCAM-1, ICAM-1 and E-selectin clusters interact with their respective binding partners on leukocytes and induce Src and Pyk2 activation. Together with Rac1 and RhoA, the tyrosine kinases cause an increase in intracellular calcium levels in ECs, triggering VE-cadherin phosphorylation and adherens junction opening [54, 352, 835]. Inhibition of endothelial Src results in the abrogation of neutrophil endothelial transmigration [352].

In addition to leukocyte adhesion and transendothelial migration, leukocyte chemotaxis is regulated by tyrosine kinase activity (Fig. 5.4). Upon chemokine binding, GPCRs initiate signaling cascades involving tyrosine kinase effectors [836]. SFKs Hck and Fgr as well as Syk are required for leukocyte actin remodeling and thus adhesion, polarization and chemotaxis towards CX_3CL1 and Lyn and Fyn were shown to mediate adhesion and migration ability [836-841]. In addition, Syk is involved in the activation of Cdc42, Rac and WASP/WAVE through PI3K in chemotaxis towards CX_3CL1 [836]. Hck was shown to mediate ECM proteolysis to enable macrophage mesenchymal migration [842]. Further, Hck and Lyn as well as downstream ERK and p38 signaling are required for monocyte chemotaxis towards E-selectin [351]. Hck, Fgr and c-Abl activate Cdc42 and Rac and regulate migration [350]. BTK was found to mediate macrophage chemotaxis towards CCL2 and promote directional neutrophil chemotaxis, as its inhibition resulted in reduced chemotaxis but increased chemokinesis upon exposure to fMLP [377, 843].

Receptor tyrosine kinase CSF-1R mediates monocyte and macrophage chemotaxis towards CSF-1. Upon ligand binding, the receptor dimerizes, leading to the autophosphorylation of cytoplasmic tyrosine residues, which creates binding sites for SFKs and PI3K [836]. SFKs Hck and Lck are required for CSF-1-elicited macrophage chemotaxis. Lck is thought to phosphorylate Vav, which is recruited to the plasma membrane in a PI3K-dependent manner and initiates actin remodeling required for

macrophage chemotaxis [836, 844]. CSF-1R activation also results in the downstream activation of Cdc42, Rac and WAVE, leading to actin polymerization and cell movement [836]. SFK Hck has been shown to phosphorylate and activate WASP in primary macrophages [845]. Since macrophages migrate through both amoeboid and mesenchymal motility, they depend on the formation of firm adhesions. Upon interactions with ECM, non-receptor tyrosine kinases FAK and Pyk2 are phosphorylated [836]. In osteoclasts, Pyk2 was shown to directly bind to CSF-1R and, together with SFKs, phosphorylates paxillin, which causes macrophage spreading and adhesion [846]. Pyk2 induces PIP_3 production, increases intracellular calcium levels and activates Rho, thereby mediating the polarization of macrophages as well as the detachment from the surface which is required for cell movement [847, 848]. In macrophages, FAK can bind to PI3K upon CSF-1R activation and SFKs then bind to FAK and paxillin, resulting in the formation of lamellipodia, adhesion and chemotaxis [848-852]. While Syk is not required for macrophage chemotaxis towards CSF-1, it is essential for actin remodeling, adhesion and directed cell motility towards fMLP, CCL2 and CX_3CL1 [841, 853].

These findings reported in the literature show that tyrosine kinases play important roles in endothelial adhesion, transmigration as well as chemotaxis of neutrophils, monocytes and macrophages in inflammation (Fig. 5.4). Targeting specific tyrosine kinases with tyrosine kinase inhibitors is therefore an attractive approach to suppress these processes in an inflammatory setting.

5.1.2.2 Targeting leukocyte chemokines in inflammation

Considering the essential role of leukocyte migration in the initiation and amplification of inflammation, targeting this process seems like a promising strategy to treat inflammatory diseases.

Inflammatory neutrophil infiltration in cancer is linked to worse response to treatment and lower survival rates [854, 855]. Therefore, Guo et *al.* carried out a phase 1 clinical trial in

which they targeted CXCR2, which mediates the recruitment of polymorphonuclear myeloid-derived suppressor cells (PMN-MDSCs) to the tumor [856, 857]. The authors treated patients with metastatic castration-resistant prostate cancer with CXCR2 (IL-8 receptor) inhibitor AZD5069 and prostate-cancer therapeutic enzalutamide. They found that AZD5069 dose-dependently reduced numbers of blood neutrophils and lowered PMN-MDSC levels in the tumor. In addition, CXCR2 inhibition reversed resistance to androgen receptor signaling inhibitors and had long-lasting anti-tumor effects in a subset of patients [857]. A phase 1/2 clinical trial is currently investigating the effect of CXCR2 inhibitor AZD5069 treatment in combination with durvalumab in patients with advanced HCC (trial number ISRCTN12669009) [858].

Avacopan is a small molecule inhibitor of the C5a receptor, which detects complement factor C5a. The chemoattractant induces the recruitment and activation of inflammatory neutrophils, monocytes, T cells and eosinophils, which drives disease pathology in antineutrophil cytoplasmic antibody-associated vasculitis (AAV) [859, 860]. The disease is commonly treated with glucocorticoids, however, they can increase morbidity and mortality [861]. Therefore, a phase 2 clinical trial evaluated the effect of avacopan on AAV patients compared to standard of care (SOC) prednisone and found similar clinical responses in both treatment groups, indicating that avacopan is not inferior to prednisone and may therefore be considered a replacement for high-dose glucocorticoids [861]. Another phase 2 trial investigated the safety of avacopan treatment in AAV patients and reported that the inhibitor was well tolerated and that higher drug doses improved time to remission [862]. In a phase 3 clinical trial, AAV patients were either treated with avacopan or prednisone in combination with cyclophosphamide or rituximab. The C5a receptor inhibitor significantly increased sustained remission rates compared to prednisone [863]. Consequently, avacopan received FDA approval as an add-on treatment for adult AAV patients in 2021 [864].

Elevated chemokine levels have been detected in the synovium and the serum of RA patients and were shown to drive inflammatory leukocyte recruitment and angiogenesis [865]. Therefore, phase 1 and 2 clinical trials set out to investigate therapeutic effects of anti-CXCL10, CCL2, CCR2 and CX_3CL1 antibodies as well as CCR1 and CCR5 small molecule inhibitors [866]. However, most clinical trials were unsuccessful, possibly due to the redundancy of chemokine signaling in RA [867]. A phase 2 study investigated the effect of human anti-CXCL10 monoclonal antibody MDX-1100 in combination with methotrexate in RA patients. MDX-1100 caused significantly higher American College of Rheumatology 20 % improvement criteria (ACR20, indicating 20 % improvement in certain RA scores) response rates [868].

The success of AZD5069, MDX-1100 and avacopan in clinical trials demonstrate that therapeutically targeting leukocyte infiltration is a promising strategy to treat a wide range of inflammatory diseases. Therefore, *in vitro* chemotaxis, transmigration or adhesion assays may represent powerful tools to identify and characterize inhibitors of neutrophil and monocyte chemotaxis in inflammation.

5.1.3 The role of NF-κB in leukocyte adhesion, transendothelial migration and chemotaxis in inflammation

NF-κB activation in inflammation mediates leukocyte adhesion, endothelial transmigration and chemotaxis. The transcription factor induces the expression of adhesion molecules ICAM-1 and VCAM-1 on ECs and promotes the production of GM-CSF, CCL2 and other chemokines, which recruit monocytes [869-871]. Large amounts of IL-6, another target of NF-κB, are secreted by the aortic adventitia in vascular inflammation during atherosclerotic lesion development in mice on a high-fat diet [872]. This led Brasier to propose that in this setting, NF-κB-mediated IL-6 production causes monocyte activation and recruitment through outside-in signaling, resulting in further production of CCL2 and IL-6 [870].

In addition, studies have shown that in a mouse model of skin inflammation, PKCα induced NF-κB activation, which resulted in TNFα, CXCL2 and KC production. Inhibition of NF-κB attenuated secretion of both cytokines and neutrophil chemoattractants. Similarly, blocking NF-κB in primary keratinocytes inhibited neutrophil chemotaxis *in vitro* [873]. NF-κB activation is also required for CCR1-mediated chemotaxis of THP-1 monocytes [874, 875]. In fibroblast, macrophage and neutrophil chemotaxis towards HMGB1, IKKα and IKKβ as well as p52/RelB are essential for cell polarization, cell orientation and migration [876, 877]. In addition, IKKα and IKKβ initiate non-canonical and canonical NF-κB signaling pathways, which are crucial for fibroblast and macrophage chemotaxis towards CXCL12. IKKα also modulates cell polarization and migration speed during CXCL12-elicited chemotaxis [878]. These findings demonstrate that NF-κB plays an important role in adhesion and cell migration in an inflammatory environment by promoting the expression of adhesion molecules and chemokines as well as mediating cell polarization and migration speed during chemotaxis.

5.1.4 Drug repurposing to target leukocyte adhesion, transendothelial migration and chemotaxis

5.1.4.1 Targeting monocyte/neutrophil adhesion and transendothelial migration

Given the important role dysregulated leukocyte-endothelial adhesion plays in the recruitment of inflammatory cells in pathologic inflammation, Sun et *al.* sought to identify drug repurposing candidates that can potently and specifically inhibit monocyte adhesion [879]. In a high-throughput screen (with a Z' score of 0.7), they used LPS-stimulated HUVECs that were pre-treated with 1 μM of 2791 FDA-approved medicines before co-culture with calcein-AM-labeled THP1 monocytes for 15 min. Fluorescence intensity was used as a read-out to determine the number of adhered labeled THP1 monocytes and Bay11-7082 was used as a positive control. The screen identified lifitegrast, approved for the treatment of dry eye disease, as an inhibitor of monocyte adhesion, which may directly block the interaction of THP1 and EC adhesion molecules. The drug was

developed by rational design to block the interaction of LFA-1 and ICAM-1, validating the screening results [880]. Its anti-inflammatory properties were successfully confirmed in a mouse model of poly(I:C)D-GalN-induced acute liver injury. Therapeutic i.p. lifitegrast administration reduced serum ALT levels (liver damage marker), pro-inflammatory cytokine expression, NF-κB signaling as well as CCL2 and CXCL10 expression in the liver with effect sizes comparable to those of dexamethasone [879].

Another drug repurposing study identified FDA-approved statin simvastatin as an inhibitor of neutrophil adhesion. In a static adhesion assay, TNFα-activated primary human neutrophils were pre-treated with simvastatin and incubated on fibronectin-coated plates for 30 min. Neutrophil adhesion was determined by measuring MPO levels compared to a standard curve [881]. 10 µM simvastatin reduced neutrophil adhesion by inhibiting TNFα-mediated upregulation of CD11b surface levels on neutrophils, possibly through inhibition of Rho kinase [881].

Recently, Galkina et *al.* reported that imipramine, an FDA-approved anti-depressant, can reduce neutrophil adhesion and activation [882]. As previous studies had highlighted the neuro-inflammatory component of depression [883], the authors pre-treated primary human neutrophils with LPS and imipramine before incubation on fibronectin-coated plates. To quantify neutrophil adhesion, MPO production was assessed in a colorimetric assay. 100 µM and 10 µM imipramine inhibited neutrophil adhesion and the secretion of MMP-9 and NGAL, which re-organize the ECM to promote cell migration. However, the anti-depressant also promoted neutrophil ROS production and apoptosis [882].

Dabrafenib is FDA-approved for the treatment of glioma and metastatic solid tumors with V600E mutations in the gene of serine/threonine kinase B-Raf. In a screen of 327 FDA-approved medicines, Lee et *al.* identified the kinase inhibitor as a suppressor of PolyP65-induced vascular inflammation [884]. 5 µM and 10 µM dabrafenib were shown to inhibit LPS- and PolyP65-induced HUVEC expression of adhesion molecules VCAM, ICAM and

E-selectin as well as adhesion of fluorescein-labeled primary human neutrophils to HUVEC monolayers. In addition, dabrafenib inhibited primary neutrophil migration to activated HUVECs in a trans-well migration assay [884, 885]. In LPS-induced endotoxemia *in vivo*, the kinase inhibitor dose-dependently suppressed leukocyte recruitment at doses between 9.2 and 52 mg/kg and reduced lethality [885]. Similarly, 10 and 30 µg/mouse dabrafenib increased survival rates in a PolyP-induced lethality model and the cecal ligation puncture sepsis model [884].

5.1.4.2 Targeting monocyte/neutrophil chemotaxis

Following adhesion and transendothelial migration into the tissue, monocytes and neutrophils follow gradients of chemoattractants to migrate to sites of inflammation. Therefore, various drug repurposing studies aimed to identify candidates that inhibit the production of chemokines and leukocyte migration towards chemokine gradients in inflammation.

A recent study reported that anti-malarial drug atovaquone inhibits neutrophil chemotaxis by decreasing CD11b surface expression and promotes disease resolution in DSS-induced colitis *in vivo*. *In vitro*, the drug repurposing candidate inhibited primary human neutrophil chemotaxis towards fMLF in a trans-well migration assay by reducing CD11b surface levels [886].

Colchicine is FDA-approved for gout prophylaxis as well as the treatment of acute gout flares and familial Mediterranean fever and was recently the first anti-inflammatory drug to receive FDA approval to protect atherosclerosis patients from cardiovascular events [887, 888]. Due to neutrophils lacking the efflux pump P-glycoprotein, colchicine was shown to accumulate in neutrophils and therefore preferentially affect neutrophil functions [889]. Colchicine inhibits neutrophil chemotaxis, which was already demonstrated in 1965 using the Boyden chamber migration assay [889, 890]. Through its effects on tubulin organization, colchicine reduces IL-1β or TNFα-mediated

endothelial cell adhesiveness by re-distributing surface E-selectin at doses as low as 3 nM. At 0.3 µM, the drug additionally inhibited the expression of L-selectin on neutrophils, which was also observed in peripheral blood neutrophils from colchicine-treated volunteers [891]. A recent clinical study reported that short-term colchicine treatment reduced transcoronary levels of chemokines CCL2, CCL5 and CX_3CL1 in patients with acute coronary syndrome (ACS). In monocytes isolated from colchicine-treated patients, the intracellular concentrations of these chemokines were reduced. *In vitro*, colchicine inhibited primary human monocyte chemotaxis in a trans-well migration assay [892].

Cilostazol is a phosphodiesterase type III inhibitor and received FDA approval for the treatment of claudication and restenosis after angioplasty. Chuang et *al.* showed that cilostazol dose-dependently reduces monocyte chemotaxis towards CCL2 in a trans-well migration assay by decreasing surface CCR2 levels in THP1 monocytes and human primary PBMCs and by suppressing CCR2-mediated p38 MAPK signaling. In addition, CCL2-activated THP1 monocytes showed reduced adherence to a HUVEC monolayer after cilostazol-treatment [893]. Similar effects were observed with type I angiotensin II receptor antagonist losartan, which is approved for the treatment of hypertension and diabetic nephropathy [894]. It inhibited THP1 and PBMC chemotaxis towards CCL2 in a trans-well migration assay by reducing CCR2 surface levels and CCL2-induced ERK phosphorylation in THP1 monocytes [895]. In addition, the study found that losartan inhibited monocyte recruitment *in vivo* in experimental lung metastasis models [895].

BTK inhibitor and FDA-approved anti-cancer drug ibrutinib was found to dose-dependently inhibit BMDM chemotaxis towards a C5a gradient in a real-time xCELLigence trans-well migration assay. Similarly, pre-treatment with 10 µM ibrutinib reduced human primary monocyte chemotaxis towards CCL2. These effects translated into ZIP as an *in vivo* model of acute inflammation. Ibrutinib-treated mice showed reduced peritoneal neutrophil and monocyte recruitment after zymosan challenge [377].

These published findings demonstrate that trans-well chemotaxis assays as well as static adhesion assays are useful tools to identify FDA-approved drug repurposing candidates that inhibit neutrophil or monocyte endothelial adhesion or transmigration as well as chemotaxis *in vitro*. Many studies further showed that these *in vitro* findings translated to anti-inflammatory effects of these drug repurposing candidates in *in vivo* models of inflammation. Therefore, drug repurposing seems like a promising strategy to target inflammatory leukocyte recruitment in inflammation.

5.2 Original hypothesis and experimental aims of the chapter

In Chapter 3, I showed that tyrosine kinase inhibition by regorafenib and sorafenib reduces LPS-induced CSF-1R phosphorylation, NF-κB signaling and the expression and protein production of NF-κB targets including TNFα, IL-1β and IL-6 as well as monocyte/ macrophage chemoattractant CCL2. In addition, I demonstrated in Chapter 4 that both TKIs inhibit macrophage KC/IL-8 production upon NLRP3 inflammasome activation by LPS+MSU/CPPD crystals *in vitro* and reduce peritoneal CCL2 and IL-1β levels early in MSU crystal-induced peritonitis *in vivo*. This correlated with a reduction in peritoneal neutrophil and monocyte recruitment at 4 h and 16 h post i.p. MSU crystal challenge.

NF-κB is known to play an important role in leukocyte chemotaxis by activating endothelial cells and leukocytes through production of cytokines TNFα, IL-1β and IL-6 or chemokines KC/CCL2, up-regulating adhesion molecule expression as well as by mediating leukocyte polarization and directional migration. Therefore, I hypothesize that NF-κB inhibitor regorafenib can inhibit endothelial adhesion and transmigration of monocytes and neutrophils as well as chemotaxis of macrophages and monocytes towards gradients of pro-inflammatory chemokines. I further hypothesize that this effect will translate into acute inflammation *in vivo*, where TKI inhibition by regorafenib may affect leukocyte mobilization.

The experimental aims of this chapter were to:

1. Assess the effect of regorafenib on primary murine macrophage and THP1-Dual monocyte chemotaxis towards gradients of different pro-inflammatory chemoattractants.
2. Investigate the effect of regorafenib on activated primary human endothelial cell adhesion and transmigration by primary human neutrophils and monocytes.
3. Explore the dynamics of monocyte and neutrophil mobilization in acute inflammation *in vivo*.

Static migration assays investigating primary human neutrophil and monocyte endothelial adhesion and transmigration were assisted by Jenefa Begum and Areeba Fatima and informed by discussions with Prof. Asif Iqbal at the University of Birmingham.

5.3 Results

5.3.1 Effect of regorafenib and sorafenib on macrophage and monocyte chemotaxis

To measure macrophage and monocyte chemotaxis *in vitro*, I decided to use the xCELLigence Real-Time Cell analyzer (RTCA-DP) to detect cell migration in real-time [431]. This system measures cell migration from a top well towards a chemokine gradient in the bottom well through a filter with 8 µm pores. During migration, cells adhere to gold electrodes underneath the porous filter, which causes an increase in electrical impedance, from which the cell index (CI) can be calculated (Fig. 5.5A). Therefore, an increased amount of migrated and electrode-adhered cells correlates to an increased CI. To eliminate random, non-directional cell movement, data was normalized to control wells containing cells without a chemokine gradient [431].

5.3.1.1 C5a-elicited macrophage chemotaxis

To investigate the effect of TK inhibition by regorafenib and sorafenib on macrophage chemotaxis, we chose to use C5a as a chemoattractant for initial chemotaxis experiments. The complement component potently recruits and activates monocytes, neutrophils and macrophages and is therefore involved in the pathology of various inflammatory diseases such as sepsis, periodontitis, cancer and glomerular disease [896-898].

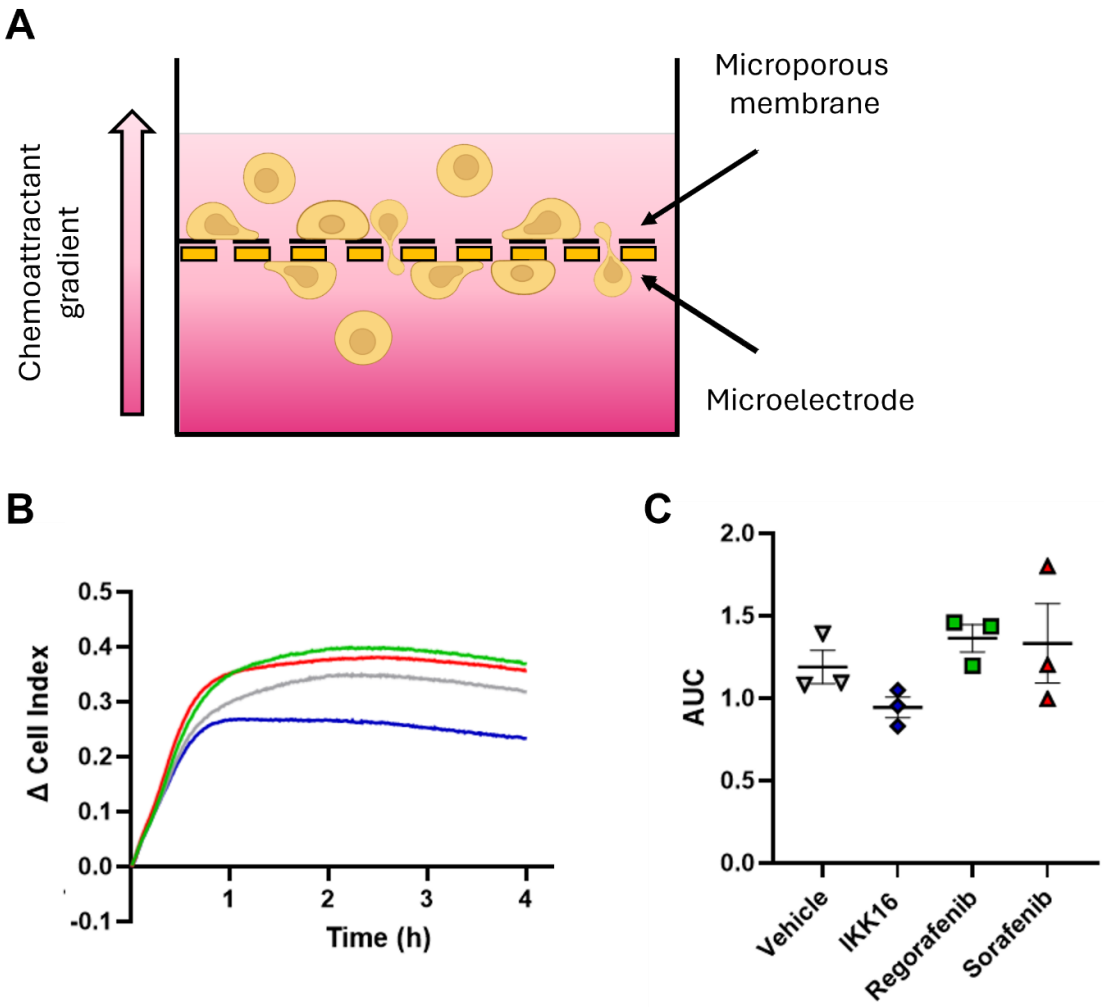


Fig. 5. 5 TKI inhibition by regorafenib or sorafenib does not affect BMDM chemotaxis towards C5a. (A) Experimental setup of xCELLigence chemotaxis assay using CIM-16 plates. **(B)** Traces from RTCA-DP software of BMDMs migrating towards C5a (10 nM). Cells were pretreated with 3 µM regorafenib (green), sorafenib (red), DMSO vehicle (grey) or 1 µM IKK16 (blue) for 1 h before exposure to C5a. Normalization to medium only. **(C)** Quantified migration (as area under the curve (AUC) of Δ cell index). Mean ±SEM, n=3. One-way ANOVA with Dunnett's multiple comparisons test.

Therefore, C5a was used as a chemoattractant to validate macrophage chemotaxis assays in previous studies in the Greaves lab [819, 899]. Taylor et *al.* found that for the xCELLigence real-time chemotaxis assay, $1x10^5$ cell/well is the optimal density for BMDMs [431]. To determine the concentration of C5a that would elicit a maximal chemotaxis response in BMDMs, Dr. Agata Rumianek tested the migratory response of BMDMs to 19 concentrations of C5a, ranging from 0.003 pM to 300 nm, and found that 10 nM C5a caused the largest migratory response [899]. Therefore, this concentration was chosen to investigate the effect of regorafenib and sorafenib on BMDM chemotaxis.

Before exposure to the C5a gradient in the bottom well for 4 h, BMDMs were incubated with 3 µM regorafenib or sorafenib, 1 µM IKK16 or DMSO vehicle for 1 h in the top well. Normalized traces of cell index (Fig. 5.5B) and the corresponding area under the curve (Fig. 5.5C) revealed that neither regorafenib, sorafenib nor IKK16 significantly affected C5a-elicited BMDM chemotaxis.

5.3.3.2 CSF-1-elicited macrophage chemotaxis

Therefore, I decided to test CSF-1 as a chemoattractant for BMDMs in the xCELLigence real-time chemotaxis assay. As described in section 1.2.2.2.2, CSF-1 binding to macrophage CSF-1R initiates macrophage chemotaxis and recruits macrophages to sites of pathologic inflammation. To identify a CSF-1 concentration that elicits maximal BMDM chemotaxis, I exposed BMDMs to a range of CSF-1 concentrations, ranging from 0.1 ng/ml to 100 ng/ml (Fig. 5.6A). The area under the curve of cell index traces showed that 30 ng/ml caused maximal BMDM migration, whereas higher and lower concentrations resulted in a smaller migratory response (Fig. 5.6B).

Therefore, 30 ng/ml CSF-1 was chosen for further experiments. BMDMs were pre-treated with 3 µM regorafenib or sorafenib, 1 µM IKK16 or DMSO vehicle for 1 h before exposure to the CSF-1 gradient in the bottom well. Real-time cell migration was measured for 4 h. Normalized traces of CI (Fig. 5.6C) and the corresponding AUCs (Fig.

5.6D) show that regorafenib, sorafenib and IKK inhibitor IKK16 significantly reduced BMDM chemotaxis towards CSF-1. Considering that macrophage migration was reduced to a similar extent in regorafenib/sorafenib treated macrophages (83 % and 73 % decrease) and in BMDMs treated with IKK-inhibitor IKK16 (70 % decrease), this effect may be mediated by inhibition of NF-κB signaling.

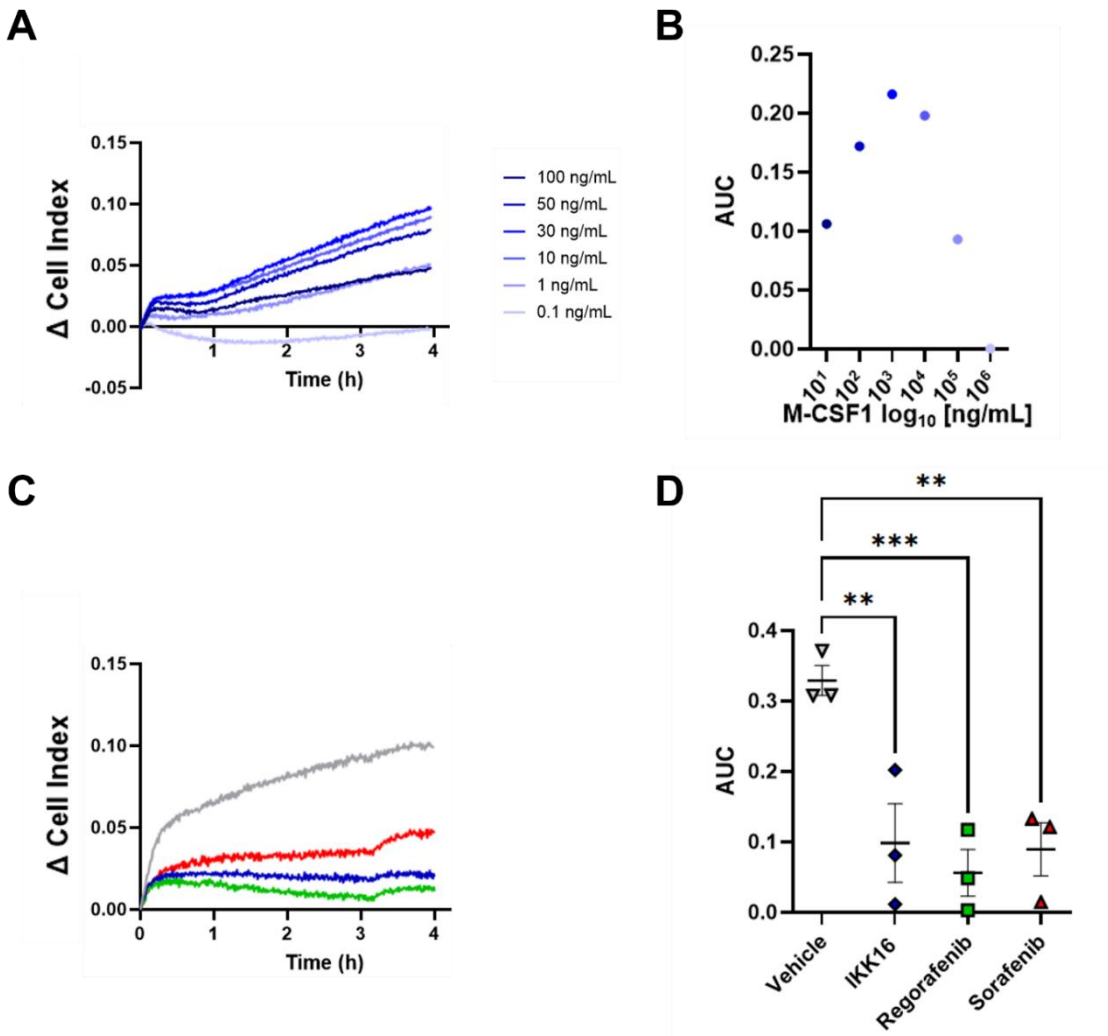


Fig. 5. 6 TKI inhibition by regorafenib or sorafenib reduces BMDM chemotaxis towards CSF-1 (A) Traces from RTCA-DP software of BMDMs migrating towards indicated concentrations of CSF-1. Normalization to medium only. **(B)** Quantified migration (as AUC of Δ cell index). **(C)** Traces from RTCA-DP software of BMDMs migrating towards CSF-1 (30 ng/ml). Cells were pretreated with 3 µM regorafenib (green), sorafenib (red), DMSO vehicle (grey) or 1 µM IKK16 (blue) for 1 h before exposure to CSF-1. Normalization to medium only. **(D)** Quantified migration (as AUC of Δ cell index). Mean ±SEM, n=3. One-way ANOVA with Dunnett's multiple comparisons test.

Of note, DMSO vehicle itself (Fig. 5.6C) seemed to change the shape of the cell index trace (Fig. 5.6A). A study by Yao et *al.* suggests that DMSO does not change the

chemotactic properties of microglia [900]. However, DMSO-treated microglia were observed to undergo morphological changes, characterized by larger processes [901]. This is in line with the finding that DMSO can cause cytoskeletal re-arrangements and increased adhesion of epithelial melanoma cells [902]. Therefore, DMSO may change the shape of the cell index trace of BMDMs migrating towards a gradient of CSF-1 by causing morphological changes which affect electrical impedance. Therefore, further experiments include DMSO vehicle as a control to reliably assess the effects of regorafenib and sorafenib on leukocyte chemotaxis.

5.3.3.3 CCL2-elicited monocyte chemotaxis

In Chapters 3 and 4, I found that regorafenib inhibits CCL2 protein production in LPS-stimulated macrophages *in vitro* and in the peritoneum in MSU crystal-challenged mice *in vivo*. Therefore, I sought to investigate if regorafenib could also reduce monocyte chemotaxis towards CCL2 when it is already present in the medium. To identify the appropriate concentration of CCL2 to use in the xCELLigence real-time chemotaxis assay, I exposed THP1-Dual monocytes to 6 concentrations of human recombinant CCL2, ranging from 0.1 ng/ml to 100 ng/ml (Fig. 5.7A). I found that 50 ng/ml elicited maximal monocyte chemotaxis and therefore chose this concentration for further experiments (Fig. 5.7B). THP1-Dual monocytes were pre-incubated with 3 µM regorafenib or DMSO vehicle for 1 h before they were added to the top well and were exposed to a gradient of CCL2 in the bottom well for 4 h (Fig. 5.7C). Analysis of the area under the curve of normalized CI traces (Fig. 5.7D) revealed that regorafenib significantly reduced monocyte chemotaxis towards CCL2 by 80 % compared to vehicle.

Using the xCELLigence trans-well real-time chemotaxis assay, we have shown here that TKI inhibition by regorafenib can reduce primary murine BMDM chemotaxis towards M-CSF-1 but not towards C5a. In addition, the TKI inhibited THP1-Dual monocyte migration towards CCL2.

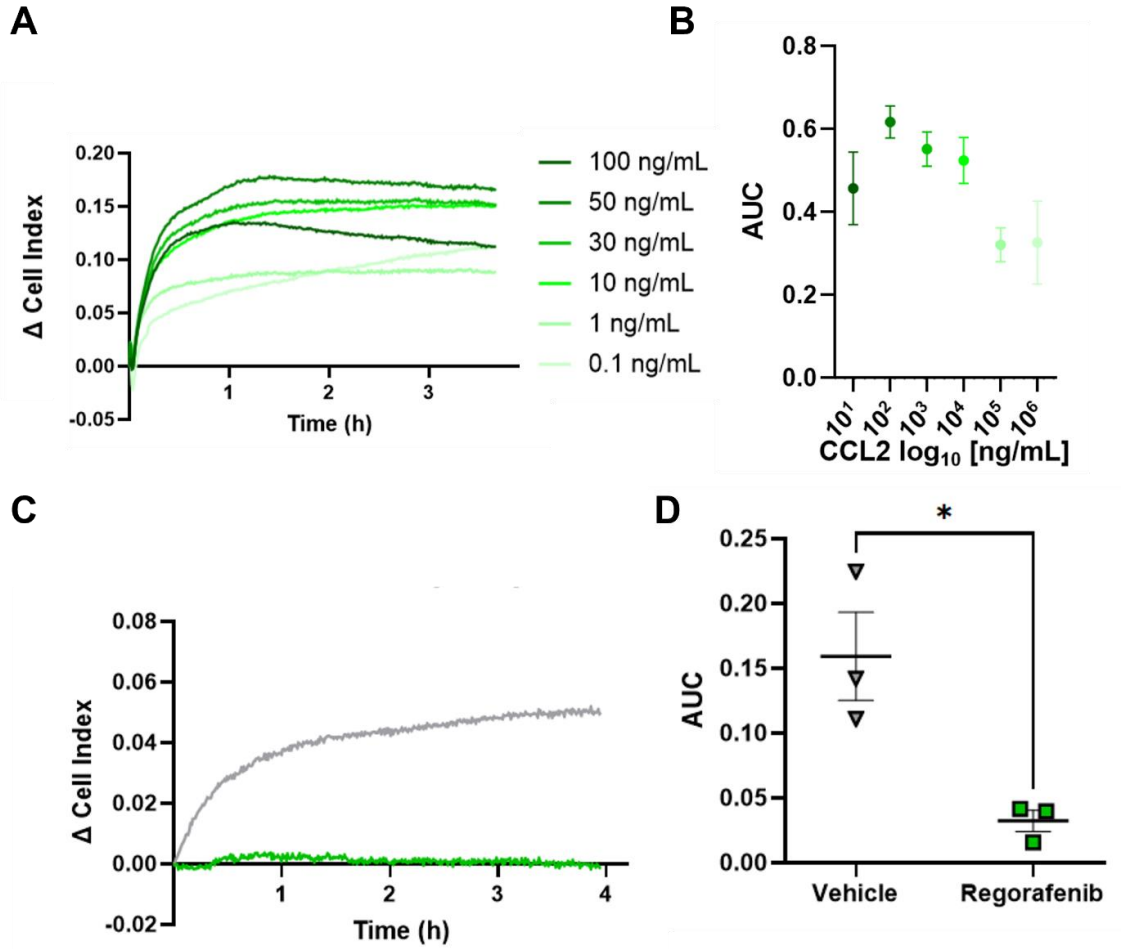


Fig. 5. 7 TKI inhibition by regorafenib reduces THP1-Dual monocyte chemotaxis towards CCL2 (A) Traces from RTCA-DP software of THP1-Dual monocytes migrating towards indicated concentrations of CCL2. Normalization to medium only. **(B)** Quantified migration (as AUC of Δ cell index). **(C)** Traces from RTCA-DP software of THP1-Dual monocytes migrating towards CCL2 (50 ng/ml). Cells were pretreated with 3 µM regorafenib (green) or DMSO vehicle (grey) for 1 h before exposure to CCL2. Normalization to medium only. **(D)** Quantified migration (as AUC of Δ cell index). Mean ±SEM, n=3. Unpaired student's t-test.

5.3.2 Effect of regorafenib on human primary neutrophil and monocyte endothelial cell adhesion

Given regorafenib inhibits macrophage and monocyte chemotaxis *in vitro* and the recruitment of neutrophils and monocytes in models of acute peritoneal inflammation *in vivo*, I aimed to investigate whether the TKI affects neutrophil and monocyte adhesion or transendothelial migration.

As described above, static migration assays using human primary endothelial cells and human primary monocytes or neutrophils are useful tools to characterize inhibitors of

leukocyte adhesion or endothelial transmigration. They allow separate pre-treatment of ECs and monocytes/neutrophils to assess a drug's effect on leukocyte adhesion and migration. Attached (phase bright), activated (phase grey) and transmigrated (phase dark) leukocytes can be easily counted using phase contrast microscopy [434]. Therefore, we decided to activate human primary dermal blood endothelial cells (HDBECs) with TNFα (100 U/ml) for 4 h before adding neutrophils or monocytes. TNFα is physiologically produced by resident macrophages during inflammation and initiates the activation of endothelial cells. Consequently, ECs up-regulate the expression of adhesion molecules like selectins, which recognize glycoprotein ligands [52-54]. E- and P-selectin expression, responsible for leukocyte capture by endothelial cells, is maximally induced 4 h after TNFα stimulation [903, 904]. In addition, ICAM-1 and VCAM-1, which mediate leukocyte adhesion, are also up-regulated by ECs 4 h after exposure to TNFα [905, 906]. To differentiate between any effects of regorafenib on EC activation and effects on neutrophils or monocytes, we pre-treated ECs with 3 µM regorafenib, sorafenib or DMSO vehicle for 1 h before addition of TNFα for 4 h. Subsequently, the remaining TNFα was removed before untreated monocytes or neutrophils were added for 7 min. Alternatively, non-drug-treated ECs were stimulated with TNFα for 4 h, then TNFα was removed and neutrophils or monocytes, which had been pre-treated with 3 µM regorafenib, sorafenib or DMSO vehicle, were added to the EC monolayer. After allowing monocytes or neutrophils to migrate for 7 min, non-adherent cells were removed and the remaining leukocytes and ECs were fixed for imaging.

5.3.2.1 Effect on ECs during monocyte adhesion and migration

To investigate whether regorafenib affects monocyte transendothelial migration through effects on the endothelial monolayer, HDBECs were pre-treated with 3 µM regorafenib before stimulation with TNFα for 4 h and the subsequent addition of monocytes (Fig. 5.8A).

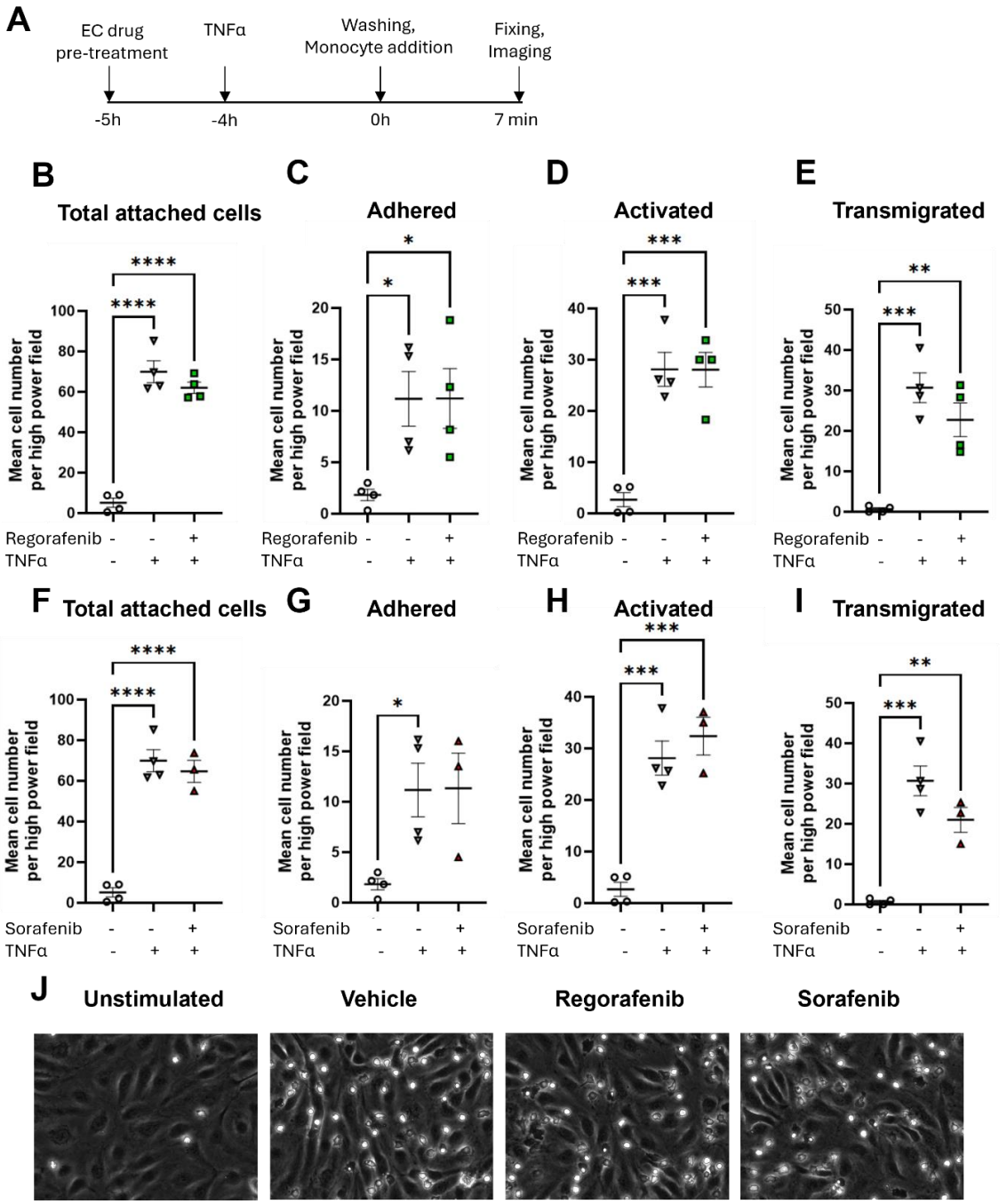


Fig. 5. 8 Regorafenib EC pre-treatment does not affect monocyte adhesion or transmigration. (A) Experimental outline. HDBECs were pre-treated with 3 µM regorafenib (green squares), sorafenib (red triangles) or DMSO vehicle (grey triangles) for 1 h before TNFα (100 U/ml) stimulation for 4 h. After removing TNFα, primary human monocytes were added for 7 min before fixing and imaging. Mean number of total cells **(B/F)**, adhered cells **(C/G)**, activated cells **(D/H)** and transmigrated cells **(E/I)** per high power field. **(J)** Representative images of cell migration after 7 min in different treatment groups. Mean ±SEM, n=3-4. One-way ANOVA with Dunnett's multiple comparisons test.

TNFα stimulation significantly increased the total number of cells attached to the activated endothelial monolayer (Fig. 5.8B/F and 5.8J). Further, we observed a

significant increase in the number of surface adhered cells (Fig. 5.8C and 5.8G), the number of activated cells in the process of migrating (Fig. 5.8D and 5.8H) as well as the number of cells that had undergone endothelial transmigration (Fig. 5.8E and 5.8I) upon TNFα stimulation. Regorafenib did not significantly reduce monocyte adhesion or transmigration through its effects on ECs, even though the number of transmigrated monocytes was less elevated in the regorafenib-treated group than in the vehicle group compared to non-TNFα-stimulated ECs (Fig. 5.8E). Sorafenib did not significantly affect monocyte adhesion, activation or transendothelial migration compared to vehicle control (Fig. 5.8F-I). However, similar to regorafenib, there was a trend towards the number of transmigrated monocytes being less elevated in the sorafenib group compared to non-TNFα-stimulated ECs (Fig. 5.8I).

5.3.2.2 Effect on monocytes during EC adhesion and migration

Pre-treatment of monocytes with regorafenib before addition to TNFα-activated ECs did not affect monocyte adhesion or transendothelial migration (Fig. 5.9A). We did not observe any changes in the number of total attached monocytes (Fig. 5.9B), adhered monocytes (Fig. 5.9C), activated monocytes (Fig. 5.9C) or transmigrated monocytes (Fig. 5.9E) between the vehicle and the regorafenib group (Fig. 5.9J). Similar to regorafenib, pre-treatment of monocytes with sorafenib did not significantly reduce the total number of attached monocytes (Fig. 5.9F), monocyte adhesion (Fig. 5.9G), activation (Fig. 5.9H) or transendothelial migration to activated endothelial cells (Fig. 5.9I and 5.9J).

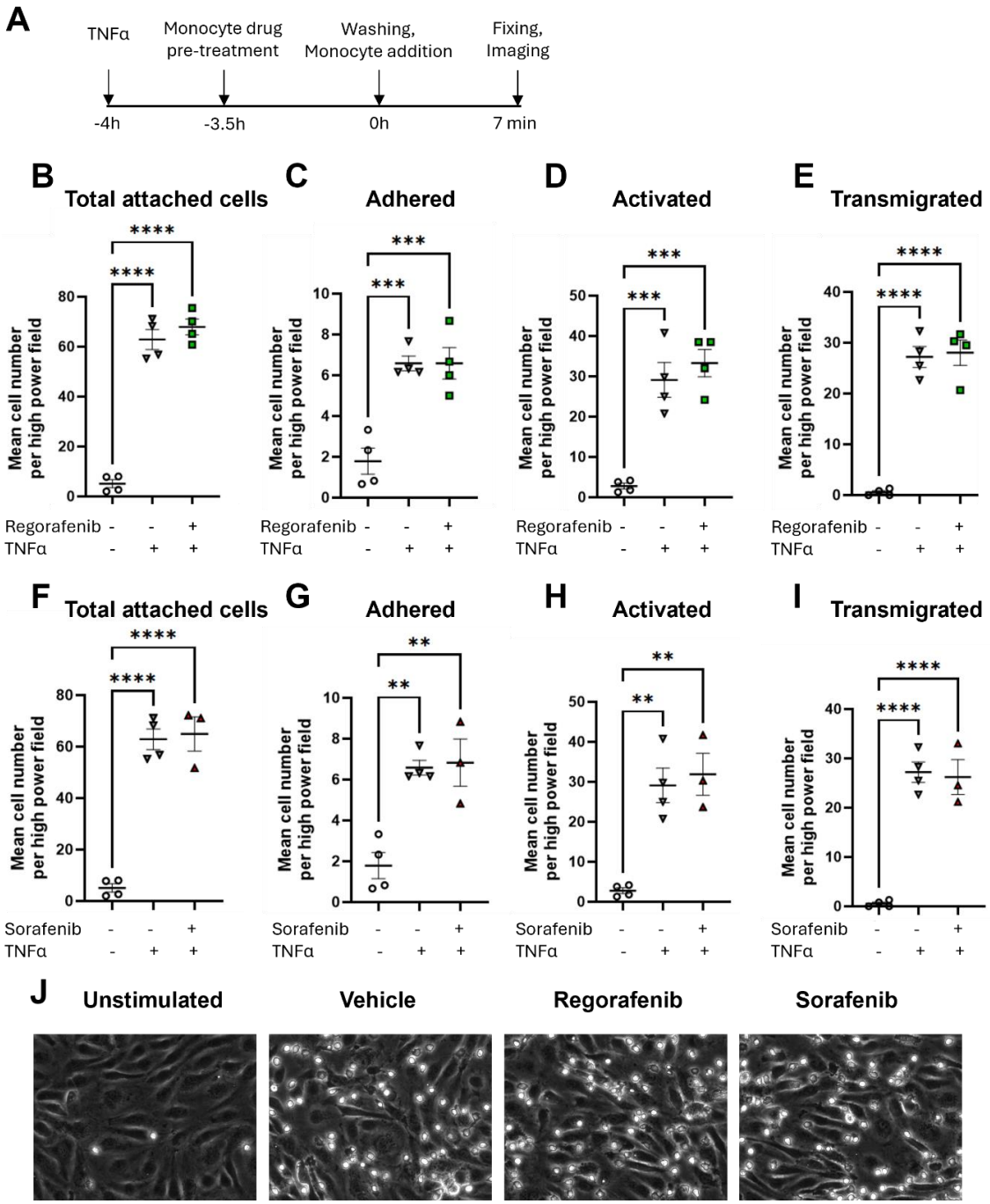


Fig. 5. 9 Regorafenib monocyte pre-treatment does not affect adhesion or endothelial transmigration. (A) Experimental outline. HDBECs were activated with TNFα (100 U/ml) for 4 h. Primary human monocytes were pre-treated with 3 µM regorafenib (green squares), sorafenib (red triangles) or DMSO vehicle (grey triangles) for 30 min. After removing TNFα, monocytes were added for 7 min before fixing and imaging. Mean number of total cells **(B/F)**, adhered cells **(C/G)**, activated cells **(D/H)** and transmigrated cells **(E/I)** per high power field. **(J)** Representative images of cell migration after 7 min in different treatment groups. Mean ±SEM, n=3-4. One-way ANOVA with Dunnett's multiple comparisons test.

5.3.2.3 Effect on ECs during neutrophil adhesion and migration

Given regorafenib and sorafenib reduce neutrophil recruitment in acute inflammation *in vivo*, we investigated whether the TKIs can modulate neutrophil adhesion or transendothelial migration through their effects on endothelial cell activation (Fig. 5.10A).

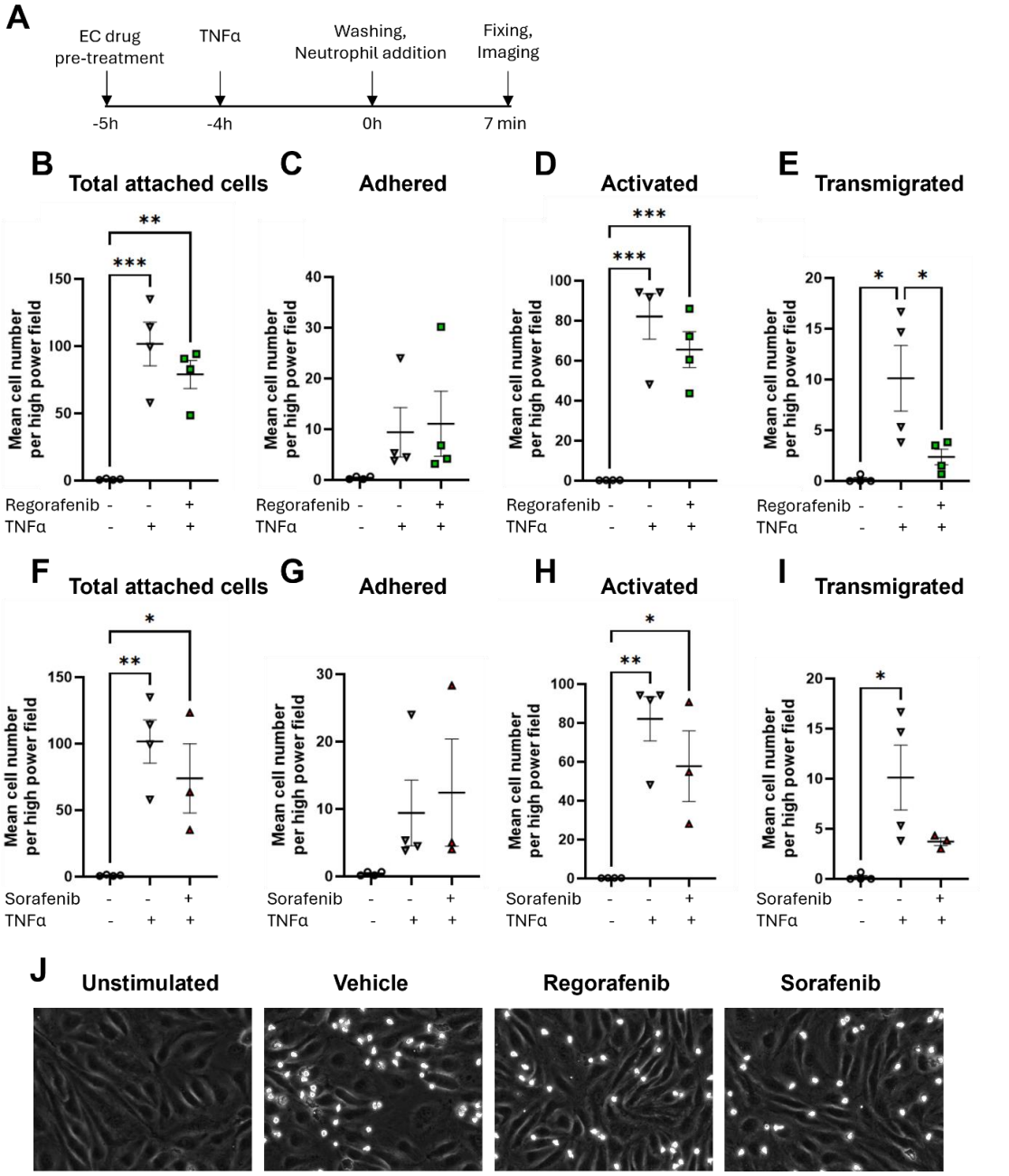


Fig. 5. 10 Regorafenib EC pre-treatment reduces neutrophil transmigration. (A) Experimental outline. HDBECs were pre-treated with 3 µM regorafenib (green squares), sorafenib (red triangles) or DMSO vehicle (grey triangles) for 1 h before TNFα (100 U/ml) stimulation for 4 h. After removing TNFα, primary human neutrophils were added for 7 min before fixing and imaging. Mean number of total cells **(B/F)**, adhered cells **(C/G)**, activated cells **(D/H)** and transmigrated cells **(E/I)** per high power field. **(J)** Representative images of cell migration after 7 min in different treatment groups. Mean ±SEM, n=3-4. One-way ANOVA with Dunnett's multiple comparisons test.

TNFα stimulation significantly increased neutrophil attachment to the activated endothelial monolayer (Fig. 5.10B) as well as the number of activated (Fig. 5.10D) and transmigrated (Fig. 5.10E) neutrophils (Fig. 5.10J). When ECs were pre-treated with regorafenib before TNFα-stimulation and subsequent neutrophil addition, the number of total attached neutrophils was slightly less elevated than in vehicle-treated ECs compared to non-TNFα-treated ECs (Fig. 5.10B). While regorafenib did not affect the number of activated neutrophils (Fig. 5.10D), it significantly reduced the number of neutrophils that had undergone transendothelial migration after 7 min compared to vehicle by 77 % (Fig. 5.10E and 5.10J). Similar to regorafenib, sorafenib pre-treatment of ECs prior to the addition of neutrophils did not significantly reduce neutrophil adhesion (Fig. 5.10F-G) or activation (Fig. 5.10H). Sorafenib reduced the number of neutrophils that had undergone transendothelial migration at 7 min by 63 % but this decrease did not reach statistical significance. However, unlike in the vehicle-treated group, the number of transmigrated neutrophils was not significantly elevated after sorafenib treatment compared to non-TNFα stimulated controls (Fig. 5.10I and 5.10J).

5.3.2.4 Effect on neutrophils during EC adhesion and migration

Next, we investigated whether neutrophil but not EC pre-treatment with regorafenib or sorafenib affects neutrophil adhesion or transmigration (Fig. 5.11A). We found that when neutrophils were exposed to regorafenib before incubation with TNFα-activated ECs, the number of total attached neutrophils did not change between the vehicle-treated and the regorafenib-treated group (Fig. 5.11B).

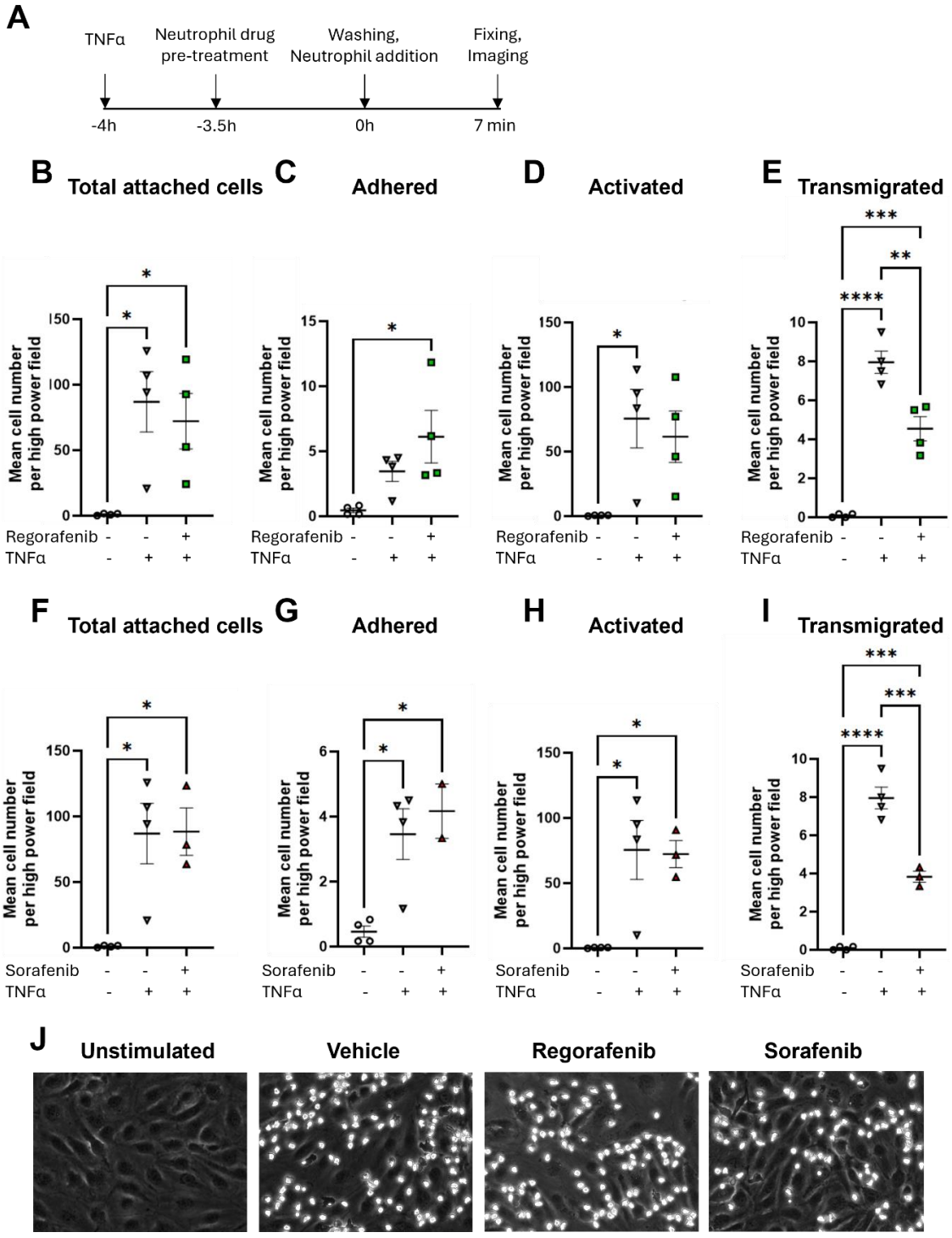


Fig. 5. 11 Regorafenib neutrophil pre-treatment reduces endothelial transmigration. (A) Experimental outline. HDBECs were activated with TNFα (100 U/ml) for 4 h., Primary human neutrophils were pre-treated with 3 µM regorafenib (green squares), sorafenib (red triangles) or DMSO vehicle (grey triangles) for 30 min. After removing TNFα, neutrophils were added for 7 min before fixing and imaging. Mean number of total cells **(B/F)**, adhered cells **(C/G)**, activated cells **(D/H)** and transmigrated cells **(E/I)** per high power field. **(J)** Representative images of cell migration after 7 min in different treatment groups. Mean ±SEM, n=3-4. One-way ANOVA with Dunnett's multiple comparisons test.

The number of adhered neutrophils was only significantly increased in the regorafenib but not the vehicle group compared to non-TNFα-stimulated ECs (Fig. 5.11C), while the number of activated neutrophils was only significantly increased in the vehicle but not in the regorafenib group compared to unstimulated ECs (Fig. 5.11D), suggesting slower activation of neutrophils after regorafenib treatment. Regorafenib significantly reduced the number of neutrophils that had transmigrated through the EC monolayer compared to vehicle by 43 % (Fig. 5.11E and 5.11J). Similar to regorafenib, sorafenib pre-treatment of neutrophils prior to the addition to activated ECs did not affect neutrophil adhesion (Fig. 5.11F-G) or activation (Fig. 5.11H) but significantly reduced the number of neutrophils that had undergone transendothelial migration at 7 min by 52 % (Fig. 5.11I and 5.11J).

Our findings demonstrate that regorafenib does not affect monocyte adhesion, activation or endothelial transmigration in this static migration assay *in vitro*. However, the drug repurposing candidate reduced transendothelial migration of primary human neutrophils through TNFα-stimulated ECs both by acting on the endothelial cells as well as on the neutrophils directly.

5.3.3 Effect of regorafenib on myeloid cell mobilization *in vivo*

During acute inflammation, monocytes and neutrophils are readily recruited from reservoirs in the spleen and enter blood circulation to reach the site of inflammation [907, 908]. In Chapter 4, we observed that regorafenib can reduce peritoneal neutrophil and monocyte recruitment following MSU crystal challenge. Therefore, we investigated whether regorafenib affects neutrophil or monocyte mobilization from their reservoir in the spleen (Fig. 5.12B-D) and whether the TKI would affect the number of circulating neutrophils and monocytes in the blood (Fig. 5.12E-G).

Mice were prophylactically administered with 30 mg/kg regorafenib or vehicle before intraperitoneal MSU crystal challenge for 4 h (Fig. 5.12A). We detected a similar number of CD45⁺ lymphocytes in the spleen of sham and MSU-challenged mice (Fig. 5.12B).

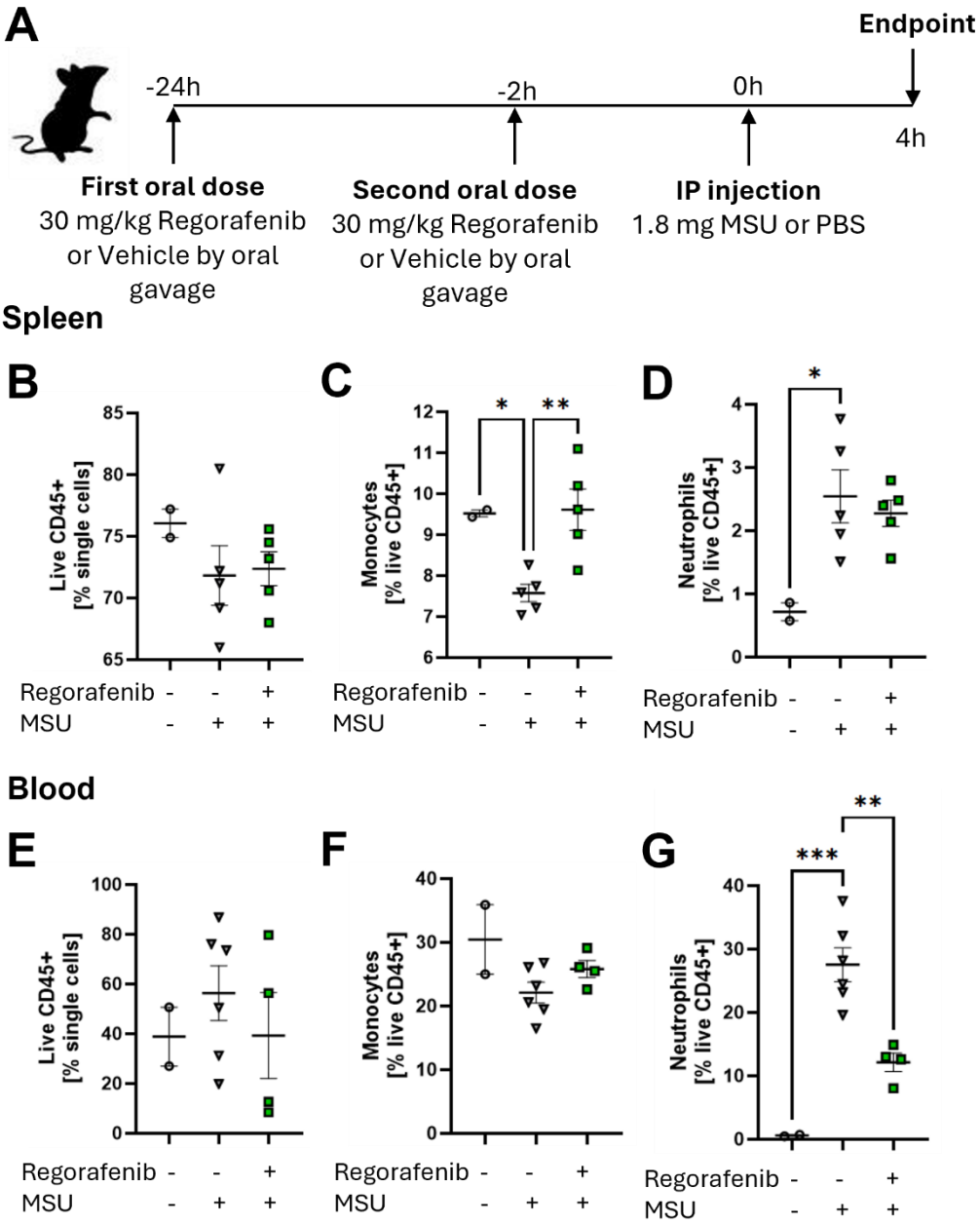


Fig. 5. 12 Regorafenib retains monocytes in the spleen and reduces circulating neutrophil numbers. (A) Mice were orally administered with regorafenib (30 mg/kg, green squares) or vehicle (grey triangles) 24 h and 2 h before i.p. injection of MSU crystals (1.8 µg) for 4 h. The spleen was harvested and live CD45⁺ lymphocytes **(B)**, monocytes **(C)** and neutrophils **(D)** were counted. Blood was harvested and live CD45⁺ lymphocytes **(E)**, monocytes **(F)** and neutrophils **(G)** were counted. Means ± SEM of 2-6 mice per group. One-way ANOVA with Dunnett's multiple comparisons test.

MSU crystal injection caused a significant reduction of monocyte numbers in the spleen of vehicle-treated mice, indicating the release of monocytes from their splenic reservoir (Fig. 5.12C). Interestingly, we found that regorafenib retained monocytes in the spleen, with comparable splenic monocyte numbers in regorafenib-treated mice and in sham mice (Fig. 5.12C). 4 h after MSU crystal challenge, splenic neutrophil numbers significantly increased in vehicle-treated mice compared to sham mice (Fig. 5.12D). While regorafenib did not significantly decrease splenic neutrophil numbers compared to vehicle, splenic neutrophil numbers were not significantly elevated in regorafenib-treated mice compared to sham mice either.

4 h after MSU crystal challenge, circulating blood $CD45^+$ lymphocytes were not significantly increased (Fig. 5.12E). Similarly, blood monocyte numbers remained unchanged between all three treatment groups (Fig. 5.12F). However, the number of circulating neutrophils significantly increased in vehicle-treated mice 4 h after MSU crystal injection (Fig. 5.12G). TKI inhibition by regorafenib significantly reduced the number of circulating neutrophils compared to vehicle (Fig. 5.12G).

5.4 Discussion

In this chapter, I aimed to assess the effect of regorafenib on primary murine BMDM and human THP1-Dual monocyte chemotaxis towards gradients of different pro-inflammatory chemoattractants. In the xCELLigence real-time chemotaxis assay, I found that regorafenib and sorafenib significantly inhibited BMDM chemotaxis towards CSF-1 (Fig. 5.6) but did not affect macrophage migration elicited by complement peptide C5a (Fig. 5.5). In addition to reducing LPS-induced CCL2 protein production by BMDMs *in vitro* (Fig. 3.10) and in the peritoneum of MSU crystal-challenged mice *in vivo* (Fig. 4.7), regorafenib also directly inhibited THP1-Dual monocyte chemotaxis towards CCL2 in the xCELLigence real-time chemotaxis assay (Fig. 5.7). *In vitro* and *in vivo*, we showed that regorafenib can reduce pro-inflammatory cytokine production and the secretion of

monocyte and neutrophil chemoattractants CCL2 and IL-8/KC. Therefore, I sought to investigate the effect of regorafenib on human primary monocyte and neutrophil adhesion and the transmigration through TNFα-activated primary human HDBECs in a static migration assay. Here, we report for the first time that regorafenib inhibits transendothelial migration of neutrophils through its effects on endothelial cells and neutrophils directly (Fig. 5.10-5.11). In addition, we demonstrate that *in vivo*, regorafenib modulates leukocyte mobilization by retaining monocytes in the spleen and reducing circulating neutrophil numbers in MSU crystal-induced peritonitis at 4 h (Fig. 5.12).

5.4.1 Targeting tyrosine kinases to modulate leukocyte adhesion, transendothelial migration and chemotaxis

As described above, previous findings reported in the literature demonstrate that tyrosine kinases play an important role in endothelial adhesion, transmigration as well as chemotaxis of neutrophils, monocytes and macrophages in inflammation (Fig. 5.4). Targeting specific tyrosine kinases with tyrosine kinase inhibitors can successfully suppress these processes in an inflammatory setting. In Chapter 3, we have shown that regorafenib inhibits LPS-induced CSF-1R phosphorylation in macrophages. CSF-1R is a key target to reduce macrophage chemotaxis in inflammation (Fig. 5.4). Indeed, studies have shown that pharmacologic inhibition of CSF-1R with TKIs GW2580, PLX5622 or KI20227 can reduce monocyte or microglia infiltration, inflammation and atherosclerotic plaque formation, LPS-induced retina inflammation or experimental autoimmune encephalitis (EAE) *in vivo* (Fig. 5.13) [909, 910]. Here, we found that regorafenib and sorafenib significantly inhibit BMDM chemotaxis towards CSF-1 (Fig. 5.6).

In Chapter 3, we also showed that regorafenib inhibits early Src phosphorylation and the activation of p38 in macrophages upon LPS exposure. Both Src and p38 are heavily implicated in leukocyte adhesion, transmigration and chemotaxis [53, 73, 911, 912]. Pharmacological targeting of p38 with small molecule inhibitors SKF86002 or SB203580

was reported to effectively reduce leukocyte intraluminal migration, transendothelial migration and chemotaxis *in vivo* [911, 912]. Src inhibition by TKI PP2 inhibited leukocyte slow rolling, adhesion, endothelial transmigration as well as chemotaxis (Fig. 5.13) [348, 349, 351, 352, 843]. In agreement with these reported findings, we demonstrated that regorafenib can reduce CCL2-induced monocyte chemotaxis *in vitro* (Fig. 5.7) and inhibit MSU crystal-induced neutrophil and monocyte recruitment *in vivo* (Fig. 4.7 and 4.9). In addition, regorafenib reduced neutrophil transmigration through TNFα-stimulated endothelial cells (Fig. 5.10E and 5.11E).

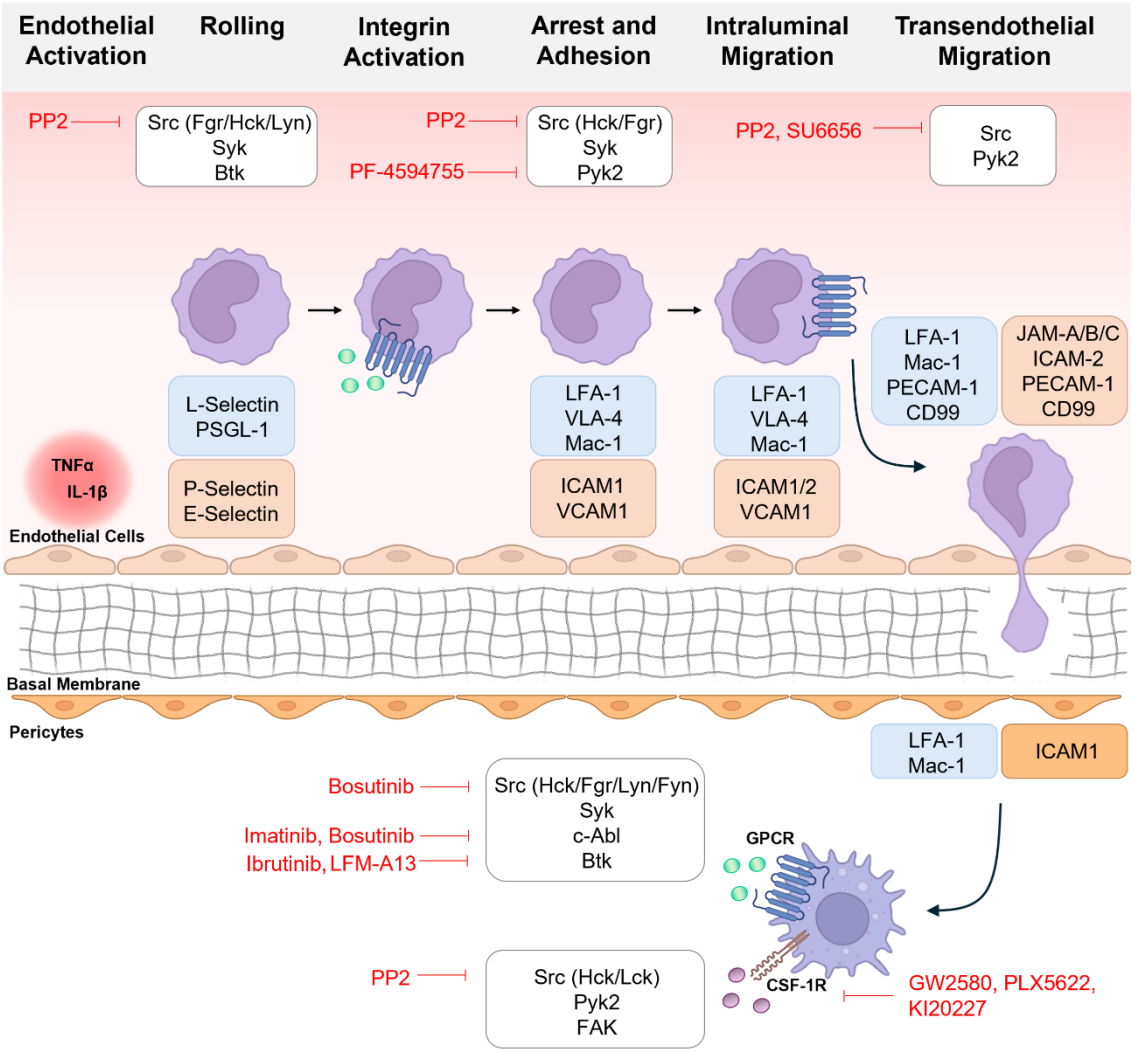


Fig. 5. 13 Tyrosine kinases in leukocyte extravasation and chemotaxis. Pharmaceutical targeting of tyrosine kinases that mediate processes during leukocyte extravasation and chemotaxis can reduce leukocyte recruitment and macrophage chemotaxis in inflammation. Figure adapted from [59] and includes findings described in [348-353]. Created with BioRender and PowerPoint.

As discussed above, NF-κB plays an important role in leukocyte adhesion, endothelial transmigration and chemotaxis. The transcription factor promotes the expression of endothelial and leukocyte adhesion molecules and drives cell polarization and chemotaxis. Considering that regorafenib reduces NF-κB activation, the TKI's inhibitory effects on macrophage and monocyte chemotaxis as well as neutrophil transendothelial migration may in part be mediated by its ability to inhibit NF-κB signaling. This hypothesis is supported by the finding that regorafenib reduced CSF-1-elicited macrophage chemotaxis to a similar extent as IKK-inhibitor IKK16.

5.4.2.2 Targeting tyrosine kinases to suppress leukocyte mobilization in acute inflammation

Previous studies have reported the role of tyrosine kinases in leukocyte mobilization in inflammation. Purvis et *al.* showed that BTK modulates monocyte and neutrophil recruitment to the blood and thus to the site of inflammation in zymosan-induced peritonitis. Pharmacological BTK inhibition significantly decreased neutrophil and monocyte numbers in the blood as well as in the peritoneum at 16 h post-zymosan challenge [377].

Receptor tyrosine kinases VEGFR, FGFR and PDGFR, which are reported targets of regorafenib, have also been linked to inflammatory monocyte and neutrophil recruitment during inflammation [913, 914]. During skin inflammation induced by TNFα in rats, VEGF increased monocyte recruitment by up-regulating E- and P-selectin expression at 2 h [913]. In this model, FGF increased both neutrophil and monocyte infiltration by enhancing integrin expression and leukocyte chemotaxis [913]. PDGF was found to elicit monocyte and neutrophil chemotaxis in Boyden chamber assays [914].

CCR2, which is bound by chemokine CCL2, was shown to specifically elicit the early recruitment of $Ly6C^{hi}$ inflammatory monocytes from the spleen. Leuschner et *al.* developed nanoparticles loaded with siRNA to target CCR2 expression in spleen

monocytes, which retained the cells in the spleen, lowered circulating monocyte numbers and prevented their recruitment to the site of inflammation in atherosclerotic plaques, myocardial infarct or diabetes in mice [915]. Similarly, bindarit, which targets NF-κB and CCL2, was shown to reduce circulating pro-inflammatory monocyte numbers in the blood and to suppress inflammation in diabetes-associated periodontitis and atherosclerosis [916, 917]. In Chapter 4, I found that tyrosine kinase inhibition by regorafenib resulted in reduced peritoneal NF-κB-driven CCL2 production. This may, in part, be responsible for the retention of monocytes in the spleen of regorafenib-treated mice.

5.5 Limitations of this study

Here, we demonstrated the ability of regorafenib to attenuate primary human neutrophil and monocyte transmigration through HDBEC monolayers in a static migration assay. However, shear force is an important factor that activates LFA-1 and promotes firm endothelial adhesion of leukocytes to vascular endothelial cells as well as their coordinated intraluminal migration. Therefore, future studies could explore the effect of regorafenib on neutrophil and monocyte adhesion and transendothelial migration in an adhesion under shear flow assay, potentially using commercially available Ibidi µ-slides. The slides can be seeded with monolayers of HDBECs, which can be activated with TNFα after regorafenib pre-treatment and subsequently, human primary neutrophils or monocytes can be flowed through the chamber to mimic physiological conditions under blood flow. This would allow for a detailed investigation of the TKI's effect on leukocyte rolling velocity that is impacted by the activity of tyrosine kinase Src, which we have validated as a target of regorafenib. In addition, performing adhesion under flow assays may reveal effects of regorafenib on the strength of adhesion molecule interactions, which is also mediated in part by SFKs. Using live cell imaging, the effect on the processes of leukocyte rolling, adhesion and transendothelial migration could be separately investigated. Such studies are time-consuming and require specialized

equipment, which is why we opted for static migration assays for initial investigations of regorafenib's effect on leukocyte adhesion and transmigration. After having demonstrated the effects of regorafenib on neutrophil transendothelial migration, adhesion under shear flow assays could help dissect the mechanism and provide further insights into its anti-inflammatory properties. In addition, flow cytometry assays could be employed to detect changes in adhesion molecule expression on activated ECs or neutrophils treated with the TKI to determine how regorafenib modulates transendothelial migration on a molecular level.

We investigated the effects of regorafenib on macrophage and monocyte chemotaxis in the xCELLigence real-time trans-well chemotaxis assay. However, this assay does not take into account the physiological 3D structure of tissues with varying porosity and stiffness, which impact directional cell movement. This may be especially important considering macrophage chemotaxis, unlike monocyte or neutrophil chemotaxis, relies on a combination of amoeboid and mesenchymal motility and depends on the degradation of the ECM around the cell. In addition, the trans-well migration assay does not allow the assessment of migration directionality or velocity. Therefore, 3D chemotaxis assays could provide further information on regorafenib's effects on monocyte and macrophage chemotaxis in an environment that more closely resembles that found *in vivo*. Again, commercially available Ibidi µ-Slides could be used for live tracking of the morphology, speed and migration path of regorafenib-treated macrophages or monocytes through a 3D matrix towards a defined chemoattractant gradient.

When exploring how tyrosine kinase inhibition by regorafenib affects myeloid cell recruitment to the peritoneum, we investigated monocyte and neutrophil mobilization from their splenic reservoir and the number of circulating neutrophils and monocytes in the blood. We found that regorafenib prevents monocyte release from the spleen 4 h after peritoneal MSU crystal challenge but did not affect splenic neutrophil numbers.

Considering that the number of circulating neutrophils in the blood was decreased, regorafenib may suppress neutrophil mobilization from other reservoirs, such as the lung or the bone marrow. While we did not analyze monocyte and neutrophil numbers in the bone marrow or lung at 4 h post-MSU crystal challenge in this thesis, future studies could investigate whether tyrosine kinase or NF-κB inhibition affects myeloid cell recruitment from these reservoirs.

5.6 Summary

In this chapter, I found that in a real-time trans-well chemotaxis assay, pre-treatment with sorafenib or regorafenib can reduce primary murine macrophage chemotaxis towards a gradient of CSF-1. In addition, regorafenib suppressed THP1-Dual monocyte migration towards CCL2. Our findings in a static migration assay revealed that regorafenib and sorafenib inhibit the transmigration of primary human neutrophils through TNFα-activated primary HDBEC monolayers. *In vivo*, tyrosine kinase inhibition by regorafenib prevented monocyte mobilization from the spleen and decreased the number of circulating neutrophils in the blood at 4 h post-MSU crystal challenge.

Chapter 6: Conclusions and future work

6.1 Summary and discussion of key findings

One of the key aims of this thesis was to identify drug repurposing candidates with underexplored anti-inflammatory activity. In an initial screen, I identified FDA-approved tyrosine kinase inhibitors regorafenib and sorafenib as NF-κB inhibitors in macrophage inflammation. I then validated the anti-inflammatory activity of the drug repurposing candidates in different inflammatory settings *in vitro* and in a model of acute inflammation *in vivo*.

The first aim of this study was to use a reliable and reproducible cell-based assay to identify FDA-approved tyrosine kinase inhibitors with novel anti-inflammatory properties in human and murine macrophages/monocytes and to determine their mechanism of action *in vitro* (Chapter 3). Here, I made the following key findings:

- According to its Z'-score, the QuantiBlue assay using NF-κB reporter cell lines and positive control IKK16 is an excellent assay to screen for novel NF-κB inhibitors in macrophages and monocytes.
- Screening of a Tocriscreen Kinase Inhibitor Library containing 80 commercially available small molecule kinase inhibitors identified kinase targets that, when inhibited, reduce NF-κB activation in the macrophage reporter cell lines.
- FDA-approved tyrosine kinase inhibitors regorafenib and sorafenib dose-dependently inhibit NF-κB activation in murine macrophage RAW-Blue and human monocyte THP1-Dual reporter cell lines without affecting cell viability at relevant concentrations (below 10 µM).
- Regorafenib and sorafenib suppress NF-κB-dependent pro-inflammatory mediator expression and protein production in primary murine BMDMs, human THP1-Dual macrophages as well as human primary monocyte-derived macrophages upon LPS or LPS+IFN-γ stimulation.

- Regorafenib and sorafenib reduce NF-κB activation and pro-inflammatory mediator production in BMDMs and THP1-Dual macrophages stimulated with a wide range of PAMPs and DAMPs.
- Regorafenib and sorafenib inhibit NF-κB activation by reducing phosphorylation of upstream kinases CSF-1R, Src and p38 in RAW-Blue macrophages.
- Regorafenib modulates BMDM polarization.
- The anti-inflammatory activity of regorafenib is not mediated by effects on TLR4 internalization.

The second aim of my thesis was to investigate the effect of regorafenib and sorafenib on NF-κB-dependent NLRP3 inflammasome priming and activation *in vitro* and to validate the anti-inflammatory effect of both drug repurposing candidates in an *in vivo* model of acute inflammation driven by NF-κB-dependent NLRP3 inflammasome activation (Chapter 4). Regarding this aim, I found that:

- Regorafenib and sorafenib reduce NLRP3 inflammasome activation in RAW-Blue macrophages by inhibiting NF-κB-mediated NLRP3 inflammasome priming but not its assembly directly.
- Both TKIs attenuate IL-1β and IL-8/KC protein production in BMDMs and THP1-Dual macrophages upon LPS+CPPD or LPS+MSU crystal stimulation.
- *In vivo*, prophylactic oral administration of regorafenib or sorafenib reduces neutrophil and monocyte influx as well as inflammatory cytokine and chemokine expression and protein production in mice with MSU crystal-induced peritonitis.
- Therapeutic i.p. regorafenib administration has anti-inflammatory effects in MSU crystal-induced peritonitis at 16 h.
- Both regorafenib and NSAID indomethacin have anti-inflammatory effects in MSU crystal-induced peritonitis at 16 h, which are mediated by different

mechanisms. Regorafenib is lacking the NSAID's gastrointestinal toxicity but induces hepatotoxicity.

- The anti-inflammatory mechanism of regorafenib *in vivo* is mediated by its inhibition of NF-κB-mediated NLRP3 inflammasome priming as indicated by its reduction of IL-1β and pro-Caspase1 levels in the peritoneum.

The final aim of this study was to investigate the mechanism underlying regorafenib's inhibition of leukocyte recruitment *in vitro* and *in vivo* (Chapter 5). Here, I made the following key findings:

- Regorafenib and sorafenib inhibit BMDM chemotaxis towards CSF-1.
- Regorafenib reduces THP1-Dual monocyte chemotaxis towards CCL2.
- Regorafenib and sorafenib suppress transmigration of primary human neutrophils through TNFα-activated primary endothelial cells.
- Regorafenib's, and to a lesser extent sorafenib's, inhibition of neutrophil transendothelial migration is mediated by effects on endothelial cells and on neutrophils directly.
- *In vivo*, regorafenib retains monocytes in the spleen and reduces circulating neutrophil numbers in the blood 4 h post i.p. MSU crystal challenge.

6.2 The future of TKIs regorafenib and sorafenib as therapeutics for inflammatory diseases

In this thesis, I have identified regorafenib and sorafenib as inhibitors of NF-κB activation and associated downstream production of pro-inflammatory mediators in macrophages *in vitro*. These anti-inflammatory effects translated into MSU crystal-induced peritonitis, an *in vivo* model of acute inflammation (Chapter 4). Mechanistically, these effects may be mediated by the TKI's inhibition of NF-κB-dependent NLRP3 inflammasome priming (Fig. 4.2) and the reduction of NF-κB-driven monocyte chemoattractant production both *in vitro* (Fig. 3.7) and *in vivo* (Fig. 4.7 and 4.10). Further, regorafenib and to a lesser

extent sorafenib directly attenuate macrophage and monocyte chemotaxis and neutrophil transendothelial migration *in vitro* (Chapter 5). Our experiments using a variety of PAMPs and DAMPs to stimulate NF-κB activation and TNFα production in BMDMs and THP1-Dual macrophages revealed that regorafenib and sorafenib most likely do not exert their anti-inflammatory effects by targeting the receptors or the Myddosome directly (Fig. 3.13). Our findings indicate that in macrophages, the TKIs likely simultaneously target tyrosine kinases as well as p38 upstream of p65, which results in the combined downstream inhibition of NF-κB activation. However, further experiments are needed to elucidate at which exact stages NF-κB signaling is inhibited by the drug repurposing candidates. In the past, studies investigating targets of regorafenib and sorafenib either tested target affinity in cell-free assays or in cancer cells. Therefore, future studies could explore proteome-wide kinase-drug interactions and kinase phosphorylation in macrophages by employing label-free thermal shift assays utilizing mass spectrometry, such as mass spectrometry-based cellular thermal shift assays (MS-CETSA) [918-920]. Here, we have identified p65 and the NLRP3 inflammasome as *in vivo* targets of regorafenib, but further studies are required to investigate the exact mechanism with which regorafenib inhibits these targets and modulates processes like leukocyte recruitment and migration in inflammation *in vivo*. Assays such as MS-CETSA can be employed on intact cells like peritoneal exudate cells or whole tissues like the peritoneal lining, allowing for target identification of regorafenib *in vivo* [920].

In Chapter 3 and 4, I investigated the anti-inflammatory effect of regorafenib and sorafenib on macrophages and monocytes. However, our *in vivo* data as well as the data obtained from static migration assays suggest that the anti-inflammatory effect of the TKIs is not macrophage- or monocyte-restricted. Rather, both drugs seem to also modulate neutrophil migration as well as endothelial and mesothelial cell function in inflammation. However, this study did not investigate the effects on inflammatory

signaling pathways in these different cell types. Therefore, future studies could elucidate differences or similarities in the anti-inflammatory mechanism of regorafenib in macrophages compared to neutrophils or non-immune cells like endothelial or mesothelial cells.

In addition, our *in vivo* studies focused on the effects of our drug repurposing candidates on early inflammatory processes in acute inflammation. Therefore, effects on processes involved in pathogen clearance and inflammation resolution like phagocytosis, tissue repair and efferocytosis *in vivo* remain unexplored. So far, few compounds have been identified that both inhibit inflammation and enhance tissue repair. Only a small subset of these compounds have been tested in clinical trials and so far, none have received FDA approval [441]. As traditional *de novo* drug discovery has fallen short of meeting the unmet need for anti-inflammatory medicines that both decrease inflammatory mediator production and enhance endogenous anti-inflammatory and pro-repair pathways, drug repurposing assays have been developed to screen specifically for medicines that enhance tissue repair, both *in vivo* and *in vitro*. Phenotypic screens in zebrafish have been used for the identification of anti-inflammatory drugs that target both the recruitment and resolution phases of neutrophil inflammatory responses [921, 922]. Screens were designed to identify compounds that specifically enhance disease-relevant pro-repair pathways, like screens for anti-inflammatory neuroprotective or myelin repair-enhancing drugs for the treatment of MS [458, 923-925] or wound healing assays [609]. Such phenotypic screens could be employed to identify FDA-approved medicines with novel anti-inflammatory and pro-repair effects directly in a complex organism *in vivo* or in assays that measure pro-repair effects specifically relevant to inflammatory diseases of interest *in vitro*. This could also enhance the clinical predictivity of drug repurposing screens.

To identify macrophage-targeting anti-inflammatory pro-repair drugs, efferocytosis or macrophage-reprogramming transcriptional screens have been developed [610, 926]. Further, a screen using primary human synovial fibroblasts from healthy donors and RA patients was used to identify drugs for RA that inhibit synovial fibroblast activation, characterized by their secretion of pro-inflammatory mediators. The screen was carried out in a high-throughput format using an ELISA-type Luminex analysis assay that allows the assessment of 48 cytokines in each synovial fluid before and after incubation with synovial fibroblasts [927]. This screen could be adapted to screen for drug repurposing candidates that increase pro-repair mediators like IL-10 or TGF-β. While the use of synovial fibroblasts from RA patients directly reveals repurposing candidates with disease-relevant effects, these samples are precious and hard to obtain. Therefore, a primary screen could be carried out using BMDMs and hit compounds could subsequently be tested for their effect on synovial fibroblast activation. In addition, the effect of repurposing candidates on macrophage efferocytosis of apoptotic cells, which is a critical step in inflammation resolution, could be measured quantitatively using BMDMs and ImageStream imaging. Apoptosis can be induced by dexamethasone or UV treatment prior to staining cells with cell-trace-CSFE. BMDMs can then be co-cultured with the apoptotic cells and subsequently be stained with anti-F4/80-APC. Induction of apoptosis is confirmed with flow cytometry and ImageStream can be used to detect macrophages engulfing apoptotic cells [928].

In our *in vivo* experiments in Chapter 4, we aimed to compare the anti-inflammatory effects of regorafenib to an NSAID commonly used to treat gouty inflammation. Therefore, we chose indomethacin as an appropriate control as it is the gold standard treatment and was the first NSAID used for gout treatment [929, 930]. However, when choosing an indomethacin dose corresponding to that of regorafenib in our previous *in vivo* studies, we were limited by the NSAID's toxicity in mice. Cancer patients take 160

mg of regorafenib per day [708], while indomethacin is administered at 150-200 mg per day for the treatment of gout [714]. Taking into account the differences in body surface area between humans and mice [752], I calculated that a dose of 30 mg/kg regorafenib in mice corresponds to 2.4 mg/kg in humans, which is slightly higher than the dose taken by cancer patients (160 mg/day = 2 mg/kg/day in an average 80 kg adult). Dosing mice with 5 mg/kg indomethacin however corresponds to 0.4 mg/kg in humans. This is about 5-6 times lower than the daily dose of 1.9-2.5 mg/kg/day taken for the treatment of gout by an average adult human patient. Therefore, the anti-inflammatory effects of regorafenib cannot be compared directly to those of indomethacin in our study. However, despite the dose difference, our results indicate that our drug repurposing candidate identified through our cell-based screening approach has anti-inflammatory effects in *vivo* and that TKIs could be repurposed or re-designed as a new class of anti-inflammatory drugs as alternatives to current anti-inflammatories like NSAIDs.

Regarding the pharmacokinetic properties of regorafenib after oral gavage, we relied on previous reports investigating the plasma concentration after orally administering mice with 10 mg/kg regorafenib [427]. While we used the same vehicle as in the study performed by Kort et *al.* [427], pharmacodynamics were determined in FVB mice instead of C57BL/6 mice used in this thesis. In addition, only 10 mg/kg regorafenib were administered before measuring regorafenib concentrations in the plasma over time, while we mostly used 30 mg/kg regorafenib. Further, we induced acute inflammation in the peritoneum but regorafenib concentrations in the peritoneum over time were not measured. Therefore, measuring plasma and peritoneal regorafenib levels in C57BL/6 mice after oral administration with 10 mg/kg and 30 mg/kg regorafenib would be useful to understand the pharmacodynamics of the TKI in our *in vivo* model of acute inflammation.

In our *in vivo* studies, we compared the anti-inflammatory effects of 10 mg/kg and 30 mg/kg regorafenib in MSU crystal-induced peritonitis at 4 h. We decided to use 30 mg/kg regorafenib in further studies as the higher dose more effectively reduced neutrophil influx and only 30 mg/kg regorafenib significantly reduced IL-1β and CCL2 levels in the peritoneum compared to vehicle (Fig. 4.7). Our dosing regimen designed around the pharmacokinetics of regorafenib required three oral drug doses within 30 h. Therefore, we administered 90 mg/kg regorafenib within 30 h, which corresponds to the amount of regorafenib cancer patients take over 3.6 days. While lower regorafenib doses may not have sufficient anti-inflammatory effects, the high regorafenib dose required to suppress inflammation *in vivo* may make it difficult to translate our animal studies into the clinic.

As described above, regorafenib frequently causes liver toxicity in cancer patients, which can result in severe liver damage and even death [789, 793]. In addition, regorafenib has been shown to cause neutropenia, which may explain some of the TKI's effects on neutrophil infiltration during inflammation [786, 787]. Considering that regorafenib was administered at 3.6 times the daily dose within 30 h, side effects may be even more severe. Here, we observed the reduction of liver function as indicated by elevated serum bilirubin levels and possibly the onset of liver damage indicated by elevated ALT and AST serum levels after three oral doses of regorafenib. While the drug repurposing candidate did not cause gastrointestinal damage in mice, unlike NSAID indomethacin, the high dose required for the anti-inflammatory effect of regorafenib *in vivo* combined with its liver toxicity could severely limit its use as a therapeutic for acute gout flare-ups. However, by comparing regorafenib to NSAID indomethacin, we did demonstrate that TKIs could represent a new class of anti-inflammatory drugs and our drug repurposing strategy could be employed to identify other tyrosine kinase inhibitors with more favorable side effect profiles.

Adverse effects of tyrosine kinase inhibitors are thought to mostly be due to off-target effects. Sorafenib was shown to be relatively promiscuous, especially since it bound approx. 10 % of kinases with an affinity in the 10-fold range of that of primary target VEGFR, unlike most other tested kinase inhibitors [794-796]. Regorafenib has an even broader kinase target spectrum than sorafenib [621], indicating even lower selectivity and explaining the more frequent hepatotoxic events observed in patients. The risk of developing these side effects may be outweighed by the benefits of sorafenib or regorafenib treatment in cancer, but this may not be the case in other disorders like inflammatory diseases. Therefore, future efforts could focus on minimizing adverse events by reducing off-target effects through targeted drug delivery. This was shown to be an effective strategy to reduce inflammation and prevent systemic adverse effects [931].

Macrophage-specific drug delivery can be achieved by coupling drugs to nanocarrier dextran sulfate, which is recognized by class A scavenger receptors on inflammatory macrophages [803-805]. Other studies used “eat me” signal phosphatidylserine (PS)-containing liposomes to target anti-inflammatory cytokine IL-10 or diabetes drug pioglitazone to macrophages, resulting in anti-inflammatory *in vivo* effects mediated by macrophage M2 polarization [931-934]. A similar strategy could be employed to specifically target regorafenib to pro-inflammatory macrophages to minimize off-target effects and associated adverse events.

A recent study demonstrated that intra-articular treatment of mice with MSU crystal-induced acute arthritis with PLGA nanoparticles containing the TKI imatinib can significantly reduce disease severity and allow for the use of lower therapeutic doses by prolonging the drug’s half-life [687]. This strategy could help reduce rapid metabolization and dose-related side effects of regorafenib.

Alternatively, regorafenib could be used as a pharmacological scaffold serving as a starting point for drug re-engineering efforts. This strategy may lack many benefits of drug repurposing but could identify structurally similar compounds with enhanced anti-inflammatory effects and reduced side effect profiles. In addition, computational shape similarity methods like the widely used Rapid Overlay of Chemical Structures (ROCS) or Quantitative Structure-Activity Relationship (QSAR) models could be employed to find compounds with closely related structures or predicted on-target activity and have proven helpful in identifying novel anti-inflammatories [935-938].

In this thesis, I have demonstrated that our drug repurposing pipeline, which includes cell-based screening using macrophage/monocyte reporter cell lines, subsequent hit validation using primary murine and human macrophages and finally *in vivo* studies using a simple model of acute peritoneal inflammation, is a robust strategy to identify novel anti-inflammatory properties of FDA-approved medicines. Based on previous drug repurposing studies in the lab that identified anti-inflammatory activities of approved KIs [377, 939], we decided to screen a panel of 80 kinase inhibitor tool compounds as a basis for further drug repurposing screens. Considering the side effect profiles of many kinase inhibitors due to off-target effects and the challenges of developing KIs that are entirely specific to one kinase [782, 940], future drug repurposing efforts could include a wider variety of drug classes. In addition, we screened only a limited number of compounds. Therefore, screening more FDA-approved medicines or late-stage clinical trial candidates could identify drugs with enhanced anti-inflammatory activities and more favorable side effect profiles compared to regorafenib.

With artificial intelligence (AI)-based drug repurposing strategies becoming increasingly sophisticated [498, 941], such approaches could be coupled with our cell-based drug repurposing screen and subsequent *in vivo* studies to identify new indications for existing medicines [441]. AI-based method deepDTnet for example was developed to identify

new drug-target interactions based on previously reported interactions. The system contains complex chemical, phenotypic and genomic data sets and was employed to screen a library containing FDA-approved compounds [498]. DeepDTnet successfully identified drugs interacting with transcription factor ROR-γt, which regulates Th17 cell differentiation and is therefore linked to the pathology of inflammatory diseases such as MS [498, 941]. The study identified anti-cancer drug topotecan as a drug repurposing candidate, which was confirmed in the EAE *in vivo* model of MS [498]. This study demonstrates that AI approaches can successfully integrate information on drugs, diseases and targets/genes to predict promising drug repurposing candidates, which can subsequently be tested in *in vitro* and *in vivo* studies to validate anti-inflammatory activities.

While regorafenib had promising efficacy towards reducing inflammation, it is unlikely to be a viable candidate for the treatment of anti-inflammatory diseases on account of its hepatotoxicity. However, I have demonstrated in this study that our drug repurposing approach relying on a robust NF-κB macrophage/monocyte reporter assay can identify drug repurposing candidates with new anti-inflammatory properties in macrophages, which translated into *in vivo* studies of acute inflammation. Therefore, this approach presents a promising strategy to identify more anti-inflammatory medicines to address the increasing need for new effective and safe anti-inflammatory drugs.

References

1. Medzhitov, R., *Origin and physiological roles of inflammation.* Nature, 2008. **454**(7203): p. 428-435.
2. Iqbal, A.J., E.A. Fisher, and D.R. Greaves, *Inflammation-a Critical Appreciation of the Role of Myeloid Cells.* Microbiol Spectr, 2016. **4**(5).
3. Millman, A., et al., *An expanded arsenal of immune systems that protect bacteria from phages.* Cell Host & Microbe, 2022. **30**(11): p. 1556-1569.e5.
4. Wilkin, J., *Review of Pathologies on MOR 693: An Allosaurus from the Late Jurassic of Wyoming and Implications for Understanding Allosaur Immune Systems*. 2019.
5. Granger DN, S.E., *Chapter 2, Historical Perspectives*, in *Inflammation and the Microcirculation*. 2010, Morgan & Claypool Life Sciences: San Rafael (CA).
6. Ley, K., *Chapter 1, History of inflammation research*, in *Physiology of Inflammation*. 2001, Oxford University Press. p. 1-10.
7. Metchnikoff, E., *Lectures on the comparative pathology of inflammation delivered at the Pasteur Institute in 1891*. 1893: Рипол Классик.
8. Underhill, D.M., et al., *Élie Metchnikoff (1845–1916): celebrating 100 years of cellular immunology and beyond.* Nature Reviews Immunology, 2016. **16**(10): p. 651-656.
9. Gordon, S., *Elie Metchnikoff, the Man and the Myth.* Journal of Innate Immunity, 2016. **8**(3): p. 223-227.
10. Tauber, A.I., *Metchnikoff and the phagocytosis theory.* Nature Reviews Molecular Cell Biology, 2003. **4**(11): p. 897-901.
11. Cannon, W.B., *ORGANIZATION FOR PHYSIOLOGICAL HOMEOSTASIS.* Physiological Reviews, 1929. **9**(3): p. 399-431.
12. Billman, G.E., *Homeostasis: The Underappreciated and Far Too Often Ignored Central Organizing Principle of Physiology.* Front Physiol, 2020. **11**: p. 200.
13. Meizlish, M.L., et al., *Tissue Homeostasis and Inflammation.* Annual Review of Immunology, 2021. **39**(1): p. 557-581.
14. Feehan, K.T. and D.W. Gilroy, *Is Resolution the End of Inflammation?* Trends in Molecular Medicine, 2019. **25**(3): p. 198-214.
15. Kolaczkowska, E. and P. Kubes, *Neutrophil recruitment and function in health and inflammation.* Nature Reviews Immunology, 2013. **13**(3): p. 159-175.
16. Fullerton, J.N. and D.W. Gilroy, *Resolution of inflammation: a new therapeutic frontier.* Nature Reviews Drug Discovery, 2016. **15**(8): p. 551-567.
17. Serhan, C.N., et al., *Resolution of inflammation: state of the art, definitions and terms.* Faseb j, 2007. **21**(2): p. 325-32.
18. Gilroy, D. and R. De Maeyer. *New insights into the resolution of inflammation*. in *Seminars in immunology*. 2015. Elsevier.
19. Newson, J., et al., *Resolution of acute inflammation bridges the gap between innate and adaptive immunity.* Blood, The Journal of the American Society of Hematology, 2014. **124**(11): p. 1748-1764.
20. León, B., M. López-Bravo, and C. Ardavín, *Monocyte-derived dendritic cells formed at the infection site control the induction of protective T helper 1 responses against Leishmania.* Immunity, 2007. **26**(4): p. 519-531.
21. Yona, S., et al., *Fate mapping reveals origins and dynamics of monocytes and tissue macrophages under homeostasis.* Immunity, 2013. **38**(1): p. 79-91.
22. Marshall, J.S., et al., *An introduction to immunology and immunopathology.* Allergy, Asthma & Clinical Immunology, 2018. **14**(2): p. 49.
23. Roh, J.S. and D.H. Sohn, *Damage-Associated Molecular Patterns in Inflammatory Diseases.* Immune Netw, 2018. **18**(4): p. e27.

24. Brubaker, S.W., et al., *Innate Immune Pattern Recognition: A Cell Biological Perspective.* Annual Review of Immunology, 2015. **33**(1): p. 257-290.
25. Li, D. and M. Wu, *Pattern recognition receptors in health and diseases.* Signal Transduction and Targeted Therapy, 2021. **6**(1): p. 291.
26. Baines, K.J., J.L. Simpson, and P.G. Gibson, *17 - Biology of Neutrophils*, in *Middleton's Allergy (Eighth Edition)*, N.F. Adkinson, et al., Editors. 2014, W.B. Saunders: London. p. 280-291.
27. Hoffbrand, V., *Phagocytes*, in *Hoffbrand's Essential Haematology*. 2024, Wiley.
28. Evrard, M., et al., *Developmental Analysis of Bone Marrow Neutrophils Reveals Populations Specialized in Expansion, Trafficking, and Effector Functions.* Immunity, 2018. **48**(2): p. 364-379.e8.
29. Othman, A., M. Sekheri, and J.G. Filep, *Roles of neutrophil granule proteins in orchestrating inflammation and immunity.* The FEBS Journal, 2022. **289**(14): p. 3932-3953.
30. Rørvig, S., et al., *Ficolin-1 is present in a highly mobilizable subset of human neutrophil granules and associates with the cell surface after stimulation with fMLP.* Journal of leukocyte biology, 2009. **86**(6): p. 1439-1449.
31. Christoffersson, G. and M. Phillipson, *The neutrophil: one cell on many missions or many cells with different agendas?* Cell and Tissue Research, 2018. **371**(3): p. 415-423.
32. de Oliveira, S., E.E. Rosowski, and A. Huttenlocher, *Neutrophil migration in infection and wound repair: going forward in reverse.* Nat Rev Immunol, 2016. **16**(6): p. 378-91.
33. Park, S.A. and Y.M. Hyun, *Neutrophil Extravasation Cascade: What Can We Learn from Two-photon Intravital Imaging?* Immune Netw, 2016. **16**(6): p. 317-321.
34. Song, Z., et al., *Molecular regulation of neutrophil swarming in health and disease: Lessons from the phagocyte oxidase.* iScience, 2023. **26**(10): p. 108034.
35. Brown, L. and B.G. Yipp, *Neutrophil swarming: Is a good offense the best defense?* iScience, 2023. **26**(9): p. 107655.
36. Pérez-Figueroa, E., et al., *Neutrophils: Many Ways to Die.* Frontiers in Immunology, 2021. **12**.
37. Colotta, F., et al., *Modulation of granulocyte survival and programmed cell death by cytokines and bacterial products.* Blood, 1992. **80**(8): p. 2012-2020.
38. Lee, A., M.K.B. Whyte, and C. Haslett, *Inhibition of apoptosis and prolongation of neutrophil functional longevity by inflammatory mediators.* Journal of Leukocyte Biology, 1993. **54**(4): p. 283-288.
39. Kobayashi, Y., *The role of chemokines in neutrophil biology.* Front Biosci, 2008. **13**: p. 2400-7.
40. Xu, Q., et al., *Neutrophil reverse migration.* Journal of Inflammation, 2022. **19**(1): p. 22.
41. Leiding, J.W., *Neutrophil Evolution and Their Diseases in Humans.* Front Immunol, 2017. **8**: p. 1009.
42. Mank V, A.W., Brown K. *Leukocytosis*. StatPearls 2023 4.12.2023 [cited 2024 3.1.]; Available from: https://www.ncbi.nlm.nih.gov/books/NBK560882/.
43. Ferrata, A. and A. Pappenheim, *Ueber die verschiedenen Lymphoiden Zellformen des normalen und pathologischen Blutes.* Folia Haematol I Teil Arch, 1910.
44. Ginhoux, F. and S. Jung, *Monocytes and macrophages: developmental pathways and tissue homeostasis.* Nature Reviews Immunology, 2014. **14**(6): p. 392-404.
45. Shi, C. and E.G. Pamer, *Monocyte recruitment during infection and inflammation.* Nat Rev Immunol, 2011. **11**(11): p. 762-74.
46. Auffray, C., et al., *Monitoring of blood vessels and tissues by a population of monocytes with patrolling behavior.* Science, 2007. **317**(5838): p. 666-670.

47. Tsou, C.-L., et al., *Critical roles for CCR2 and MCP-3 in monocyte mobilization from bone marrow and recruitment to inflammatory sites.* The Journal of clinical investigation, 2007. **117**(4): p. 902-909.
48. Wolf, A.A., et al., *The Ontogeny of Monocyte Subsets.* Frontiers in Immunology, 2019. **10**.
49. Kapellos, T.S., et al., *Human Monocyte Subsets and Phenotypes in Major Chronic Inflammatory Diseases.* Frontiers in Immunology, 2019. **10**.
50. Guilliams, M., A. Mildner, and S. Yona, *Developmental and Functional Heterogeneity of Monocytes.* Immunity, 2018. **49**(4): p. 595-613.
51. Wagner, D.D. and P.S. Frenette, *The vessel wall and its interactions.* Blood, 2008. **111**(11): p. 5271-5281.
52. Nourshargh, S. and R. Alon, *Leukocyte Migration into Inflamed Tissues.* Immunity, 2014. **41**(5): p. 694-707.
53. Morikis, V.A. and S.I. Simon, *Neutrophil Mechanosignaling Promotes Integrin Engagement With Endothelial Cells and Motility Within Inflamed Vessels.* Frontiers in Immunology, 2018. **9**.
54. Gerhardt, T. and K. Ley, *Monocyte trafficking across the vessel wall.* Cardiovascular research, 2015. **107**(3): p. 321-330.
55. An, G., et al., *P-selectin glycoprotein ligand-1 is highly expressed on Ly-6Chi monocytes and a major determinant for Ly-6Chi monocyte recruitment to sites of atherosclerosis in mice.* Circulation, 2008. **117**(25): p. 3227-37.
56. Walcheck, B., et al., *Neutrophil-neutrophil interactions under hydrodynamic shear stress involve L-selectin and PSGL-1. A mechanism that amplifies initial leukocyte accumulation of P-selectin in vitro.* The Journal of clinical investigation, 1996. **98**(5): p. 1081-1087.
57. Medrano-Bosch, M., et al., *Monocyte-endothelial cell interactions in vascular and tissue remodeling.* Frontiers in Immunology, 2023. **14**.
58. Maas, S.L., O. Soehnlein, and J.R. Viola, *Organ-Specific Mechanisms of Transendothelial Neutrophil Migration in the Lung, Liver, Kidney, and Aorta.* Frontiers in Immunology, 2018. **9**.
59. Beat Imhof, Y.E., Abcam. *Leukocyte recruitment in inflammation*. 2011 [cited 2024 09.02.]; Available from: https://docs.abcam.com/pdf/cardiovascular/Leukocyte-Recruitment-in-Inflammation.pdf.
60. Proebstl, D., et al., *Pericytes support neutrophil subendothelial cell crawling and breaching of venular walls in vivo.* Journal of Experimental Medicine, 2012. **209**(6): p. 1219-1234.
61. Angelini, D.J., et al., *TNF-α increases tyrosine phosphorylation of vascular endothelial cadherin and opens the paracellular pathway through fyn activation in human lung endothelia.* American Journal of Physiology-Lung Cellular and Molecular Physiology, 2006. **291**(6): p. L1232-L1245.
62. Pérez Castrillón, J.L., et al., *Leukocyte chemotaxis.* Allergol Immunopathol (Madr), 1988. **16**(4): p. 279-83.
63. Leber, T., *Die Entstehung der Entzündung und die Wirkung der entzündungerregenden Schädlichkeiten: nach vorzugsweise am Auge angestellten Untersuchungen*. 1891: Engelmann.
64. Rumianek, A.N. and D.R. Greaves, *How Have Leukocyte In Vitro Chemotaxis Assays Shaped Our Ideas about Macrophage Migration?* Biology (Basel), 2020. **9**(12).
65. Frow, E.K., J. Reckless, and D.J. Grainger, *Tools for anti-inflammatory drug design: In vitro models of leukocyte migration.* Medicinal Research Reviews, 2004. **24**(3): p. 276-298.

66. Petri, B. and M.-J. Sanz, *Neutrophil chemotaxis.* Cell and Tissue Research, 2018. **371**(3): p. 425-436.
67. Hughes, C.E. and R.J.B. Nibbs, *A guide to chemokines and their receptors.* Febs j, 2018. **285**(16): p. 2944-2971.
68. Zarbock, A. and K. Ley, *Mechanisms and consequences of neutrophil interaction with the endothelium.* The American journal of pathology, 2008. **172**(1): p. 1-7.
69. Kamp, M.E., Y. Liu, and A. Kortholt, *Function and Regulation of Heterotrimeric G Proteins during Chemotaxis.* Int J Mol Sci, 2016. **17**(1).
70. Li, Z., et al., *Directional Sensing Requires Gβγ-Mediated PAK1 and PIXα-Dependent Activation of Cdc42.* Cell, 2003. **114**(2): p. 215-227.
71. Manser, E., et al., *PAK kinases are directly coupled to the PIX family of nucleotide exchange factors.* Molecular cell, 1998. **1**(2): p. 183-192.
72. Daniels, R.H., F.T. Zenke, and G.M. Bokoch, *αPix stimulates p21-activated kinase activity through exchange factor-dependent and-independent mechanisms.* Journal of Biological Chemistry, 1999. **274**(10): p. 6047-6050.
73. Metzemaekers, M., M. Gouwy, and P. Proost, *Neutrophil chemoattractant receptors in health and disease: double-edged swords.* Cellular & Molecular Immunology, 2020. **17**(5): p. 433-450.
74. Dong, X., et al., *P-Rex1 is a primary Rac2 guanine nucleotide exchange factor in mouse neutrophils.* Current Biology, 2005. **15**(20): p. 1874-1879.
75. Kunisaki, Y., et al., *DOCK2 is a Rac activator that regulates motility and polarity during neutrophil chemotaxis.* The Journal of cell biology, 2006. **174**(5): p. 647-652.
76. Hannigan, M., et al., *Neutrophils lacking phosphoinositide 3-kinase γ show loss of directionality during N-formyl-Met-Leu-Phe-induced chemotaxis.* Proceedings of the National Academy of Sciences, 2002. **99**(6): p. 3603-3608.
77. Pollitt, A.Y. and R.H. Insall, *WASP and SCAR/WAVE proteins: the drivers of actin assembly.* J Cell Sci, 2009. **122**(Pt 15): p. 2575-8.
78. Inoue, T. and T. Meyer, *Synthetic activation of endogenous PI3K and Rac identifies an AND-gate switch for cell polarization and migration.* PloS one, 2008. **3**(8): p. e3068.
79. Tang, W., et al., *A PLCβ/PI3Kγ-GSK3 signaling pathway regulates cofilin phosphatase slingshot2 and neutrophil polarization and chemotaxis.* Dev Cell, 2011. **21**(6): p. 1038-50.
80. Li, H., et al., *Association between Gαi2 and ELMO1/Dock180 connects chemokine signalling with Rac activation and metastasis.* Nature communications, 2013. **4**(1): p. 1706.
81. Wu, J., et al., *Homer3 regulates the establishment of neutrophil polarity.* Molecular biology of the cell, 2015. **26**(9): p. 1629-1639.
82. Kamakura, S., et al., *The cell polarity protein mInsc regulates neutrophil chemotaxis via a noncanonical G protein signaling pathway.* Developmental cell, 2013. **26**(3): p. 292-302.
83. Mao, J., et al., *Guanine nucleotide exchange factor GEF115 specifically mediates activation of Rho and serum response factor by the G protein alpha subunit Galpha13.* Proc Natl Acad Sci U S A, 1998. **95**(22): p. 12973-6.
84. Kozasa, T., et al., *p115 RhoGEF, a GTPase Activating Protein for Gα₁₂ and Gα₁₃.* Science, 1998. **280**(5372): p. 2109-2111.
85. Hart, M.J., et al., *Direct Stimulation of the Guanine Nucleotide Exchange Activity of p115 RhoGEF by Gα₁₃.* Science, 1998. **280**(5372): p. 2112-2114.
86. Gambardella, L. and S. Vermeren, *Molecular players in neutrophil chemotaxis—focus on PI3K and small GTPases.* Journal of Leukocyte Biology, 2013. **94**(4): p. 603-612.

87. Hirsch, E., et al., *Central Role for G Protein-Coupled Phosphoinositide 3-Kinase γ in Inflammation.* Science, 2000. **287**(5455): p. 1049-1053.
88. Sasaki, T., et al., *Function of PI3Kγ in thymocyte development, T cell activation, and neutrophil migration.* Science, 2000. **287**(5455): p. 1040-1046.
89. Funamoto, S., et al., *Spatial and temporal regulation of 3-phosphoinositides by PI 3-kinase and PTEN mediates chemotaxis.* Cell, 2002. **109**(5): p. 611-623.
90. Iijima, M. and P. Devreotes, *Tumor suppressor PTEN mediates sensing of chemoattractant gradients.* Cell, 2002. **109**(5): p. 599-610.
91. Li, Z., et al., *Regulation of PTEN by Rho small GTPases.* Nature cell biology, 2005. **7**(4): p. 399-404.
92. Cui, K., et al., *Distinct Migratory Properties of M1, M2, and Resident Macrophages Are Regulated by αDβ2 and αMβ2 Integrin-Mediated Adhesion.* Frontiers in Immunology, 2018. **9**.
93. Friedl, P. and B. Weigelin, *Interstitial leukocyte migration and immune function.* Nature Immunology, 2008. **9**(9): p. 960-969.
94. Horwitz, R. and D. Webb, *Cell migration.* Current Biology, 2003. **13**(19): p. R756-R759.
95. Webb, S.E., J.W. Pollard, and G.E. Jones, *Direct observation and quantification of macrophage chemoattraction to the growth factor CSF-1.* Journal of Cell Science, 1996. **109**(4): p. 793-803.
96. KANAGASUNDARAM, V., A. JAWOROWSKI, and J.A. HAMILTON, *Association between phosphatidylinositol-3 kinase, Cbl and other tyrosine phosphorylated proteins in colony-stimulating factor-1-stimulated macrophages.* Biochemical Journal, 1996. **320**(1): p. 69-77.
97. Vanhaesebroeck, B., et al., *Distinct PI (3) Ks mediate mitogenic signalling and cell migration in macrophages.* Nature cell biology, 1999. **1**(1): p. 69-71.
98. Jones, G.E., *Cellular signaling in macrophage migration and chemotaxis.* Journal of Leukocyte Biology, 2000. **68**(5): p. 593-602.
99. Lin, E.Y., et al., *Colony-stimulating factor 1 promotes progression of mammary tumors to malignancy.* J Exp Med, 2001. **193**(6): p. 727-40.
100. Wyckoff, J., et al., *A paracrine loop between tumor cells and macrophages is required for tumor cell migration in mammary tumors.* Cancer Res, 2004. **64**(19): p. 7022-9.
101. Pierce, J.H., et al., *Macrophage-colony-stimulating factor (CSF-1) induces proliferation, chemotaxis, and reversible monocytic differentiation in myeloid progenitor cells transfected with the human c-fms/CSF-1 receptor cDNA.* Proceedings of the National Academy of Sciences of the United States of America, 1990. **87**(15): p. 5613-5617.
102. Webb, S.E., J.W. Pollard, and G.E. Jones, *Direct observation and quantification of macrophage chemoattraction to the growth factor CSF-1.* J Cell Sci, 1996. **109 (Pt 4)**: p. 793-803.
103. Nakano, K., et al., *Rheumatoid synovial endothelial cells produce macrophage colony-stimulating factor leading to osteoclastogenesis in rheumatoid arthritis.* Rheumatology, 2006. **46**(4): p. 597-603.
104. Park, Y.M. and B.S. Bochner, *Eosinophil survival and apoptosis in health and disease.* Allergy Asthma Immunol Res, 2010. **2**(2): p. 87-101.
105. Roitt, I.M., J. Brostoff, and D.K. Male, *Immunology*. 2001: Mosby.
106. Yousefi, S., et al., *Catapult-like release of mitochondrial DNA by eosinophils contributes to antibacterial defense.* Nature medicine, 2008. **14**(9): p. 949-953.
107. Rosenberg, H.F. and J.B. Domachowske, *Eosinophils, eosinophil ribonucleases, and their role in host defense against respiratory virus pathogens.* Journal of leukocyte biology, 2001. **70**(5): p. 691-698.

108. Adamko, D.J., et al., *Ovalbumin sensitization changes the inflammatory response to subsequent parainfluenza infection: eosinophils mediate airway hyperresponsiveness, M2 muscarinic receptor dysfunction, and antiviral effects.* The Journal of experimental medicine, 1999. **190**(10): p. 1465-1478.
109. Inoue, Y., et al., *Nonpathogenic, environmental fungi induce activation and degranulation of human eosinophils.* The Journal of Immunology, 2005. **175**(8): p. 5439-5447.
110. Rubin, E. and F. Gorstein, *Rubin's Pathology: Clinicopathologic Foundations of Medicine*. 2004: Lippincott Williams & Wilkins.
111. Stone, K.D., C. Prussin, and D.D. Metcalfe, *IgE, mast cells, basophils, and eosinophils.* J Allergy Clin Immunol, 2010. **125**(2 Suppl 2): p. S73-80.
112. Gurish, Michael F. and K.F. Austen, *Developmental Origin and Functional Specialization of Mast Cell Subsets.* Immunity, 2012. **37**(1): p. 25-33.
113. Abraham, S.N. and A.L. St John, *Mast cell-orchestrated immunity to pathogens.* Nat Rev Immunol, 2010. **10**(6): p. 440-52.
114. Miyake, K., J. Ito, and H. Karasuyama, *Role of Basophils in a Broad Spectrum of Disorders.* Frontiers in Immunology, 2022. **13**.
115. Patente, T.A., et al., *Human Dendritic Cells: Their Heterogeneity and Clinical Application Potential in Cancer Immunotherapy.* Frontiers in Immunology, 2019. **9**.
116. Steinman , R.M. and Z.A. Cohn *IDENTIFICATION OF A NOVEL CELL TYPE IN PERIPHERAL LYMPHOID ORGANS OF MICE : I. MORPHOLOGY, QUANTITATION, TISSUE DISTRIBUTION.* Journal of Experimental Medicine, 1973. **137**(5): p. 1142-1162.
117. Collin, M. and V. Bigley, *Human dendritic cell subsets: an update.* Immunology, 2018. **154**(1): p. 3-20.
118. Balan, S., M. Saxena, and N. Bhardwaj, *Chapter One - Dendritic cell subsets and locations*, in *International Review of Cell and Molecular Biology*, C. Lhuillier and L. Galluzzi, Editors. 2019, Academic Press. p. 1-68.
119. Ye, Y., et al., *Plasmacytoid dendritic cell biology and its role in immune-mediated diseases.* Clin Transl Immunology, 2020. **9**(5): p. e1139.
120. Eisenbarth, S.C., *Dendritic cell subsets in T cell programming: location dictates function.* Nature Reviews Immunology, 2019. **19**(2): p. 89-103.
121. Scandella, E., et al., *CCL19/CCL21-triggered signal transduction and migration of dendritic cells requires prostaglandin E2.* Blood, 2004. **103**(5): p. 1595-601.
122. Banchereau, J. and R.M. Steinman, *Dendritic cells and the control of immunity.* Nature, 1998. **392**(6673): p. 245-252.
123. Tai, Y., et al., *Molecular Mechanisms of T Cells Activation by Dendritic Cells in Autoimmune Diseases.* Front Pharmacol, 2018. **9**: p. 642.
124. Domogalla, M.P., et al., *Tolerance through Education: How Tolerogenic Dendritic Cells Shape Immunity.* Frontiers in Immunology, 2017. **8**.
125. Merien, F., *A Journey with Elie Metchnikoff: From Innate Cell Mechanisms in Infectious Diseases to Quantum Biology.* Front Public Health, 2016. **4**: p. 125.
126. Metchnikoff, E., *Lectures on the Comparative Pathology of Inflammation* 1893, London: Kegan Paul, Trench, Trubner & Co.
127. Aschoff, L., *Das reticulo-endotheliale System*. 1924: Springer.
128. van Furth, R., et al., *The mononuclear phagocyte system: a new classification of macrophages, monocytes, and their precursor cells.* Bull World Health Organ, 1972. **46**(6): p. 845-52.
129. Van Furth, R., et al., *Methods for studying mononuclear phagocytes.* by DO Adams, PJ Edelson, and H. Koren, Academic Press, New York, 1981: p. 243-251.

130. Nussenzweig, M.C. and R.M. Steinman, *Contribution of dendritic cells to stimulation of the murine syngeneic mixed leukocyte reaction.* Journal of Experimental Medicine, 1980. **151**(5): p. 1196-1212.
131. Crocker, P. and S. Gordon, *Isolation and characterization of resident stromal macrophages and hematopoietic cell clusters from mouse bone marrow.* The Journal of experimental medicine, 1985. **162**(3): p. 993-1014.
132. Gordon, S. and A. Plüddemann, *Tissue macrophages: heterogeneity and functions.* BMC Biology, 2017. **15**(1): p. 53.
133. Dobzhansky, T., *Nothing in Biology Makes Sense except in the Light of Evolution.* The American Biology Teacher, 1973. **35**(3): p. 125-129.
134. Fenton, C., *Siamon Gordon: The Father of F4/80*, S. Gordon, Editor. 2023, BioRad.
135. van Furth, R. and Z.A. Cohn, *The origin and kinetics of mononuclear phagocytes.* J Exp Med, 1968. **128**(3): p. 415-35.
136. van Furth, R. and M.M. Diesselhoff-den Dulk, *Dual origin of mouse spleen macrophages.* J Exp Med, 1984. **160**(5): p. 1273-83.
137. Hashimoto, D., et al., *Tissue-resident macrophages self-maintain locally throughout adult life with minimal contribution from circulating monocytes.* Immunity, 2013. **38**(4): p. 792-804.
138. Epelman, S., Kory J. Lavine, and Gwendalyn J. Randolph, *Origin and Functions of Tissue Macrophages.* Immunity, 2014. **41**(1): p. 21-35.
139. Bogunovic, M., et al., *Origin of the lamina propria dendritic cell network.* Immunity, 2009. **31**(3): p. 513-525.
140. Tamoutounour, S., et al., *Origins and functional specialization of macrophages and of conventional and monocyte-derived dendritic cells in mouse skin.* Immunity, 2013. **39**(5): p. 925-938.
141. A-Gonzalez, N., et al., *The nuclear receptor LXRα controls the functional specialization of splenic macrophages.* Nature immunology, 2013. **14**(8): p. 831-839.
142. Gomez Perdiguero, E., et al., *Tissue-resident macrophages originate from yolk-sac-derived erythro-myeloid progenitors.* Nature, 2015. **518**(7540): p. 547-551.
143. Ginhoux, F. and M. Guilliams, *Tissue-Resident Macrophage Ontogeny and Homeostasis.* Immunity, 2016. **44**(3): p. 439-449.
144. Wu, Y. and K.K. Hirschi, *Tissue-Resident Macrophage Development and Function.* Front Cell Dev Biol, 2020. **8**: p. 617879.
145. Stein, M., et al., *Interleukin 4 potently enhances murine macrophage mannose receptor activity: a marker of alternative immunologic macrophage activation.* Journal of Experimental Medicine, 1992. **176**(1): p. 287-292.
146. Doyle, A.G., et al., *Interleukin-13 alters the activation state of murine macrophages in vitro: Comparison with interleukin-4 and interferon-γ.* European Journal of Immunology, 1994. **24**(6): p. 1441-1445.
147. Nathan, C.F., et al., *Identification of interferon-gamma as the lymphokine that activates human macrophage oxidative metabolism and antimicrobial activity.* The Journal of experimental medicine, 1983. **158**(3): p. 670-689.
148. Mosmann, T.R., et al., *Two types of murine helper T cell clone. I. Definition according to profiles of lymphokine activities and secreted proteins.* The Journal of Immunology, 1986. **136**(7): p. 2348-2357.
149. Mills, C.D., et al., *M-1/M-2 Macrophages and the Th1/Th2 Paradigm1.* The Journal of Immunology, 2000. **164**(12): p. 6166-6173.
150. Mantovani, A., et al., *The chemokine system in diverse forms of macrophage activation and polarization.* Trends in Immunology, 2004. **25**(12): p. 677-686.

151. Rőszer, T., *Understanding the Mysterious M2 Macrophage through Activation Markers and Effector Mechanisms.* Mediators Inflamm, 2015. **2015**: p. 816460.
152. Liu, Y., et al., *Metabolic reprogramming in macrophage responses.* Biomarker Research, 2021. **9**(1): p. 1.
153. Martinez, F.O. and S. Gordon, *The M1 and M2 paradigm of macrophage activation: time for reassessment.* F1000Prime Rep, 2014. **6**: p. 13.
154. Murray, P.J., *Macrophage Polarization.* Annual Review of Physiology, 2017. **79**(1): p. 541-566.
155. Davis, M.J., et al., *Macrophage M1/M2 polarization dynamically adapts to changes in cytokine microenvironments in Cryptococcus neoformans infection.* mBio, 2013. **4**(3): p. e00264-13.
156. Murray, P.J., et al., *Macrophage activation and polarization: nomenclature and experimental guidelines.* Immunity, 2014. **41**(1): p. 14-20.
157. Xuan, W., et al., *The chemotaxis of M1 and M2 macrophages is regulated by different chemokines.* Journal of Leukocyte Biology, 2014. **97**(1): p. 61-69.
158. Biorad. *Mini-review: Macrophage Polarization*. [cited 2024 11.03.]; Available from: https://www.bio-rad-antibodies.com/macrophage-polarization-minireview.html.
159. Gensel, J.C., et al., *Predictive screening of M1 and M2 macrophages reveals the immunomodulatory effectiveness of post spinal cord injury azithromycin treatment.* Scientific Reports, 2017. **7**(1): p. 40144.
160. Arango Duque, G. and A. Descoteaux, *Macrophage cytokines: involvement in immunity and infectious diseases.* Front Immunol, 2014. **5**: p. 491.
161. Dinarello, C.A., *Historical insights into cytokines.* Eur J Immunol, 2007. **37 Suppl 1**(Suppl 1): p. S34-45.
162. Murphy, K.M., C. Weaver, and C. Janeway, *Janeway's Immunobiology*. 2017: Garland Science.
163. García Morán GA, P.-M.R., Cardona AG, *Cytokines, chemokines and growth factors*, in *Autoimmunity: From Bench to Bedside*, S.Y. Anaya JM, Rojas-Villarraga A, Editor. 2013, Bogota (Colombia): El Rosario University.
164. Zhang, J.M. and J. An, *Cytokines, inflammation, and pain.* Int Anesthesiol Clin, 2007. **45**(2): p. 27-37.
165. Unanue, E., et al., *Regulation of immunity and inflammation by mediators from macrophages.* The American journal of pathology, 1976. **85**(2): p. 465.
166. Neurath, M.F., *Cytokines in inflammatory bowel disease.* Nature Reviews Immunology, 2014. **14**(5): p. 329-342.
167. Schulte, W., J. Bernhagen, and R. Bucala, *Cytokines in sepsis: potent immunoregulators and potential therapeutic targets--an updated view.* Mediators Inflamm, 2013. **2013**: p. 165974.
168. Hasanvand, A., *COVID-19 and the role of cytokines in this disease.* Inflammopharmacology, 2022. **30**(3): p. 789-798.
169. Comerford, I. and S.R. McColl, *Mini-review series: focus on chemokines.* Immunology & Cell Biology, 2011. **89**(2): p. 183-184.
170. Davenport, R.D., *An introduction to chemokines and their roles in transfusion medicine.* Vox Sanguinis, 2009. **96**(3): p. 183-198.
171. Raman, D., T. Sobolik-Delmaire, and A. Richmond, *Chemokines in health and disease.* Exp Cell Res, 2011. **317**(5): p. 575-89.
172. Pelus, L.M. and S. Fukuda, *Peripheral blood stem cell mobilization: The CXCR2 ligand GROβ rapidly mobilizes hematopoietic stem cells with enhanced engraftment properties.* Experimental Hematology, 2006. **34**(8): p. 1010-1020.

173. Moser, B., et al., *Neutrophil-activating properties of the melanoma growth-stimulatory activity.* Journal of Experimental Medicine, 1990. **171**(5): p. 1797-1802.
174. Schumacher, C., et al., *High- and low-affinity binding of GRO alpha and neutrophil-activating peptide 2 to interleukin 8 receptors on human neutrophils.* Proc Natl Acad Sci U S A, 1992. **89**(21): p. 10542-6.
175. Appay, V. and S.L. Rowland-Jones, *RANTES: a versatile and controversial chemokine.* Trends Immunol, 2001. **22**(2): p. 83-7.
176. Lee, D., et al., *CXCL5 secreted from macrophages during cold exposure mediates white adipose tissue browning.* J Lipid Res, 2021. **62**: p. 100117.
177. Deng, J., et al., *CXCL5: A coachman to drive cancer progression.* Frontiers in Oncology, 2022. **12**.
178. Chang, M.S., et al., *Cloning and characterization of the human neutrophil-activating peptide (ENA-78) gene.* J Biol Chem, 1994. **269**(41): p. 25277-82.
179. Vilotić, A., et al., *IL-6 and IL-8: An Overview of Their Roles in Healthy and Pathological Pregnancies.* Int J Mol Sci, 2022. **23**(23).
180. Petrovic-Djergovic, D., et al., *CXCL10 induces the recruitment of monocyte-derived macrophages into kidney, which aggravate puromycin aminonucleoside nephrosis.* Clin Exp Immunol, 2015. **180**(2): p. 305-15.
181. Leventis, P.A. and S. Grinstein, *The distribution and function of phosphatidylserine in cellular membranes.* Annual review of biophysics, 2010. **39**: p. 407-427.
182. Truman, L.A., et al., *CX3CL1/fractalkine is released from apoptotic lymphocytes to stimulate macrophage chemotaxis.* Blood, The Journal of the American Society of Hematology, 2008. **112**(13): p. 5026-5036.
183. Fukumoto, N., et al., *Critical roles of CXC chemokine ligand 16/scavenger receptor that binds phosphatidylserine and oxidized lipoprotein in the pathogenesis of both acute and adoptive transfer experimental autoimmune encephalomyelitis.* The Journal of Immunology, 2004. **173**(3): p. 1620-1627.
184. Pontejo, S.M. and P.M. Murphy, *Chemokines act as phosphatidylserine-bound "find-me" signals in apoptotic cell clearance.* PLoS Biol, 2021. **19**(5): p. e3001259.
185. Palmieri, E.M., et al., *Nitric Oxide in Macrophage Immunometabolism: Hiding in Plain Sight.* Metabolites, 2020. **10**(11).
186. Tripathi, P., et al., *The role of nitric oxide in inflammatory reactions.* FEMS Immunology & Medical Microbiology, 2007. **51**(3): p. 443-452.
187. Brunet, L.R., *Nitric oxide in parasitic infections.* Int Immunopharmacol, 2001. **1**(8): p. 1457-67.
188. Rath, M., et al., *Metabolism via Arginase or Nitric Oxide Synthase: Two Competing Arginine Pathways in Macrophages.* Front Immunol, 2014. **5**: p. 532.
189. Knab, K., D. Chambers, and G. Krönke, *Synovial Macrophage and Fibroblast Heterogeneity in Joint Homeostasis and Inflammation.* Frontiers in Medicine, 2022. **9**.
190. Culemann, S., et al., *Locally renewing resident synovial macrophages provide a protective barrier for the joint.* Nature, 2019. **572**(7771): p. 670-675.
191. Dehlin, M., L. Jacobsson, and E. Roddy, *Global epidemiology of gout: prevalence, incidence, treatment patterns and risk factors.* Nat Rev Rheumatol, 2020. **16**(7): p. 380-390.
192. Steiger, S. and J.L. Harper, *Mechanisms of Spontaneous Resolution of Acute Gouty Inflammation.* Current Rheumatology Reports, 2013. **16**(1): p. 392.
193. Jeong, J.H., et al., *Prominent Inflammatory Features of Monocytes/Macrophages in Acute Calcium Pyrophosphate Crystal Arthritis: a Comparison with Acute Gouty Arthritis.* Immune Netw, 2019. **19**(3): p. e21.

194. Jeong, J.H., et al., *CD14+ Cells with the Phenotype of Infiltrated Monocytes Consist of Distinct Populations Characterized by Anti-inflammatory as well as Pro-inflammatory Activity in Gouty Arthritis.* Frontiers in Immunology, 2017. **8**.
195. Lan, Z., et al., *Mechanosensitive TRPV4 is required for crystal-induced inflammation.* Annals of the Rheumatic Diseases, 2021. **80**(12): p. 1604-1614.
196. Zhao, L., et al., *Distinct macrophage polarization in acute and chronic gout.* Laboratory Investigation, 2022. **102**(10): p. 1054-1063.
197. Liu, L., et al., *Recent Insights Into the Role of Macrophages in Acute Gout.* Front Immunol, 2022. **13**: p. 955806.
198. Rose, D.M., et al., *Transglutaminase 2 limits murine peritoneal acute gout-like inflammation by regulating macrophage clearance of apoptotic neutrophils.* Arthritis & Rheumatism: Official Journal of the American College of Rheumatology, 2006. **54**(10): p. 3363-3371.
199. Savill, J.S., et al., *Macrophage phagocytosis of aging neutrophils in inflammation. Programmed cell death in the neutrophil leads to its recognition by macrophages.* The Journal of clinical investigation, 1989. **83**(3): p. 865-875.
200. Jeong, J.H., et al., *Neutrophil extracellular trap clearance by synovial macrophages in gout.* Arthritis Res Ther, 2021. **23**(1): p. 88.
201. Fadok, V.A., et al., *Macrophages that have ingested apoptotic cells in vitro inhibit proinflammatory cytokine production through autocrine/paracrine mechanisms involving TGF-beta, PGE2, and PAF.* The Journal of clinical investigation, 1998. **101**(4): p. 890-898.
202. Ren, Y. and J. Savill, *Proinflammatory cytokines potentiate thrombospondin-mediated phagocytosis of neutrophils undergoing apoptosis.* Journal of immunology (Baltimore, Md.: 1950), 1995. **154**(5): p. 2366-2374.
203. Martin, W.J., et al., *Monosodium urate monohydrate crystal–recruited noninflammatory monocytes differentiate into M1-like proinflammatory macrophages in a peritoneal murine model of gout.* Arthritis & Rheumatism, 2011. **63**(5): p. 1322-1332.
204. Kemble, S. and A.P. Croft, *Critical Role of Synovial Tissue–Resident Macrophage and Fibroblast Subsets in the Persistence of Joint Inflammation.* Frontiers in Immunology, 2021. **12**.
205. Landis, R.C., et al., *Safe disposal of inflammatory monosodium urate monohydrate crystals by differentiated macrophages.* Arthritis Rheum, 2002. **46**(11): p. 3026-33.
206. Fava, R., et al., *Active and latent forms of transforming growth factor beta activity in synovial effusions.* The Journal of experimental medicine, 1989. **169**(1): p. 291-296.
207. Scanu, A., et al., *Cytokine levels in human synovial fluid during the different stages of acute gout: role of transforming growth factor β1 in the resolution phase.* Annals of the rheumatic diseases, 2012. **71**(4): p. 621-624.
208. Yagnik, D.R., et al., *Macrophage release of transforming growth factor β1 during resolution of monosodium urate monohydrate crystal–induced inflammation.* Arthritis & Rheumatism, 2004. **50**(7): p. 2273-2280.
209. Xu, Y., et al., *Immune Effects of Macrophages in Rheumatoid Arthritis: A Bibliometric Analysis From 2000 to 2021.* Frontiers in Immunology, 2022. **13**.
210. Martin, W.J., M. Walton, and J. Harper, *Resident macrophages initiating and driving inflammation in a monosodium urate monohydrate crystal–induced murine peritoneal model of acute gout.* Arthritis & Rheumatism, 2009. **60**(1): p. 281-289.
211. Alivernini, S., et al., *Distinct synovial tissue macrophage subsets regulate inflammation and remission in rheumatoid arthritis.* Nature Medicine, 2020. **26**(8): p. 1295-1306.

212. Huang, Q.-Q., et al., *Critical role of synovial tissue–resident macrophage niche in joint homeostasis and suppression of chronic inflammation.* Science Advances, 2021. **7**(2): p. eabd0515.
213. Chakarov, S., et al., *Two distinct interstitial macrophage populations coexist across tissues in specific subtissular niches.* Science, 2019. **363**(6432): p. eaau0964.
214. Zhang, F., et al., *Defining inflammatory cell states in rheumatoid arthritis joint synovial tissues by integrating single-cell transcriptomics and mass cytometry.* Nature Immunology, 2019. **20**(7): p. 928-942.
215. Brunet, A., et al., *NR4A1-dependent Ly6Clow monocytes contribute to reducing joint inflammation in arthritic mice through Treg cells.* European Journal of Immunology, 2016. **46**(12): p. 2789-2800.
216. Misharin, A.V., et al., *Nonclassical Ly6C(-) monocytes drive the development of inflammatory arthritis in mice.* Cell Rep, 2014. **9**(2): p. 591-604.
217. Puchner, A., et al., *Non-classical monocytes as mediators of tissue destruction in arthritis.* Annals of the Rheumatic Diseases, 2018. **77**(10): p. 1490-1497.
218. Hirose, S., et al., *Monocyte subsets involved in the development of systemic lupus erythematosus and rheumatoid arthritis.* International Immunology, 2019. **31**(11): p. 687-696.
219. Kawanaka, N., et al., *CD14+, CD16+ blood monocytes and joint inflammation in rheumatoid arthritis.* Arthritis & Rheumatism, 2002. **46**(10): p. 2578-2586.
220. Rossol, M., et al., *The CD14brightCD16+ monocyte subset is expanded in rheumatoid arthritis and promotes expansion of the Th17 cell population.* Arthritis & Rheumatism, 2012. **64**(3): p. 671-677.
221. Tsukamoto, M., et al., *Increased circulating CD14brightCD16+ intermediate monocytes are regulated by TNF-α and IL-6 axis in accordance with disease activity in patients with rheumatoid arthritis.* Clin Exp Rheumatol, 2018. **36**(4): p. 540-544.
222. Tsukamoto, M., et al., *CD14 bright CD16+ intermediate monocytes are induced by interleukin-10 and positively correlate with disease activity in rheumatoid arthritis.* Arthritis research & therapy, 2017. **19**: p. 1-10.
223. Seeling, M., et al., *Inflammatory monocytes and Fcγ receptor IV on osteoclasts are critical for bone destruction during inflammatory arthritis in mice.* Proc Natl Acad Sci U S A, 2013. **110**(26): p. 10729-34.
224. Rana, A.K., et al., *Monocytes in rheumatoid arthritis: Circulating precursors of macrophages and osteoclasts and, their heterogeneity and plasticity role in RA pathogenesis.* International Immunopharmacology, 2018. **65**: p. 348-359.
225. Komano, Y., et al., *Identification of a human peripheral blood monocyte subset that differentiates into osteoclasts.* Arthritis Research & Therapy, 2006. **8**(5): p. R152.
226. Sprangers, S., et al., *Different Blood-Borne Human Osteoclast Precursors Respond in Distinct Ways to IL-17A.* Journal of Cellular Physiology, 2016. **231**(6): p. 1249-1260.
227. Xiao, Y. and L. Zhang, *Mechanistic and therapeutic insights into the function of NLRP3 inflammasome in sterile arthritis.* Frontiers in Immunology, 2023. **14**.
228. Wang, W., et al., *Targeting macrophage polarization as a promising therapeutic strategy for the treatment of osteoarthritis.* Int Immunopharmacol, 2023. **116**: p. 109790.
229. Park, J.-Y., et al., *Triamcinolone–Gold Nanoparticles Repolarize Synoviocytes and Macrophages in an Inflamed Synovium.* ACS Applied Materials & Interfaces, 2020. **12**(35): p. 38936-38949.
230. Vande Walle, L. and M. Lamkanfi, *Drugging the NLRP3 inflammasome: from signalling mechanisms to therapeutic targets.* Nat Rev Drug Discov, 2024. **23**(1): p. 43-66.

231. Klück, V., et al., *Dapansutrile, an oral selective NLRP3 inflammasome inhibitor, for treatment of gout flares: an open-label, dose-adaptive, proof-of-concept, phase 2a trial.* The Lancet Rheumatology, 2020. **2**(5): p. e270-e280.
232. Akira, S., S. Uematsu, and O. Takeuchi, *Pathogen recognition and innate immunity.* Cell, 2006. **124**(4): p. 783-801.
233. Duan, T., et al., *Toll-Like Receptor Signaling and Its Role in Cell-Mediated Immunity.* Frontiers in Immunology, 2022. **13**.
234. Iwasaki, A. and R. Medzhitov, *Toll-like receptor control of the adaptive immune responses.* Nature immunology, 2004. **5**(10): p. 987-995.
235. Sameer, A.S. and S. Nissar, *Toll-Like Receptors (TLRs): Structure, Functions, Signaling, and Role of Their Polymorphisms in Colorectal Cancer Susceptibility.* Biomed Res Int, 2021. **2021**: p. 1157023.
236. Anderson, K.V., G. Jürgens, and C. Nüsslein-Volhard, *Establishment of dorsal-ventral polarity in the Drosophila embryo: genetic studies on the role of the Toll gene product.* Cell, 1985. **42**(3): p. 779-789.
237. Lemaitre, B., et al., *The dorsoventral regulatory gene cassette spätzle/Toll/cactus controls the potent antifungal response in Drosophila adults.* Cell, 1996. **86**(6): p. 973-983.
238. Rosetto, M., et al., *Signals from the IL-1 Receptor Homolog, Toll, Can Activate an Immune Response in a Drosophila Hemocyte Cell Line.* Biochemical and Biophysical Research Communications, 1995. **209**(1): p. 111-116.
239. Medzhitov, R., P. Preston-Hurlburt, and C.A. Janeway, *A human homologue of the Drosophila Toll protein signals activation of adaptive immunity.* Nature, 1997. **388**(6640): p. 394-397.
240. Takeuchi, O. and S. Akira, *Pattern Recognition Receptors and Inflammation.* Cell, 2010. **140**(6): p. 805-820.
241. Blikslager, A.T., et al., *Restoration of Barrier Function in Injured Intestinal Mucosa.* Physiological Reviews, 2007. **87**(2): p. 545-564.
242. Fore, F., et al., *TLR10 and Its Unique Anti-Inflammatory Properties and Potential Use as a Target in Therapeutics.* Immune Netw, 2020. **20**(3): p. e21.
243. Behzadi, P., H.A. García-Perdomo, and T.M. Karpiński, *Toll-Like Receptors: General Molecular and Structural Biology.* Journal of Immunology Research, 2021. **2021**: p. 9914854.
244. Asami, J. and T. Shimizu, *Structural and functional understanding of the toll-like receptors.* Protein Sci, 2021. **30**(4): p. 761-772.
245. Joosten, L.A.B., et al., *Toll-like receptors and chronic inflammation in rheumatic diseases: new developments.* Nature Reviews Rheumatology, 2016. **12**(6): p. 344-357.
246. Fitzgerald, K.A. and J.C. Kagan, *Toll-like Receptors and the Control of Immunity.* Cell, 2020. **180**(6): p. 1044-1066.
247. Gioannini, T.L. and J.P. Weiss, *Regulation of interactions of Gram-negative bacterial endotoxins with mammalian cells.* Immunologic Research, 2007. **39**(1): p. 249-260.
248. Lin, S.-C., Y.-C. Lo, and H. Wu, *Helical assembly in the MyD88–IRAK4–IRAK2 complex in TLR/IL-1R signalling.* Nature, 2010. **465**(7300): p. 885-890.
249. Dorrington, M.G. and I.D.C. Fraser, *NF-κB Signaling in Macrophages: Dynamics, Crosstalk, and Signal Integration.* Frontiers in Immunology, 2019. **10**(705).
250. Sharma, S., et al., *Triggering the interferon antiviral response through an IKK-related pathway.* Science, 2003. **300**(5622): p. 1148-1151.
251. Fitzgerald, K.A., et al., *IKKε and TBK1 are essential components of the IRF3 signaling pathway.* Nature immunology, 2003. **4**(5): p. 491-496.

252. Sen, R. and D. Baltimore, *Multiple nuclear factors interact with the immunoglobulin enhancer sequences.* Cell, 1986. **46**(5): p. 705-716.
253. Amiri, K.I. and A. Richmond, *Role of nuclear factor-kappa B in melanoma.* Cancer Metastasis Rev, 2005. **24**(2): p. 301-13.
254. Chen, F., L.M. Demers, and X. Shi, *Upstream signal transduction of NF-κB activation.* Current Drug Targets-Inflammation & Allergy, 2002. **1**(2): p. 137-149.
255. Ben-Neriah, Y., *Regulatory functions of ubiquitination in the immune system.* Nat Immunol, 2002. **3**(1): p. 20-6.
256. Kumar, A., et al., *Nuclear factor-kappaB: its role in health and disease.* J Mol Med (Berl), 2004. **82**(7): p. 434-48.
257. Liu, T., et al., *NF-κB signaling in inflammation.* Signal transduction and targeted therapy, 2017. **2**: p. 17023.
258. Yu, H., et al., *Targeting NF-κB pathway for the therapy of diseases: mechanism and clinical study.* Signal Transduction and Targeted Therapy, 2020. **5**(1): p. 209.
259. Nabel, G.J. and I.M. Verma, *Proposed NF-kappa B/I kappa B family nomenclature.* Genes Dev, 1993. **7**(11): p. 2063.
260. Hayden, M.S., A.P. West, and S. Ghosh, *NF-κB and the immune response.* Oncogene, 2006. **25**(51): p. 6758-6780.
261. Oeckinghaus, A. and S. Ghosh, *The NF-kappaB family of transcription factors and its regulation.* Cold Spring Harb Perspect Biol, 2009. **1**(4): p. a000034.
262. Mussbacher, M., et al., *Cell Type-Specific Roles of NF-κB Linking Inflammation and Thrombosis.* Frontiers in Immunology, 2019. **10**(85).
263. Zhang, H. and S.C. Sun, *NF-κB in inflammation and renal diseases.* Cell Biosci, 2015. **5**: p. 63.
264. Schröfelbauer, B., et al., *NEMO ensures signaling specificity of the pleiotropic IKKβ by directing its kinase activity toward IκBα.* Molecular cell, 2012. **47**(1): p. 111-121.
265. Karin, M. and M. Delhase, *The I kappa B kinase (IKK) and NF-kappa B: key elements of proinflammatory signalling.* Semin Immunol, 2000. **12**(1): p. 85-98.
266. Sun, S.C. and S.C. Ley, *New insights into NF-kappaB regulation and function.* Trends Immunol, 2008. **29**(10): p. 469-78.
267. Kanarek, N. and Y. Ben-Neriah, *Regulation of NF-κB by ubiquitination and degradation of the IκBs.* Immunological reviews, 2012. **246**(1): p. 77-94.
268. Hayden, M.S. and S. Ghosh, *NF-κB, the first quarter-century: remarkable progress and outstanding questions.* Genes & development, 2012. **26**(3): p. 203-234.
269. Beinke, S. and S.C. Ley, *Functions of NF-kappaB1 and NF-kappaB2 in immune cell biology.* Biochem J, 2004. **382**(Pt 2): p. 393-409.
270. Sun, S.C., *Non-canonical NF-κB signaling pathway.* Cell Res, 2011. **21**(1): p. 71-85.
271. Sun, S.C. and Z.G. Liu, *A special issue on NF-κB signaling and function.* Cell Res, 2011. **21**(1): p. 1-2.
272. Jin, J., et al., *Noncanonical NF-κB pathway controls the production of type I interferons in antiviral innate immunity.* Immunity, 2014. **40**(3): p. 342-54.
273. Sun, S.-C., *The non-canonical NF-κB pathway in immunity and inflammation.* Nature Reviews Immunology, 2017. **17**(9): p. 545-558.
274. Habib, A.A., et al., *The epidermal growth factor receptor engages receptor interacting protein and nuclear factor-κB (NF-κB)-inducing kinase to activate NF-κB: identification of a novel receptor-tyrosine kinase signalosome.* Journal of Biological Chemistry, 2001. **276**(12): p. 8865-8874.
275. Alberti, C., et al., *Ligand-dependent EGFR activation induces the co-expression of IL-6 and PAI-1 via the NFkB pathway in advanced-stage epithelial ovarian cancer.* Oncogene, 2012. **31**(37): p. 4139-4149.

276. Hoesel, B. and J.A. Schmid, *The complexity of NF-κB signaling in inflammation and cancer.* Molecular Cancer, 2013. **12**(1): p. 86.
277. Kato Jr, T., et al., *CK2 is a C-terminal IκB kinase responsible for NF-κB activation during the UV response.* Molecular cell, 2003. **12**(4): p. 829-839.
278. Takada, Y., et al., *Hydrogen peroxide activates NF-κB through tyrosine phosphorylation of IκBα and serine phosphorylation of p65: evidence for the involvement of IκBα kinase and Syk protein-tyrosine kinase.* Journal of Biological Chemistry, 2003. **278**(26): p. 24233-24241.
279. Guo, H., J.B. Callaway, and J.P. Ting, *Inflammasomes: mechanism of action, role in disease, and therapeutics.* Nat Med, 2015. **21**(7): p. 677-87.
280. Demarco, B., K. Chen, and P. Broz, *Cross talk between intracellular pathogens and cell death.* Immunological Reviews, 2020. **297**.
281. Barnett, K.C., et al., *A 360° view of the inflammasome: Mechanisms of activation, cell death, and diseases.* Cell, 2023. **186**(11): p. 2288-2312.
282. Műzes, G. and F. Sipos, *Inflammasomes Are Influenced by Epigenetic and Autophagy Mechanisms in Colorectal Cancer Signaling.* International Journal of Molecular Sciences, 2024. **25**(11): p. 6167.
283. Sciences, A.L. *The Expert in Inflammasome Research - From Innate to Adaptive Immunity*. 2023 [cited 2024 09.07.]; Available from: https://adipogen.com/pub/media/wysiwyg/Catalogs/PDFs-URLs/Inflammasome_Brochure_2023_URLs.pdf.
284. Pandey, A., et al., *Cell biology of inflammasome activation.* Trends in Cell Biology, 2021. **31**(11): p. 924-939.
285. Martinon, F., K. Burns, and J. Tschopp, *The Inflammasome: A Molecular Platform Triggering Activation of Inflammatory Caspases and Processing of proIL-&#x3b2.* Molecular Cell, 2002. **10**(2): p. 417-426.
286. Dinarello, C.A., *Immunological and inflammatory functions of the interleukin-1 family.* Annual review of immunology, 2009. **27**: p. 519-550.
287. Ihim, S.A., et al., *Interleukin-18 cytokine in immunity, inflammation, and autoimmunity: Biological role in induction, regulation, and treatment.* Front Immunol, 2022. **13**: p. 919973.
288. Kelley, N., et al., *The NLRP3 Inflammasome: An Overview of Mechanisms of Activation and Regulation.* Int J Mol Sci, 2019. **20**(13).
289. Swanson, K.V., M. Deng, and J.P.Y. Ting, *The NLRP3 inflammasome: molecular activation and regulation to therapeutics.* Nature Reviews Immunology, 2019. **19**(8): p. 477-489.
290. Ma, Q., *Pharmacological Inhibition of the NLRP3 Inflammasome: Structure, Molecular Activation, and Inhibitor-NLRP3 Interaction.* Pharmacol Rev, 2023. **75**(3): p. 487-520.
291. Fischer, F.A., et al., *TBK1 and IKKε act like an OFF switch to limit NLRP3 inflammasome pathway activation.* Proc Natl Acad Sci U S A, 2021. **118**(38).
292. Paik, S., et al., *An update on the regulatory mechanisms of NLRP3 inflammasome activation.* Cellular & Molecular Immunology, 2021. **18**(5): p. 1141-1160.
293. González Moro, A., et al., *NLRP3 Inflammasome in Vascular Disease: A Recurrent Villain to Combat Pharmacologically.* Antioxidants, 2022. **11**: p. 269.
294. Bulté, D., et al., *Inflammasomes: Mechanisms of Action and Involvement in Human Diseases.* Cells, 2023. **12**(13): p. 1766.
295. Arbore, G. and C. Kemper, *A novel 'Complement - Metabolism - Inflammasome Axis' as a key regulator of immune cell effector function.* European Journal of Immunology, 2016. **46**.

296. Lee, D.J., et al., *Regulation and Function of the Caspase-1 in an Inflammatory Microenvironment.* J Invest Dermatol, 2015. **135**(8): p. 2012-2020.
297. Robinson, D.R., Y.M. Wu, and S.F. Lin, *The protein tyrosine kinase family of the human genome.* Oncogene, 2000. **19**(49): p. 5548-57.
298. Shibuya, M., *Vascular Endothelial Growth Factor (VEGF) and Its Receptor (VEGFR) Signaling in Angiogenesis: A Crucial Target for Anti- and Pro-Angiogenic Therapies.* Genes Cancer, 2011. **2**(12): p. 1097-105.
299. Liu, Y., et al., *Recent progress on vascular endothelial growth factor receptor inhibitors with dual targeting capabilities for tumor therapy.* J Hematol Oncol, 2022. **15**(1): p. 89.
300. Hiratsuka, S., et al., *Hiratsuka, S., Minowa, O., Kuno, J., Noda, T. & Shibuya, M. Flt-1 lacking the tyrosine kinase domain is sufficient for normal development and angiogenesis In mice. Proc. Natl. Acad. Sci. USA 95, 9349-9354.* Proceedings of the National Academy of Sciences of the United States of America, 1998. **95**: p. 9349-54.
301. Barleon, B., et al., *Migration of human monocytes in response to vascular endothelial growth factor (VEGF) is mediated via the VEGF receptor flt-1.* Blood, 1996. **87**(8): p. 3336-3343.
302. Muramatsu, M., et al., *Vascular Endothelial Growth Factor Receptor-1 Signaling Promotes Mobilization of Macrophage Lineage Cells from Bone Marrow and Stimulates Solid Tumor Growth.* Cancer Research, 2010. **70**(20): p. 8211-8221.
303. Kerber, M., et al., *Flt-1 Signaling in Macrophages Promotes Glioma Growth In vivo.* Cancer Research, 2008. **68**(18): p. 7342-7351.
304. Krysiak, O., et al., *Soluble Vascular Endothelial Growth Factor Receptor-1 (sFLT-1) Mediates Downregulation of FLT-1 and Prevents Activated Neutrophils From Women With Preeclampsia From Additional Migration by VEGF.* Circulation Research, 2005. **97**(12): p. 1253-1261.
305. Wheeler, K.C., et al., *VEGF may contribute to macrophage recruitment and M2 polarization in the decidua.* PLOS ONE, 2018. **13**(1): p. e0191040.
306. Dineen, S.P., et al., *Vascular endothelial growth factor receptor 2 mediates macrophage infiltration into orthotopic pancreatic tumors in mice.* Cancer Res, 2008. **68**(11): p. 4340-6.
307. Okikawa, S., et al., *Inhibition of the VEGF signaling pathway attenuates tumor-associated macrophage activity in liver cancer.* Oncol Rep, 2022. **47**(4): p. 71.
308. Liu, X., et al., *Fruquintinib inhibits VEGF/VEGFR2 axis of choroidal endothelial cells and M1-type macrophages to protect against mouse laser-induced choroidal neovascularization.* Cell Death & Disease, 2020. **11**(11): p. 1016.
309. Beazley-Long, N., et al., *VEGFR2 promotes central endothelial activation and the spread of pain in inflammatory arthritis.* Brain, Behavior, and Immunity, 2018. **74**: p. 49-67.
310. Scaldaferri, F., et al., *VEGF-A Links Angiogenesis and Inflammation in Inflammatory Bowel Disease Pathogenesis.* Gastroenterology, 2009. **136**(2): p. 585-595.e5.
311. Granito, A., et al., *Experience with regorafenib in the treatment of hepatocellular carcinoma.* Therapeutic Advances in Gastroenterology, 2021. **14**: p. 17562848211016959.
312. He, Y., et al., *Targeting PI3K/Akt signal transduction for cancer therapy.* Signal Transduction and Targeted Therapy, 2021. **6**(1): p. 425.
313. Liang, J., et al., *The C-kit receptor-mediated signal transduction and tumor-related diseases.* Int J Biol Sci, 2013. **9**(5): p. 435-43.
314. Sudhesh Dev, S., et al., *Receptor Tyrosine Kinases and Their Signaling Pathways as Therapeutic Targets of Curcumin in Cancer.* Frontiers in Pharmacology, 2021. **12**.

315. Niu, M., et al., *Advances of Targeted Therapy for Hepatocellular Carcinoma.* Frontiers in Oncology, 2021. **11**.
316. Ullrich, K., et al., *BAY 43-9006/Sorafenib blocks CSF1R activity and induces apoptosis in various classical Hodgkin lymphoma cell lines.* Br J Haematol, 2011. **155**(3): p. 398-402.
317. Alu, A., et al., *BTK inhibitors in the treatment of hematological malignancies and inflammatory diseases: mechanisms and clinical studies.* Journal of Hematology & Oncology, 2022. **15**.
318. Heldin, C.-H. and B. Westermark, *Mechanism of Action and In Vivo Role of Platelet-Derived Growth Factor.* Physiological Reviews, 1999. **79**(4): p. 1283-1316.
319. Yang, P., et al., *Role of PDGF-D and PDGFR-β in neuroinflammation in experimental ICH mice model.* Exp Neurol, 2016. **283**(Pt A): p. 157-64.
320. He, C., et al., *PDGFRβ signalling regulates local inflammation and synergizes with hypercholesterolaemia to promote atherosclerosis.* Nature Communications, 2015. **6**(1): p. 7770.
321. Martinet, Y., et al., *Activated human monocytes express the c-sis proto-oncogene and release a mediator showing PDGF-like activity.* Nature, 1986. **319**(6049): p. 158-160.
322. Antoniades, H.N., et al., *Platelet-derived growth factor in idiopathic pulmonary fibrosis.* J Clin Invest, 1990. **86**(4): p. 1055-64.
323. Ogawa, T., et al., *Macrophages in lung fibrosis.* Int Immunol, 2021. **33**(12): p. 665-671.
324. Nakagawa, M., et al., *A decline in platelet activation and inflammatory cell infiltration is associated with the phenotypic redifferentiation of neointimal smooth muscle cells after bare-metal stent implantation in acute coronary syndrome.* J Atheroscler Thromb, 2010. **17**(7): p. 675-87.
325. Bethel-Brown, C., et al., *Platelet-derived growth factor (PDGF)-BB-mediated induction of monocyte chemoattractant protein 1 in human astrocytes: implications for HIV-associated neuroinflammation.* Journal of Neuroinflammation, 2012. **9**(1): p. 262.
326. Ma, Q., et al., *PDGFR-α inhibition preserves blood-brain barrier after intracerebral hemorrhage.* Annals of Neurology, 2011. **70**(6): p. 920-931.
327. Hume, D.A. and K.P.A. MacDonald, *Therapeutic applications of macrophage colony-stimulating factor-1 (CSF-1) and antagonists of CSF-1 receptor (CSF-1R) signaling.* Blood, 2012. **119**(8): p. 1810-1820.
328. Xiang, C., H. Li, and W. Tang, *Targeting CSF-1R represents an effective strategy in modulating inflammatory diseases.* Pharmacological Research, 2023. **187**: p. 106566.
329. Kumari, A., O. Silakari, and R.K. Singh, *Recent advances in colony stimulating factor-1 receptor/c-FMS as an emerging target for various therapeutic implications.* Biomedicine & Pharmacotherapy, 2018. **103**: p. 662-679.
330. Stanley, E.R. and V. Chitu, *CSF-1 receptor signaling in myeloid cells.* Cold Spring Harb Perspect Biol, 2014. **6**(6).
331. Lindau, R., et al., *Interleukin-34 is present at the fetal–maternal interface and induces immunoregulatory macrophages of a decidual phenotype in vitro.* Human reproduction, 2018. **33**(4): p. 588-599.
332. Svensson, J., et al., *Macrophages at the fetal–maternal interface express markers of alternative activation and are induced by M-CSF and IL-10.* The Journal of Immunology, 2011. **187**(7): p. 3671-3682.
333. Huang, S.C., et al., *Metabolic Reprogramming Mediated by the mTORC2-IRF4 Signaling Axis Is Essential for Macrophage Alternative Activation.* Immunity, 2016. **45**(4): p. 817-830.
334. Martinez, F.O., et al., *Transcriptional Profiling of the Human Monocyte-to-Macrophage Differentiation and Polarization: New Molecules and Patterns of Gene Expression1.* The Journal of Immunology, 2006. **177**(10): p. 7303-7311.

335. Mitrasinovic, O.M., et al., *Macrophage colony stimulating factor promotes phagocytosis by murine microglia.* Neuroscience Letters, 2003. **344**(3): p. 185-188.
336. Uemura, Y., et al., *The selective M-CSF receptor tyrosine kinase inhibitor Ki20227 suppresses experimental autoimmune encephalomyelitis.* Journal of neuroimmunology, 2008. **195**(1-2): p. 73-80.
337. Nissen, J.C., et al., *Csf1R inhibition attenuates experimental autoimmune encephalomyelitis and promotes recovery.* Experimental Neurology, 2018. **307**: p. 24-36.
338. Wies Mancini, V.S.B., et al., *Microglial modulation through colony-stimulating factor-1 receptor inhibition attenuates demyelination.* Glia, 2019. **67**(2): p. 291-308.
339. Hu, X., et al., *Imatinib inhibits CSF1R that stimulates proliferation of rheumatoid arthritis fibroblast-like synoviocytes.* Clinical & Experimental Immunology, 2019. **195**(2): p. 237-250.
340. Garcia, S., et al., *Colony-stimulating factor (CSF) 1 receptor blockade reduces inflammation in human and murine models of rheumatoid arthritis.* Arthritis Research & Therapy, 2016. **18**(1): p. 75.
341. Zhuang, L., et al., *Interleukin-34-NF-κB signaling aggravates myocardial ischemic/reperfusion injury by facilitating macrophage recruitment and polarization.* eBioMedicine, 2023. **95**.
342. Wang, Y., et al., *M-CSF Induces Monocyte Survival by Activating NF-κB p65 Phosphorylation at Ser276 via Protein Kinase C.* PLOS ONE, 2011. **6**(12): p. e28081.
343. Aleshin, A. and R.S. Finn, *SRC: a century of science brought to the clinic.* Neoplasia, 2010. **12**(8): p. 599-607.
344. Szilveszter, K.P., T. Németh, and A. Mócsai, *Tyrosine Kinases in Autoimmune and Inflammatory Skin Diseases.* Front Immunol, 2019. **10**: p. 1862.
345. K, K.B., et al., *Protein Tyrosine Kinases: Their Roles and Their Targeting in Leukemia.* Cancers (Basel), 2021. **13**(2).
346. Byeon, S.E., et al., *The Role of Src Kinase in Macrophage-Mediated Inflammatory Responses.* Mediators of Inflammation, 2012. **2012**: p. 512926.
347. Byeon, S., et al., *The Role of Src Kinase in Macrophage-Mediated Inflammatory Responses.* Mediators of inflammation, 2012. **2012**: p. 512926.
348. Sumagin, R., J.M. Kuebel, and I.H. Sarelius, *Leukocyte rolling and adhesion both contribute to regulation of microvascular permeability to albumin via ligation of ICAM-1.* Am J Physiol Cell Physiol, 2011. **301**(4): p. C804-13.
349. Shao, B., et al., *Signal-dependent Slow Leukocyte Rolling Does Not Require Cytoskeletal Anchorage of P-selectin Glycoprotein Ligand-1 (PSGL-1) or Integrin αLβ2*.* Journal of Biological Chemistry, 2012. **287**(23): p. 19585-19598.
350. Baruzzi, A., et al., *c-Abl and Src-family kinases cross-talk in regulation of myeloid cell migration.* FEBS Letters, 2010. **584**(1): p. 15-21.
351. Kumar, P., S. Hosaka, and A.E. Koch, *Soluble E-selectin induces monocyte chemotaxis through Src family tyrosine kinases.* J Biol Chem, 2001. **276**(24): p. 21039-45.
352. Allingham, M.J., J.D. van Buul, and K. Burridge, *ICAM-1-Mediated, Src- and Pyk2-Dependent Vascular Endothelial Cadherin Tyrosine Phosphorylation Is Required for Leukocyte Transendothelial Migration1.* The Journal of Immunology, 2007. **179**(6): p. 4053-4064.
353. Canino, J., et al., *The proline-rich tyrosine kinase Pyk2 modulates integrin-mediated neutrophil adhesion and reactive oxygen species generation.* Biochimica et Biophysica Acta (BBA) - Molecular Cell Research, 2020. **1867**(10): p. 118799.

354. Hunter, S., et al., *Fc gamma RIIA-mediated phagocytosis and receptor phosphorylation in cells deficient in the protein tyrosine kinase Src.* Experimental hematology, 1993. **21**(11): p. 1492-1497.
355. Tang, C.-H., et al., *Lipoteichoic acid enhances IL-6 production in human synovial fibroblasts via TLR2 receptor, PKCδ and c-Src dependent pathways.* Biochemical Pharmacology, 2010. **79**(11): p. 1648-1657.
356. Hsieh, H.-L., et al., *Lipoteichoic Acid Induces Matrix Metalloproteinase-9 Expression via Transactivation of PDGF Receptors and NF-κB Activation in Rat Brain Astrocytes.* Neurotoxicity Research, 2010. **17**(4): p. 344-359.
357. Leu, T.H., et al., *Lipopolysaccharide-induced c-Src expression plays a role in nitric oxide and TNFalpha secretion in macrophages.* Mol Immunol, 2006. **43**(4): p. 308-16.
358. Meng, F. and C.A. Lowell, *Lipopolysaccharide (LPS)-induced macrophage activation and signal transduction in the absence of Src-family kinases Hck, Fgr, and Lyn.* J Exp Med, 1997. **185**(9): p. 1661-70.
359. Stefanová, I., et al., *Lipopolysaccharide induces activation of CD14-associated protein tyrosine kinase p53/56lyn.* J Biol Chem, 1993. **268**(28): p. 20725-8.
360. English, B.K., et al., *Hck tyrosine kinase activity modulates tumor necrosis factor production by murine macrophages.* J Exp Med, 1993. **178**(3): p. 1017-22.
361. Boulet, I., et al., *Lipopolysaccharide- and interferon-gamma-induced expression of hck and lyn tyrosine kinases in murine bone marrow-derived macrophages.* Oncogene, 1992. **7**(4): p. 703-10.
362. English, B.K., et al., *Bacterial LPS and IFN-gamma trigger the tyrosine phosphorylation of vav in macrophages: evidence for involvement of the hck tyrosine kinase.* J Leukoc Biol, 1997. **62**(6): p. 859-64.
363. Orlicek, S.L., J.H. Hanke, and B.K. English, *THE SRC FAMILY-SELECTIVE TYROSINE KINASE INHIBITOR PP1 BLOCKS LPS AND IFN-α-MEDIATED TNF AND iNOS PRODUCTION IN MURINE MACROPHAGES.* Shock, 1999. **12**(5): p. 350-354.
364. Chen, Y.-J., et al., *Eps8 Protein Facilitates Phagocytosis by Increasing TLR4-MyD88 Protein Interaction in Lipopolysaccharide-stimulated Macrophages *.* Journal of Biological Chemistry, 2012. **287**(22): p. 18806-18819.
365. Rozkiewicz, D., et al., *Bruton's Tyrosine Kinase Inhibitors (BTKIs): Review of Preclinical Studies and Evaluation of Clinical Trials.* Molecules, 2023. **28**(5).
366. Zarrin, A.A., et al., *Kinase inhibition in autoimmunity and inflammation.* Nature Reviews Drug Discovery, 2021. **20**(1): p. 39-63.
367. Mangla, A., et al., *Pleiotropic consequences of Bruton tyrosine kinase deficiency in myeloid lineages lead to poor inflammatory responses.* Blood, 2004. **104**(4): p. 1191-1197.
368. Horwood, N.J., et al., *Bruton's Tyrosine Kinase Is Required for TLR2 and TLR4-Induced TNF, but Not IL-6, Production1.* The Journal of Immunology, 2006. **176**(6): p. 3635-3641.
369. Gray, P., et al., *MyD88 Adapter-like (Mal) Is Phosphorylated by Bruton's Tyrosine Kinase during TLR2 and TLR4 Signal Transduction *.* Journal of Biological Chemistry, 2006. **281**(15): p. 10489-10495.
370. Doyle, S.L., C.A. Jefferies, and L.A. O'Neill, *Bruton's Tyrosine Kinase Is Involved in p65-mediated Transactivation and Phosphorylation of p65 on Serine 536 during NFκB Activation by Lipopolysaccharide *.* Journal of Biological Chemistry, 2005. **280**(25): p. 23496-23501.
371. Jefferies, C.A., et al., *Bruton's Tyrosine Kinase Is a Toll/Interleukin-1 Receptor Domain-binding Protein That Participates in Nuclear Factor κB Activation by Toll-like Receptor 4 *.* Journal of Biological Chemistry, 2003. **278**(28): p. 26258-26264.

372. Purvis, G.S.D., et al., *Inhibition of Bruton's TK regulates macrophage NF-κB and NLRP3 inflammasome activation in metabolic inflammation.* British Journal of Pharmacology, 2020. **177**(19): p. 4416-4432.
373. Liu, X., et al., *Human NACHT, LRR, and PYD domain–containing protein 3 (NLRP3) inflammasome activity is regulated by and potentially targetable through Bruton tyrosine kinase.* Journal of Allergy and Clinical Immunology, 2017. **140**(4): p. 1054-1067. e10.
374. Bittner, Z.A., et al., *BTK operates a phospho-tyrosine switch to regulate NLRP3 inflammasome activity.* J Exp Med, 2021. **218**(11).
375. Ito, M., et al., *Bruton's tyrosine kinase is essential for NLRP3 inflammasome activation and contributes to ischaemic brain injury.* Nat Commun, 2015. **6**: p. 7360.
376. Benner, B., et al., *Evidence for interaction of the NLRP3 inflammasome and Bruton's tyrosine kinase in tumor-associated macrophages: implications for myeloid cell production of interleukin-1beta.* Oncoimmunology, 2019. **8**(11): p. 1659704.
377. Purvis, G.S.D., et al., *Bruton's TK regulates myeloid cell recruitment during acute inflammation.* British Journal of Pharmacology, 2022. **179**(11): p. 2754-2770.
378. Di Paolo, J.A., et al., *Specific Btk inhibition suppresses B cell– and myeloid cell–mediated arthritis.* Nature Chemical Biology, 2011. **7**(1): p. 41-50.
379. Xu, D., et al., *RN486, a selective Bruton's tyrosine kinase inhibitor, abrogates immune hypersensitivity responses and arthritis in rodents.* J Pharmacol Exp Ther, 2012. **341**(1): p. 90-103.
380. O'Riordan, C.E., et al., *Bruton's Tyrosine Kinase Inhibition Attenuates the Cardiac Dysfunction Caused by Cecal Ligation and Puncture in Mice.* Front Immunol, 2019. **10**: p. 2129.
381. Mina-Osorio, P., et al., *Suppression of glomerulonephritis in lupus-prone NZB × NZW mice by RN486, a selective inhibitor of Bruton's tyrosine kinase.* Arthritis Rheum, 2013. **65**(9): p. 2380-91.
382. Rankin, A.L., et al., *Selective inhibition of BTK prevents murine lupus and antibody-mediated glomerulonephritis.* J Immunol, 2013. **191**(9): p. 4540-50.
383. Evonuk, K.S., et al., *Bruton's tyrosine kinase inhibition reduces disease severity in a model of secondary progressive autoimmune demyelination.* Acta Neuropathol Commun, 2023. **11**(1): p. 115.
384. Weber, H., et al. *Fenebrutinib reduces disease activity in a mouse model of inflammatory multiple sclerosis, which is associated with reduced microglial activation*. in *Congress of the European Committee for Treatment and Research in Multiple Sclerosis*. 2021.
385. Gruber, R., et al., *Evaluating the Effect of a Bruton's Tyrosine Kinase Inhibitor in a Murine Experimental Autoimmune Encephalomyelitis Model of Multiple Sclerosis (P2-3.012).* Neurology, 2023. **100**(17_supplement_2): p. 1825.
386. Miklos, D., et al., *Ibrutinib for chronic graft-versus-host disease after failure of prior therapy.* Blood, 2017. **130**(21): p. 2243-2250.
387. Wongrakpanich, S., et al., *A Comprehensive Review of Non-Steroidal Anti-Inflammatory Drug Use in The Elderly.* Aging Dis, 2018. **9**(1): p. 143-150.
388. Habib, I., et al., *Nonsteroidal Anti-inflammatory Drugs and Inflammatory Bowel Disease: Pathophysiology and Clinical Associations.* Inflammatory Bowel Diseases, 2014. **20**(12): p. 2493-2502.
389. Ricciotti, E. and G.A. FitzGerald, *Prostaglandins and inflammation.* Arterioscler Thromb Vasc Biol, 2011. **31**(5): p. 986-1000.

390. McAdam, B.F., et al., *Effect of regulated expression of human cyclooxygenase isoforms on eicosanoid and isoeicosanoid production in inflammation.* The Journal of Clinical Investigation, 2000. **105**(10): p. 1473-1482.
391. Crofford, L.J., et al., *Cyclooxygenase-1 and -2 expression in rheumatoid synovial tissues. Effects of interleukin-1 beta, phorbol ester, and corticosteroids.* The Journal of Clinical Investigation, 1994. **93**(3): p. 1095-1101.
392. Nakao, S., et al., *Activation of NFκB is necessary for IL-1β-induced cyclooxygenase-2 (COX-2) expression in human gingival fibroblasts.* Molecular and Cellular Biochemistry, 2000. **209**(1): p. 113-118.
393. Janjic, J.M., et al., *Low-dose NSAIDs reduce pain via macrophage targeted nanoemulsion delivery to neuroinflammation of the sciatic nerve in rat.* J Neuroimmunol, 2018. **318**: p. 72-79.
394. Williams, J.A. and E. Shacter, *Regulation of Macrophage Cytokine Production by Prostaglandin E₂: DISTINCT ROLES OF CYCLOOXYGENASE-1 AND -2 *.* Journal of Biological Chemistry, 1997. **272**(41): p. 25693-25699.
395. Haimerl, P., et al., *Inflammatory macrophage memory in nonsteroidal anti-inflammatory drug–exacerbated respiratory disease.* Journal of Allergy and Clinical Immunology, 2021. **147**(2): p. 587-599.
396. Na, Y.R., et al., *Consistent inhibition of cyclooxygenase drives macrophages towards the inflammatory phenotype.* PLoS One, 2015. **10**(2): p. e0118203.
397. Cho, J.Y., *Immunomodulatory effect of nonsteroidal anti-inflammatory drugs (NSAIDs) at the clinically available doses.* Archives of Pharmacal Research, 2007. **30**(1): p. 64-74.
398. Simoni, R.D., R.L. Hill, and M. Vaughan, *The Isolation of Thyroxine and Cortisone: the Work of Edward C. Kendall.* Journal of Biological Chemistry, 2002. **277**(21): p. 21-22.
399. Sarett, L.H., *PARTIAL SYNTHESIS OF PREGNENE-4-TRIOL-17(β),20(β),21-DIONE-3,11 AND PREGNENE-4-DIOL-17(β),21-TRIONE-3,11,20 MONOACETATE.* Journal of Biological Chemistry, 1946. **162**(3): p. 601-631.
400. Timmermans, S., J. Souffriau, and C. Libert, *A General Introduction to Glucocorticoid Biology.* Front Immunol, 2019. **10**: p. 1545.
401. Yang, R. and Y. Yu, *Glucocorticoids are double-edged sword in the treatment of COVID-19 and cancers.* Int J Biol Sci, 2021. **17**(6): p. 1530-1537.
402. Bekhbat, M., S.A. Rowson, and G.N. Neigh, *Checks and balances: The glucocorticoid receptor and NFκB in good times and bad.* Front Neuroendocrinol, 2017. **46**: p. 15-31.
403. Scheinman, R.I., et al., *Role of Transcriptional Activation of IκBα in Mediation of Immunosuppression by Glucocorticoids.* Science, 1995. **270**(5234): p. 283-286.
404. WIDÉN, C., J.-Å. GUSTAFSSON, and A.-C. WIKSTRÖM, *Cytosolic glucocorticoid receptor interaction with nuclear factor-kappaB proteins in rat liver cells.* Biochemical Journal, 2003. **373**(1): p. 211-220.
405. Ray, A. and K.E. Prefontaine, *Physical association and functional antagonism between the p65 subunit of transcription factor NF-kappa B and the glucocorticoid receptor.* Proceedings of the National Academy of Sciences, 1994. **91**(2): p. 752-756.
406. Mukaida, N., et al., *Novel mechanism of glucocorticoid-mediated gene repression. Nuclear factor-kappa B is target for glucocorticoid-mediated interleukin 8 gene repression.* Journal of Biological Chemistry, 1994. **269**(18): p. 13289-13295.
407. De Bosscher, K., et al., *Glucocorticoid-mediated repression of nuclear factor-κBdependent transcription involves direct interference with transactivation.* Proceedings of the National Academy of Sciences, 1997. **94**(25): p. 13504-13509.
408. De Bosscher, K., et al., *Glucocorticoids repress NF-κB-driven genes by disturbing the interaction of p65 with the basal transcription machinery, irrespective of coactivator*

levels in the cell. Proceedings of the National Academy of Sciences, 2000. **97**(8): p. 3919-3924.
409. Nelson, G., et al., *NF-κB signalling is inhibited by glucocorticoid receptor and STAT6 via distinct mechanisms.* Journal of Cell Science, 2003. **116**(12): p. 2495-2503.
410. Scheinman, R.I., et al., *Characterization of Mechanisms Involved in Transrepression of NF-κB by Activated Glucocorticoid Receptors.* Molecular and Cellular Biology, 1995. **15**(2): p. 943-953.
411. Barnes, P.J., *Glucocorticosteroids: current and future directions.* British Journal of Pharmacology, 2011. **163**(1): p. 29-43.
412. Oray, M., et al., *Long-term side effects of glucocorticoids.* Expert Opinion on Drug Safety, 2016. **15**(4): p. 457-465.
413. Benjamin O, G.A., Lappin SL. *Disease-Modifying Antirheumatic Drugs (DMARD)*. 2023 07.2023 [cited 202425.03.; Available from: https://www.ncbi.nlm.nih.gov/books/NBK507863/.
414. Findeisen, K.E., J. Sewell, and A.J.K. Ostor, *Biological Therapies for Rheumatoid Arthritis: An Overview for the Clinician.* Biologics, 2021. **15**: p. 343-352.
415. Chi, X.K., et al., *Combining nanotechnology with monoclonal antibody drugs for rheumatoid arthritis treatments.* J Nanobiotechnology, 2023. **21**(1): p. 105.
416. Wolmarans, D.W., S. Brand, and L. Brand, *A Quick and Painless Reminder: The Pharmacotherapy of Rheumatoid Arthritis in Primary Practice.* South African Family Practice, 2018. **60**.
417. Botz, B., K. Bölcskei, and Z. Helyes, *Challenges to develop novel anti-inflammatory and analgesic drugs.* Wiley Interdiscip Rev Nanomed Nanobiotechnol, 2017. **9**(3).
418. Seyhan, A., *Lost in translation: the valley of death across preclinical and clinical divide – identification of problems and overcoming obstacles.* Translational Medicine Communications, 2019. **4**.
419. Chaffey, L., A. Roberti, and D.R. Greaves, *Drug repurposing in cardiovascular inflammation: Successes, failures, and future opportunities.* Front Pharmacol, 2022. **13**: p. 1046406.
420. Diseases, N.I.o.D.a.D.a.K. *LiverTox: Clinical and Research Information on Drug-Induced Liver Injury*. Nonsteroidal Antiinflammatory Drugs (NSAIDs) 2012 18.03.2020 [cited 2024 21.03.]; Available from: https://www.ncbi.nlm.nih.gov/books/NBK548614/.
421. Ghlichloo I, G.V. *Nonsteroidal Anti-Inflammatory Drugs (NSAIDs)*. 2023 May 2023 [cited 2024 12.01.]; Available from: https://www.ncbi.nlm.nih.gov/books/NBK547742/.
422. Ponticelli, C. and F. Locatelli, *Glucocorticoids in the Treatment of Glomerular Diseases: Pitfalls and Pearls.* Clinical Journal of the American Society of Nephrology, 2018. **13**: p. CJN.12991117.
423. Moreni, G., et al., *Bridging the gap between emerging models and humans by learning from polio animal studies: A systematic review.* Clinical and Translational Discovery, 2022. **2**(2): p. e42.
424. Loewa, A., J.J. Feng, and S. Hedtrich, *Human disease models in drug development.* Nature Reviews Bioengineering, 2023. **1**(8): p. 545-559.
425. Seok, J., et al., *Genomic responses in mouse models poorly mimic human inflammatory diseases.* Proc Natl Acad Sci U S A, 2013. **110**(9): p. 3507-12.
426. Spalinger, M.R. and M. Scharl, *Mono Sodium Urate Crystal-induced Peritonitis for in vivoAssessment of Inflammasome Activation.* Bio Protoc, 2018. **8**(5): p. e2754.
427. Kort, A., et al., *Brain and Testis Accumulation of Regorafenib is Restricted by Breast Cancer Resistance Protein (BCRP/ABCG2) and P-glycoprotein (P-GP/ABCB1).* Pharm Res, 2015. **32**(7): p. 2205-16.

428. Chaffey, L.E., et al., *Drug repurposing screen identifies novel anti-inflammatory activity of sunitinib in macrophages.* European Journal of Pharmacology, 2024. **969**: p. 176437.
429. Riedhammer, C., D. Halbritter, and R. Weissert, *Peripheral blood mononuclear cells: isolation, freezing, thawing, and culture.* Multiple Sclerosis: Methods and Protocols, 2016: p. 53-61.
430. Chaffey, L., *Anti-inflammatory activity of repurposed tyrosine kinase inhibitors in macrophages*, in *Sir William Dunn School of Pathology*. 2023, University of Oxford.
431. Taylor, L., et al., *In Vitro Migration Assays.* Methods Mol Biol, 2018. **1784**: p. 197-214.
432. Sun, M., et al., *A dynamic real-time method for monitoring epithelial barrier function in vitro.* Analytical Biochemistry, 2012. **425**(2): p. 96-103.
433. Iqbal, A.J., et al., *A Real Time Chemotaxis Assay Unveils Unique Migratory Profiles amongst Different Primary Murine Macrophages.* PLOS ONE, 2013. **8**(3): p. e58744.
434. Mansour, A.A., et al., *Galectin-9 supports primary T cell transendothelial migration in a glycan and integrin dependent manner.* Biomedicine & Pharmacotherapy, 2022. **151**: p. 113171.
435. Maguire, O., et al., *Quantifying nuclear p65 as a parameter for NF-κB activation: Correlation between ImageStream cytometry, microscopy, and Western blot.* Cytometry A, 2011. **79**(6): p. 461-9.
436. Parisi, D., et al., *Drug repositioning or target repositioning: A structural perspective of drug-target-indication relationship for available repurposed drugs.* Computational and Structural Biotechnology Journal, 2020. **18**: p. 1043-1055.
437. Nosengo, N., *Can you teach old drugs new tricks?* Nature, 2016. **534**(7607): p. 314-316.
438. Scannell, J.W., et al., *Diagnosing the decline in pharmaceutical R&D efficiency.* Nat Rev Drug Discov, 2012. **11**(3): p. 191-200.
439. Insights, G.M., *Anti-inflammatory Drugs Market - By Drug Class (Anti-inflammatory Biologics, Corticosteroids), Treatment (Arthritis, Multiple Sclerosis) Route of Administration (Oral, Topical), Sales Channel (Prescription, Over-the-Counter) & Forecast 2023 - 2032* 2023.
440. Abani, O., et al., *Tocilizumab in patients admitted to hospital with COVID-19 (RECOVERY): a randomised, controlled, open-label, platform trial.* The Lancet, 2021. **397**(10285): p. 1637-1645.
441. Roberti, A., L.E. Chaffey, and D.R. Greaves, *NF-κB Signaling and Inflammation—Drug Repurposing to Treat Inflammatory Disorders?* Biology, 2022. **11**(3): p. 372.
442. Okamoto, H. and A. Kobayashi, *Tyrosine kinases in rheumatoid arthritis.* Journal of Inflammation, 2011. **8**(1): p. 21.
443. Nejatbakhsh Samimi, L., et al., *NF-κB signaling in rheumatoid arthritis with focus on fibroblast-like synoviocytes.* Autoimmunity Highlights, 2020. **11**(1): p. 11.
444. Gomez-Puerta, J.A. and A. Mócsai, *Tyrosine kinase inhibitors for the treatment of rheumatoid arthritis.* Curr Top Med Chem, 2013. **13**(6): p. 760-73.
445. Ding, Q., et al., *Signaling pathways in rheumatoid arthritis: implications for targeted therapy.* Signal Transduction and Targeted Therapy, 2023. **8**(1): p. 68.
446. Day, E., et al., *Inhibition of collagen-induced discoidin domain receptor 1 and 2 activation by imatinib, nilotinib and dasatinib.* European journal of pharmacology, 2008. **599**(1-3): p. 44-53.
447. Guo, K., et al., *Treatment Effects of the Second-Generation Tyrosine Kinase Inhibitor Dasatinib on Autoimmune Arthritis.* Frontiers in immunology, 2019. **9**: p. 3133-3133.
448. Matsuda, K., N. Shiba, and K. Hiraoka, *New Insights into the Role of Synovial Fibroblasts Leading to Joint Destruction in Rheumatoid Arthritis.* Int J Mol Sci, 2023. **24**(6).

449. Wilkinson, G.F. and K. Pritchard, *In vitro screening for drug repositioning.* J Biomol Screen, 2015. **20**(2): p. 167-79.
450. Kaur, G. and J.M. Dufour, *Cell lines: Valuable tools or useless artifacts.* Spermatogenesis, 2012. **2**(1): p. 1-5.
451. Chaffey, L., A. Roberti, and D.R. Greaves, *Drug repurposing in cardiovascular inflammation: Successes, failures, and future opportunities.* Frontiers in Pharmacology, 2022. **13**.
452. Etzion, Y., et al., *An Unbiased Chemical Biology Screen Identifies Agents That Modulate Uptake of Oxidized LDL by Macrophages.* Circulation Research, 2009. **105**(2): p. 148-157.
453. Hoeffner, N., A. Paul, and Y.-H. Goo, *Drug screen identifies verteporfin as a regulator of lipid metabolism in macrophage foam cells.* Scientific Reports, 2023. **13**(1): p. 19588.
454. Zhao, X. and C. Jacob, *Mechanisms of Demyelination and Remyelination Strategies for Multiple Sclerosis.* Int J Mol Sci, 2023. **24**(7).
455. Mei, F., et al., *Micropillar arrays as a high-throughput screening platform for therapeutics in multiple sclerosis.* Nature Medicine, 2014. **20**(8): p. 954-960.
456. Cree, B.A.C., et al., *Clemastine rescues myelination defects and promotes functional recovery in hypoxic brain injury.* Brain, 2017. **141**(1): p. 85-98.
457. Mei, F., et al., *Accelerated remyelination during inflammatory demyelination prevents axonal loss and improves functional recovery.* Elife, 2016. **5**: p. e18246.
458. Mei, F., et al., *Micropillar arrays as a high-throughput screening platform for therapeutics in multiple sclerosis.* Nat Med, 2014. **20**(8): p. 954-960.
459. Liu, J., et al., *Clemastine Enhances Myelination in the Prefrontal Cortex and Rescues Behavioral Changes in Socially Isolated Mice.* The Journal of Neuroscience, 2016. **36**(3): p. 957-962.
460. Li, Z., et al., *Clemastine rescues behavioral changes and enhances remyelination in the cuprizone mouse model of demyelination.* Neuroscience Bulletin, 2015. **31**(5): p. 617-625.
461. Zada, D., et al., *Pharmacological treatment and BBB-targeted genetic therapy for MCT8-dependent hypomyelination in zebrafish.* Disease Models & Mechanisms, 2016. **9**(11): p. 1339-1348.
462. Su, W.J., et al., *Clemastine Alleviates Depressive-Like Behavior Through Reversing the Imbalance of Microglia-Related Pro-inflammatory State in Mouse Hippocampus.* Front Cell Neurosci, 2018. **12**: p. 412.
463. Apolloni, S., et al., *Actions of the antihistaminergic clemastine on presymptomatic SOD1-G93A mice ameliorate ALS disease progression.* J Neuroinflammation, 2016. **13**(1): p. 191.
464. Leurs, R., M.K. Church, and M. Taglialatela, *H1-antihistamines: inverse agonism, anti-inflammatory actions and cardiac effects.* Clinical & Experimental Allergy, 2002. **32**(4): p. 489-498.
465. Yuan, X., et al., *Clemastine Fumarate Protects Against Myocardial Ischemia Reperfusion Injury by Activating the TLR4/PI3K/Akt Signaling Pathway.* Front Pharmacol, 2020. **11**: p. 28.
466. Green, A.J., et al., *Clemastine fumarate as a remyelinating therapy for multiple sclerosis (ReBUILD): a randomised, controlled, double-blind, crossover trial.* Lancet, 2017. **390**(10111): p. 2481-2489.
467. Nainu, F., et al., *Fruit fly for anticancer drug discovery and repurposing.* Ann Med Surg (Lond), 2023. **85**(2): p. 337-342.

468. Hope, K.A., et al., *An in vivo drug repurposing screen and transcriptional analyses reveals the serotonin pathway and GSK3 as major therapeutic targets for NGLY1 deficiency.* PLoS Genet, 2022. **18**(6): p. e1010228.
469. Lublin, A., et al., *FDA-approved drugs that protect mammalian neurons from glucose toxicity slow aging dependent on cbp and protect against proteotoxicity.* PLoS One, 2011. **6**(11): p. e27762.
470. Haerkens, F., et al., *A new use for old drugs: identifying compounds with an anti-obesity effect using a high through-put semi-automated Caenorhabditis elegans screening platform.* Heliyon, 2022. **8**(8): p. e10108.
471. Xie, Y., A.H. Meijer, and M.J.M. Schaaf, *Modeling Inflammation in Zebrafish for the Development of Anti-inflammatory Drugs.* Front Cell Dev Biol, 2020. **8**: p. 620984.
472. Meeker, N.D. and N.S. Trede, *Immunology and zebrafish: Spawning new models of human disease.* Developmental & Comparative Immunology, 2008. **32**(7): p. 745-757.
473. Traver, D., et al., *The zebrafish as a model organism to study development of the immune system.* Advances in immunology, 2003. **81**: p. 253-330.
474. Rihel, J., et al., *Zebrafish behavioral profiling links drugs to biological targets and rest/wake regulation.* Science, 2010. **327**(5963): p. 348-51.
475. Hall, C.J., et al., *Repositioning drugs for inflammatory disease – fishing for new anti-inflammatory agents.* Disease Models & Mechanisms, 2014. **7**(9): p. 1069-1081.
476. Mertens, S., et al., *Drug-repurposing screen on patient-derived organoids identifies therapy-induced vulnerability in KRAS-mutant colon cancer.* Cell Rep, 2023. **42**(4): p. 112324.
477. Mao, Y., et al., *Drug repurposing screening and mechanism analysis based on human colorectal cancer organoids.* Protein & Cell, 2023.
478. de Poel, E., et al., *FDA-approved drug screening in patient-derived organoids demonstrates potential of drug repurposing for rare cystic fibrosis genotypes.* J Cyst Fibros, 2023. **22**(3): p. 548-559.
479. Spelier, S., et al., *High-throughput functional assay in cystic fibrosis patient-derived organoids allows drug repurposing.* ERJ Open Research, 2023. **9**(1): p. 00495-2022.
480. Leibowitz, S.M. and J. Yan, *NF-κB Pathways in the Pathogenesis of Multiple Sclerosis and the Therapeutic Implications.* Front Mol Neurosci, 2016. **9**: p. 84.
481. Zhou, Y., et al., *Nuclear Factor κB (NF-κB)-Mediated Inflammation in Multiple Sclerosis.* Front Immunol, 2020. **11**: p. 391.
482. Bärnthaler, T., et al., *Imatinib stimulates prostaglandin E(2) and attenuates cytokine release via EP4 receptor activation.* J Allergy Clin Immunol, 2019. **143**(2): p. 794-797.e10.
483. Ciarcia, R., et al., *Imatinib treatment inhibit IL-6, IL-8, NF-KB and AP-1 production and modulate intracellular calcium in CML patients.* J Cell Physiol, 2012. **227**(6): p. 2798-803.
484. Wolf, A.M., et al., *The kinase inhibitor imatinib mesylate inhibits TNF-α production in vitro and prevents TNF-dependent acute hepatic inflammation.* Proceedings of the National Academy of Sciences of the United States of America, 2005. **102**(38): p. 13622-13627.
485. Azizi, G., et al., *Effects of imatinib mesylate in mouse models of multiple sclerosis and in vitro determinants.* Iran J Allergy Asthma Immunol, 2014. **13**(3): p. 198-206.
486. Mukherjee, S., et al., *Pharmacologic targeting of a stem/progenitor population in vivo is associated with enhanced bone regeneration in mice.* The Journal of clinical investigation, 2008. **118**(2): p. 491-504.

487. Fissolo, N., et al., *Dual inhibition of proteasomal and lysosomal proteolysis ameliorates autoimmune central nervous system inflammation.* European journal of immunology, 2008. **38**(9): p. 2401-2411.
488. Schmidt, N., et al., *Targeting the proteasome: partial inhibition of the proteasome by bortezomib or deletion of the immunosubunit LMP7 attenuates experimental colitis.* Gut, 2010. **59**(7): p. 896-906.
489. Basler, M., et al., *Prevention of experimental colitis by a selective inhibitor of the immunoproteasome.* The Journal of Immunology, 2010. **185**(1): p. 634-641.
490. Lassoued, S., et al., *Bortezomib improved the joint manifestations of rheumatoid arthritis in three patients.* Joint Bone Spine, 2019. **86**(3): p. 381-382.
491. Herrington, F.D., R.J. Carmody, and C.S. Goodyear, *Modulation of NF-κB Signaling as a Therapeutic Target in Autoimmunity.* Journal of Biomolecular Screening, 2016. **21**(3): p. 223-242.
492. Liu, J., et al., *Bortezomib followed by autologous stem cell transplantation in a patient with rheumatoid arthritis: A case report and review of the literature.* Medicine (Baltimore), 2016. **95**(52): p. e5760.
493. Verbrugge, S.E., et al., *Proteasome inhibitors as experimental therapeutics of autoimmune diseases.* Arthritis Research & Therapy, 2015. **17**(1): p. 17.
494. Wakita, H., et al., *Ibudilast, a phosphodiesterase inhibitor, protects against white matter damage under chronic cerebral hypoperfusion in the rat.* Brain Research, 2003. **992**(1): p. 53-59.
495. Kiebala, M. and S.B. Maggirwar, *Ibudilast, a pharmacologic phosphodiesterase inhibitor, prevents human immunodeficiency virus-1 Tat-mediated activation of microglial cells.* PLoS One, 2011. **6**(4): p. e18633.
496. Ghazi, A., et al. *Ibudilast and octreotide can ameliorate acute pancreatitis via downregulation of the inflammatory cytokines and Nuclear Factor- Kappa B expression*. 2019.
497. Feng, J., et al., *Ibudilast, a nonselective phosphodiesterase inhibitor, regulates Th1/Th2 balance and NKT cell subset in multiple sclerosis.* Multiple Sclerosis Journal, 2004. **10**(5): p. 494-498.
498. Zeng, X., et al., *Target identification among known drugs by deep learning from heterogeneous networks.* Chem Sci, 2020. **11**(7): p. 1775-1797.
499. Chang, B.Y., et al., *The Bruton tyrosine kinase inhibitor PCI-32765 ameliorates autoimmune arthritis by inhibition of multiple effector cells.* Arthritis Research & Therapy, 2011. **13**(4): p. R115.
500. Pan, Z., et al., *Discovery of Selective Irreversible Inhibitors for Bruton's Tyrosine Kinase.* ChemMedChem, 2007. **2**(1): p. 58-61.
501. Purvis, G.S.D., et al., *Inhibition of Bruton's TK regulates macrophage NF-κB and NLRP3 inflammasome activation in metabolic inflammation.* Br J Pharmacol, 2020. **177**(19): p. 4416-4432.
502. Lee, S.W., et al., *Bortezomib attenuates murine collagen-induced arthritis.* Ann Rheum Dis, 2009. **68**(11): p. 1761-7.
503. Baig, M.S., et al., *Repurposing Thioridazine (TDZ) as an anti-inflammatory agent.* Scientific Reports, 2018. **8**(1): p. 12471.
504. Fei, F., et al., *Effects of nilotinib on regulatory T cells: the dose matters.* Molecular Cancer, 2010. **9**(1): p. 22.
505. Fei, F., et al., *Tyrosine Kinase Inhibitors Dasatinib, Nilotinib and Imatinib Have an Impact on Both CD8+ T Lymphocytes and CD4+CD25+FoxP3+ Regulatory T Cells by Downregulation of the NF-κB Pathway.* Blood, 2007. **110**(11): p. 2368.

506. Cooper, M.J., et al., *Application of multiplexed kinase inhibitor beads to study kinome adaptations in drug-resistant leukemia.* PLoS One, 2013. **8**(6): p. e66755.
507. Auphan, N., et al., *Immunosuppression by glucocorticoids: inhibition of NF-κB activity through induction of IκB synthesis.* Science, 1995. **270**(5234): p. 286-290.
508. Kandasamy, M., *NF-κB signalling as a pharmacological target in COVID-19: potential roles for IKKβ inhibitors.* Naunyn Schmiedebergs Arch Pharmacol, 2021. **394**(3): p. 561-567.
509. *Dexamethasone in Hospitalized Patients with Covid-19.* New England Journal of Medicine, 2020. **384**(8): p. 693-704.
510. Shakoory, B., et al., *Interleukin-1 receptor blockade is associated with reduced mortality in sepsis patients with features of the macrophage activation syndrome: Re-analysis of a prior Phase III trial.* Critical care medicine, 2016. **44**(2): p. 275.
511. Dimopoulos, G., et al., *Favorable anakinra responses in severe Covid-19 patients with secondary hemophagocytic lymphohistiocytosis.* Cell host & microbe, 2020. **28**(1): p. 117-123. e1.
512. Pontali, E., et al., *Safety and efficacy of early high-dose IV anakinra in severe COVID-19 lung disease.* Journal of Allergy and Clinical Immunology, 2020. **146**(1): p. 213-215.
513. Cavalli, G., et al., *Interleukin-1 blockade with high-dose anakinra in patients with COVID-19, acute respiratory distress syndrome, and hyperinflammation: a retrospective cohort study.* The Lancet Rheumatology, 2020. **2**(6): p. e325-e331.
514. Huet, T., et al., *Anakinra for severe forms of COVID-19: a cohort study.* The Lancet Rheumatology, 2020. **2**(7): p. e393-e400.
515. Navarro-Millán, I., et al., *Use of anakinra to prevent mechanical ventilation in severe COVID-19: A case series.* Arthritis & Rheumatology, 2020. **72**(12): p. 1990-1997.
516. Hughes, J.P., et al., *Principles of early drug discovery.* Br J Pharmacol, 2011. **162**(6): p. 1239-49.
517. Zhang, J.H., T.D. Chung, and K.R. Oldenburg, *A Simple Statistical Parameter for Use in Evaluation and Validation of High Throughput Screening Assays.* J Biomol Screen, 1999. **4**(2): p. 67-73.
518. Bray MA, C.A. *Advanced Assay Development Guidelines for Image-Based High Content Screening and Analysis*. Assay Guidance Manual 2017 08.07.2017 [cited 2024 23.01.]; Available from: https://www.ncbi.nlm.nih.gov/books/NBK126174/.
519. Guo, K., J. Ma, and W. Liang, *Effects of SB202190 on expression levels of IL-6 and NF-κB in flap ischemia-reperfusion injury.* Exp Ther Med, 2018. **16**(3): p. 2522-2526.
520. Park, J.M., et al., *Signaling Pathways and Genes that Inhibit Pathogen-Induced Macrophage Apoptosis— CREB and NF-κB as Key Regulators.* Immunity, 2005. **23**(3): p. 319-329.
521. Shan, Y., et al., *Sulforaphane down-regulates COX-2 expression by activating p38 and inhibiting NF-kappaB-DNA-binding activity in human bladder T24 cells.* Int J Oncol, 2009. **34**(4): p. 1129-34.
522. Sørensen, M.G., et al., *Screening of protein kinase inhibitors identifies PKC inhibitors as inhibitors of osteoclastic acid secretion and bone resorption.* BMC Musculoskeletal Disorders, 2010. **11**(1): p. 250.
523. Agbottah, E., et al., *Two specific drugs, BMS-345541 and purvalanol A induce apoptosis of HTLV-1 infected cells through inhibition of the NF-kappaB and cell cycle pathways.* AIDS Res Ther, 2008. **5**: p. 12.
524. Liu, L., et al., *Cyclin-dependent kinase inhibitors block leukocyte adhesion and migration.* J Immunol, 2008. **180**(3): p. 1808-17.
525. Coldewey, S.M., et al., *Inhibition of IκB kinase reduces the multiple organ dysfunction caused by sepsis in the mouse.* Dis Model Mech, 2013. **6**(4): p. 1031-42.

526. Fong, C.H., et al., *An antiinflammatory role for IKKbeta through the inhibition of "classical" macrophage activation.* J Exp Med, 2008. **205**(6): p. 1269-76.
527. Ogawa, H., et al., *IκB kinase β inhibitor IMD-0354 suppresses airway remodelling in a Dermatophagoides pteronyssinus-sensitized mouse model of chronic asthma.* Clin Exp Allergy, 2011. **41**(1): p. 104-15.
528. Sugita, A., et al., *Antiallergic and Anti-Inflammatory Effects of a Novel IκB Kinase β Inhibitor, IMD-0354, in a Mouse Model of Allergic Inflammation.* International Archives of Allergy and Immunology, 2009. **148**(3): p. 186-198.
529. Yanai, A., et al., *Activation of IκB Kinase β and NF-κB Is Essential for Helicobacter pylori-Induced Chronic Gastritis in Mongolian Gerbils.* Infection and Immunity, 2008. **76**(2): p. 781-787.
530. Ottosen, E.R., et al., *Synthesis and structure-activity relationship of aminobenzophenones. A novel class of p38 MAP kinase inhibitors with high antiinflammatory activity.* J Med Chem, 2003. **46**(26): p. 5651-62.
531. Usui, T., et al., *Eukaryotic elongation factor 2 kinase regulates the development of hypertension through oxidative stress-dependent vascular inflammation.* Am J Physiol Heart Circ Physiol, 2013. **305**(5): p. H756-68.
532. Li, W., et al., *Fluoxetine regulates eEF2 activity (phosphorylation) via HDAC1 inhibitory mechanism in an LPS-induced mouse model of depression.* Journal of Neuroinflammation, 2021. **18**(1): p. 38.
533. Birkenkamp, K.U., et al., *The p38 MAP kinase inhibitor SB203580 enhances nuclear factor-kappa B transcriptional activity by a non-specific effect upon the ERK pathway.* Br J Pharmacol, 2000. **131**(1): p. 99-107.
534. Herman, A.P., et al., *Peripheral injection of SB203580 inhibits the inflammatory-dependent synthesis of proinflammatory cytokines in the hypothalamus.* Biomed Res Int, 2014. **2014**: p. 475152.
535. Jia, Y.-T., et al., *Activation of p38 MAPK by Reactive Oxygen Species Is Essential in a Rat Model of Stress-Induced Gastric Mucosal Injury.* The Journal of Immunology, 2007. **179**(11): p. 7808-7819.
536. King, E.M., et al., *Inhibition of NF-kappaB-dependent transcription by MKP-1: transcriptional repression by glucocorticoids occurring via p38 MAPK.* J Biol Chem, 2009. **284**(39): p. 26803-15.
537. Underwood, D.C., et al., *SB 239063, a potent p38 MAP kinase inhibitor, reduces inflammatory cytokine production, airways eosinophil infiltration, and persistence.* J Pharmacol Exp Ther, 2000. **293**(1): p. 281-8.
538. Jia, Y.T., et al., *Activation of p38 MAPK by reactive oxygen species is essential in a rat model of stress-induced gastric mucosal injury.* J Immunol, 2007. **179**(11): p. 7808-19.
539. Youssif, C., et al., *Myeloid p38α signaling promotes intestinal IGF-1 production and inflammation-associated tumorigenesis.* EMBO Mol Med, 2018. **10**(7).
540. Li, Z., et al., *Co-targeting EGFR and IKKβ/NF-κB signalling pathways in head and neck squamous cell carcinoma: a potential novel therapy for head and neck squamous cell cancer.* British Journal of Cancer, 2019. **120**(3): p. 306-316.
541. Noguchi, T., et al., *Gefitinib initiates sterile inflammation by promoting IL-1β and HMGB1 release via two distinct mechanisms.* Cell Death & Disease, 2021. **12**(1): p. 49.
542. Miyake, K., et al., *Epidermal growth factor receptor-tyrosine kinase inhibitor (gefitinib) augments pneumonitis, but attenuates lung fibrosis in response to radiation injury in rats.* J Med Invest, 2012. **59**(1-2): p. 174-85.
543. Paez-Mayorga, J., et al., *Ponatinib Activates an Inflammatory Response in Endothelial Cells via ERK5 SUMOylation.* Front Cardiovasc Med, 2018. **5**: p. 125.

544. Chen, S., et al., *Ponatinib Protects Mice From Lethal Influenza Infection by Suppressing Cytokine Storm.* Frontiers in Immunology, 2019. **10**.
545. Momeny, M., et al., *Anti-tumour activity of tivozanib, a pan-inhibitor of VEGF receptors, in therapy-resistant ovarian carcinoma cells.* Sci Rep, 2017. **7**: p. 45954.
546. Brooks, M.B., *Erlotinib and gefitinib, epidermal growth factor receptor kinase inhibitors, may treat non-cancer-related tumor necrosis factor-α mediated inflammatory diseases.* Oncologist, 2013. **18**(1): p. e3-5.
547. Xue, Q., et al., *Erlotinib protests against LPS-induced parthanatos through inhibiting macrophage surface TLR4 expression.* Cell Death Discovery, 2021. **7**(1): p. 181.
548. De, S., et al., *Erlotinib protects against LPS-induced Endotoxicity because TLR4 needs EGFR to signal.* Proceedings of the National Academy of Sciences, 2015. **112**(31): p. 9680-9685.
549. Blakely, C.M., et al., *NF-κB-activating complex engaged in response to EGFR oncogene inhibition drives tumor cell survival and residual disease in lung cancer.* Cell Rep, 2015. **11**(1): p. 98-110.
550. Rasmi, R.R., K.M. Sakthivel, and C. Guruvayoorappan, *NF-κB inhibitors in treatment and prevention of lung cancer.* Biomedicine & Pharmacotherapy, 2020. **130**: p. 110569.
551. Liu, F., et al., *Nintedanib, a triple tyrosine kinase inhibitor, attenuates renal fibrosis in chronic kidney disease.* Clin Sci (Lond), 2017. **131**(16): p. 2125-2143.
552. Li, X., et al., *Nintedanib ameliorates imiquimod-induced psoriasis in mice by inhibiting NF-κB and VEGFR2 signaling.* Int Immunopharmacol, 2021. **100**: p. 108129.
553. Feng, L., et al., *Synergistic Inhibition of Renal Fibrosis by Nintedanib and Gefitinib in a Murine Model of Obstructive Nephropathy.* Kidney Diseases, 2021. **7**(1): p. 34-49.
554. Wollin, L., et al., *Antifibrotic and anti-inflammatory activity of the tyrosine kinase inhibitor nintedanib in experimental models of lung fibrosis.* J Pharmacol Exp Ther, 2014. **349**(2): p. 209-20.
555. Gad, E.S., et al., *The Anti-fibrotic and Anti-inflammatory Potential of Bone Marrow-Derived Mesenchymal Stem Cells and Nintedanib in Bleomycin-Induced Lung Fibrosis in Rats.* Inflammation, 2020. **43**(1): p. 123-134.
556. Puhl, A.C., et al., *Vandetanib Reduces Inflammatory Cytokines and Ameliorates COVID-19 in Infected Mice.* bioRxiv, 2021.
557. Tang, D., et al., *Apatinib-induced NF-κB inactivation sensitizes triple-negative breast cancer cells to doxorubicin.* Am J Transl Res, 2020. **12**(7): p. 3741-3753.
558. Maroufi, N.F., et al., *The apatinib inhibits breast cancer cell line MDA-MB-231 in vitro by inducing apoptosis, cell cycle arrest, and regulating nuclear factor-κB (NF-κB) and mitogen-activated protein kinase (MAPK) signaling pathways.* Breast Cancer, 2020. **27**(4): p. 613-620.
559. He, X., et al., *Apatinib Inhibits the Invasion and Metastasis of Liver Cancer Cells by Downregulating MMP-Related Proteins via Regulation of the NF-κB Signaling Pathway.* BioMed Research International, 2020. **2020**: p. 3126182.
560. Chong D, G.G., Li D, Yang Y, Wang R, *Remission of Psoriasis during Treatment with Apatinib in a Patient with Rectal Cancer.* J Dermatol Res Ther, 2019. **5:068**.
561. Weng, M.C., et al., *Regorafenib inhibits tumor progression through suppression of ERK/NF-κB activation in hepatocellular carcinoma bearing mice.* Biosci Rep, 2018. **38**(3).
562. Weng, M.-C., et al., *Apoptosis induction and AKT/NF-κB inactivation are associated with regroafenib-inhibited tumor progression in non-small cell lung cancer in vitro and in vivo.* Biomedicine & Pharmacotherapy, 2019. **116**: p. 109032.

563. Tsai, J.-J., P.-J. Pan, and F.-T. Hsu, *Regorafenib induces extrinsic and intrinsic apoptosis through inhibition of ERK/NF-κB activation in hepatocellular carcinoma cells.* Oncol Rep, 2017. **37**(2): p. 1036-1044.
564. Liu, Y.C., R.H. Wu, and W.S. Wang, *Regorafenib diminishes the expression and secretion of angiogenesis and metastasis associated proteins and inhibits cell invasion via NF-κB inactivation in SK-Hep1 cells.* Oncol Lett, 2017. **14**(1): p. 461-467.
565. WU, J.-Y., et al., *Induction of Apoptosis and Inhibition of EGFR/NF-κB Signaling Are Associated With Regorafenib-sensitized Non-small Cell Lung Cancer to Cisplatin.* In Vivo, 2021. **35**(5): p. 2569-2576.
566. Canning, P., et al., *Inflammatory Signaling by NOD-RIPK2 Is Inhibited by Clinically Relevant Type II Kinase Inhibitors.* Chem Biol, 2015. **22**(9): p. 1174-84.
567. Han, K.M., et al., *Regorafenib Regulates AD Pathology, Neuroinflammation, and Dendritic Spinogenesis in Cells and a Mouse Model of AD.* Cells, 2020. **9**(7).
568. Spirina, L.V., et al., *Effect of Targeted Therapy With Pazopanib on Expression Levels of Transcription, Growth Factors and Components of AKT/m-TOR Signaling Pathway in Patients with Renal Cell Carcinoma.* Asian Pac J Cancer Prev, 2017. **18**(11): p. 2977-2983.
569. Spirina, L., Usynin, E. , Kondakova, I. , Yurmazov, Z. and Slonimskaya, E, *Molecular Markers of Kidney Cancer Progression, Association with Efficiency of Pazopanib Therapy.* Journal of Biomedical Science and Engineering, 2015. **8**: p. 756-766.
570. Kim, J., et al., *Sorafenib Modulates the LPS- and Aβ-Induced Neuroinflammatory Response in Cells, Wild-Type Mice, and 5xFAD Mice.* Front Immunol, 2021. **12**: p. 684344.
571. Martens, S., et al., *Sorafenib tosylate inhibits directly necrosome complex formation and protects in mouse models of inflammation and tissue injury.* Cell Death & Disease, 2017. **8**(6): p. e2904-e2904.
572. Zahavi, T., et al., *Sorafenib treatment during partial hepatectomy reduces tumorgenesis in an inflammation-associated liver cancer model.* Oncotarget, 2015. **7**(4).
573. Zanotto-Filho, A., et al., *Sorafenib improves alkylating therapy by blocking induced inflammation, invasion and angiogenesis in breast cancer cells.* Cancer Lett, 2018. **425**: p. 101-115.
574. Wu, C.H., et al., *Sorafenib Induces Apoptosis and Inhibits NF-κB-mediated Anti-apoptotic and Metastatic Potential in Osteosarcoma Cells.* Anticancer Res, 2021. **41**(3): p. 1251-1259.
575. Dudgeon, C., et al., *Inhibiting oncogenic signaling by sorafenib activates PUMA via GSK3β and NF-κB to suppress tumor cell growth.* Oncogene, 2012. **31**(46): p. 4848-4858.
576. Li, J., et al., *Sorafenib inhibits caspase-1 expression through suppressing TLR4/stat3/SUMO1 pathway in hepatocellular carcinoma.* Cancer Biology & Therapy, 2018. **19**(11): p. 1057-1064.
577. Miller, S.C., et al., *Identification of known drugs that act as inhibitors of NF-kappaB signaling and their mechanism of action.* Biochemical pharmacology, 2010. **79**(9): p. 1272-1280.
578. Canacankatan, N., et al., *Effect of axitinib on inflammation in experimental corneal neovascularization model in rats Axitinibin sıçanlarda deneysel kornea neovascularizasyon modelinde inflamasyona etkisi.* Cukurova Medical Journal, 2018. **43**: p. 275-284.

579. Du Four, S., et al., *Axitinib increases the infiltration of immune cells and reduces the suppressive capacity of monocytic MDSCs in an intracranial mouse melanoma model.* Oncoimmunology, 2015. **4**(4): p. e998107.
580. Heine, A., et al., *The VEGF-Receptor Inhibitor Axitinib Impairs Dendritic Cell Phenotype and Function.* PLoS One, 2015. **10**(6): p. e0128897.
581. Heusschen, R., et al., *SRC kinase inhibition with saracatinib limits the development of osteolytic bone disease in multiple myeloma.* Oncotarget, 2016. **7**(21): p. 30712-29.
582. Gage, M., et al., *Saracatinib, a Src Tyrosine Kinase Inhibitor, as a Disease Modifier in the Rat DFP Model: Sex Differences, Neurobehavior, Gliosis, Neurodegeneration, and Nitro-Oxidative Stress.* Antioxidants, 2022. **11**(1): p. 61.
583. Sharma, S., et al., *Mechanisms of disease-modifying effect of saracatinib (AZD0530), a Src/Fyn tyrosine kinase inhibitor, in the rat kainate model of temporal lobe epilepsy.* Neurobiology of Disease, 2021. **156**: p. 105410.
584. Chen, Y.-J., et al., *Anti-inflammatory effect of afatinib (an EGFR-TKI) on OGD-induced neuroinflammation.* Scientific Reports, 2019. **9**(1): p. 2516.
585. Liu, X., et al., *Case Report: Afatinib-Induced Interstitial Pneumonia: Experiences and Lessons From Two Patients.* Frontiers in Pharmacology, 2021. **12**.
586. Kimura, T., et al., *Immunomodulatory activity of lenvatinib contributes to antitumor activity in the Hepa1-6 hepatocellular carcinoma model.* Cancer Sci, 2018. **109**(12): p. 3993-4002.
587. Torrens, L., et al., *Immunomodulatory Effects of Lenvatinib Plus Anti–Programmed Cell Death Protein 1 in Mice and Rationale for Patient Enrichment in Hepatocellular Carcinoma.* Hepatology, 2021. **74**(5): p. 2652-2669.
588. Liu, Y.C., et al., *Lenvatinib Inhibits AKT/NF-κB Signaling and Induces Apoptosis Through Extrinsic/Intrinsic Pathways in Non-small Cell Lung Cancer.* Anticancer Res, 2021. **41**(1): p. 123-130.
589. Liu, Y.C., et al., *Lenvatinib Induces AKT/NF-κB Inactivation, Apoptosis Signal Transduction and Growth Inhibition of Non-small Cell Lung Cancer In Vivo.* Anticancer Res, 2021. **41**(6): p. 2867-2874.
590. Chao, T.-L., et al., *Abstract 966: Lenvatinib induces apoptosis and inhibits metastasis through downregulate Wnt/GSK3β/NF-κB in hepatocellular carcinoma.* Cancer Research, 2021. **81**(13 Supplement): p. 966-966.
591. Wang, L., et al., *Pexidartinib (PLX3397) through restoring hippocampal synaptic plasticity ameliorates social isolation-induced mood disorders.* Int Immunopharmacol, 2022. **113**(Pt B): p. 109436.
592. Dunn, T.N., et al., *Inhibition of CSF1R and KIT With Pexidartinib Reduces Inflammatory Signaling and Cell Viability in Endometriosis.* Endocrinology, 2024. **165**(4).
593. Colado, A., et al., *Effect of the BTK inhibitor ibrutinib on macrophage- and γδ T cell-mediated response against Mycobacterium tuberculosis.* Blood Cancer Journal, 2018. **8**(11): p. 100.
594. O'Riordan, C.E., et al., *X-linked immunodeficient mice with no functional Bruton's tyrosine kinase are protected from sepsis-induced multiple organ failure.* Frontiers in immunology, 2020. **11**: p. 581758.
595. Hart, R. and D.R. Greaves, *Chemerin Contributes to Inflammation by Promoting Macrophage Adhesion to VCAM-1 and Fibronectin through Clustering of VLA-4 and VLA-5.* The Journal of Immunology, 2010. **185**(6): p. 3728-3739.
596. Ciesielska, A., M. Matyjek, and K. Kwiatkowska, *TLR4 and CD14 trafficking and its influence on LPS-induced pro-inflammatory signaling.* Cellular and Molecular Life Sciences, 2021. **78**(4): p. 1233-1261.

597. Sasaki, R., et al., *Different Mechanisms of Action of Regorafenib and Lenvatinib on Toll-Like Receptor-Signaling Pathways in Human Hepatoma Cell Lines.* Int J Mol Sci, 2020. **21**(9).
598. Li, X., et al., *Sorafenib inhibits LPS-induced inflammation by regulating Lyn-MAPK-NF-kB/AP-1 pathway and TLR4 expression.* Cell Death Discov, 2022. **8**(1): p. 281.
599. Richard, K., S.N. Vogel, and D.J. Perkins, *Quantitation of TLR4 Internalization in Response to LPS in Thioglycollate Elicited Peritoneal mouse Macrophages by Flow Cytometry.* Bio Protoc, 2019. **9**(18).
600. Ponzoni, M., et al., *Targeting Macrophages as a Potential Therapeutic Intervention: Impact on Inflammatory Diseases and Cancer.* Int J Mol Sci, 2018. **19**(7).
601. Wynn, T.A., A. Chawla, and J.W. Pollard, *Macrophage biology in development, homeostasis and disease.* Nature, 2013. **496**(7446): p. 445-455.
602. Liddiard, K., et al., *Macrophage heterogeneity and acute inflammation.* European Journal of Immunology, 2011. **41**(9): p. 2503-2508.
603. Utomo, L., et al., *Guiding synovial inflammation by macrophage phenotype modulation: an in vitro study towards a therapy for osteoarthritis.* Osteoarthritis and Cartilage, 2016. **24**(9): p. 1629-1638.
604. Zhou, T., et al., *An injectable hydrogel dotted with dexamethasone acetate-encapsulated reactive oxygen species-scavenging micelles for combinatorial therapy of osteoarthritis.* Materials Today Nano, 2022. **17**: p. 100164.
605. Li, D., et al., *Metformin attenuates osteoarthritis by targeting chondrocytes, synovial macrophages and adipocytes.* Rheumatology, 2023. **62**(4): p. 1652-1661.
606. Kanigur Sultuybek, G., T. Soydas, and G. Yenmis, *NF-κB as the mediator of metformin's effect on ageing and ageing-related diseases.* Clinical and Experimental Pharmacology and Physiology, 2019. **46**(5): p. 413-422.
607. Auphan, N., et al., *Immunosuppression by glucocorticoids: inhibition of NF-kappa B activity through induction of I kappa B synthesis.* Science, 1995. **270**(5234): p. 286-90.
608. Rodell, C.B., P.D. Koch, and R. Weissleder, *Screening for new macrophage therapeutics.* Theranostics, 2019. **9**(25): p. 7714-7729.
609. Zordan, M.D., et al., *A high throughput, interactive imaging, bright-field wound healing assay.* Cytometry A, 2011. **79**(3): p. 227-32.
610. Hu, G., et al., *High-throughput phenotypic screen and transcriptional analysis identify new compounds and targets for macrophage reprogramming.* Nature Communications, 2021. **12**(1): p. 773.
611. Li, D., et al., *The dysregulation of immune cells induced by uric acid: mechanisms of inflammation associated with hyperuricemia and its complications.* Front Immunol, 2023. **14**: p. 1282890.
612. Sedger, L.M. and M.F. McDermott, *TNF and TNF-receptors: From mediators of cell death and inflammation to therapeutic giants – past, present and future.* Cytokine & Growth Factor Reviews, 2014. **25**(4): p. 453-472.
613. Farhana A, K.Y. *Biochemistry, Lipopolysaccharide*. 2023 17.4.2023 [cited 2024 17.01.]; Available from: https://www.ncbi.nlm.nih.gov/books/NBK554414/.
614. Chen, S., et al., *Macrophages in immunoregulation and therapeutics.* Signal Transduction and Targeted Therapy, 2023. **8**(1): p. 207.
615. Wassenaar, T.M. and K. Zimmermann, *Lipopolysaccharides in Food, Food Supplements, and Probiotics: Should We be Worried?* Eur J Microbiol Immunol (Bp), 2018. **8**(3): p. 63-69.
616. Page, M.J., D.B. Kell, and E. Pretorius, *The Role of Lipopolysaccharide-Induced Cell Signalling in Chronic Inflammation.* Chronic Stress, 2022. **6**: p. 24705470221076390.

617. InvivoGen. *RIG-I-Like Receptors & Cytosolic DNA Sensors*. [cited 2024 18.01.]; Available from: https://www.invivogen.com/review-rlr.
618. Wu, Y. and B.P. Zhou, *TNF-α/NF-κB/Snail pathway in cancer cell migration and invasion.* British Journal of Cancer, 2010. **102**(4): p. 639-644.
619. Inc., B.H.P. *Treatment With NEXAVAR (Sorafenib)*. 2015 06.2020 [cited 2024 18.01.]; Available from: https://labeling.bayerhealthcare.com/html/products/pi/Nexavar_PI.pdf.
620. Li, X., et al., *Sorafenib inhibits LPS-induced inflammation by regulating Lyn-MAPK-NF-kB/AP-1 pathway and TLR4 expression.* Cell Death Discovery, 2022. **8**(1): p. 281.
621. Goel, G., *Evolution of regorafenib from bench to bedside in colorectal cancer: Is it an attractive option or merely a "me too" drug?* Cancer Manag Res, 2018. **10**: p. 425-437.
622. Wilhelm, S.M., et al., *Regorafenib (BAY 73-4506): A new oral multikinase inhibitor of angiogenic, stromal and oncogenic receptor tyrosine kinases with potent preclinical antitumor activity.* International Journal of Cancer, 2011. **129**(1): p. 245-255.
623. Grothey, A., et al., *Evolving role of regorafenib for the treatment of advanced cancers.* Cancer Treatment Reviews, 2020. **86**: p. 101993.
624. Liu, Y.-C., et al., *Regorafenib suppresses epidermal growth factor receptor signaling-modulated progression of colorectal cancer.* Biomedicine & Pharmacotherapy, 2020. **128**: p. 110319.
625. Grünewald, S., et al., *Effects of regorafenib on the mononuclear/phagocyte system and how these contribute to the inhibition of colorectal tumors in mice.* European Journal of Medical Research, 2023. **28**(1): p. 147.
626. Ou, D.L., et al., *Regorafenib enhances antitumor immunity via inhibition of p38 kinase/Creb1/Klf4 axis in tumor-associated macrophages.* J Immunother Cancer, 2021. **9**(3).
627. Saleh, R., et al., *CSF-1 in Inflammatory and Arthritic Pain Development.* The Journal of Immunology, 2018. **201**(7): p. 2042-2053.
628. Onuora, S., *Antibody against CSF-1 receptor protects bone and cartilage.* Nature Reviews Rheumatology, 2014. **10**(5): p. 260-260.
629. Hu, X., et al., *Imatinib inhibits CSF1R that stimulates proliferation of rheumatoid arthritis fibroblast-like synoviocytes.* Clin Exp Immunol, 2019. **195**(2): p. 237-250.
630. Dalbeth, N., et al., *Enhanced osteoclastogenesis in patients with tophaceous gout: Urate crystals promote osteoclast development through interactions with stromal cells.* Arthritis & Rheumatism, 2008. **58**(6): p. 1854-1865.
631. Alvarado-Vazquez, P.A., et al., *Intra-articular administration of an antibody against CSF-1 receptor reduces pain-related behaviors and inflammation in CFA-induced knee arthritis.* Neuroscience Letters, 2015. **584**: p. 39-44.
632. Tan, Y., et al., *Mechanisms of Toll-like Receptor 4 Endocytosis Reveal a Common Immune-Evasion Strategy Used by Pathogenic and Commensal Bacteria.* Immunity, 2015. **43**(5): p. 909-22.
633. Lin, Y.-C., et al., *The Tyrosine Kinase Syk Differentially Regulates Toll-like Receptor Signaling Downstream of the Adaptor Molecules TRAF6 and TRAF3.* Science Signaling, 2013. **6**(289): p. ra71-ra71.
634. Tsukamoto, H., et al., *Lipopolysaccharide (LPS)-binding protein stimulates CD14-dependent Toll-like receptor 4 internalization and LPS-induced TBK1–IKKε–IRF3 axis activation.* Journal of Biological Chemistry, 2018. **293**(26): p. 10186-10201.
635. Yao, X., et al., *Leukadherin-1-Mediated Activation of CD11b Inhibits LPS-Induced Pro-inflammatory Response in Macrophages and Protects Mice Against Endotoxic Shock by Blocking LPS-TLR4 Interaction.* Frontiers in Immunology, 2019. **10**.

636. Zanoni, I., et al., *CD14 Controls the LPS-Induced Endocytosis of Toll-like Receptor 4.* Cell, 2011. **147**(4): p. 868-880.
637. Rajaiah, R., et al., *CD14 dependence of TLR4 endocytosis and TRIF signaling displays ligand specificity and is dissociable in endotoxin tolerance.* Proceedings of the National Academy of Sciences, 2015. **112**(27): p. 8391-8396.
638. Ling, G.S., et al., *Integrin CD11b positively regulates TLR4-induced signalling pathways in dendritic cells but not in macrophages.* Nature Communications, 2014. **5**(1): p. 3039.
639. Ghosh, M., et al., *CD13 Restricts TLR4 Endocytic Signal Transduction in Inflammation.* J Immunol, 2015. **194**: p. 4466-76.
640. Zanoni, I., et al., *CD14 controls the LPS-induced endocytosis of Toll-like receptor 4.* Cell, 2011. **147**(4): p. 868-80.
641. Qian, C., et al., *Heterogeneous macrophages: Supersensors of exogenous inducing factors.* Scand J Immunol, 2019. **90**(1): p. e12768.
642. Trojan, J. and O. Waidmann, *Role of regorafenib as second-line therapy and landscape of investigational treatment options in advanced hepatocellular carcinoma.* J Hepatocell Carcinoma, 2016. **3**: p. 31-36.
643. Velcicky, J., et al., *Modulating ADME Properties by Fluorination: MK2 Inhibitors with Improved Oral Exposure.* ACS Med Chem Lett, 2018. **9**(4): p. 392-396.
644. Kissel, M., et al., *Antitumor effects of regorafenib and sorafenib in preclinical models of hepatocellular carcinoma.* Oncotarget, 2017. **8**(63): p. 107096-107108.
645. Zopf, D., et al., *Pharmacologic activity and pharmacokinetics of metabolites of regorafenib in preclinical models.* Cancer medicine, 2016. **5**(11): p. 3176-3185.
646. Saber-Mahloogi H, M.D. *Pharmacology Review- Nexavar (sorafenib tosylate)*. 2005 28.10.2005 [cited 2024 18.01.]; Available from: http://www.accessdata.fda.gov/drugsatfda_docs/nda/2005/021923_s000_Nexavar_PharmR.pdf.
647. Haralampiev, I., et al., *The interaction of sorafenib and regorafenib with membranes is modulated by their lipid composition.* Biochim Biophys Acta, 2016. **1858**(11): p. 2871-2881.
648. Georgantas, R.W., 3rd, et al., *CD34+ hematopoietic stem-progenitor cell microRNA expression and function: a circuit diagram of differentiation control.* Proc Natl Acad Sci U S A, 2007. **104**(8): p. 2750-5.
649. Copeland, S., et al., *Acute inflammatory response to endotoxin in mice and humans.* Clin Diagn Lab Immunol, 2005. **12**(1): p. 60-7.
650. Lewis, A.J., C.W. Seymour, and M.R. Rosengart, *Current Murine Models of Sepsis.* Surg Infect (Larchmt), 2016. **17**(4): p. 385-93.
651. Remick, D.G., et al., *COMPARISON OF THE MORTALITY AND INFLAMMATORY RESPONSE OF TWO MODELS OF SEPSIS: LIPOPOLYSACCHARIDE VS. CECAL LIGATION AND PUNCTURE.* Shock, 2000. **13**(2): p. 110-116.
652. Seok, J., et al., *Genomic responses in mouse models poorly mimic human inflammatory diseases.* Proceedings of the National Academy of Sciences, 2013. **110**(9): p. 3507-3512.
653. Patel, P.N., et al., *Human Experimental Endotoxemia in Modeling the Pathophysiology, Genomics, and Therapeutics of Innate Immunity in Complex Cardiometabolic Diseases.* Arteriosclerosis, Thrombosis, and Vascular Biology, 2015. **35**(3): p. 525-534.
654. Selye, H., *Use of "Granuloma Pouch" Technic in the Study of Antiphlogistic Corticoids.* Proceedings of the Society for Experimental Biology and Medicine, 1953. **82**(2): p. 328-333.
655. Duarte, D.B., M.R. Vasko, and J.C. Fehrenbacher, *Models of inflammation: carrageenan air pouch.* Curr Protoc Pharmacol, 2012. **Chapter 5**: p. Unit5.6.

656. McNeill, E., et al., *Contrasting in vitro vs. in vivo effects of a cell membrane-specific CC-chemokine binding protein on macrophage chemotaxis.* Journal of Molecular Medicine, 2014. **92**(11): p. 1169-1178.
657. Brooks, P.M., D. Burton, and M.J. Forrest, *Crystal-induced inflammation in the rat subcutaneous air-pouch.* Br J Pharmacol, 1987. **90**(2): p. 413-9.
658. Maione, F., et al., *Repetitive Exposure of IL-17 Into the Murine Air Pouch Favors the Recruitment of Inflammatory Monocytes and the Release of IL-16 and TREM-1 in the Inflammatory Fluids.* Frontiers in Immunology, 2018. **9**.
659. Edwards, J.C.W., A.D. Sedgwick, and D.A. Willoughby, *The formation of a structure with the features of synovial lining by subcutaneous injection of air: An in vivo tissue culture system.* The Journal of Pathology, 1981. **134**(2): p. 147-156.
660. Pessler, F., et al., *Identification of novel monosodium urate crystal regulated mRNAs by transcript profiling of dissected murine air pouch membranes.* Arthritis Research & Therapy, 2008. **10**(3): p. R64.
661. Yan, F., et al., *Comparison of the different monosodium urate crystals in the preparation process and pro-inflammation.* Advances in Rheumatology, 2023. **63**(1): p. 39.
662. Liu-Bryan, R., et al., *Innate immunity conferred by toll-like receptors 2 and 4 and myeloid differentiation factor 88 expression is pivotal to monosodium urate monohydrate crystal–induced inflammation.* Arthritis & Rheumatism, 2005. **52**(9): p. 2936-2946.
663. Cooper, D., et al., *Chapter Eleven - Multiple Functional Targets of the Immunoregulatory Activity of Galectin-1: Control of Immune Cell Trafficking, Dendritic Cell Physiology, and T-Cell Fate*, in *Methods in Enzymology*, M. Fukuda, Editor. 2010, Academic Press. p. 199-244.
664. Cash, J.L., G.E. White, and D.R. Greaves, *Chapter 17 Zymosan-Induced Peritonitis as a Simple Experimental System for the Study of Inflammation*, in *Methods in Enzymology*. 2009, Academic Press. p. 379-396.
665. Laurin, L.-P., et al., *Regulation of Experimental Peritonitis: A Complex Orchestration.* Nephron Experimental Nephrology, 2012. **120**(1): p. e41-e46.
666. Martinon, F., et al., *Gout-associated uric acid crystals activate the NALP3 inflammasome.* Nature, 2006. **440**(7081): p. 237-241.
667. Shi, Y., A.D. Mucsi, and G. Ng, *Monosodium urate crystals in inflammation and immunity.* Immunological Reviews, 2010. **233**(1): p. 203-217.
668. Martin, W.J. and J.L. Harper, *Innate inflammation and resolution in acute gout.* Immunology & Cell Biology, 2010. **88**(1): p. 15-19.
669. Liu, X., et al., *Rapid CCL2 Release by Membrane Stromal Cells Initiates Monosodium Urate Crystal-Induced Monocyte Recruitment in a Peritoneal Model of Gouty Inflammation.* European Journal of Inflammation, 2012. **10**(2): p. 165-174.
670. Dostert, C., et al., *Innate Immune Activation Through Nalp3 Inflammasome Sensing of Asbestos and Silica.* Science, 2008. **320**(5876): p. 674-677.
671. Martinon, F., *Update on Biology: Uric Acid and the Activation of Immune and Inflammatory Cells.* Current Rheumatology Reports, 2010. **12**(2): p. 135-141.
672. Chen, C.J., et al., *MyD88-dependent IL-1 receptor signaling is essential for gouty inflammation stimulated by monosodium urate crystals.* J Clin Invest, 2006. **116**(8): p. 2262-71.
673. Scott, P., et al., *Engagement of CD14 Mediates the Inflammatory Potential of Monosodium Urate Crystals1.* The Journal of Immunology, 2006. **177**(9): p. 6370-6378.

674. Liu-Bryan, R., et al., *TLR2 signaling in chondrocytes drives calcium pyrophosphate dihydrate and monosodium urate crystal-induced nitric oxide generation.* J Immunol, 2005. **174**(8): p. 5016-23.
675. Chen, L., et al., *Stimulation of inducible nitric oxide synthase by monosodium urate crystals in macrophages and expression of iNOS in gouty arthritis.* Nitric Oxide, 2004. **11**(3): p. 228-236.
676. Zamudio-Cuevas, Y., et al., *Molecular basis of oxidative stress in gouty arthropathy.* Clinical Rheumatology, 2015. **34**(10): p. 1667-1672.
677. Bellingan, G.J., et al., *In vivo fate of the inflammatory macrophage during the resolution of inflammation: inflammatory macrophages do not die locally, but emigrate to the draining lymph nodes.* J Immunol, 1996. **157**(6): p. 2577-85.
678. Gautier, E.L., et al., *Local apoptosis mediates clearance of macrophages from resolving inflammation in mice.* Blood, 2013. **122**(15): p. 2714-22.
679. Page, H.T., et al., *Tyrosine Kinases and Inflammatory Signalling.* Current Molecular Medicine, 2009. **9**(1): p. 69-85.
680. Okutani, D., et al., *Src protein tyrosine kinase family and acute inflammatory responses.* American Journal of Physiology-Lung Cellular and Molecular Physiology, 2006. **291**(2): p. L129-L141.
681. Macfarlane, J.G., *The role of src kinases in controlling neutrophil function in acute inflammation*, in *Institute of Cellular Medicine*. 2016, Newcastle University.
682. Tsai, Y.-F., et al., *Resveratrol suppresses neutrophil activation via inhibition of Src family kinases to attenuate lung injury.* Free Radical Biology and Medicine, 2019. **145**: p. 67-77.
683. Guo, R., et al., *Ibrutinib suppresses the activation of neutrophils and macrophages and exerts therapeutic effect on acute peritonitis induced by zymosan.* Int Immunopharmacol, 2022. **113**(Pt B): p. 109469.
684. Stadler, N., et al., *The Bruton tyrosine kinase inhibitor ibrutinib abrogates triggering receptor on myeloid cells 1-mediated neutrophil activation.* Haematologica, 2017. **102**(5): p. e191-e194.
685. Huang, J., et al., *Discovery of Ibrutinib-based BTK PROTACs with in vivo anti-inflammatory efficacy by inhibiting NF-κB activation.* European Journal of Medicinal Chemistry, 2023. **259**: p. 115664.
686. Klück, V., R. Liu, and L.A.B. Joosten, *The role of interleukin-1 family members in hyperuricemia and gout.* Joint Bone Spine, 2021. **88**(2): p. 105092.
687. Reber, L.L., et al., *The tyrosine kinase inhibitor imatinib mesylate suppresses uric acid crystal-induced acute gouty arthritis in mice.* PLoS One, 2017. **12**(10): p. e0185704.
688. Yuan, W., et al., *Autophagy induced by PP121 alleviates MSU crystal-induced acute gouty arthritis via inhibition of the NLRP3 inflammasome.* International Immunopharmacology, 2023. **123**: p. 110756.
689. Futosi, K., et al., *Myeloid Src-family kinases are critical for neutrophil-mediated autoinflammation in gout and motheaten models.* Journal of Experimental Medicine, 2023. **220**(7).
690. Yang, S.-P., et al., *Carvedilol, a new antioxidative β-blocker, blocks in vitro human peripheral blood T cell activation by downregulating NF-κB activity.* Cardiovascular Research, 2003. **59**(3): p. 776-787.
691. Wong, W.T., et al., *Repositioning of the β-Blocker Carvedilol as a Novel Autophagy Inducer That Inhibits the NLRP3 Inflammasome.* Front Immunol, 2018. **9**: p. 1920.
692. Lin, W.Y., et al., *Repositioning of the Angiotensin II Receptor Antagonist Candesartan as an Anti-Inflammatory Agent With NLRP3 Inflammasome Inhibitory Activity.* Front Immunol, 2022. **13**: p. 870627.

693. Huang, Y., et al., *Tivantinib alleviates inflammatory diseases by directly targeting NLRP3.* iScience, 2023. **26**(3): p. 106062.
694. Pan, Q., et al., *FAK inhibitor PF-562271 inhibits the migration and proliferation of high-grade serous ovarian cancer cells through FAK and FAK mediated cell cycle arrest.* Medical Oncology, 2023. **40**(8): p. 215.
695. Infante, J.R., et al., *Safety, pharmacokinetic, and pharmacodynamic phase I dose-escalation trial of PF-00562271, an inhibitor of focal adhesion kinase, in advanced solid tumors.* Journal of Clinical Oncology, 2012. **30**(13): p. 1527-1533.
696. Chung, I.C., et al., *Pyk2 activates the NLRP3 inflammasome by directly phosphorylating ASC and contributes to inflammasome-dependent peritonitis.* Scientific Reports, 2016. **6**(1): p. 36214.
697. Nolan, R.A., et al., *Dopamine activates NF-κB and primes the NLRP3 inflammasome in primary human macrophages.* Brain Behav Immun Health, 2020. **2**.
698. Groslambert, M. and B.F. Py, *Spotlight on the NLRP3 inflammasome pathway.* J Inflamm Res, 2018. **11**: p. 359-374.
699. Martinon, F., et al., *Gout-associated uric acid crystals activate the NALP3 inflammasome.* Nature, 2006. **440**(7081): p. 237-41.
700. Pang, L., et al., *Pseudogout-associated inflammatory calcium pyrophosphate dihydrate microcrystals induce formation of neutrophil extracellular traps.* J Immunol, 2013. **190**(12): p. 6488-500.
701. So, A.K. and F. Martinon, *Inflammation in gout: mechanisms and therapeutic targets.* Nature Reviews Rheumatology, 2017. **13**(11): p. 639-647.
702. Apostolakis, S., et al., *Interleukin 8 and cardiovascular disease.* Cardiovascular Research, 2009. **84**(3): p. 353-360.
703. Bishara, N., *Chapter 18 - The Use of Biomarkers for Detection of Early- and Late-Onset Neonatal Sepsis*, in *Hematology, Immunology and Infectious Disease: Neonatology Questions and Controversies (Second Edition)*, R.K. Ohls and A. Maheshwari, Editors. 2012, W.B. Saunders: Philadelphia. p. 303-315.
704. Fujishima, S., et al., *Regulation of neutrophil interleukin 8 gene expression and protein secretion by LPS, TNF-alpha, and IL-1 beta.* J Cell Physiol, 1993. **154**(3): p. 478-85.
705. Herman, J., et al., *Pro-inflammatory effects of human apatite crystals extracted from patients suffering from calcific tendinopathy.* Arthritis Research & Therapy, 2021. **23**(1): p. 131.
706. Bins, S., et al., *Influence of OATP1B1 Function on the Disposition of Sorafenib-β-D-Glucuronide.* Clinical and Translational Science, 2017. **10**(4): p. 271-279.
707. Al-Shammari, A.H., et al., *Influx and Efflux Transporters Contribute to the Increased Dermal Exposure to Active Metabolite of Regorafenib After Repeated Oral Administration in Mice.* Journal of Pharmaceutical Sciences, 2019. **108**(6): p. 2173-2179.
708. Inc., B.H.P. *STIVARGA (regorafenib)*. 2012 09.2012 [cited 2024 25.01.]; Available from: https://www.accessdata.fda.gov/drugsatfda_docs/label/2012/203085lbl.pdf.
709. Schnelzer, A.-C., *Myeloid Fra-1 expression modulates the endotoxin tolerance response in sepsis*. 2021.
710. Ghosn, E.E., et al., *Two physically, functionally, and developmentally distinct peritoneal macrophage subsets.* Proc Natl Acad Sci U S A, 2010. **107**(6): p. 2568-73.
711. Yin, C., et al., *CXCL5 activates CXCR2 in nociceptive sensory neurons to drive joint pain and inflammation in experimental gouty arthritis.* Nature Communications, 2024. **15**(1): p. 3263.
712. Lockhart, J.S. and R. Sumagin, *Non-Canonical Functions of Myeloperoxidase in Immune Regulation, Tissue Inflammation and Cancer.* Int J Mol Sci, 2022. **23**(20).

713. Cronstein, B.N. and R. Terkeltaub, *The inflammatory process of gout and its treatment.* Arthritis Research & Therapy, 2006. **8**(1): p. S3.
714. Munjal A, A.A. *Indomethacin*. 2023 31.01.2023 [cited 2023 29.11.]; Available from: https://www.ncbi.nlm.nih.gov/books/NBK555936/.
715. Yoshioka, S., et al., *Immunotoxicity of soluble β-glucans induced by indomethacin treatment.* FEMS Immunology & Medical Microbiology, 1998. **21**(3): p. 171-179.
716. Boushey, R.P., B. Yusta, and D.J. Drucker, *Glucagon-like peptide 2 decreases mortality and reduces the severity of indomethacin-induced murine enteritis.* American Journal of Physiology-Endocrinology and Metabolism, 1999. **277**(5): p. E937-E947.
717. Nadatani, Y., et al., *High mobility group box 1 promotes small intestinal damage induced by nonsteroidal anti-inflammatory drugs through Toll-like receptor 4.* Am J Pathol, 2012. **181**(1): p. 98-110.
718. River, C., *Characteristics of Early and Late Adult C57BL/6NCrl Mice*. Charles River.
719. Mazzaccara, C., et al., *Age-Related Reference Intervals of the Main Biochemical and Hematological Parameters in C57BL/6J, 129SV/EV and C3H/HeJ Mouse Strains.* PLoS One, 2008. **3**(11): p. e3772.
720. Slack, E., et al., *Innate and adaptive immunity cooperate flexibly to maintain host-microbiota mutualism.* Science, 2009. **325**(5940): p. 617-20.
721. Xiao, X., et al., *Gut Microbiota Mediates Protection Against Enteropathy Induced by Indomethacin.* Sci Rep, 2017. **7**: p. 40317.
722. Indomethacin, N.I.o.D.a.D.a.K.D.-. *LiverTox: Clinical and Research Information on Drug-Induced Liver Injury*. 2012 23.03.2018 [cited 2023 29.11.]; Available from: https://www.ncbi.nlm.nih.gov/books/NBK548001.
723. Oliveira, S.H., et al., *Neutrophil migration induced by IL-1beta depends upon LTB4 released by macrophages and upon TNF-alpha and IL-1beta released by mast cells.* Inflammation, 2008. **31**(1): p. 36-46.
724. Dalbeth, N., et al., *Gout.* The Lancet, 2021. **397**(10287): p. 1843-1855.
725. Kim, S.-K., *The Mechanism of the NLRP3 Inflammasome Activation and Pathogenic Implication in the Pathogenesis of Gout.* Journal of Rheumatic Diseases, 2022. **29**(3): p. 140-153.
726. Bryan, O. *INFLAMMASOME INHIBITORS – 21st Century Miracle Drugs: Spotlight on Clinical NLRP3 Inflammasome Inhibitors*. 2023 April 2023 [cited 2024 03.01.]; Available from: https://drug-dev.com/inglammasome-inhibitors-21st-century-miracle-drugs-spotlight-on-clinical-nlrp3-inflammasome-inhibitors/.
727. Zahid, A., et al., *Pharmacological Inhibitors of the NLRP3 Inflammasome.* Frontiers in Immunology, 2019. **10**.
728. Bonomi, M., et al., *PREVLAR: Phase 2a Randomized Trial to Assess the Safety and Efficacy of RRx-001 in the Attenuation of Oral Mucositis in Patients Receiving Head and Neck Chemoradiotherapy.* International Journal of Radiation Oncology*Biology*Physics, 2023. **116**(3): p. 551-559.
729. Oronsky, B., et al., *RRx-001: a chimeric triple action NLRP3 inhibitor, Nrf2 inducer, and nitric oxide superagonist.* Front Oncol, 2023. **13**: p. 1204143.
730. Fine, H., et al., *A multicenter, phase 1, dose escalation clinical trial (G-FORCE-1) of XRT, RRx-001 and temozolomide followed by temozolomide +/- RRx-001 in newly diagnosed glioblastoma.* Front Oncol, 2023. **13**: p. 1176448.
731. Wohlford, G.F., et al., *Phase 1B, Randomized, Double-Blinded, Dose Escalation, Single-Center, Repeat Dose Safety and Pharmacodynamics Study of the Oral NLRP3 Inhibitor Dapansutrile in Subjects With NYHA II-III Systolic Heart Failure.* J Cardiovasc Pharmacol, 2020. **77**(1): p. 49-60.

732. Klück, V., et al., *Dapansutrile, an oral selective NLRP3 inflammasome inhibitor, for treatment of gout flares: an open-label, dose-adaptive, proof-of-concept, phase 2a trial.* The Lancet Rheumatology, 2020. **2**(5): p. e270-e280.
733. Parmar, D.V., et al., *Safety, Tolerability, Pharmacokinetics, and Pharmacodynamics of the Oral NLRP3 Inflammasome Inhibitor ZYIL1: First-in-Human Phase 1 Studies (Single Ascending Dose and Multiple Ascending Dose).* Clin Pharmacol Drug Dev, 2023. **12**(2): p. 202-211.
734. Hissaria, P., et al., *Safety, Tolerability, Pharmacokinetics, and Pharmacodynamics of ZY-IL1 in Three Patients with Cryopyrin-Associated Periodic Syndromes.* Clinical Pharmacology in Drug Development. **n/a**(n/a).
735. Halia Therapeutics, I. *Halia Therapeutics Announces Positive Phase 1 Clinical Trial Results for HT-6184 at the 5th Inflammasome Therapeutics Summit*. 2023 29.11.2023 [cited 2024 29.01.]; Available from: https://haliatx.com/halia-therapeutics-announces-positive-phase-1-clinical-trial-results-for-ht-6184-at-the-5th-inflammasome-therapeutics-summit/.
736. Halia Therapeutics, I. *Halia Therapeutics Dosed its First Patient in Phase 2a Clinical Trial of HT-6184, a First-in-Class NLRP3-Inhibitor, for the Treatment of Lower-Risk Myelodysplastic Syndromes*. 2023 13.12.2023 [cited 2024 29.01.2024]; Available from: https://www.prnewswire.com/news-releases/halia-therapeutics-dosed-its-first-patient-in-phase-2a-clinical-trial-of-ht-6184-a-first-in-class-nlrp3-inhibitor-for-the-treatment-of-lower-risk-myelodysplastic-syndromes-302013467.html.
737. Biosciences, V. *Ventyx Biosciences Announces Initiation of Dosing in a Phase 1 Trial of VTX3232, a Novel CNS-Penetrant NLRP3 Inhibitor*. 2023 14.06.2023 [cited 2024 29.01.]; Available from: https://ir.ventyxbio.com/news-releases/news-release-details/ventyx-biosciences-announces-initiation-dosing-phase-1-trial/.
738. Coll, R.C., K. Schroder, and P. Pelegrín, *NLRP3 and pyroptosis blockers for treating inflammatory diseases.* Trends in Pharmacological Sciences, 2022. **43**(8): p. 653-668.
739. Harrison, D., et al., *Discovery of Clinical Candidate NT-0796, a Brain-Penetrant and Highly Potent NLRP3 Inflammasome Inhibitor for Neuroinflammatory Disorders.* Journal of Medicinal Chemistry, 2023. **66**(21): p. 14897-14911.
740. NodThera. *NodThera's NLRP3 Inhibitor NT-0796 Reverses Neuroinflammation in Parkinson's Disease Phase Ib/IIa Trial*. 2024 07. March [cited 2024 03.May]; Available from: https://www.nodthera.com/news/nodtheras-nlrp3-inhibitor-nt-0796-reverses-neuroinflammation-in-parkinsons-disease-phase-ib-iia-trial/.
741. Cooper, M. *Inzomelid completes Phase I studies and shows positive results in the treatment of Cryopyrin-Associated Periodic Syndrome (CAPS)*. 2020 26.03.2020 [cited 2024 29.01.]; Available from: https://www.linkedin.com/pulse/inzomelid-completes-phase-i-studies-shows-positive-results-cooper.
742. Inflazome. *Inflazome's Somalix Demonstrates Positive Safety, Tolerability and Pharmacodynamic Profile in its Phase I Study*. 2020 27.02.2020 [cited 2024 29.01.].
743. Klughammer, B., et al., *A randomized, double-blind phase 1b study evaluating the safety, tolerability, pharmacokinetics and pharmacodynamics of the NLRP3 inhibitor selnoflast in patients with moderate to severe active ulcerative colitis.* Clin Transl Med, 2023. **13**(11): p. e1471.
744. Schlesinger, N., et al., *Canakinumab for acute gouty arthritis in patients with limited treatment options: results from two randomised, multicentre, active-controlled, double-blind trials and their initial extensions.* Annals of the rheumatic diseases, 2012. **71**(11): p. 1839-1848.
745. Gorman, R.M., *Pharma Looks to Inflammasome Inhibitors as All-Around Therapies.* The Scientist, 2021.

746. Roddy, E. and M. Doherty, *Treatment of hyperuricaemia and gout.* Clin Med (Lond), 2013. **13**(4): p. 400-3.
747. Chi, X.-K., et al., *Combining nanotechnology with monoclonal antibody drugs for rheumatoid arthritis treatments.* Journal of Nanobiotechnology, 2023. **21**(1): p. 105.
748. Parisa, N., et al., *The inflammation process of gout arthritis and its treatment.* J Adv Pharm Technol Res, 2023. **14**(3): p. 166-170.
749. Widrich., A.F.M.R.R.G.J. *Gout*. 2022 [cited 2024 30.01.]; Available from: https://www.ncbi.nlm.nih.gov/books/NBK546606/.
750. van de Laar, C.J., et al., *Model-based cost-effectiveness analyses comparing combinations of urate lowering therapy and anti-inflammatory treatment in gout patients.* PLoS One, 2022. **17**(1): p. e0261940.
751. Jeria-Navarro, S., et al., *Effectiveness and safety of anakinra in gouty arthritis: A case series and review of the literature.* Front Med (Lausanne), 2022. **9**: p. 1089993.
752. Nair, A.B. and S. Jacob, *A simple practice guide for dose conversion between animals and human.* J Basic Clin Pharm, 2016. **7**(2): p. 27-31.
753. Owen, S. *Material Safety Data Sheet - Indomethacin*. 2013 3.12.2013 [cited 2023 29.11.2023]; Available from: https://us.vwr.com/assetsvc/asset/en_US/id/12782437/contents.
754. Yamagishi, Y., et al., *Gastroprotective Effect of Enteral Nutrition Formula in Mice Injected Subcutaneously with Indomethacin.* Nutrients, 2021. **13**(9): p. 3297.
755. Dvir, E., et al., *A Novel Phospholipid Derivative of Indomethacin, DP-155 [Mixture of 1-Steroyl and 1-Palmitoyl-2-{6-[1-(p-chlorobenzoyl)-5-methoxy-2-methyl-3-indolyl acetamido]hexanoyl}-sn-glycero-3-phosophatidyl Choline], Shows Superior Safety and Similar Efficacy in Reducing Brain Amyloid ß in an Alzheimer's Disease Model.* Journal of Pharmacology and Experimental Therapeutics, 2006. **318**(3): p. 1248-1256.
756. El-Leithy, E.S., H.K. Ibrahim, and R.M. Sorour, *In vitro and in vivo evaluation of indomethacin nanoemulsion as a transdermal delivery system.* Drug Delivery, 2015. **22**(8): p. 1010-1017.
757. Liang, X., et al., *Bidirectional interactions between indomethacin and the murine intestinal microbiota.* Elife, 2015. **4**: p. e08973.
758. Shacter, E., G.K. Arzadon, and J. Williams, *Elevation of interleukin-6 in response to a chronic inflammatory stimulus in mice: inhibition by indomethacin.* Blood, 1992. **80**(1): p. 194-202.
759. Bour, A.M., et al., *Interaction of indomethacin with cytokine production in whole blood. Potential mechanism for a brain-protective effect.* Exp Gerontol, 2000. **35**(8): p. 1017-24.
760. Shen, Y., et al., *Indomethacin enhances the cytotoxicity of recombinant human lymphotoxin alpha on tumor cells by suppressing NFkappaB signaling.* Cancer Biol Ther, 2007. **6**(9): p. 1428-33.
761. Lala V, Z.M., Minter DA. *Liver Function Tests*. 2023 30 July 2023 [cited 2024 30.04.]; Available from: https://www.ncbi.nlm.nih.gov/books/NBK482489/.
762. Guerra Ruiz, A.R., et al., *Measurement and clinical usefulness of bilirubin in liver disease.* Adv Lab Med, 2021. **2**(3): p. 352-372.
763. Meunier, L. and D. Larrey, *Drug-Induced Liver Injury: Biomarkers, Requirements, Candidates, and Validation.* Front Pharmacol, 2019. **10**: p. 1482.
764. Yamamoto, A., et al., *Sodium alginate ameliorates indomethacin-induced gastrointestinal mucosal injury via inhibiting translocation in rats.* World J Gastroenterol, 2014. **20**(10): p. 2641-52.

765. Fukumoto, K., et al., *Role of tumor necrosis factor-α in the pathogenesis of indomethacin-induced small intestinal injury in mice.* Int J Mol Med, 2011. **27**(3): p. 353-9.
766. Zhang, X., et al., *Herb-drug interaction in the protective effect of Alpinia officinarum against gastric injury induced by indomethacin based on pharmacokinetic, tissue distribution and excretion studies in rats.* Journal of Pharmaceutical Analysis, 2021. **11**(2): p. 200-209.
767. Spalinger, M.R., M. Schwarzfischer, and M. Scharl, *The Role of Protein Tyrosine Phosphatases in Inflammasome Activation.* Int J Mol Sci, 2020. **21**(15).
768. Mehta, V.B., J. Hart, and M.D. Wewers, *ATP-stimulated Release of Interleukin (IL)-1β and IL-18 Requires Priming by Lipopolysaccharide and Is Independent of Caspase-1 Cleavage *.* Journal of Biological Chemistry, 2001. **276**(6): p. 3820-3826.
769. Ahmad, S.F., et al., *Inhibition of tyrosine kinase signaling by tyrphostin AG126 downregulates the IL-21/IL-21R and JAK/STAT pathway in the BTBR mouse model of autism.* Neurotoxicology, 2020. **77**: p. 1-11.
770. Gross, O., et al., *Syk kinase signalling couples to the Nlrp3 inflammasome for anti-fungal host defence.* Nature, 2009. **459**(7245): p. 433-436.
771. Hara, H., et al., *Phosphorylation of the adaptor ASC acts as a molecular switch that controls the formation of speck-like aggregates and inflammasome activity.* Nature Immunology, 2013. **14**(12): p. 1247-1255.
772. Lin, Y.-C., et al., *Syk is involved in NLRP3 inflammasome-mediated caspase-1 activation through adaptor ASC phosphorylation and enhanced oligomerization.* Journal of Leukocyte Biology, 2015. **97**(5): p. 825-835.
773. Moran, G. and A. Elaine, *Protein Kinase Inhibitors - Selectivity or Toxicity?*, in *Protein Kinases*, S. Rajesh Kumar, Editor. 2021, IntechOpen: Rijeka. p. Ch. 2.
774. Roskoski, R., *Properties of FDA-approved small molecule protein kinase inhibitors: A 2024 update.* Pharmacological Research, 2024. **200**: p. 107059.
775. Roskoski, R., *Properties of FDA-approved small molecule protein kinase inhibitors: A 2020 update.* Pharmacological Research, 2020. **152**: p. 104609.
776. Roskoski, R., Jr., *Classification of small molecule protein kinase inhibitors based upon the structures of their drug-enzyme complexes.* Pharmacol Res, 2016. **103**: p. 26-48.
777. Kufareva, I. and R. Abagyan, *Type-II Kinase Inhibitor Docking, Screening, and Profiling Using Modified Structures of Active Kinase States.* Journal of Medicinal Chemistry, 2008. **51**(24): p. 7921-7932.
778. Namboodiri, H.V., et al., *Analysis of Imatinib and Sorafenib Binding to p38α Compared with c-Abl and b-Raf Provides Structural Insights for Understanding the Selectivity of Inhibitors Targeting the DFG-Out Form of Protein Kinases.* Biochemistry, 2010. **49**(17): p. 3611-3618.
779. Wan, P.T., et al., *Mechanism of activation of the RAF-ERK signaling pathway by oncogenic mutations of B-RAF.* Cell, 2004. **116**(6): p. 855-867.
780. McTigue, M., et al., *Molecular conformations, interactions, and properties associated with drug efficiency and clinical performance among VEGFR TK inhibitors.* Proc Natl Acad Sci U S A, 2012. **109**(45): p. 18281-9.
781. Mao, W.-f., et al., *The important roles of RET, VEGFR2 and the RAF/MEK/ERK pathway in cancer treatment with sorafenib.* Acta Pharmacologica Sinica, 2012. **33**(10): p. 1311-1318.
782. Anastassiadis, T., et al., *Comprehensive assay of kinase catalytic activity reveals features of kinase inhibitor selectivity.* Nature Biotechnology, 2011. **29**(11): p. 1039-1045.

783. Force, T., D.S. Krause, and R.A. Van Etten, *Molecular mechanisms of cardiotoxicity of tyrosine kinase inhibition.* Nature Reviews Cancer, 2007. **7**(5): p. 332-344.
784. Gerber, H.-P. and N. Ferrara, *The role of VEGF in normal and neoplastic hematopoiesis.* Journal of molecular medicine, 2003. **81**: p. 20-31.
785. Kumar, R., et al., *Myelosuppression and kinase selectivity of multikinase angiogenesis inhibitors.* British Journal of Cancer, 2009. **101**(10): p. 1717-1723.
786. Schutz, F.A.B., Y. Je, and T.K. Choueiri, *Hematologic toxicities in cancer patients treated with the multi-tyrosine kinase sorafenib: A meta-analysis of clinical trials.* Critical Reviews in Oncology/Hematology, 2011. **80**(2): p. 291-300.
787. Zhao, B. and H. Zhao, *Incidence and risk of hematologic toxicities in cancer patients treated with regorafenib.* Oncotarget, 2017. **8**(55): p. 93813-93824.
788. Diseases, N.I.o.D.a.D.a.K. *LiverTox: Clinical and Research Information on Drug-Induced Liver Injury*. Sorafenib 2012 June 2018 [cited 2024 23.02.]; Available from: https://www.ncbi.nlm.nih.gov/books/NBK548944/.
789. Diseases, N.I.o.D.a.D.a.K. *LiverTox: Clinical and Research Information on Drug-Induced Liver Injury*. Regorafenib 2012 June 2018 [cited 2024 23.02.]; Available from: www.ncbi.nlm.nih.gov/books/NBK548608/.
790. Bouitbir, J., et al., *Imatinib and dasatinib provoke mitochondrial dysfunction leading to oxidative stress in C2C12 myotubes and human RD cells.* Frontiers in pharmacology, 2020. **11**: p. 1106.
791. Paech, F., J. Bouitbir, and S. Krähenbühl, *Hepatocellular toxicity associated with tyrosine kinase inhibitors: mitochondrial damage and inhibition of glycolysis.* Frontiers in pharmacology, 2017. **8**: p. 367.
792. Van Hootegem, A., C. Verslype, and W. Van Steenbergen, *Sorafenib-Induced Liver Failure: A Case Report and Review of the Literature.* Case Reports in Hepatology, 2011. **2011**: p. 941395.
793. Zhao, B. and H. Zhao, *Incidence and risk of regorafenib-induced hepatotoxicity.* Oncotarget, 2017. **8**(48): p. 84102-84111.
794. Karaman, M.W., et al., *A quantitative analysis of kinase inhibitor selectivity.* Nature Biotechnology, 2008. **26**(1): p. 127-132.
795. Adnane, L., et al., *Sorafenib (BAY 43-9006, Nexavar), a dual-action inhibitor that targets RAF/MEK/ERK pathway in tumor cells and tyrosine kinases VEGFR/PDGFR in tumor vasculature.* Methods Enzymol, 2006. **407**: p. 597-612.
796. Uitdehaag, J.C.M. and G.J.R. Zaman, *A theoretical entropy score as a single value to express inhibitor selectivity.* BMC Bioinformatics, 2011. **12**(1): p. 94.
797. Taylor, W.J., et al., *Study for Updated Gout Classification Criteria: Identification of Features to Classify Gout.* Arthritis Care & Research, 2015. **67**(9): p. 1304-1315.
798. Culemann, S., et al., *Stunning of neutrophils accounts for the anti-inflammatory effects of clodronate liposomes.* Journal of Experimental Medicine, 2023. **220**(6).
799. Hua, L., et al., *Genetic Models of Macrophage Depletion.* Methods Mol Biol, 2018. **1784**: p. 243-258.
800. Cai, D., et al., *Current Development of Nano-Drug Delivery to Target Macrophages.* Biomedicines, 2022. **10**(5).
801. Zhao, Y., et al., *Lactoferrin-mediated macrophage targeting delivery and patchouli alcohol-based therapeutic strategy for inflammatory bowel diseases.* Acta Pharmaceutica Sinica B, 2020. **10**(10): p. 1966-1976.
802. Johnson DB, L.M., Kelley B. *Dexamethasone*. 2023 02.05.2023 [cited 2024 30.01.]; Available from: https://www.ncbi.nlm.nih.gov/books/NBK482130/.
803. Ma, L., et al., *Efficient Targeting of Adipose Tissue Macrophages in Obesity with Polysaccharide Nanocarriers.* ACS Nano, 2016. **10**(7): p. 6952-6962.

804. Prabhu, S., et al., *Nanocarriers targeting adipose macrophages increase glucocorticoid anti-inflammatory potency to ameliorate metabolic dysfunction.* Biomaterials Science, 2021. **9**(2): p. 506-518.
805. Han, J., et al., *Macrophage-Targeted Dextran Sulfate-Dexamethasone Conjugate Micelles for Effective Treatment of Rheumatoid Arthritis.* Molecules, 2023. **28**(2): p. 591.
806. Oliviero, F. and A. Scanu, *How Factors Involved in the Resolution of Crystal-Induced Inflammation Target IL-1β.* Front Pharmacol, 2017. **8**: p. 164.
807. Louwe, P.A., et al., *Recruited macrophages that colonize the post-inflammatory peritoneal niche convert into functionally divergent resident cells.* Nature Communications, 2021. **12**(1): p. 1770.
808. Harris, H., *Chemotaxis of granulocytes.* The Journal of Pathology and Bacteriology, 1953. **66**(1): p. 135-146.
809. Harris, H., *Role of Chemotaxis in Inflammation.* Physiological Reviews, 1954. **34**(3): p. 529-562.
810. Boyden, S., *THE CHEMOTACTIC EFFECT OF MIXTURES OF ANTIBODY AND ANTIGEN ON POLYMORPHONUCLEAR LEUCOCYTES.* Journal of Experimental Medicine, 1962. **115**(3): p. 453-466.
811. Zhao, W., et al., *Microfluidic devices for neutrophil chemotaxis studies.* Journal of Translational Medicine, 2020. **18**(1): p. 168.
812. Gee, A.P., *Advantages and limitations of methods for measuring cellular chemotaxis and chemokinesis.* Molecular and Cellular Biochemistry, 1984. **62**(1): p. 5-11.
813. Falk, W., R.H. Goodwin, Jr., and E.J. Leonard, *A 48-well micro chemotaxis assembly for rapid and accurate measurement of leukocyte migration.* J Immunol Methods, 1980. **33**(3): p. 239-47.
814. Gomez-Lopez, N., F. Vadillo-Ortega, and G. Estrada-Gutierrez, *Combined Boyden-Flow Cytometry Assay Improves Quantification and Provides Phenotypification of Leukocyte Chemotaxis.* PLOS ONE, 2011. **6**(12): p. e28771.
815. Irimia, D., *Microfluidic Technologies for Temporal Perturbations of Chemotaxis.* Annual review of biomedical engineering, 2010. **12**: p. 259-84.
816. Muinonen-Martin, A.J., et al., *An improved chamber for direct visualisation of chemotaxis.* PloS one, 2010. **5**(12): p. e15309.
817. Zigmond, S.H., *Ability of polymorphonuclear leukocytes to orient in gradients of chemotactic factors.* Journal of Cell Biology, 1977. **75**(2): p. 606-616.
818. Zicha, D., G.A. Dunn, and A.F. Brown, *A new direct-viewing chemotaxis chamber.* Journal of Cell Science, 1991. **99**(4): p. 769-775.
819. Deroy, C., et al., *Reconfigurable Microfluidic Circuits for Isolating and Retrieving Cells of Interest.* ACS Appl Mater Interfaces, 2022. **14**(22): p. 25209-25219.
820. Zengel, P., et al., *μ-Slide Chemotaxis: A new chamber for long-term chemotaxis studies.* BMC Cell Biology, 2011. **12**(1): p. 21.
821. Zengel, P., et al., *μ-Slide Chemotaxis: a new chamber for long-term chemotaxis studies.* BMC Cell Biol, 2011. **12**: p. 21.
822. Biswenger, V., et al., *Characterization of EGF-guided MDA-MB-231 cell chemotaxis in vitro using a physiological and highly sensitive assay system.* PLOS ONE, 2018. **13**(9): p. e0203040.
823. Visweshwaran, S.P. and T. Maritzen, *A simple 3D cellular chemotaxis assay and analysis workflow suitable for a wide range of migrating cells.* MethodsX, 2019. **6**: p. 2807-2821.

824. Van Goethem, E., et al., *Matrix Architecture Dictates Three-Dimensional Migration Modes of Human Macrophages: Differential Involvement of Proteases and Podosome-Like Structures.* The Journal of Immunology, 2009. **184**(2): p. 1049-1061.
825. Casale, T.B. and M.K. Abbas, *Comparison of leukotriene B4-induced neutrophil migration through different cellular barriers.* American Journal of Physiology-Cell Physiology, 1990. **258**(4): p. C639-C647.
826. Erger, R.A. and T.B. Casale, *Interleukin-8 is a potent mediator of eosinophil chemotaxis through endothelium and epithelium.* Am J Physiol, 1995. **268**(1 Pt 1): p. L117-22.
827. Andjelkovic, A.V., et al., *Qualitative and quantitative analysis of monocyte transendothelial migration by confocal microscopy and three-dimensional image reconstruction.* In Vitro Cell Dev Biol Anim, 2001. **37**(2): p. 111-20.
828. Jaczewska, J., et al., *TNF-α and IFN-γ promote lymphocyte adhesion to endothelial junctional regions facilitating transendothelial migration.* J Leukoc Biol, 2014. **95**(2): p. 265-74.
829. Wong, C.H.Y., B. Heit, and P. Kubes, *Molecular regulators of leucocyte chemotaxis during inflammation.* Cardiovascular Research, 2010. **86**(2): p. 183-191.
830. Schaff, U.Y., et al., *Vascular mimetics based on microfluidics for imaging the leukocyte--endothelial inflammatory response.* Lab Chip, 2007. **7**(4): p. 448-56.
831. Iqbal, A.J., et al., *Galectin-9 mediates neutrophil capture and adhesion in a CD44 and β2 integrin-dependent manner.* The FASEB Journal, 2022. **36**(1): p. e22065.
832. Simon, S.I., et al., *LEUCOCYTE RECRUITMENT UNDER FLUID SHEAR: MECHANICAL AND MOLECULAR REGULATION WITHIN THE INFLAMMATORY SYNAPSE.* Clinical and Experimental Pharmacology and Physiology, 2009. **36**(2): p. 217-224.
833. Cinamon, G. and R. Alon, *A real time in vitro assay for studying leukocyte transendothelial migration under physiological flow conditions.* Journal of Immunological Methods, 2003. **273**(1): p. 53-62.
834. Yuan, S.Y., et al., *Neutrophil transmigration, focal adhesion kinase and endothelial barrier function.* Microvasc Res, 2012. **83**(1): p. 82-8.
835. Wittchen, E.S., et al., *Trading spaces: Rap, Rac, and Rho as architects of transendothelial migration.* Current opinion in hematology, 2005. **12**(1): p. 14-21.
836. Park, H., D. Ishihara, and D. Cox, *Regulation of tyrosine phosphorylation in macrophage phagocytosis and chemotaxis.* Archives of Biochemistry and Biophysics, 2011. **510**(2): p. 101-111.
837. Chiaradonna, F., et al., *Urokinase receptor-dependent and -independent p56/59(hck) activation state is a molecular switch between myelomonocytic cell motility and adherence.* EMBO Journal, 1999. **18**(11): p. 3013-3023.
838. Ernst, M., et al., *Constitutive activation of the Src family kinase Hck results in spontaneous pulmonary inflammation and an enhanced innate immune response.* Journal of Experimental Medicine, 2002. **196**(5): p. 589-604.
839. Suen, P.W., et al., *Impaired integrin-mediated signal transduction, altered cytoskeletal structure and reduced motility in Hck/Fgr deficient macrophages.* Journal of Cell Science, 1999. **112**(22): p. 4067-4078.
840. Meng, F. and C.A. Lowell, *A β1 integrin signaling pathway involving Src-family kinases, Cbl and PI-3 kinase is required for macrophage spreading and migration.* EMBO Journal, 1998. **17**(15): p. 4391-4403.
841. Gevrey, J.C., B.M. Isaac, and D. Cox, *Syk is required for monocyte/macrophage chemotaxis to CX3CL1 (fractalkine).* Journal of Immunology, 2005. **175**(6): p. 3737-3745.

842. Cougoule, C., et al., *Three-dimensional migration of macrophages requires Hck for podosome organization and extracellular matrix proteolysis.* Blood, 2010. **115**(7): p. 1444-1452.
843. Zen, K. and Y. Liu, *Role of different protein tyrosine kinases in fMLP-induced neutrophil transmigration.* Immunobiology, 2008. **213**(1): p. 13-23.
844. Vedham, V., H. Phee, and K.M. Coggeshall, *Vav activation and function as a Rac guanine nucleotide exchange factor in macrophage colony-stimulating factor-induced macrophage chemotaxis.* Molecular and Cellular Biology, 2005. **25**(10): p. 4211-4220.
845. Cory, G.O.C., et al., *Phosphorylation of tyrosine 291 enhances the ability of WASp to stimulate actin polymerization and filopodium formation.* Journal of Biological Chemistry, 2002. **277**(47): p. 45115-45121.
846. Elsegood, C.L., et al., *M-CSF induces the stable interaction of cFms with αVβ3 integrin in osteoclasts.* International Journal of Biochemistry and Cell Biology, 2006. **38**(9): p. 1518-1529.
847. Okigaki, M., et al., *Pyk2 regulates multiple signaling events crucial for macrophage morphology and migration.* Proceedings of the National Academy of Sciences of the United States of America, 2003. **100**(19): p. 10740-10745.
848. Owen, K.A., et al., *Regulation of lamellipodial persistence, adhesion turnover, and motility in macrophages by focal adhesion kinase.* Journal of Cell Biology, 2007. **179**(6): p. 1275-1287.
849. Pixley, F.J., et al., *Protein tyrosine phosphatase φ regulates paxillin tyrosine phosphorylation and mediates colony-stimulating factor 1-induced morphological changes in macrophages.* Molecular and Cellular Biology, 2001. **21**(5): p. 1795-1809.
850. Hatch, W.C., et al., *The related adhesion focal tyrosine kinase (RAFTK) is tyrosine phosphorylated and participates in colony-stimulating factor-1/macrophage colony-stimulating factor signaling in monocyte-macrophages.* Blood, 1998. **91**(10): p. 3967-3973.
851. Cobb, B.S., et al., *Stable association of pp60src and pp59fyn with the focal adhesion-associated protein tyrosine kinase, pp125FAK.* Molecular and Cellular Biology, 1994. **14**(1): p. 147-155.
852. Brown, M.C., J.A. Perrotta, and C.E. Turner, *Identification of LIM3 as the principal determinant of paxillin focal adhesion localization and characterization of a novel motif on paxillin directing vinculin and focal adhesion kinase binding.* Journal of Cell Biology, 1996. **135**(4): p. 1109-1123.
853. Schymeinsky, J., C. Then, and B. Walzog, *The non-receptor tyrosine kinase Syk regulates lamellipodium formation and site-directed migration of human leukocytes.* Journal of Cellular Physiology, 2005. **204**(2): p. 614-622.
854. Templeton, A.J., et al., *Simple prognostic score for metastatic castration-resistant prostate cancer with incorporation of neutrophil-to-lymphocyte ratio.* Cancer, 2014. **120**(21): p. 3346-3352.
855. Valero, C., et al., *Pretreatment neutrophil-to-lymphocyte ratio and mutational burden as biomarkers of tumor response to immune checkpoint inhibitors.* Nature communications, 2021. **12**(1): p. 729.
856. Katoh, H., et al., *CXCR2-expressing myeloid-derived suppressor cells are essential to promote colitis-associated tumorigenesis.* Cancer cell, 2013. **24**(5): p. 631-644.
857. Guo, C., et al., *Targeting myeloid chemotaxis to reverse prostate cancer therapy resistance.* Nature, 2023. **623**(7989): p. 1053-1061.
858. Evans, J., et al., *A phase I/II study of the CXCR2 inhibitor, AZD5069, in combination with durvalumab, in patients (pts) with advanced hepatocellular carcinoma (HCC).* Journal of Clinical Oncology, 2023. **41**: p. TPS631-TPS631.

859. Yuan, J., et al., *C5a and its receptors in human anti-neutrophil cytoplasmic antibody (ANCA)-associated vasculitis.* Arthritis Res Ther, 2012. **14**(3): p. R140.
860. Guo, R.F. and P.A. Ward, *Role of C5a in inflammatory responses.* Annu Rev Immunol, 2005. **23**: p. 821-52.
861. Jayne, D.R.W., et al., *Randomized Trial of C5a Receptor Inhibitor Avacopan in ANCA-Associated Vasculitis.* Journal of the American Society of Nephrology, 2017. **28**(9): p. 2756-2767.
862. Merkel, P.A., et al., *Adjunctive Treatment With Avacopan, an Oral C5a Receptor Inhibitor, in Patients With Antineutrophil Cytoplasmic Antibody–Associated Vasculitis.* ACR Open Rheumatology, 2020. **2**(11): p. 662-671.
863. Jayne, D.R.W., et al., *Avacopan for the Treatment of ANCA-Associated Vasculitis.* New England Journal of Medicine, 2021. **384**(7): p. 599-609.
864. Osman, M., J.W. Cohen Tervaert, and C. Pagnoux, *Avacopan for the treatment of ANCA-associated vasculitis: an update.* Expert Rev Clin Immunol, 2023. **19**(5): p. 461-471.
865. Szekanecz, Z. and A.E. Koch, *Successes and failures of chemokine-pathway targeting in rheumatoid arthritis.* Nature Reviews Rheumatology, 2016. **12**(1): p. 5-13.
866. Miyabe, Y., et al., *Chemokines in rheumatic diseases: pathogenic role and therapeutic implications.* Nature Reviews Rheumatology, 2019. **15**(12): p. 731-746.
867. Hosoya, T., et al., *Editorial: Targeting the Chemoattractant System in Inflammation.* Frontiers in Pharmacology, 2021. **12**.
868. Yellin, M., et al., *A phase II, randomized, double-blind, placebo-controlled study evaluating the efficacy and safety of MDX-1100, a fully human anti-CXCL10 monoclonal antibody, in combination with methotrexate in patients with rheumatoid arthritis.* Arthritis & Rheumatism, 2012. **64**(6): p. 1730-1739.
869. Pahl, H.L., *Activators and target genes of Rel/NF-κB transcription factors.* Oncogene, 1999. **18**(49): p. 6853-6866.
870. Brasier, A.R., *The nuclear factor-kappaB-interleukin-6 signalling pathway mediating vascular inflammation.* Cardiovasc Res, 2010. **86**(2): p. 211-8.
871. Wang, Y., et al., *Nuclear factor kappa B regulated monocyte chemoattractant protein-1/chemokine CC motif receptor-2 expressing in spinal cord contributes to the maintenance of cancer-induced bone pain in rats.* Mol Pain, 2018. **14**: p. 1744806918788681.
872. Recinos III, A., et al., *Angiotensin II induces IL-6 expression and the Jak-STAT3 pathway in aortic adventitia of LDL receptor-deficient mice.* Atherosclerosis, 2007. **194**(1): p. 125-133.
873. Cataisson, C., et al., *Protein Kinase Cα-Mediated Chemotaxis of Neutrophils Requires NF-κB Activity but Is Independent of TNFα Signaling in Mouse Skin In Vivo1.* The Journal of Immunology, 2005. **174**(3): p. 1686-1692.
874. Ko, J., et al., *Leukotactin-1/CCL15-induced chemotaxis signaling through CCR1 in HOS cells.* FEBS Letters, 2002. **515**(1): p. 159-164.
875. Jang, S.-W., et al., *Regulation of Human LZIP Expression by NF-κB and Its Involvement in Monocyte Cell Migration Induced by Lkn-1 *.* Journal of Biological Chemistry, 2007. **282**(15): p. 11092-11100.
876. Penzo, M., et al., *Inhibitor of NF-κB Kinases α and β Are Both Essential for High Mobility Group Box 1-Mediated Chemotaxis.* The Journal of Immunology, 2010. **184**(8): p. 4497-4509.
877. Kew, R.R., et al., *The IKKα-Dependent NF-κB p52/RelB Noncanonical Pathway Is Essential To Sustain a CXCL12 Autocrine Loop in Cells Migrating in Response to HMGB1.* The Journal of Immunology, 2012. **188**(5): p. 2380-2386.

878. Penzo, M., et al., *Cell migration to CXCL12 requires simultaneous IKKα and IKKβ-dependent NF-κB signaling.* Biochimica et Biophysica Acta (BBA) - Molecular Cell Research, 2014. **1843**(9): p. 1796-1804.
879. Sun, H., et al., *Establishment and application of a high-throughput screening model for cell adhesion inhibitors.* Frontiers in Pharmacology, 2023. **14**.
880. Abidi, A., P. Shukla, and A. Ahmad, *Lifitegrast: A novel drug for treatment of dry eye disease.* J Pharmacol Pharmacother, 2016. **7**(4): p. 194-198.
881. Silveira, A.A.A., et al., *Simvastatin abrogates inflamed neutrophil adhesive properties, in association with the inhibition of Mac-1 integrin expression and modulation of Rho kinase activity.* Inflammation Research, 2013. **62**(2): p. 127-132.
882. Galkina, S.I., et al., *Inhibition of Neutrophil Secretion Upon Adhesion as a Basis for the Anti-Inflammatory Effect of the Tricyclic Antidepressant Imipramine.* Front Pharmacol, 2021. **12**: p. 709719.
883. Hashioka, S., *Antidepressants and neuroinflammation: can antidepressants calm glial rage down?* Mini Reviews in Medicinal Chemistry, 2011. **11**(7): p. 555-564.
884. Lee, S., S.-K. Ku, and J.-S. Bae, *Anti-inflammatory effects of dabrafenib on polyphosphate-mediated vascular disruption.* Chemico-Biological Interactions, 2016. **256**: p. 266-273.
885. Lee, I.-C., J. Kim, and J.-S. Bae, *Anti-inflammatory effects of dabrafenib in vitro and in vivo.* Canadian Journal of Physiology and Pharmacology, 2017. **95**(6): p. 697-707.
886. Manzanares, L.D., et al., *Atovaquone attenuates experimental colitis by reducing neutrophil infiltration of colonic mucosa.* Frontiers in Pharmacology, 2022. **13**.
887. Pharma, A. *U.S. FDA Approves First Anti-Inflammatory Drug for Cardiovascular Disease*. 2023 20.06.2023 [cited 2024 31.01.]; Available from: https://us.agephapharma.com/blog/2023/06/20/us-fda-approves-first-anti-inflammatory-drug-for-cardiovascular-disease/.
888. Weng, J.-H., et al., *Colchicine acts selectively in the liver to induce hepatokines that inhibit myeloid cell activation.* Nature Metabolism, 2021. **3**(4): p. 513-522.
889. Deftereos, S.G., et al., *Colchicine in Cardiovascular Disease: In-Depth Review.* Circulation, 2022. **145**(1): p. 61-78.
890. Caner, J.E.Z., *Colchicine inhibition of chemotaxis.* Arthritis & Rheumatism, 1965. **8**(4): p. 757-764.
891. Cronstein, B.N., et al., *Colchicine alters the quantitative and qualitative display of selectins on endothelial cells and neutrophils.* The Journal of Clinical Investigation, 1995. **96**(2): p. 994-1002.
892. Tucker, B., et al., *Colchicine as a Novel Therapy for Suppressing Chemokine Production in Patients With an Acute Coronary Syndrome: A Pilot Study.* Clinical Therapeutics, 2019. **41**(10): p. 2172-2181.
893. Chuang, S.-Y., S.-H. Yang, and J.-H.S. Pang, *Cilostazol reduces MCP-1-induced chemotaxis and adhesion of THP-1 monocytes by inhibiting CCR2 gene expression.* Biochemical and Biophysical Research Communications, 2011. **411**(2): p. 402-408.
894. Mulla S, S.W. *Losartan*. 2022 18.07.2022 [cited 2024 14.02.]; Available from: https://www.ncbi.nlm.nih.gov/books/NBK526065/.
895. Regan, D.P., et al., *The Angiotensin Receptor Blocker Losartan Suppresses Growth of Pulmonary Metastases via AT1R-Independent Inhibition of CCR2 Signaling and Monocyte Recruitment.* The Journal of Immunology, 2019. **202**(10): p. 3087-3102.
896. Guo, R.-F. and P.A. Ward, *ROLE OF C5A IN INFLAMMATORY RESPONSES.* Annual Review of Immunology, 2005. **23**(1): p. 821-852.

897. Ricklin, D. and J.D. Lambris, *Complement in Immune and Inflammatory Disorders: Pathophysiological Mechanisms.* The Journal of Immunology, 2013. **190**(8): p. 3831-3838.
898. Taylor, L., et al., *Netrin-1 Reduces Monocyte and Macrophage Chemotaxis towards the Complement Component C5a.* PLOS ONE, 2016. **11**(8): p. e0160685.
899. Rumianek, A., *New methods to study macrophage biology in vitro and in vivo.*, in *Sir William Dunn School of Pathology*. 2022, University of Oxford.
900. Yao, J., et al., *Chemotaxis by a CNS macrophage, the microglia.* Journal of Neuroscience Research, 1990. **27**(1): p. 36-42.
901. Giulian, D. and T.J. Baker, *Characterization of ameboid microglia isolated from developing mammalian brain.* J Neurosci, 1986. **6**(8): p. 2163-78.
902. Lampugnani, M.G., et al., *Effects of dimethyl sulfoxide (DMSO) on microfilament organization, cellular adhesion, and growth of cultured mouse B16 melanoma cells.* Exp Cell Res, 1987. **172**(2): p. 385-96.
903. Gotsch, U., et al., *Expression of P-selectin on endothelial cells is upregulated by LPS and TNF-alpha in vivo.* Cell Adhes Commun, 1994. **2**(1): p. 7-14.
904. Rahman, A., et al., *E-selectin expression in human endothelial cells by TNF-α-induced oxidant generation and NF-κB activation.* American Journal of Physiology-Lung Cellular and Molecular Physiology, 1998. **275**(3): p. L533-L544.
905. Cochran, D.B., et al., *Degradable poly(apigenin) polymer inhibits tumor cell adhesion to vascular endothelial cells.* Journal of Biomedical Materials Research Part B: Applied Biomaterials, 2016. **104**(7): p. 1438-1447.
906. Lee, A.S., J. Hur, and S.Y. Choi, *Isobavachalcone attenuates TNF-α-induced ICAM-1 and VCAM-1 expression in human umbilical vein endothelial cells by regulating the NF-κB signaling pathway.* Applied Biological Chemistry, 2022. **65**(1): p. 45.
907. Swirski, F.K., et al., *Identification of Splenic Reservoir Monocytes and Their Deployment to Inflammatory Sites.* Science, 2009. **325**(5940): p. 612-616.
908. De Filippo, K. and S.M. Rankin, *The Secretive Life of Neutrophils Revealed by Intravital Microscopy.* Frontiers in Cell and Developmental Biology, 2020. **8**.
909. Shaposhnik, Z., X. Wang, and A.J. Lusis, *Arterial colony stimulating factor-1 influences atherosclerotic lesions by regulating monocyte migration and apoptosis[S].* Journal of Lipid Research, 2010. **51**(7): p. 1962-1970.
910. Kokona, D., et al., *Colony-stimulating factor 1 receptor inhibition prevents disruption of the blood-retina barrier during chronic inflammation.* Journal of Neuroinflammation, 2018. **15**(1): p. 340.
911. Cara, D.C., et al., *Role of p38 Mitogen-Activated Protein Kinase in Chemokine-Induced Emigration and Chemotaxis In Vivo1.* The Journal of Immunology, 2001. **167**(11): p. 6552-6558.
912. Xu, N., M. Hossain, and L. Liu, *Pharmacological Inhibition of p38 Mitogen-Activated Protein Kinases Affects KC/CXCL1-Induced Intraluminal Crawling, Transendothelial Migration, and Chemotaxis of Neutrophils In Vivo.* Mediators of Inflammation, 2013. **2013**: p. 290565.
913. Zittermann, S.I. and A.C. Issekutz, *Endothelial growth factors VEGF and bFGF differentially enhance monocyte and neutrophil recruitment to inflammation.* Journal of Leukocyte Biology, 2006. **80**(2): p. 247-257.
914. Deuel, T.F., et al., *Chemotaxis of monocytes and neutrophils to platelet-derived growth factor.* J Clin Invest, 1982. **69**(4): p. 1046-9.
915. Leuschner, F., et al., *Therapeutic siRNA silencing in inflammatory monocytes in mice.* Nat Biotechnol, 2011. **29**(11): p. 1005-10.

916. Shen, Z., et al., *Inhibition of CCL2 by bindarit alleviates diabetes-associated periodontitis by suppressing inflammatory monocyte infiltration and altering macrophage properties.* Cellular & Molecular Immunology, 2021. **18**(9): p. 2224-2235.
917. Yin, L., et al., *Biomimetic oral targeted delivery of bindarit for immunotherapy of atherosclerosis.* Biomaterials Science, 2020. **8**(13): p. 3640-3648.
918. Ball, K.A., et al., *An isothermal shift assay for proteome scale drug-target identification.* Communications Biology, 2020. **3**(1): p. 75.
919. Paweletz, C.P., et al., *Identification of direct target engagement biomarkers for kinase-targeted therapeutics.* PLoS One, 2011. **6**(10): p. e26459.
920. Friman, T., *Mass spectrometry-based Cellular Thermal Shift Assay (CETSA®) for target deconvolution in phenotypic drug discovery.* Bioorg Med Chem, 2020. **28**(1): p. 115174.
921. Robertson, A.L., et al., *A zebrafish compound screen reveals modulation of neutrophil reverse migration as an anti-inflammatory mechanism.* Sci Transl Med, 2014. **6**(225): p. 225ra29.
922. Robertson, A.L., et al., *Identification of benzopyrone as a common structural feature in compounds with anti-inflammatory activity in a zebrafish phenotypic screen.* Disease Models & Mechanisms, 2016. **9**(6): p. 621-632.
923. Hansen, E., et al., *A versatile high throughput screening system for the simultaneous identification of anti-inflammatory and neuroprotective compounds.* J Alzheimers Dis, 2010. **19**(2): p. 451-64.
924. Manousi, A., et al., *Identification of novel myelin repair drugs by modulation of oligodendroglial differentiation competence.* eBioMedicine, 2021. **65**.
925. Lariosa-Willingham, K.D., et al., *A high throughput drug screening assay to identify compounds that promote oligodendrocyte differentiation using acutely dissociated and purified oligodendrocyte precursor cells.* BMC Research Notes, 2016. **9**(1): p. 419.
926. Santulli-Marotto, S., et al., *Discovering Molecules That Regulate Efferocytosis Using Primary Human Macrophages and High Content Imaging.* PLoS One, 2015. **10**(12): p. e0145078.
927. Jones, D.S., et al., *Profiling drugs for rheumatoid arthritis that inhibit synovial fibroblast activation.* Nature Chemical Biology, 2017. **13**(1): p. 38-45.
928. Mendoza-Reinoso, V., et al., *Unique Pro-Inflammatory Response of Macrophages during Apoptotic Cancer Cell Clearance.* Cells, 2020. **9**(2).
929. Hart, F.D. and P.L. Boardman, *INDOMETHACIN: A NEW NON-STEROID ANTI-INFLAMMATORY AGENT.* Br Med J, 1963. **2**(5363): p. 965-70.
930. Harris, M.D., L.B. Siegel, and J.A. Alloway, *Gout and hyperuricemia.* Am Fam Physician, 1999. **59**(4): p. 925-34.
931. Wang, H., et al., *Update on Nanoparticle-Based Drug Delivery System for Anti-inflammatory Treatment.* Frontiers in Bioengineering and Biotechnology, 2021. **9**.
932. Toita, R., et al., *Anti-obesity and anti-inflammatory effects of macrophage-targeted interleukin-10-conjugated liposomes in obese mice.* Biomaterials, 2016. **110**: p. 81-88.
933. Wu, Y., et al., *An apoptotic body-biomimic liposome in situ upregulates anti-inflammatory macrophages for stabilization of atherosclerotic plaques.* Journal of Controlled Release, 2019. **316**: p. 236-249.
934. Nagata, S., R. Hanayama, and K. Kawane, *Autoimmunity and the clearance of dead cells.* Cell, 2010. **140**(5): p. 619-630.
935. Kumar, A. and K.Y.J. Zhang, *Advances in the Development of Shape Similarity Methods and Their Application in Drug Discovery.* Frontiers in Chemistry, 2018. **6**.
936. Lucy, D., et al., *A Biased Agonist at Immunometabolic Receptor GPR84 Causes Distinct Functional Effects in Macrophages.* ACS Chemical Biology, 2019. **14**(9): p. 2055-2064.

937. Shukla, A., et al., *QSAR and Docking Studies on Capsazepine Derivatives for Immunomodulatory and Anti-Inflammatory Activity.* PLOS ONE, 2014. **9**(7): p. e100797.
938. Lessigiarska, I., et al., *3D-QSAR and preliminary evaluation of anti-inflammatory activity of series of N-pyrrolylcarboxylic acids.* Il Farmaco, 2005. **60**(3): p. 209-218.
939. Chaffey, L.E., et al., *Drug repurposing screen identifies novel anti-inflammatory activity of sunitinib in macrophages.* Eur J Pharmacol, 2024. **969**: p. 176437.
940. Cohen, P., D. Cross, and P.A. Jänne, *Kinase drug discovery 20 years after imatinib: progress and future directions.* Nature Reviews Drug Discovery, 2021. **20**(7): p. 551-569.
941. Gege, C., *Retinoic acid-related orphan receptor gamma t (RORγt) inverse agonists/antagonists for the treatment of inflammatory diseases – where are we presently?* Expert Opinion on Drug Discovery, 2021. **16**(12): p. 1517-1535.

Appendices

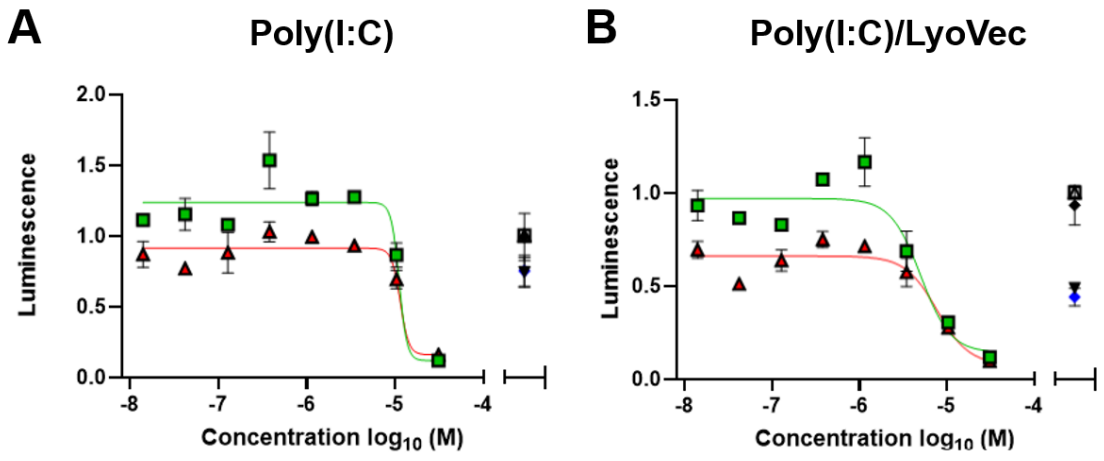
Appendix 1. Publications

Roberti A, Chaffey LE, Greaves DR. NF-κB Signaling and Inflammation-Drug Repurposing to Treat Inflammatory Disorders? Biology (Basel). 2022 Feb 26;11(3):372. doi: 10.3390/biology11030372. PMID: 35336746; PMCID: PMC8945680.

Chaffey L, **Roberti A**, Greaves DR. Drug repurposing in cardiovascular inflammation: Successes, failures, and future opportunities. Front Pharmacol. 2022 Oct 21;13:1046406. doi: 10.3389/fphar.2022.1046406. PMID: 36339576; PMCID: PMC9634418.

Chaffey LE, **Roberti A**, Bowman A, O'Brien CJ, Som L, Purvis GS, Greaves DR. Drug repurposing screen identifies novel anti-inflammatory activity of sunitinib in macrophages. Eur J Pharmacol. 2024 Apr 15;969:176437. doi: 10.1016/j.ejphar.2024.176437. Epub 2024 Feb 28. PMID: 38417608.

Appendix 2. IRF pathway activation assessment in THP1-Dual cells stimulated with Poly(I:C) and Poly(I:C)/LyoVec



Regorafenib and sorafenib do not affect IRF pathway activation in THP1-Dual cells. THP-1 Dual cells were pre-treated with indicated concentrations of regorafenib (green), sorafenib (red) or DMSO vehicle for 1 h before stimulation with **(A)** poly(I:C) (10 µg/ml) or **(B)** poly(I:C)/LyoVec (100 ng/ml) for 24 h and relative IRF pathway activation was assessed by measuring secreted Lucia luciferase activity in the supernatant by adding QUANTI-Luc™ 4 Lucia solution. Mean ±SEM, n=3 independent experiments.

Appendix 3. Project Contributions

In vivo experiments (Figures 4.6-4.16 and Figure 5.9) were performed with the help of Dr. Laura Chaffey, Nicky Hamp and Prof. Greaves. Sample processing as well as data analysis and presentation were performed by Annabell Roberti with help from Prof. Greaves.

Static migration assays investigating primary human neutrophil and monocyte endothelial adhesion and transmigration (Chapter 5, Figures 5.4-5.7) were performed by Annabell Roberti and assisted by Jenefa Begum and Areeba Fatima (Iqbal Lab). Conceptualization and experimental design were informed by discussions with Prof. Asif Iqbal at the University of Birmingham. Jenefa Begum and Areeba Fatima also helped with isolation and characterization of primary human monocytes, neutrophils and macrophages used in Figure 3.8C and Figures 5.5-5.8. Data analysis and presentation were performed by Annabell Roberti with help from Prof. Greaves.

Experiments investigating TLR4 internalization (Fig. 3.12) and macrophage polarization (Fig. 3.11) were carried out and analyzed by Annabell Roberti but assisted by Dr. Laura Chaffey.